



République Algérienne Démocratique et Populaire
Ministère de l'Enseignement Supérieur et de la Recherche
Scientifique

N° of order:

N° of serial:

Université Kasdi Merbah-Ouargla

Faculté des Mathématiques et des Sciences de la matière

Département de Chimie

THÈSE PRÉSENTÉE EN VUE DE L'OBTENTION D'UN DIPLÔME DE
DOCTORAT 3^{ème} Cycle (LMD)

Spécialité : Chimie des Produits Naturels

Intitulé :

**Investigation phytochimique et caractérisation des
activités biologiques sur des extraits bioactifs *de*
Pergularia tomentosa issue de sud d'Algérie**

Présentée par :

TOUAHRIA Tatou

Soutenue publiquement le

15/10/2023

Devant le jury composé de :

M. DENDOUGUI Hocine	Professeur	U.K.M. Ouargla	Président
M. AKKAL Salah	Professeur	U. Constantine 1	Examineur
M. HABA Hamada	Professeur	U. Batna 1	Examineur
M ^{me} . KHALLEF Sakina	M.C.A	U.K.M. Ouargla	Examinatrice
M ^{me} . HAMADA Djamila	M.C.A	U.K.M. Ouargla	Examinatrice
M. BELGUIDOUM Mahdi	M.C.A	U. Ghardaia	Invité
M ^{me} . RAHMANI Zehour	Professeur	U.K.M. Ouargla	Rapporteur

Année universitaire : 2022/2023



N° d'ordre :

N° de série :

People's Democratic Republic of Algeria
Ministry of Higher Education and Scientific Research
Kasdi Merbah-Ouargla University
Faculty of Mathematics and Material Sciences

Department of Chemistry

THESIS SUBMITTED TO OBTAINING A 3rd Cycle DOCTORAL DEGREE (LMD)

Speciality: Chemistry of Natural Products

Entitled:

**Phytochemical investigation and characterization
of biological activities of bioactive extracts of
Pergularia tomentosa from southern Algeria**

Presented by:

TOUAHRIA Tatou

Publicly defended on

15/10/2023

In front of the jury members consisting of:

Mr. DENDOUGUI Hocine	Professor	U.K.M. Ouargla	President
Mr. AKKAL Salah	Professor	U. Constantine 1	Examiner
Mr. HABA Hamada	Professor	U. Batna 1	Examiner
Ms. KHALLEF Sakina	M.C.A	U.K.M. Ouargla	Examiner
Ms. HAMADA Djamilia	M.C.A	U.K.M. Ouargla	Examiner
Mr. BELGUIDOUM Mahdi	M.C.A	U. Ghardaia	Invited
Ms. RAHMANI Zehour	Professor	U.K.M. Ouargla	Supervisor

Academic year: 2023/2022

Acknowledgements

First of all, I want to thank Almighty God, for giving me the strength, the patience, the health and the will to carry out this modest work.

This work was carried out under the direction of Professor RAHMANI Zehour, Professor at the University of Ouargla. I would like to express my warmest thanks to her for welcoming me to her research group in the laboratory of Valorisation and Promotion of Saharan Resources (VPRS), for having trusted me, encouraged, and advised me. I would also like to thank her very much for her kindness and her availability during all the stages of preparation of my doctoral thesis. I would like to thank her for the trust she has placed in me.

I would like to thank Pr. DENDOUGUI Hocine; Professor at University of Ouargla for agreeing to chair the jury. I would like to thank Gentlemen: Pr. AKKAL Salah; Professor at University of Constantine 1, Pr. HABA Hamada; Professor at the University of Batna 1, Dr. Khallef Sakina; lecturer A at University of Ouargla, and Dr. HMADA Djamilia; lecturer A at University of Ouargla, for having done me the honor of examining this work.

I express all my gratitude to Dr. BELGUIDOUM Mahdi, lecturer B at University of Ghardaia. I would like to thank him for his patience, his availability and above all his judicious advice, which contributed to fueling my reflection, and for having kindly provided useful and constructive observations during the preparation of this thesis, which have been a source of motivation for me.

I would particularly like to thank Pr. DENDOUGUI Hocine for welcoming me into his research unit, for his guidance and his kindness. I also thank him for all the efforts he has made with me in the search of natural products. I would also like to thank Pr. AKKAL Salah and Pr. HABA Hamada for their collaboration, their availability, their kindness, their advice and their help. I am very thankful to them for benefiting me from their expertise in the field of natural products chemistry.

I warmly thank Mr LAICHI Yacine; engineer of NMR service (CRAPC Bousmail) for his kindness, his welcome, his precious help and the trust he placed in me during the

Acknowledgements

performance of the NMR spectroscopic analyses. I also thank Mr. RAHMANI Youcef engineer of NMR service (CRAPC Ouargla), Mr BOUSABAA WALID and Mrs MENAA Sabah engineers of LC-MS/MS service (CRAPC Ouargla) for their non-negligible help in carrying out the spectroscopy of certain products.

I would like to thank the entire laboratory team of Research and Development Center (CRD) of SIDAL group (Baraki Algeria) in particular: Mr CHAÏBI Slimane, Mrs BOUBEKEUR Sihem, Mrs AZINE Kenza, Mrs TRIBÈCHE Noel, CHIKHI Soraya, for their contribution to the supervision of the in vivo biological activities part, and also for the availability of the means and equipment necessary for these activities.

I would like to thank Professor BELFAR Mohamed Lakhdar, Director of the VPRS Laboratory, for welcoming me into his laboratory and for his assistance and kindness. Thanks also to my best friends: Wafa and Asma, for a great time that I banked with whom, for their support, for their collaboration and their encouragement throughout this work. As well as, my colleagues and friends from the laboratory especially Zineb, Chaima, Saida, Assia, Abedeldjabar, Maroua, Mareim, Siham, Bachira, Asma, Mareim for their friendship and kindness, and all members of the VPRS laboratory. I would also like to thank my Professor MOUSSAOUI Yacine, HADJADJ Mohamed, MAHFOUD Hadj Mohammed, DEKMOUCHE Messaouda, SMARA Ouanissa, MAHFOUDI Roukaia, DOUADI Ali, RAHIM Oumlkheir, and ZENKHRI Louiza. I would like to express my thanks to all those who have contributed to my training and the realisation of my doctoral thesis from near or far.

Thanks to all

Dedications

I especially dedicate this thesis to:

My father Hamou, who always made the hard times easier for me by giving me a smile in difficult times, for his unwavering support from my birth until today, and without him I would not be here today.

The souls of my grandfather Taher and my uncle Bachir, may God have mercy on them. This thesis represents the culmination of the support and encouragement which they gave me throughout my studies. May God welcome them to his Vast Paradise.

My dear grandmother Zohra, my source of tenderness, a grandiose symbol of patience and sacrifice, and I wish her good health and long life. My grandfather

My uncles; ARIBI Karim and LARACHICHE Mohamed, I would like to thank them warmly for their kindness, their availability, their support and their help during all the stages of my preparation of this doctoral thesis.

My step mother Assia, my sisters Ftima Zohra and Tinhinane, my brother Mouhamed, all My aunts, uncles and all Touahria family

My mother Djazia, my sisters Bouchra and Zineb, my brother Yahia, my maternal aunts especially Ratiba, my maternal uncles, my grandmother Kalthoum, my grandfather Kouider and all Oulad Sidi Saleh family

All my cousins especially Khadija and Djawahir, my friends Roumaissa, Amel and Iman

Abstract

This work is devoted to the phytochemical and biological study of the Algerian plant belonging to Asclepiadaceae family named *Pergularia tomentosa*. The Phytochemical screening which was performed on leaves and stems crud extracts, showed that this plant is rich of various secondary metabolites. Five leaves and five stems extracts were obtained using different solvent with increasing polarity. The assessment of the total phenolics (TPC), flavonoids (TFC) and tannins (TTC) contents showed that the leaves extracts have high contain of TPC, TFC and TTC compared with stems extracts. Reducing power of molybdenum Mo (VI) and DPPH assays were employed in order to measure antioxidant capacity of the different stems and leaves extracts. The leaves extracts also give the best antioxidant capacity. *In vitro* anti-diabetic activity was carried out on some leaves and stems extracts using inhibition of α -amylase enzyme method.

Acute toxicity, anti-inflammatory and sedative activities were performed in order to evaluate *in vivo* biological activity of both aqueous and crud extracts of *P.tomentosa*, using male and female albino mice. Oral administration of the extracts at single dose of 2000 mg/kg did not cause any symptoms of intoxication in all animals treated. In the other hand, this oral administration inhibits the development of paw edema with a percentage of inhibition estimated by 77.25% for aqueous extract. As well as, this administration also reduced the movement of the animal treated with percentage of reduction of movement of 60.00 % for crude extract; these results indicate that these extracts have good anti-inflammatory and sedative activities.

In order to isolate alkaloids from *P.tomentosa*, specific alkaloids extraction, isolation and purification were performed. The isolation and purification were performed using different chromatographic methods which are: silica gel column, C18 column, TLC and PTLC. This phytochemical investigation led us to obtain 26 pure alkaloids. Chemical structure of 5 alkaloids were determined using NMR experiments (^1H , ^{13}C , HSQC, HMBC and COSY). All these compounds are reported in our study for the first time as new compounds. The phytochemical study of combine butanol and ethyl acetate extracts using different chromatographic methods such as silica gel column, Sephadex LH-20 column, C18 column, TLC and PTLC, led us to obtain 5 cardenolide glycosides, 2 flavonoids and 1 phenolic compound. The chemical structures of 6 compounds were determined using

Abstract

different NMR spectroscopic analysis methods (^1H , ^{13}C , DEPT135, DEPT90, HSQC, TOCSY-HSQC, HMBC and COSY). Among those compounds, 4 compounds are isolated for the first time as new compounds.

Keywords: *Pergularia tomentosa*, antioxidant capacity, acute toxicity, anti-inflammatory activity, sedative activity, alkaloids, cardenolide glycosides.

Résumé

Ce travail est consacré à l'étude phytochimique et biologique d'une plante Algérienne appartenant à la famille d'Asclepiadaceae nommée *Pergularia tomentosa*. Les tests Phytochimique qui ont été réalisés sur les extraits brut de feuilles et de tiges, a montré que cette plante est riche en différents métabolites secondaires. Cinq extraits de feuilles et de tiges ont été obtenus en utilisant différents solvants de polarité croissante. L'évaluation des teneurs en composés phénoliques totaux (TPC), en flavonoïdes (TFC) et en tanins (TTC) a montré que les extraits de feuilles ont une teneur élevée en TPC, TFC et TTC par rapport aux extraits de tiges. Le test du pouvoir réducteur du molybdène Mo (VI) et de DPPH ont été réalisés afin de mesurer la capacité antioxydante des différents extraits de tiges et de feuilles. Les extraits de feuilles donnent également la meilleure capacité antioxydante. L'activité antidiabétique *in vitro* a été réalisée sur certains extraits de feuilles et de tiges en utilisant la méthode d'inhibition de l'enzyme α -amylase

La toxicité aiguë, l'activité anti-inflammatoires et l'activité sédatives ont été réalisées afin d'évaluer l'activité biologique *in vivo* des extraits aqueux et brut de *P. tomentosa*, en utilisant des souris albinos mâles et femelles. L'administration orale des extraits à une dose unique de 2000 mg/kg n'a provoqué aucun symptôme d'intoxication chez tous les animaux traités. En revanche, cette administration orale inhibe le développement de l'œdème de la patte avec un pourcentage d'inhibition estimé à 77.25% pour l'extrait aqueuse. De plus, cette administration a également réduit le mouvement de l'animal traité avec un pourcentage de réduction de mouvement de 60,00 % pour l'extrait brut; ces résultats indiquent que ces extraits ont une bonne activité anti-inflammatoire et sédative.

Afin d'isoler les alcaloïdes de *P. tomentosa*, l'extraction spécifiques d'alcaloïdes, l'isolement et le purification de ces composés ont été effectués. L'isolement et la purification ont été réalisés en utilisant différentes méthodes chromatographiques qui sont : colonne de gel de silice, colonne C18, CCM et CCMP. Cette investigation phytochimique nous a conduit à obtenir 26 alcaloïdes purs. Les structures chimiques des cinq alcaloïdes ont été déterminée à l'aide d'expériences de NMR (^1H , ^{13}C , HSQC, HMBC et COSY). Tous ces composés sont rapportés dans notre étude pour la première fois en tant que de nouveaux composés. L'étude phytochimique des extraits combinés de butanol et d'acétate d'éthyle à l'aide de différentes méthodes chromatographiques telles que la colonne de gel de silice, la colonne Sephadex LH-20, la colonne C18, la CCM et la CCMP, nous a conduit à obtenir 5 cardénolides

Résumé

glycosidiques, 2 flavonoïdes et 1 composé phénolique. Les structures chimiques de 6 composés ont été déterminées à l'aide de différentes méthodes d'analyse spectroscopique RMN (^1H , ^{13}C , DEPT135, DEPT90, HSQC, TOCSY-HSQC, HMBC et COSY). Parmi ces composés, 4 composés sont isolés pour la première fois en tant que nouveaux composés.

Mots clés : *Pergularia tomentosa*, capacité antioxydante, toxicité aiguë, activité anti-inflammatoire, activité sédatrice, alcaloïdes, cardénolides glycosidiques

ملخص

خصص هذا العمل للدراسة الفيتو كيميائية والبيولوجية للنبات الجزائري الذي ينتمي إلى عائلة Asclepiadaceae المسمى *Pergularia tomentosa*. وقد أظهر الفحص الكيميائي النباتي الذي تم إجراؤه على المستخلصات الخام للأوراق والسيقان أن هذا النبات غني بمختلف منتجات الايض الثانوي. تمكنا من الحصول على خمس مستخلصات للأوراق واخرى للسيقان باستخدام مذيبات ذات قطبية متزايدة. أظهرت نتائج تجارب تحديد محتويات الفينولات الكلية (TPC)، الفلافونويدات (TFC) والعفصيات (TTC) أن مستخلصات الأوراق تحتوي على نسبة عالية من TPC، TFC و TTC مقارنة بمستخلصات السيقان. خلال هذه الدراسة قمنا بإجراء اختبار القدرة الارجاعية للموليبدينوم (VI) واختبار DPPH من أجل قياس نشاط مضادات الأكسدة للمستخلصات المختلفة للسيقان والأوراق. اظهرت مستخلصات الأوراق أيضًا قدرة مضادة للأكسدة جيدة مقارنة بتلك التي أظهرتها مستخلصات السيقان. كما قمنا كذلك بإجراء اختبار الفعالية المضاد للسكري في المختبر على بعض مستخلصات الأوراق والسيقان باستخدام طريقة تثبيط إنزيم الفا-أميلاز.

من اجل دراسة الفعالية البيولوجية في الجسم الحي للمستخلصين المائي والخام لنبات *P. tomentosa*، قنا بإجراء تجارب تحديد السمية الحادة والفعالية المضادة للالتهابات بالإضافة الى الفعالية المسكنة للنشاط الحركي، باستخدام مجموعة من الفئران البيضاء من جنس ذكور وإناث. التجريع الفموي للمستخلصين بجرعة وحيدة مقدارها 2000 ملغ / كغ لم يسبب أي أعراض تسمم لدى جميع الحيوانات المعالجة. من ناحية أخرى، فإن هذه الجرعة تثبط تطور وذمة القدم مع نسبة تثبيط تقدر بـ 77.25% بالنسبة للمستخلص المائي. بالإضافة إلى ذلك، قللت هذه المستخلصات أيضًا من حركة الحيوان المعالج بنسبة انخفاض في الحركة تقدر بـ 60.00% للمستخلص الخام. تشير هذه النتائج إلى أن هذه المستخلصات لها نشاط مضاد للالتهابات ونشاط مهدئ جيد.

من اجل عزل القلويدات من نبات *P. tomentosa*، تمكنا من اجراء استخلاص نوعي لها وعزلها وتنقيتها. العزل والتنقية لهذه المركبات تم باستخدام طرق كروماتوغرافيا مختلفة وهي: عمود هلام السيليك، عمود C18، كروماتوغرافيا الطبقة الرقيقة التحليلية والتحضيرية. مكننا هذا التحليل الفيتو كيميائي من الحصول على ستة وعشرون قلويدا نقيا. تمكنا من تحديد التركيب الكيميائي لخمس قلويدات

باستخدام تجارب الرنين المغناطيسي النووي (^{13}C RMN، ^1H RMN، HSQC، HMBC و COSY). يعتبر فصل جميع هذه المركبات في دراستنا لأول مرة كمركبات جديدة. الدراسة الفيتو كيميائية لمجموع مستخلصي البوتانول وخرلات الإيثيل باستخدام مختلف الطرق الكروماتوغرافيا مثل عمود هلام السيليك، عمود سيفاديكس LH-20، عمود C18، وكروماتوغرافيا الطبقة الرقيقة التحليلية والتحضيرية؛ مكننا من الحصول على خمس جليكوسيدات الكاردينوليد، ومركب فلافونويدي ومركب فينولي. تمكنا من تحديد البنى الكيميائية لستة مركبات باستخدام مختلف طرق التحليل الطيفي بالرنين المغناطيسي النووي (^{13}C RMN، ^1H RMN، DEPT90، DEPT135، HSQC، TOCSY-HSQC، HMBC و COSY). 4 مركبات من بين المركبات المعزولة تم عزلها لأول مرة كمركبات جديدة.

الكلمات المفتاحية: *Pergularia tomentosa*، القدرة المضادة للأكسدة، السمية الحادة، النشاط المضاد للالتهابات، النشاط المهدئ، قلويدات، جليكوسيدات الكاردينوليد.

List of Figures

Figure	Page
Figure I-A-01: Photo of different parts of <i>Pergularia tomentosa</i> (Photo taken on 28/10/2021)	8
Figure I-A-02: Geographical distribution of <i>P. tomentosa</i> in the world	10
Figure I-B-01: Protocol of alkaloids extraction by apolar organic solvents in an alkaline medium	31
Figure I-B-02: Protocol of alkaloids extraction in an acid medium	32
Figure I-B-03: Base structure of cardenolide (1) and bufadienolide (2)	33
Figure I-B-04: Predicted steps of cardenolide aglycone biosynthesis pathway	34
Figure I-B-05: Chemical structures of sugar units that are linked to cardenolides aglycone.	36
Figure I-B-06: Chemical structures of some cardenolides and cardenolide glycosides isolated from different plants	36
Figure I-C-01: Electron transfer (ET) mechanism of the antioxidant activity of phenolic compounds	41
Figure I-C-02: Hydrogen-atom transfer (HAT) mechanism of the antioxidant activity of phenolic compounds	42
Figure I-C-03: Mechanism of inhibition of DPPH \cdot by phenolic compounds	43
Figure II-A-01: Herbarium specimens of <i>Pergularia tomentosa</i>	52
Figure II-A-02: Plastic cages of mice.....	60
Figure II-A-03: Acute toxicity test (administration and observation of treated mice).....	61
Figure II-A-04: Anti-inflammatory test	62

List of Figures

Figure II-A-05: An actimeter device.....	64
Figure II-A-06: Sedative test.....	64
Figure II-B-01: Protocol of extraction of alkaloids.....	68
Figure II-B-02: Monitoring of fractionation of alkaloids extract.....	69
Figure II-B-03: TLC test of alkaloids isolated from <i>P. tomentosa</i>	71
Figure II-B-04: Fractionation Scheme of alkaloid extract	73
Figure II-B-05: protocol of extraction of cardenolides and phenolic compounds.	75
Figure II-B-06: Monitoring of fractionation of combined extracts (EtOAc and n-butanol extracts).....	76
Figure II-B-07: Fractionation of combined extracts (EtOAc and butanol extracts).....	78
Figure III-A-01: Gallic acid calibration curve	82
Figure III-A-02: Total phenolic content (TPC).....	84
Figure III-A-03: Quercetin calibration curve	84
Figure III-A-04: Total flavonoid content (TFC)	86
Figure III-A-05: Catechin calibration curve	87
Figure III-A-06: Total tannin content (TTC)	88
Figure III-A-07: Variation of DPPH inhibition as a function of concentration of the leaves extracts	89
Figure III-A-08: Variation of DPPH inhibition as a function of concentration of the stems extracts	90
Figure III-A-09: Curves representing the reducing power of the leaves extracts.	92
Figure III-A-10: Curves representing the reducing power of the stems extracts.....	92
Figure III-A-11: Inhibition percentage of α -amylase activity of <i>P. tomentosa</i> extracts.....	96
Figure III-A-12: Maltose calibration curve.....	97

List of Figures

Figure III-A-13: Velocity of inhibition of α -amylase enzyme in the presence and absence of extract.....	97
Figure III-A-14: Velocity of inhibition of α -amylase enzyme in the presence and absence of acarbose.....	98
Figure III-A-15: Anti-inflammatory effect of the aqueous extract, the crude extract and ibuprofen.....	99
Figure III-A-16: Sedative activity of the aqueous extract, the crude extract and haloperidol.....	101
Figure III-B-01: ^1H NMR spectrum (400 MHz, CDCl_3) of compound P8.....	103
Figure III-B-02: ^{13}C NMR spectrum (150 MHz, CDCl_3) of compound P8.....	104
Figure III-B-03: Basic structure of pyrrolizidine alkaloid.....	104
Figure III-B-04: Basic structure of macrocyclic diester pyrrolizidine alkaloid.....	105
Figure III-B-05: Structures of otonecine-type pyrrolizidine alkaloid.....	106
Figure III-B-06-a: HSQC expansion spectrum [4.4 - 0.6 ppm] (600 MHz, CDCl_3) of compound P8.....	107
Figure III-B-06-b: HSQC expansion spectrum [7.4 - 5.7 ppm] (600 MHz, CDCl_3) of compound P8.....	108
Figure III-B-07: HMBC expansion spectrum (600 MHz, CDCl_3) of compound P8 (correlation of H-1, H-5 $_{\alpha}$, H-5 $_{\beta}$ and N-CH $_3$).....	109
Figure III-B-08: Correlation of basic structure (correlation of H-1, H-5 $_{\alpha}$, H-5 $_{\beta}$ and N-CH $_3$) according to HMBC spectrum of compound P8.....	110
Figure III-B-09: HMBC expansion spectrum (600 MHz, CDCl_3) of compound P8 (correlation of methyl groups H $_3$ -18, H $_3$ -19 and H $_3$ -20).....	111
Figure III-B-10: Correlation of methyl groups (H $_3$ -18, H $_3$ -19 and H $_3$ -20) according to HMBC spectrum of compound P8.....	111

List of Figures

Figure III-B- 11-a: HMBC expansion spectrum (600 MHz, CDCl ₃) of compound P8 (correlation H-17 and H-16)	112
Figure III-B- 11-b: HMBC expansion spectrum (600 MHz, CDCl ₃) of compound P8 (correlation H-24 and N-CH ₃)	113
Figure III-B-12: Correlation H-17, H-16 and H-24 according to HMBC spectrum of compound P8	113
Figure III-B-13: COSY spectrum (600 MHz, CDCl ₃) of compound P8.....	114
Figure III-B-14: Correlation of compound P8 according to COSY spectrum.....	115
Figure III-B-15: Chemical structure of compound P8, which is an alkaloid named Tomentonecine A	117
Figure III-B-16: ¹ H NMR spectrum (600 MHz, CDCl ₃) of compound P13.....	119
Figure III-B-17: NMR ¹³ C spectrum (100 MHz, CDCl ₃) of compound P13	120
Figure III-B-18-a: HSQC expansion spectrum [2.8 - 0.7 ppm] (600 MHz, CDCl ₃) of compound P13	122
Figure III-B-18-b: HSQC expansion spectrum [6.4 – 4.3 ppm] (600 MHz, CDCl ₃) of compound P13	122
Figure III-B-19: HMBC expansion spectrum (600 MHz, CDCl ₃) of compound P13 (correlation of H-1 and H ₂ -5).....	124
Figure III-B-20: Correlation of H-1, H-5 _α and H-5 _β according to HMBC spectrum of compound P13	124
Figure III-B-21: HMBC expansions spectrum (600 MHz, CDCl ₃) of compound P13 (correlation of methyl groups H-18, H-19 and H-20).....	125
Figure III-B-22: Correlation of methyl groups H ₃ -18, H ₃ -19 and H ₃ -20 according to HMBC spectrum of compound P13	126

List of Figures

Figure III-B-23-a: HMBC expansion spectrum (600 MHz, CDCl ₃) of compound P13 (correlation of H-16 and H-17)	127
Figure III-B-23-b: HMBC expansion spectrum (600 MHz, CDCl ₃) of compound P13 (correlation of H ₃ -24)	127
Figure III-B-24: Correlation of H-16, H-17, H-23 and H ₃ -24 according to HMBC spectrum of compound P13	128
Figure III-B-25: HMBC expansion spectrum (600 MHz, CDCl ₃) of compound P13 (correlation of H ₃ -22)	129
Figure III-B-26: Correlation of H ₃ -22 according to HMBC spectrum of compound P13 ...	129
Figure III-B-27: COSY spectrum (600 MHz, CDCl ₃) of compound P13	130
Figure III-B-28: Correlation of compound P13 according to COSY spectrum	130
Figure III-B-29: Chemical structure of compound P13, which is an alkaloid named Tomentonecine B	133
Figure III-B-30-a: ¹ H NMR expansion spectrum [6.9 – 3.5 ppm] (600 MHz, CDCl ₃) of compound P5	135
Figure III-B-30-b: ¹ H NMR expansion spectrum [2.6 – 0.7 ppm] (600 MHz, CDCl ₃) of compound P5	135
Figure III-B-31: Basic structure of compound P5	136
Figure III-B-32: HSQC expansion spectrum (600 MHz, CDCl ₃) of compound P5	138
Figure III-B-33: HMBC expansion spectrum (600 MHz, CDCl ₃) of compound P5 (correlation of methyl groups H-19 and H-20)	139
Figure III-B-34-a: HMBC expansions spectra (600 MHz, CDCl ₃) of compound P5 (correlation of methyl groups H ₃ -18, H ₃ -22, H ₃ -25)	140
Figure III-B-34-b: HMBC expansions spectra (600 MHz, CDCl ₃) of compound P5 (correlation of methyl group H ₃ -26)	141

List of Figures

Figure III-B-35: Correlation of methyl groups (H3-18, H3-22, H3-25 and H-26) according to HMBC spectrum of compound P5.....	141
Figure III-B-36: Chemical structure of compound P5, which is an alkaloid named Tomentonecine C	143
Figure III-B-37: ¹ H NMR spectrum (600 MHz, CDCl ₃) of Compound P20.....	145
Figure III-B-38: ¹³ C NMR spectrum (150 MHz, CDCl ₃) of compound P20	146
Figure III-B-39-a: HSQC expansion spectrum [3.01 – 0.6 ppm] (600 MHz, CDCl ₃) of compound P20	147
Figure III-B-39-b: HSQC expansion spectrum [6.2 – 3.2 ppm] (600 MHz, CDCl ₃) of compound P20	148
Figure III-B-40: Structures of retronecine-type pyrrolizidine alkaloid.....	149
Figure III-B-41: HMBC expansions spectrum (600 MHz, CDCl ₃) of compound P20 (correlation of H-9 _α , H-9 _β , H-13, and H ₃ -28)	150
Figure III-B-42: Correlation of methyl groups (H ₃ -28H-9 _α , H-9 _β and H-13) according to HMBC spectrum of compound P20.....	150
Figure III-B-43: Chemical structure of compound P20, which is an alkaloid named Tomentonecine D	152
Figure III-B-44: ¹ H NMR spectrum (600 MHz, CDCl ₃) of compound P10.....	153
Figure III-B-45: ¹³ C NMR spectrum (150 MHz, CDCl ₃) of compound P10	154
Figure III-B-46: HSQC expansion spectrum (600 MHz, CD ₃ Cl) of compound P10	155
Figure III-B-47: HMBC expansion spectrum (600 MHz, CDCl ₃) of compound P10 (correlation of H-3 _α , H-3 _β , H-5 _α , H-5 _β and N-CH ₃).....	157
Figure III-B-48: Correlation of H-3 _α , H-3 _β , H-5 _α , H-5 _β and N-CH ₃) according to HMBC spectrum of compound P10	157

List of Figures

Figure III-B-49: HMBC expansion spectrum (600 MHz, CDCl ₃) of compound P10 (correlation of H-7 and H-9)	158
Figure III-B-50: Correlation of H-7 and H-9 according to HMBC spectrum of compound P10	159
Figure III-B-51: HMBC expansion spectrum (600 MHz, CDCl ₃) of compound P10 (correlation of methyl groups H ₃ -20 and H ₃ -29)	160
Figure III-B-52: Correlation of methyl groups H ₃ -20 and H ₃ -29 according to HMBC spectrum of compound P10	160
Figure III-B-53-a: HMBC expansions spectrum (600 MHz, CDCl ₃) of compound P10 (correlation of dihydroxyvinyloxy group groups H-17 and H-19)	161
Figure III-B-53-b: HMBC expansions spectrum (600 MHz, CDCl ₃) of compound P10 (correlation of N-CH ₃ and H-5 _α with C-30)	162
Figure III-B-54: Correlation of 2,2-dihydroxyvinyloxy group groups (H-17, H-19 and C-30) according to HMBC spectrum of compound P10	162
Figure III-B-55: Chemical structure of compound P10, which is an alkaloid named Tomentonecine E	164
Figure III-B-56: ¹ H NMR spectrum (400 MHz, CD ₃ OD) of compound PV	167
Figure III-B-57: ¹³ C NMR spectrum (100 MHz, CD ₃ OD) of compound PV	168
Figure III-B-58: ¹³ C NMR DEPT 135 spectrum (100 MHz, CD ₃ OD) of compound PV	169
Figure III-B-59: ¹³ C NMR DEPT 90 spectrum (100 MHz, CD ₃ OD) of compound PV	169
Figure III-B-60: HSQC expansions spectrum (400 MHz, CD ₃ OD) of compound PV	172
Figure III-B-61: Correlation of H-1 _α , H-1 _β , H-4 _α and H-4 _β according to HMBC spectrum of compound PV	173
Figure III-B-62: Correlation of H-17, H ₃ -18 and H ₂ -19 according to HMBC spectrum of compound PV	174

List of Figures

Figure III-B-63: Correlation of H-21 _α , H-21 _β and H-22 according to HMBC spectrum of compound PV.....	175
Figure III-B-64: Correlation of H-1', H-4' _α , H-4' _β and H ₂ -6' according to HMBC spectrum of compound PV.....	176
Figure III-B-65-a: HMBC expansions spectrum [4.0 – 0.4 ppm] (400 MHz, CD ₃ OD) of..	176
compound PV.....	176
Figure III-B-65-b: HMBC expansions spectrum [6.1 – 3.8 ppm] (400 MHz, CD ₃ OD) of compound PV.....	177
Figure III-B-66: COSY correlations of sugar part of compound PV	177
Figure III-B-67: COSY correlations of aglycon part of compound PV	178
Figure III-B-68: COSY spectrum (400 MHz, CD ₃ OD) of compound PV.....	179
Figure III-B-69: Chemical structure of compound PV, which is a cardenolides glycoside named Ghalakinoside	180
Figure III-B-70: ¹ H NMR spectrum (400 MHz, CD ₃ OD) of compound PN.....	182
Figure III-B-71: ¹³ C NMR spectrum (100 MHz, CD ₃ OD) of compound PN.....	183
Figure III-B-72: ¹³ C NMR DEPT 135 spectrum (100 MHz, CD ₃ OD) of compound PN....	184
Figure III-B-73: ¹³ C NMR DEPT 90 spectrum (100 MHz, CD ₃ OD) of compound PN.....	184
Figure III-B-74-a: HSQC expansion spectrum [3.6 – 0.4 ppm] (100 MHz, CD ₃ OD) of compound PN.....	187
Figure III-B-74-b: HSQC expansion spectrum [6.1 – 3.0 ppm] (100 MHz, CD ₃ OD) of compound PN.....	188
Figure III-B-75: Correlation of H-1 _α , H-1 _β , H-2 and H-4 _α according to HMBC spectrum of compound PN.....	189
Figure III-B-76: Correlation of H ₃ -18, H-21 _α , H-21 _β and H-22 according to HMBC spectrum of compound PN	189

List of Figures

Figure III-B-77: Correlation of H-1' and H ₂ -6' according to HMBC spectrum of compound PN	190
Figure III-B-78-a: HMBC expansions spectrum [3.6 – 0.4 ppm] (400 MHz, CD ₃ Cl) of compound PN.....	190
Figure III-B-78-b: HMBC expansions spectrum [3.6 – 3.0 ppm] (400 MHz, CD ₃ Cl) of compound PN.....	191
Figure III-B-79: COSY correlations of sugar part of compound PN	191
Figure III-B-80: COSY correlations of aglycon part of compound PN.....	192
Figure III-B-81: COSY spectrum (400 MHz, CD ₃ OD) of compound PN.....	193
Figure III-B-82: Chemical structure of PN, which is a cardenolides glycoside named.....	194
12β-hydroxycalactin	194
Figure III-B-83: ¹ H NMR spectrum (400 MHz, CD ₃ OD) of compound PVe	196
Figure III-B-84: ¹³ C NMR spectrum (100 MHz, CD ₃ OD) of compound PVe	197
Figure III-B-85: ¹³ C NMR DEPT 135 spectrum (100 MHz, CD ₃ OD) of compound PVe ..	197
Figure III-B-86: ¹³ C NMR DEPT 90 spectrum (100 MHz, CD ₃ OD) of compound PVe	198
Figure III-B-87-a: HSQC expansions spectrum [2.7 - 0.7 ppm] (100 MHz, CD ₃ OD) of compound PVe.....	201
Figure III-B-87-b: HSQC expansions spectrum [5.8 – 2.7 ppm] (100 MHz, CD ₃ OD) of compound PVe.....	201
Figure III-B-88: COSY correlations of sugar part of compound PVe	202
Figure III-B-89 COSY correlations of aglycone part of compound PVe.....	203
Figure III-B-90: COSY spectrum (400 MHz, CD ₃ OD) of compound PVe	203
Figure III-B-91: Chemical structure of compound PVe, which is a cardenolides glycoside named 2-hydroxycorotoxigenin-3-O-glucopyranoside	204
Figure III-B-92: ¹ H NMR spectrum (400 MHz, CD ₃ OD) of compound PM	207

List of Figures

Figure III-B-93: ^{13}C NMR spectrum (100 MHz, CD_3OD) of compound PM	208
Figure III-B-94: ^{13}C NMR DEPT 135 spectrum (100 MHz, CD_3OD) of compound PM ...	208
Figure III-B-95: ^{13}C NMR DEPT 90 spectrum (100 MHz, CD_3OD) of compound PM	209
Figure III-B-96: HSQC expansions spectrum (400 MHz, CD_3OD) of compound PM.....	212
Figure III-B-97: Correlation of H-4 $_{\alpha}$, H-17 and H-18 according to HMBC spectrum of compound PM.....	213
Figure III-B-98: Correlation of H-19 $_{\alpha}$, H-19 $_{\beta}$ H-21 $_{\alpha}$ and H-21 $_{\beta}$ according to HMBC spectrum of compound PM.....	214
Figure III-B-99: correlation of sugar part according to HMBC spectrum of compound PM	215
Figure III-B-100: HMBC spectrum (400 MHz, CD_3OD) of compound PM.....	215
Figure III-B-101: COSY correlations of sugar part of compound PM	216
Figure III-B-102: COSY correlations of aglycon part of compound PM	217
Figure III-B-103: COSY spectrum (400 MHz, CD_3OD) of compound PM	217
Figure III-B-104: chemical structure of compound PM which is a cardenolides glycoside named 3-oxo,19-O-β-D-glucopyranosylcoroglaucigenin	218
Figure III-B-105: The UV spectral series of compound PJ	220
Figure II-B-106: ^1H NMR spectrum (400 MHz, CD_3OD) of compound PJ.....	221
Figure III-B-107: ^{13}C NMR spectrum (100 MHz, CD_3OD) of compound PJ	222
Figure III-B-108: ^{13}C NMR DEPT 135 spectrum (100 MHz, CD_3OD) of compound PJ ...	222
Figure III-B-109: ^{13}C NMR DEPT 90 spectrum (100 MHz, CD_3OD) of compound PJ.....	223
Figure III-B-110-a: HSQC expansions spectrum [5.2 – 2.1 ppm] (400 MHz, CD_3OD) of compound PJ.....	225
Figure III-B-110-b: HSQC expansions spectrum [8.2 – 6.7 ppm] (400 MHz, CD_3OD) of compound PJ.....	225

List of Figures

Figure III-B-111: correlation of H-2'/6' and H-3'/5' according to HMBC spectrum of compound PJ.....	226
Figure III-B-112: correlation of protons of sugar part according to HMBC spectrum of compound PJ.....	227
Figure III-B-113-a: HMBC spectrum [5.2 – 3.1 ppm] (400 MHz, CD ₃ OD) of compound PJ.....	228
Figure III-B-113-b: HMBC spectrum [8.4 – 6.5 ppm] (400 MHz, CD ₃ OD) of compound PJ.....	228
Figure III-B-114: COSY correlations of aromatic and sugar protons of compound PJ.....	229
Figure III-B-115-a: COSY spectrum [8.3 – 6.7 ppm] (400 MHz, CD ₃ OD) of compound PJ.....	229
Figure III-B-115-b: COSY spectrum [5.4 – 3.0 ppm] (400 MHz, CD ₃ OD) of compound PJ.....	230
Figure III-B-116: Chemical structure of compound PJ, which is a flavonoid named 6,8-dihydroxyKaempferol-3-O-β-glucopyranosyl	230
.....	232
Figure III-B-117: ¹ H NMR spectrum (400 MHz, CD ₃ OD) of compound PR.....	232
Figure III-B-118: ¹³ C NMR spectrum (150 MHz, CD ₃ OD) of compound PR.....	233
Figure III-B-119: ¹³ C NMR DEPT 135 spectrum (100 MHz, CD ₃ OD) of compound PR..	233
Figure III-B-120: ¹³ C NMR DEPT 90 spectrum (100 MHz, CD ₃ OD) of compound PR...	234
Figure III-B-121-a: HSQC spectrum [5.4 – 0.2 ppm] (600 MHz, CD ₃ OD) of compound PR.....	236
Figure III-B-121-b: HSQC spectrum [6.8 – 6.4 ppm] (600 MHz, CD ₃ OD) of compound PR.....	236

List of Figures

Figure III-B-122: HSQC-TOCSY correlation of H-3, H-4, H-6 and H-4''' of compound PR	237
Figure III-B-123: HSQC-TOCSY correlation of the sugar part of compound PR	238
Figure III-B-124-a: HSQC-TOCSY expansion spectrum [5.0 -1.0 ppm] (600 MHz, CD ₃ OD) of compound PR	238
Figure III-B-124-b: HSQC-TOCSY expansion spectrum [7.2 – 2.8 ppm] (600 MHz, CD ₃ OD) of compound PR	239
Figure III-B-125: HMBC correlation of H-3 and OCH ₃ of compound PR.....	239
Figure III-B-126: HMBC spectrum (400 MHz, CD ₃ OD) of compound PR.....	240
Figure III-B-127: COSY correlation of H-1', H-2' and H-6'' of compound PR.....	241
Figure III-B-128: COSY correlation of sugar part of compound PR.....	242
Figure III-B-129: COSY spectrum (400 MHz, CD ₃ OD) of compound PR.....	242
Figure III-B-130: chemical structure of compound PR, which is a phenolic compound named 5-[(2-O-β-glucopyranosyl)ethoxy]-2-methoxy-phenol-O-α-rhamnopyranosyl...	243

List of Tables

Table	Page
Table I-A-01: Structures of cardenolide glycosides isolated from genus <i>Pergularia</i>	12
Table I-A-02: Structures of cardenolides isolated from genus <i>Pergularia</i>	15
Table I-A-03: Structures of triterpenes isolated from genus <i>Pergularia</i>	16
Table I-A-04: Structures of other compounds isolated from genus of <i>Pergularia</i>	20
Table I-B- 01: Main types of alkaloids and their chemical groups	25
Table III-A-01: Chemical screening of <i>Pergularia tomentosa</i>	81
Table III-A-02: Total phenolic content (TPC) of different stems and leaves extracts of <i>P. tomentosa</i>	82
Table III-A-03: Total flavonoid content (TFC) of different stems and leaves extracts of <i>P. tomentosa</i>	85
Table III-A-04: Total tannins content (TTC) of different stems and leaves extracts of <i>P. tomentosa</i>	87
Table III-A-05: Results of the antiradical activity evaluated by the DPPH [*] test	90
Table III-A-06: Results of reducing power test (AEAC)	92
Table III-A-07-a: results of linear correlation between the IC ₅₀ and AEAC values and the total polyphenols, flavonoids and tannins content of stems extracts	94
Table III-A-07-b: results of linear correlation between the IC ₅₀ and AEAC values and the total polyphenols, flavonoids and tannins content of leaves extracts	94
Table III-A-08: Percentage of inhibition of α -amylase	95
Table III-A-09: Anti-inflammatory effect of the aqueous extract, the crude extract and ibuprofen on edema induced by carrageenin	99

List of Tables

Table III-A-10: Results of sedative activity of aqueous extract, crude extract and Haloperidol	101
Table III-B-01: Chemical shifts of ^1H (400 MHz) and ^{13}C (150 MHz) NMR in CDCl_3 of compound P8 (δ in ppm and J in Hz).....	115
Table III-B-02: Chemical shifts of ^1H (600 MHz) and ^{13}C (100 MHz) NMR in CDCl_3 of alkaloid P13 (δ in ppm and J in Hz).....	131
Table III-B-03: Chemical shifts of ^1H (600 MHz) and ^{13}C (150 MHz) NMR in CDCl_3 of alkaloid P5 (δ in ppm and J in Hz).....	142
Table III-B-04: Chemical shifts of ^1H (600 MHz) and ^{13}C (150 MHz) NMR in CDCl_3 of alkaloid P20 (δ in ppm and J in Hz).....	151
Table III-B-05: Chemical shifts of ^1H (600 MHz) and ^{13}C (150 MHz) NMR in CDCl_3 of alkaloid P10 (δ in ppm and J in Hz).....	163
Table III-B-06: Chemical shifts of ^1H (400 MHz) and ^{13}C (100 MHz) NMR in CD_3OD of compound PV (δ in ppm and J in Hz).....	170
Table III-B-07: Chemical shifts of ^1H (400 MHz) and ^{13}C (100 MHz) NMR in CD_3OD of compound PN (δ in ppm and J in Hz).....	185
Table III-B-08: Chemical shifts of ^1H (400 MHz) and ^{13}C (100 MHz) NMR in CD_3OD of compound PVe (δ in ppm and J in Hz).....	199
Table III-B-09: Chemical shifts of ^1H (400 MHz) and ^{13}C (100 MHz) NMR in CD_3OD of compound PM (δ in ppm and J in Hz).....	210
Table III-B-10: UV spectral series data (λ_{max} nm) of compound PJ	219
Table III-B-11: Chemical shifts of ^1H (100 MHz) and ^{13}C (75 MHz) NMR in CD_3OD of compound PJ (δ in ppm and J in Hz).....	223
Table III-B-12: Chemical shifts of ^1H (400 MHz) and ^{13}C (150 MHz) NMR in CD_3OD of compound PR (δ in ppm and J in Hz).....	235

List of Tables

Table III-B-13: Chemical structure of the compounds isolated from <i>P.tomentosa</i>	247
---------------------------------------------------------------------------------------------------	-----

List of Abbreviations

δ	Chemical shift
EtOAc	Ethyl acetate
AEAC	Ascorbic Acid Equivalent Antioxidant Capacity
BHA	Butylated Hydroxy Anisole
BHT	Butylated Hydroxy Toluene
CC	Column Chromatography
C18	C-18 grafted silica
COSY	COrrrelation SpectroscopY
D	Doublet
Dd	Doublet of Doublets
DEPT	Distorsionless Enhancement by Polarization Transfer
DPPH	1,1-Diphenyl-2- Picryl Hydrazine
HMBC	Heteronuclear Multiple Bond Coherence
HSQC	Heteronuclear Single Quantum Coherence
Hz	Hertz
J	Coupling constant
L	Leaves
LD₅₀	The amount of a substance that causes the death of 50% of a group of test animals
m	Multiplet
NMR	Nuclear Magnetic Resonance

List of Abbreviations

<i>P</i>	Pergularia
PTLC	Preparative Thin-layer Chromotography
ppm	Parties par million
TLC	Thin-layer Chromotography
t	Triplet
s	Singlet
S	Stems

Content

Acknowledgements	III
Dedications	V
Abstract.....	VI
Résumé	VIII
ملخص	X
List of Figures.....	XII
List of Tables	XXIV
List of Abbreviation.....	XXVII
General introduction	1

PART I: THEORETICAL PART

Chapter A: botanical presentation of Pergularia tomentosa

I-A-1-Asclepiadaceae family.....	6
I-A-2-Pergularia genus	6
I-A-3-Description of <i>Pergularia tomentosa</i> specie	7
I-A-4-Description of the harvest area	9
I-A-5-Classification of <i>Pergularia tomentosa</i>	9
I-A-6-Synonyms and traditional names of <i>P.tomentosa</i>	9
I-A-7-Geographical distribution of <i>P.tomentosa</i>	10

Content

I-A-8-Traditional uses of <i>P.tomentosa</i>	10
I-A-9-Biological activities of <i>P.tomentosa</i>	11
I-A-10-Major secondary metabolites previously isolated from <i>Pergularia</i> genus.....	12

Chapter B: Alkaloids and cardenolides

I-B-1-Alkaloids.....	24
I-B-1-1-Definition of alkaloids	24
I-B-1-2-History of alkaloids	24
I-B-1-3-Classification of alkaloids	25
I-B-1-4-Distribution of alkaloids	29
I-B-1-5-Physicochemical properties of alkaloids	29
I-B-1-6-Extraction of alkaloids.....	30
I-B-1-7-Role pharmacology of alkaloids	32
I-B-2-Cardenolides	33
I-B-2-1-Definition of cardenolides	33
I-B-2-2-Biosynthesis of cardenolides.....	34
I-B-2-3-Structural description of cardenolides glycosides	35
I-B-2-4-Distribution of cardenolides	37
I-B-2-5-Physico-chemical properties of cardenolides	37
I-B-2-6-Biological activities of cardenolides.....	37

Chapter C: Biological activities

I-C-1-Biological activities	40
-----------------------------------	----

Content

I-C-2-Definition of free radicals	40
I-C-3-Source of reactive oxygen species (ROS)	40
I-C-4-Antioxidant activity	40
I-C-4-1-Mechanisms of scavenge free radicals by antioxidants (phenolic compounds)	41
I-C-4-1-1-Electron transfer (ET) mechanism.....	41
I-C-4-1-2-Hydrogen atom transfer (HAT)	41
I-C-4-2-Methods of determination of antioxidant activity	42
I-C-4-2-1-DPPH (2,2-diphenyl-1-picrylhydrazyl) radical scavenging method	42
I-C-4-2-2-Total antioxidant capacity (TAC).....	43
I-C-5-Antidiabetic activity	43
I-C-5-1-Definition of diabetes	43
I-C-5-2-Classification of diabetes.....	44
I-C-5-2-1-Insulin-dependent diabetes (type I diabetes)	44
I-C-5-2-2-Non-insulin dependent (type II diabetes)	44
I-C-5-2-3-Gestational diabetes	44
I-C-5-2-4-Other types of diabetes	44
I-C-5-3-Definition of α -amylase	44
I-C-6-Toxicity.....	45
I-C-6-1-Definition of toxicity	45
I-C-6-1-1-Acute toxicity	45
I-C-6-1-2-Sub-acute toxicity	45

Content

I-C-6-1-3-Chronic toxicity	46
I-C-7-Anti-inflammatory activity	46
I-C-7-1-Definition of inflammation	46
I-C-7-1-1-Acute inflammation	46
I-C-7-1-2-Chronic inflammation.....	46
I-C-7-2-Anti-inflammatory agents.....	47
I-C-7-2-1-Nonsteroidal anti-inflammatory drugs (NSAIDs)	47
I-C-7-2-2-Steroidal anti-inflammatory drugs (AISDs)	47
I-C-7-2-3-Naturel anti-inflammatory drugs	47
I-C-8-Sedative activity	48
I-C-8-1-Definition of pain.....	48
I-C-8-1-1-Types of pain	48
I-C-8-2-Definition of sedation	48
I-C-8-3-Sedative drugs.....	49

PART II: MATERIAL AND METHOD

ChapterA: Qualitative and Biological study of P. tomentosa

II-A-1-Preparation of Sample	52
II-A-2-Phytochemical screening.....	52
II-A-3-Quantitative study	54
II-A-3-1-Dosage of Total Phenolic Content	54

Content

II-A-3-2-Dosage of flavonoids	55
II-A-3-3-Dosage of condensed tannins	55
II-A-4-Evaluation of <i>in vitro</i> biological activities (antioxidant and antidiabetic activity	56
II-A-4-1-Antioxidant activity.....	56
II-A-4-1-1-DPPH [•] radical scavenging test	56
II-A-4-1-2-Reducing power of molybdenum Mo (VI) test.....	57
II-A-4-2-Antidiabetic activity	58
II-A-5-Evaluation of <i>in vivo</i> biological activities (acute toxicity, anti-inflammatory and	
sedative activities)	59
II-A-5-1-Determination of acute toxicity.....	60
II-A-5-2-Anti-inflammatory test	61
II-A-5-3-Sedative activity	63

B-Phytochemical study of P. tomentosa

II-B-1-Extraction, isolation and purification of alkaloids	67
II-B-1-1-Extraction of alkaloids	67
II-B-1-2-Isolation and purification of alkaloids.....	69
II-B-2-Extraction, isolation and purification of cardenolides and phenolic compounds .	74
II-B-2-1-Extraction of cardenolides and phenolic compounds.....	74
II-B-2-2-Isolation and purification of cardenolides and phenolic compounds.....	76

PART III: RESULTS AND DISCUSSION

Chapter A: Qualitative and Biological study of P. tomentosa

III-A-1-Phytochemical tests	81
III-A-2-Quantitative study	82
III-A-2-1-Total Phenolic Content (TPC)	82
III-B-2-2-Total flavonoids content (TFC)	84
III-A-2-3-Total tannins content (TTC)	86
III-A-3-Evaluation of in vitro biological activities (antioxidant and antidiabetic activities)	89
III-A-3-1-Antioxidant activity	89
III-A-3-1-1-DPPH• radical scavenging test	89
III-A-3-1-2- Reducing power of molybdenum Mo (VI) test.....	91
III-A-3-2-Antidiabetic activity.....	95
III-A-3-2-1-Determination of percentage of inhibition of α -amylase activity	95
III-A-3-2-2-Determination of velocity of α -amylase activity	96
III-A-4-Evaluation of in vivo biological activities (acute toxicity, anti-inflammatory and sedative activities)	98
III-A-4-1-Determination of acute toxicity	98
III-A-4-2-Anti-inflammatory test.....	99
III-A-4-3-Sedative activity.....	100

Chapter B: Phytochemical study of P. tomentosa

Content

III-B-1-Structural elucidation of alkaloids isolated from <i>P.tomentosa</i>	103
III-B-1-1-Compound P8.....	103
III-B-1-2-Compound P13.....	118
III-B-1-3-Compound P5.....	133
III-B-1-4-Compound P20.....	144
III-B-1-5-Compound P10.....	152
III-B-2- Structural elucidation of cardenolide glycosides isolated from <i>P.tomentosa</i> ...	165
III-B-2-1-Compound PV	165
III-B-2-2-Compound PN.....	180
III-B-2-3-Compound PVe	194
III-B-2-4-Compound M	205
III-B-3- Structural elucidation of phenolic compounds isolated from <i>P.tomentosa</i>	218
III-B-3-1-Compound PJ	218
III-B-3-2-Compound PR.....	231
General conclusion	245
References	254

General introduction

General introduction

Plants represent an inexhaustible source of active compounds whose their traditional use has been known for a long time. A majority of the world's population, especially in developing countries, treat their illnesses with traditional herbal remedies due to absence of a modern medical system. This type of medicine is known as phytotherapy. Study of natural substances for therapeutic purposes is nowadays experiencing unprecedented interest. The selection of plant material is the first step in a phytochemical study. This step requires an ethno-pharmacological and pharmacological study, which can guide the phytochemists when harvesting plants.

Algeria has a great climatic and taxonomic diversity, which gives it a considerable floristic richness. Its flora includes thousands of species presenting material for scientific research. The Algerian flora is estimated at more than 3152 species belonging to several botanical families [1] of which 650 species are Shahrin species [1]. Among these species, a significant number (15%) are endemic species [2].

Asclepiadaceae family is named milk-weed family due to its richness in latex. Plants belonging to this family are perennial shrubs and herbs, which distributed through the tropics and temperate areas of the world [3]. This family is renowned for cardenolides-containing plants, such as plants belonging to the genera of *Asclepias*, *Pergularia*, *Gomphocarpus* and *Calotropis*, which usually develop secretory tissues (laticifers) that produce white corrosive latex [4], which has been used in the treatment of skin infections, such as that has been used in the treatment of skin infections, such as *Tinea capitis* [5].

Pergularia genus is one of the most important genera of Asclepiadaceae family; this genus consists of two species: *Pergularia daemia* and *Pergularia tomentosa*. According to Quezel P. and Santa S., only *P. tomentosa* species is present in Algeria [2]. It is distributed in the Northern and Central Sahara of Algeria [1]. *Pergularia* genus is known for its richness in secondary metabolites especially cardenolides, cardenolide glycosides and triterpenoides which have biological interest.

The species studied in our work is named *Pergularia tomentosa*, it is known for its toxicity; it cannot be consumed in the green state. This plant is rich in cardenolides and cardenolide glycosides; which are used, in low concentrations, to increase the contractile

force of the heart and decrease its rate of contraction by inhibiting the cellular Na⁺/K⁺-ATPase, as well as, they possess antitumour activities against different cancer types [6]. The aim of our work is the isolation and the identification of bioactive compounds from *P. tomentosa* in particular alkaloids, which are minor compounds in this plant (according to the literatures). We noted that the isolation and identification of alkaloids from this plant are done for the first time.

This work was carried out in laboratory of Valorization and Promotion of Saharan Resources (VPRS), Kasdi Merbah University Ouargla, as well as, the Research and Development Center (CRD) of SIDAL group, Baraki Algeria. The NMR analyses (NMR 600 MHz and NMR 400 MHz) of the isolated compounds in this study, were carried out in Scientific and Technical Research Center of Physico-Chemical Analysis (Bou Ismail and Ouargla centers). This study is part of the search for new natural substances of therapeutic interest.

This doctoral thesis started with an abstract followed by a general introduction, and it is subdivided into three main parts; a theoretical part, an experimental part and results and discussion part, where each part contains distinct chapters. It ends with a bibliography.

- ❖ The first part is the theoretical part; it consists of three chapters: the botanical presentation and previous studies, some secondary metabolites and biological activities:
 - The first chapter is devoted to the botanical description of Asclepiadaceae family, *Pergularia* genus, and *Pergularia tomentosa* species, as well as the chemical studies carried out on *Pergularia* genus (*Pergularia tomentosa* and *Pergularia daemia*).
 - The second chapter includes the study of secondary metabolites; we distinguish in particular alkaloid and cardenolide compounds, on the side of chemical structure, biosynthesis, distribution, classification and biological properties.
 - The third chapter based on general information of the different biological activities performed in our study (antioxidant, anti-diabetic, toxicity, anti-inflammatory and sedative activities).
- ❖ The second part is the experimental part; it is devoted to the presentation of materials and methods used in our personal work, comprising two chapters:

- The first chapter describes the qualitative and biological studies carried out on the different extracts of *Pergularia tomentosa*. It consists of:
 - ✓ Evaluation of phytochemical screening and dosage of total phenols, flavonoids and tannins.
 - ✓ Evaluation of biological activities *in vitro*: antioxidant activities by the methods of DPPH[•] radical scavenging and reducing power of molybdenum Mo (VI) activities, as well as anti-diabetic activity using inhibition of activity of α -amylase enzyme method.
 - ✓ Evaluation of biological activities *in vivo*: the acute toxicity of the extracts as well as their anti-inflammatory and sedative activities.
- The second chapter presents all the experimental procedures of maceration, extraction, fractionation, isolation and purification, which lead to obtain thirty-four pure compounds, which are twenty-six alkaloids, five cardenolide glycosides, two flavonoids and one phenolic compound.
- ❖ The third part is the results and discussion part; it includes two chapters:
 - The first chapter includes the results obtained as well as the discussion related to the qualitative and biological studies of the different extracts.
 - The second chapter includes the results obtained and the discussion related to the structural determination of eleven isolated secondary metabolites, based on various nuclear magnetic resonance experiments (¹H, ¹³C, HSQC, TOCSY-HSQC, HMBC and COSY).

PART I: THEORETICAL PART

Chapter A: botanical presentation

I-A-1-Asclepiadaceae family

Asclepiadaceae family is a subfamily in the Apocynaceae family. It was separated from Apocynaceae family by BROWN in 1810 due to the difference in pollination, in which Asclepiadaceae was defined by having pollen coalescing into masses that are fixed or applied to the stigma [style-head], in a determinate manner. In the other hand, Asclepiadaceae and Apocynaceae have the same chemotaxonomy [7].

Asclepiadaceae family contains 250 genera and 2000 species [8], majority of them are poisonous as well as revealing medicinal properties [9]. It is subdivided into three subfamilies which are: Periplocoideae, Secamonoideae and Asclepiadoideae. It has wide distribution in the world especially subtropics and tropics [10].

The plants belonging to Asclepiadaceae family are perennial herbs, vines, or shrubs, mostly with milky sap (that is why it is called milkweed family) [8]. Many members plants of this family have xerophytic stems, which are cylindrical photosynthetic stems with long internodes [11]. They have opposite leaves, simple, entire and the fruits are many-seeded, ovoid to lanceolate follicle [8]. The seeds in Asclepiadaceae plants are flattened ovate structures, closely imbricated within the fruits [11].

Plants belonging to the milkweed family are rich in steroidal glycosides [12], cardenolides and cardiac glycosides [13]. Cardenolides and cardiac glycosides are abundant especially in the genera of *Asclepias*, *Pergularia*, *Gomphocarpus* and *Calotropis* [3]. These compounds are characterized by their activity against a large range of cancer cell types [12] as well as the wide use in cardiology [13]. This family is also a source of alkaloid compounds especially phenanthroindolizidine alkaloids, their presence has been established in several species of five genera, *Tylophora*, *Cynanchum*, *Vincetoxicum*, and *Antitoxicum* [14]. In this family, little work has been recorded on the flavonoid glycosides [15].

I-A-2-Pergularia genus

The genus of *Pergularia* is one of the most important genera of Asclepiadaceae family, it is established by Linnaeus [16]. In this genus two species are recognised: *Pergularia daemia* and *Pergularia tomentosa* [17]. *Pergularia tomentosa* is widely distributed in the Sahara Desert and the Horn of Africa to Sinai, Jordan, Arabia, the deserts of southern and

eastern Iran, Afghanistan and Pakistan, it is replacing *Pergularia daemia* in the northern deserts. While *Pergularia daemia* widespread in driest tropical or subtropical regions of sub-Saharan Africa, Arabian Peninsula and Indian subcontinent [17].

Genus of *Pergularia* is characterized by possessing a pairwise fruits that are almost always covered with soft spines [18] and the heart-shaped leaves[17].

This genus was transferred from the subtribe Cynanchinae to the subtribe Asclepiadinae because it contains of 7 β ,8 β -Epoxyecdysteroid glycoside with 4,6-dideoxyhexosulose as sugar component which are found only in *Asclepias*, *Calotropis*, *Gomphocarpus* and *Pergularia* [18].

I-A-3-Description of *Pergularia tomentosa* species

Pergularia tomentosa L. is herbaceous or semi-woody plant, its flowers are white, purple and fragrant. Its twigs are containing a latex [19]. The leaves of this plant are opposite, oval or rounded, heart-shaped at the base and its color is almond green. *Tomentosa* means as hairy, because the plant covered by a lot of small hairs which causes a greenish color [20]. Its fruits are composed of two follicle which bear small spicks. Its stems are covered with short greenish hairs. The bushy appearance of this plant is due to the warp of young twigs frequently around the old ones [21].

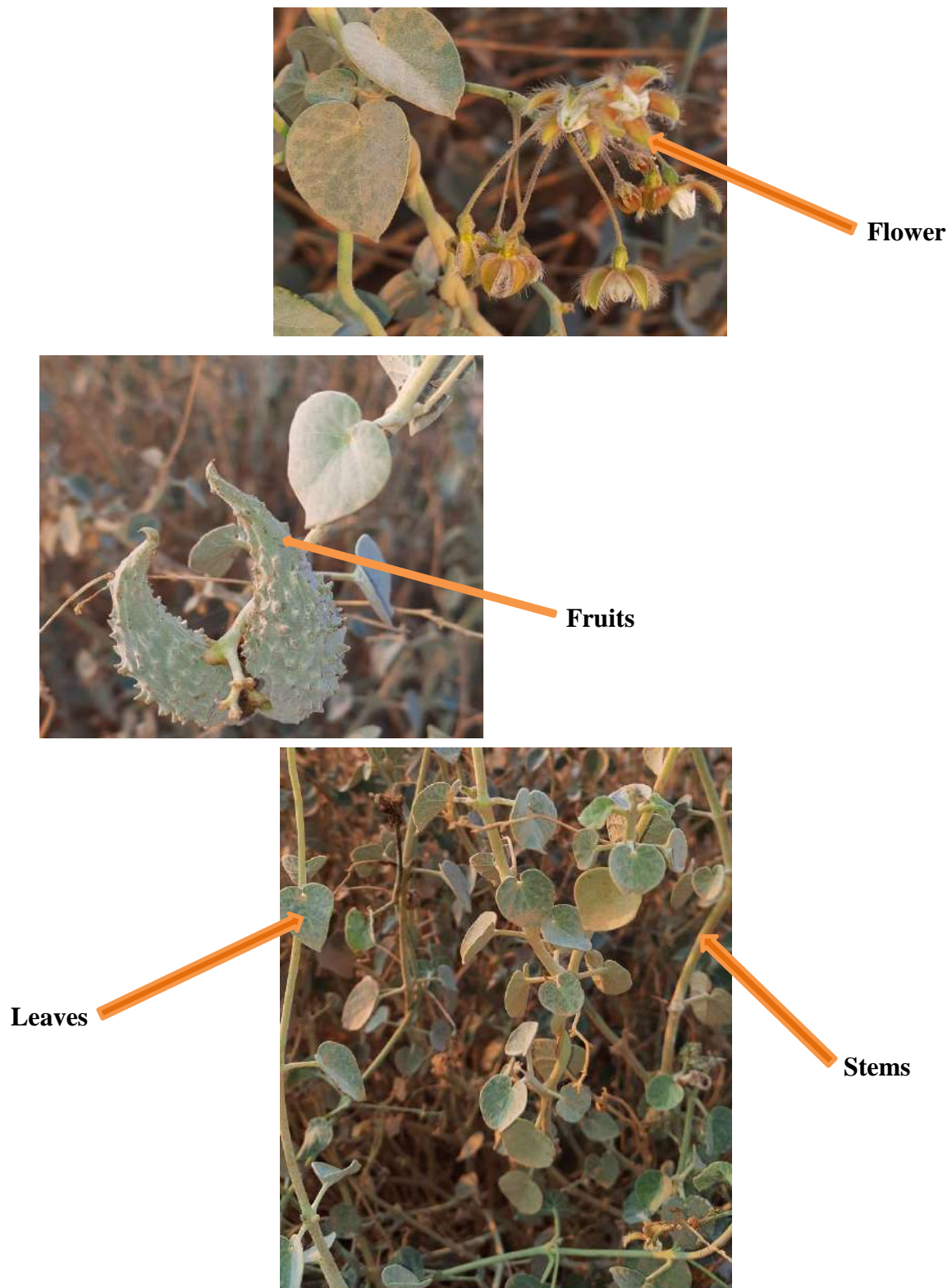


Figure I-A-01: Photo of different parts of *Pergularia tomentosa* (Photo taken on 28/10/2021)

I-A-4-Description of the harvest area

Pergularia tomentosa was harvested from M'Zab Valley which is located in the wilaya of Ghardaïa, about 600 km south of the capital Algiers, and is part of the northern part of the Saharan platform at 32° 30' north latitude and 3° 45' longitude [22]. The climate of this valley is Saharan climate, characterized by hot summers and mild winters. The temperature is marked by large amplitude between day and night, summer and winter temperatures. The hot period starts in May and lasts until the month of September. The lowest average temperatures are recorded in January, 12°C and the highest in July, 40°C [23].

I-A-5-Classification of *Pergularia tomentosa*

The systematic classification of this plant is presented below [24]:

Kingdom: plantae

Subkingdom: Tracheobionta

Super division: Spermatophyta

Division: Magnoliophyta

Class: Magnoliopsida

Subclass: Asteridae

Order: Gentianales

Family: Asclepiadaceae

Genus: *Pergularia*

Species: *Pergularia tomentosa* L.

I-A-6-Synonyms and traditional names of *P. tomentosa*

P. tomentosa is known also by this synonyms: *Daemia tomentosa*, *Telosma tomentosa* and *Daemia cordata* [24].

This plant has several vernacular names that differ from the region to another, in **Algeria** it is called Ghoulga, tellakh, sellaha, tashkat, dellakal; in **Nigeria** : fatakko,

malaiduwa, bakambi, damargu rafi, sellenke; in **Mauritanie**: umu éjlud [24], in **Tunisia**: Bou Hliba [25].

I-A-7-Geographical distribution of *P.tomentosa*

In horn of Africa, this plant is widely distributed, it is found in: north Sudan, Egypt, Ethiopia, Algeria, Jordan, Niger, Kenya [20] and Tunisia (south Sfax) [25], it is found also in Middle East (Iran, Oman, Pakistan, Afghanistan, Saudi Arabia) [20]. Figure I-A-02 illustrates geographical distribution of *P. tomentosa* in the world.

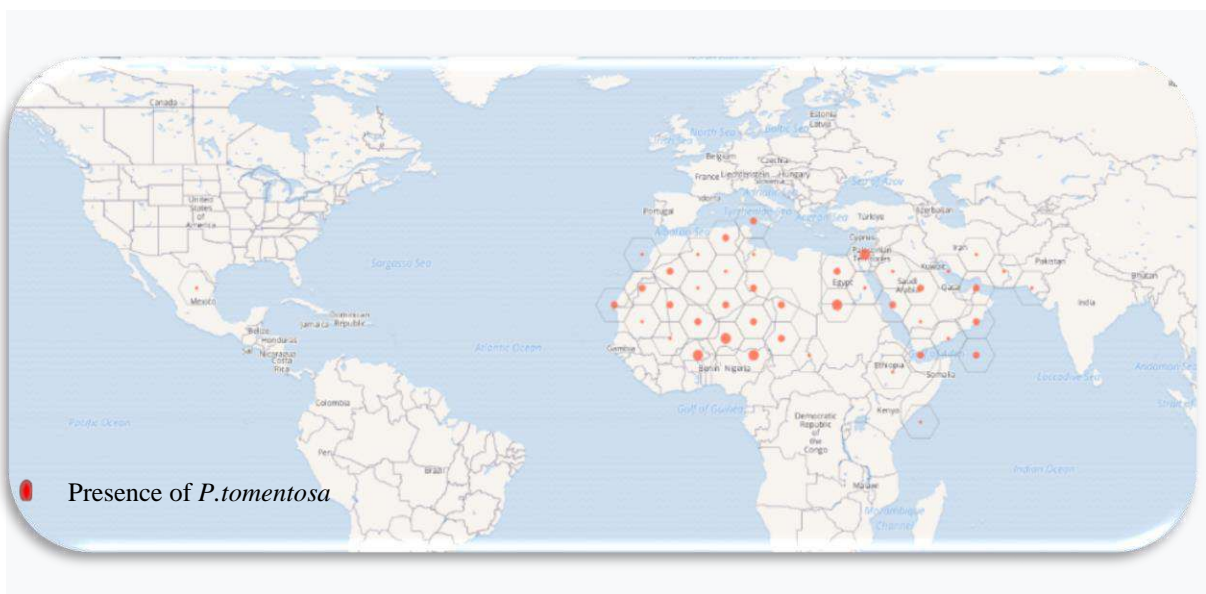


Figure I-A-02: Geographical distribution of *P. tomentosa* in the world [26]

I-A-8-Traditional uses of *P. tomentosa*

In folk medicine, this plant is widely used as an antirheumatic, laxative, abortive, asthma, bronchitis, treatment of some skin diseases, helminthiases, allergies and constipation [20]. It is used also for treatment of tonsillitis, ringworm and hypoglycemic [22, 23].

In addition, the leaves of this plant are applied to snake and scorpion bites, are used also as treatment of tumors and warts [24]. In cosmetic, it is used as depilatory [25].

I-A-9-Biological activities of *P. tomentosa*

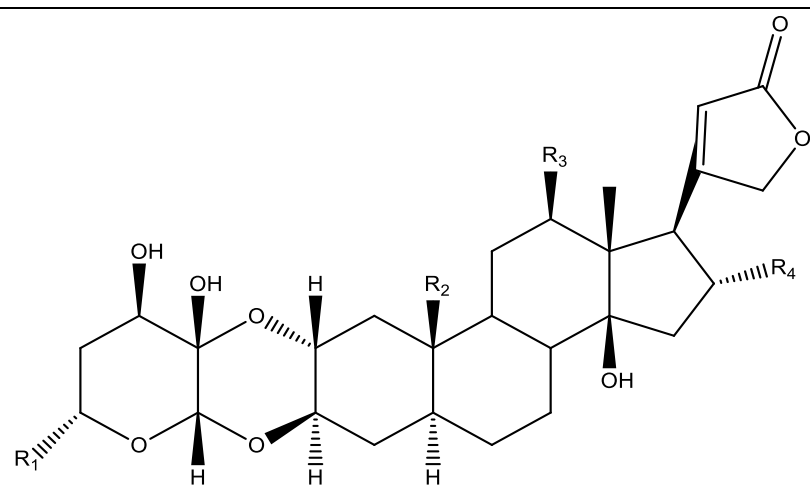
P.tomentosa is the source of secondary metabolites which have therapeutic properties, this made researches study the biological activity of this plant. There are several studies reported the biological activities of different parts of *P.tomentosa*:

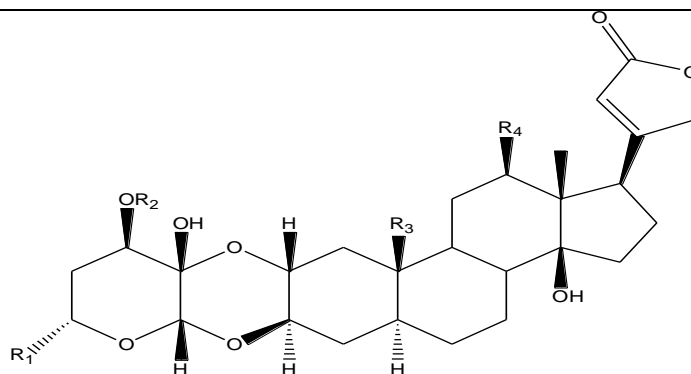
- I. Lahmar *et al.* reported that stems and fruits extracts of *P.tomentosa* exhibit an antifungal activity against *Fusarium Oxysporum f.sp. lycopersici* [25].
- M.S., Hifnawy *et al.* study the cardiotoxic activity of different aqueous extracts (root, aerial parts and leaves extracts) and isolated compounds. The results of this study demonstrated that the highest cardiotoxic activity was produced from the ghalakinoside followed by calactin and the most cardioactive extract was that of the roots, followed by the aerial parts and leaves respectively [27].
- M. Hosseini *et al.* reported that the root extract of *P.tomentosa* showed strong antiangiogenic effect with minimal adverse viability impacts [28].
- W. Abu Rayyan *et al.* reported that ethanol extract showed a broad inhibition activity against the five strains (*S. aureus*, *S. epidermidis*, *E. coli*, *S. typhi* and *C. albicans*) whereas ethyl acetate fraction had the most effective MIC values against only three strains (*S. epidermidis*, *S. typhi*, and *C. albicans*) [29].
- F. Acheuk *et al.* reported that *P. tomentosa* may be a promising naturally occurring agent for locust larval control [30].
- E. Nabih Ads *et al.* study the cytotoxic effects of methanolic and latex extract of *P. tomentosa*, the results of their study showed that the methanol extract of *P. tomentosa* has higher cytotoxic effect as compared to the latex extract, this enables the methanolic extract to be used as an antitumor [5].
- SH. Hosseini *et al.* reported that *P. tomentosa* showed a reasonable reduction in blood glucose level and induced beneficial effect on lipid profile [31].
- Antioxidant activity of *P.tomentosa* was studied. R. Yakubu *et al.* had used DPPH test in order to evaluate antioxidant activity of this plant. They reported that crude extract have highest antioxidant activity, followed by the basic fraction (alkaloid) respectively compared to acidic and methanolic fraction, whereas Hexane has the lowest activity [32].

I-A-10-Major secondary metabolites previously isolated from *Pergularia* genus

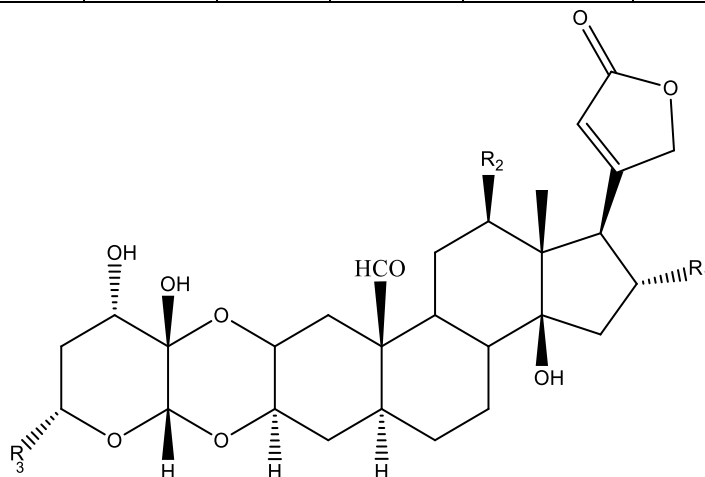
Previous studies reported that *Pergularia* genus is rich in cardenolides and cardenolide glycosides which have been isolated from two species *P. tomentosa* and *P. daemia*. Thirty-one compounds and seventeen compounds have been isolated and identified from various parts of *P. tomentosa* and *P. Daemia*, respectively. Cardenolides, cardenolide glycosides and taraxasterol-type triterpenes are the main class of secondary metabolites which have been found in these species. The identified structures are summarized in Table I-A-01, I-A-02, I-A-03 and I-A-04.

Table I-A-01: Structures of cardenolide glycosides isolated from genus *Pergularia*

						
Compound	R ₁	R ₂	R ₃	R ₄	Species	Reference
6'-hydroxycalactin	CH ₂ OH	CHO	H	H	<i>P. tomentosa</i>	[13]
6'-hydroxy-16 α -acetoxycalactin	CH ₂ OH	CHO	H	OCOCH ₃	<i>P. tomentosa</i>	
16 α -hydroxycalactin	CH ₃	CHO	H	OH	<i>P. tomentosa</i>	
ghalakinoside	CH ₂ OH	CH ₂ OH	OH	H	<i>P. tomentosa</i>	[12, 13]
calactin	CH ₃	CHO	H	H	<i>P. tomentosa</i> <i>P. daemia</i>	[12, 13, 33]

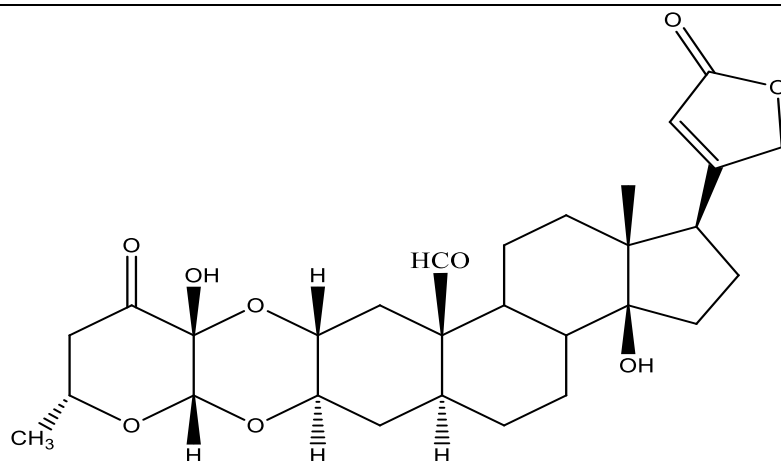


Compound	R ₁	R ₂	R ₃	R ₄	Species	Reference
3'-O-β-D-glucopyranosylcalactin	CH ₃	β-D-Glc	CHO	H	<i>P. tomentosa</i>	[12, 13, 34]
12 β-hydroxycalactin	CH ₃	H	CHO	OH	<i>P. tomentosa</i>	
12-dehydroxyghalaktinoside	CH ₂ OH	H	CH ₂ OH	H	<i>P. tomentosa</i>	
6'-dehydroxyghalaktinoside	CH ₃	H	CH ₂ OH	OH	<i>P. tomentosa</i>	

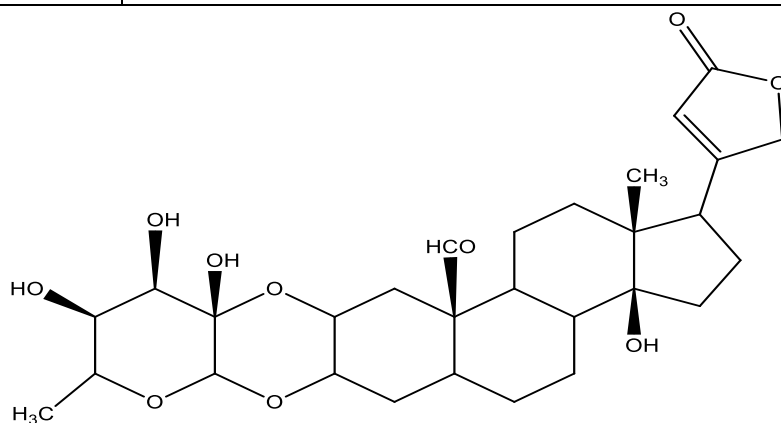


Compound	R ₁	R ₂	R ₃	Species	Reference
Pergularotoside	H	OH	CH ₂ OH	<i>P. tomentosa</i>	[27]
16α-Acetycalotropin	OAc	H	CH ₃	<i>P. tomentosa</i>	[35]
12β-hydroxycalotropin	H	OH	CH ₃	<i>P. tomentosa</i>	[36]
calotrooin	H	H	CH ₃	<i>P. daemia</i>	[33]
16α-hydroxycalotropin	OH	H	CH ₃	<i>P. tomentosa</i>	[34]
6'-hydroxycalotropin	H	H	CH ₂ OH	<i>P. tomentosa</i>	[34]

Theoretical Part : Botanical Presentation

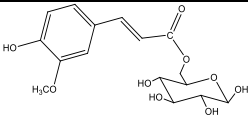


Compound	Species	Reference
Uscharidin	<i>P. tomentosa</i> , <i>P. daemia</i>	[36, 37]



Compound	Species	Reference
Calotoxin	<i>P. daemia</i>	[33]

Table I-A-02: Structures of cardenolides isolated from genus *Pergularia*

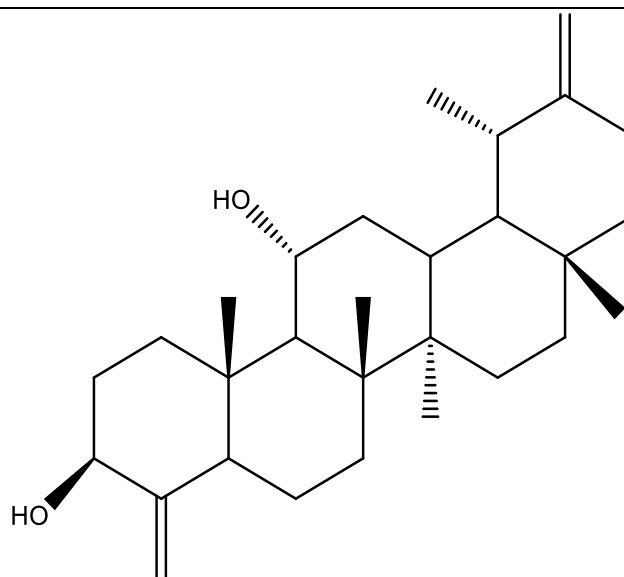
Compound	R ₁	R ₂	R ₃	Species	Reference
Desglucouzarin	Glu	CH ₃	H	<i>P. tomentosa</i>	[3]
Coroglaucigenin	H	CH ₂ OH	H	<i>P. tomentosa</i> <i>P. daemia</i>	[3, 33]
Glucocoroglaucigenin	Glu	CH ₂ OH	H	<i>P. tomentosa</i>	[34]
Uzarigenin	H	CH ₃	H	<i>P. tomentosa</i> , <i>P. daemia</i>	[3, 37]
Uzarigenin-3-O-glucopyranoside	Glu	CH ₃	H	<i>P. tomentosa</i>	[27]
6'-O-feruloyl-desglucouzarin		CH ₃	H	<i>P. tomentosa</i>	[34]
12β-hydroxycoroglaucigenin	H	CH ₂ OH	OH	<i>P. tomentosa</i>	[34]

Compound	R	Species	Reference
Corotoxigenin	H	<i>P. daemia</i>	[33]
Calotropagenin	OH	<i>P. daemia</i>	

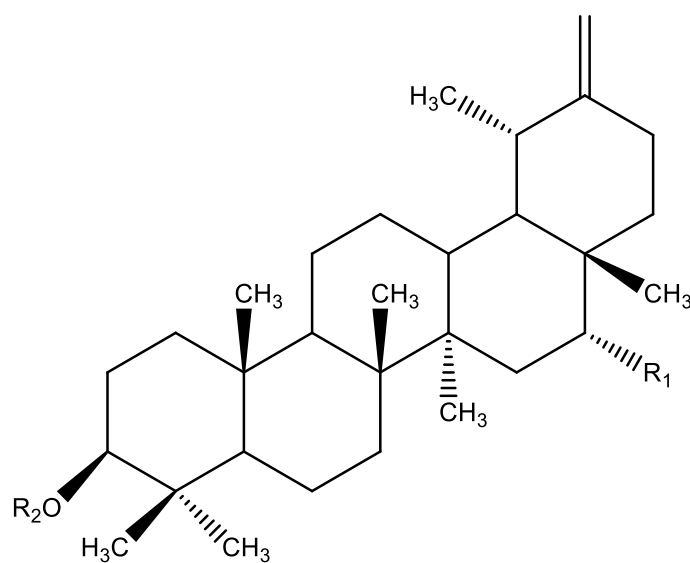
Table I-A-03: Structures of triterpenes isolated from genus *Pergularia*

Compound	Species	Reference
Pergularine A	<i>P. tomentosa</i>	[38]

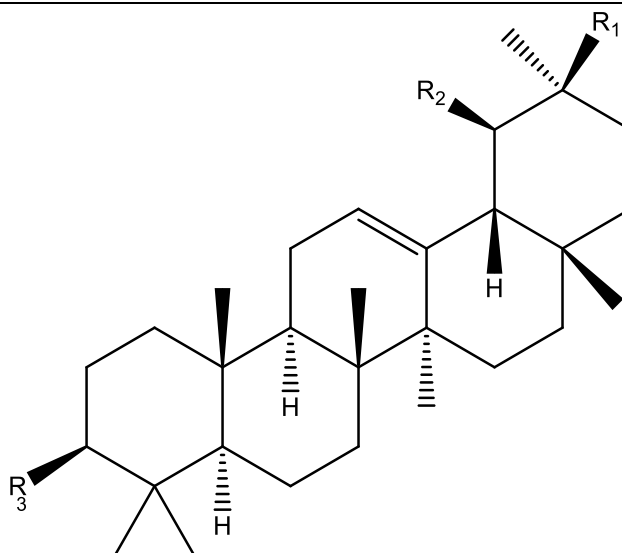
Theoretical Part : Botanical Presentation



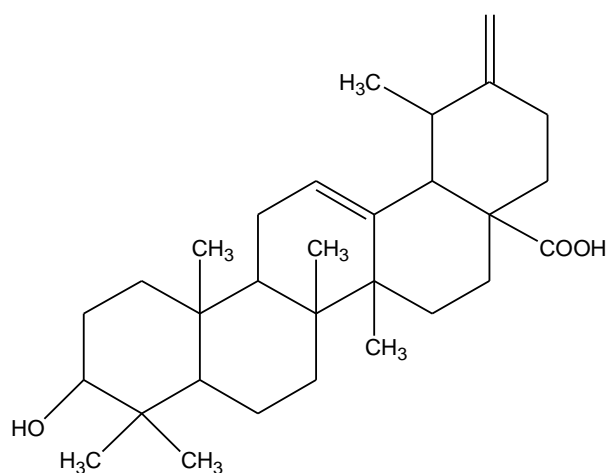
Compound	Species	Reference
Pergularine B	<i>P.tomentosa</i>	[38]



Compound	R ₁	R ₂		Species	Reference
16- α -hydroxytaraxasterol-3-acetate	OH	COCH ₃		<i>P. tomentosa</i>	[36]
Taraxasterol	H	H		<i>P. tomentosa</i>	

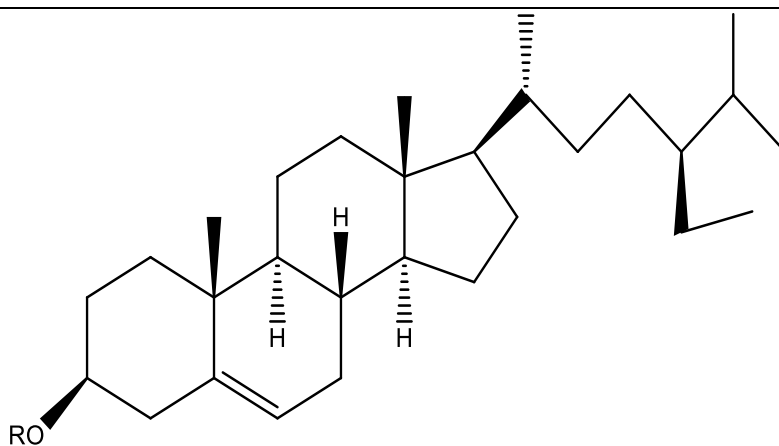


Compound	R ₁	R ₂	R ₃	Species	Reference
α-amyrine	H	CH ₃	OH	<i>P. tomentosa</i> <i>P. daemia</i>	[36, 37]
3 β -O-acetyl-α-amyrine	H	CH ₃	OAc	<i>P. tomentosa</i>	[39]
β-amyrine	CH ₃	H	OH	<i>P. daemia</i>	[37]

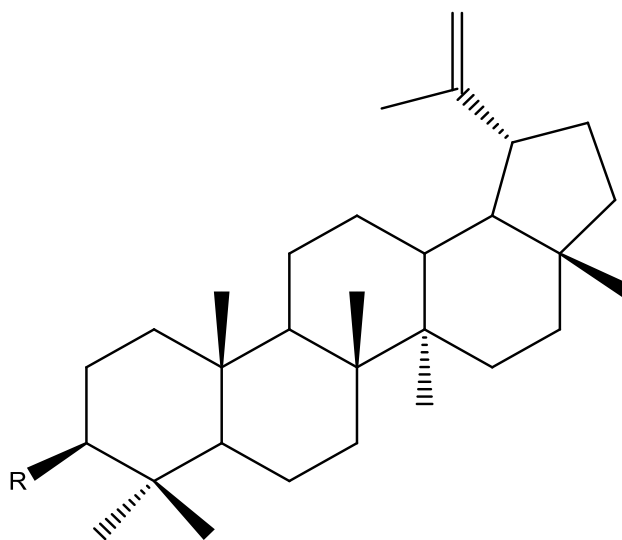


Compound	Species	Reference
Epi-micromeric acid	<i>P. tomentosa</i>	[36]

Theoretical Part : Botanical Presentation



Compound	R	Species	Reference
β -Sitosterol	H	<i>P. daemia</i>	[33]
β -Sitosterol glucoside	Glu	<i>P. tomentosa</i>	[3]
		<i>P. daemia</i>	[33]



Compound	R	Species	Reference
Lupeol	OH	<i>P. daemia</i>	[33]
3-O-acetyl lupeol	OAc	<i>P. tomentosa</i>	[39]

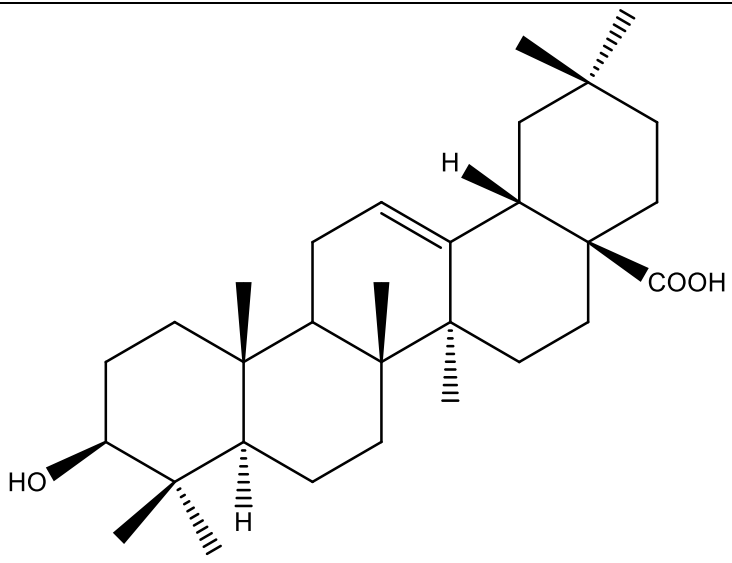
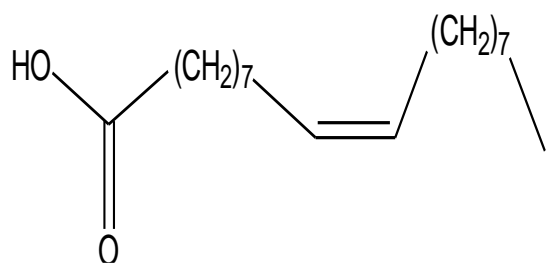
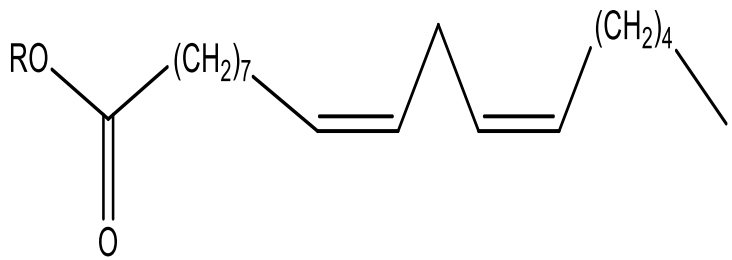
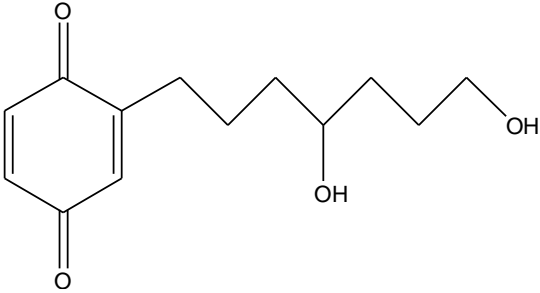
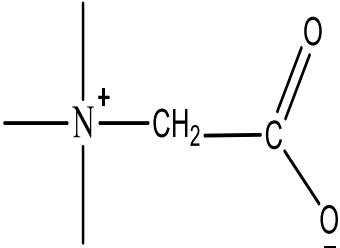
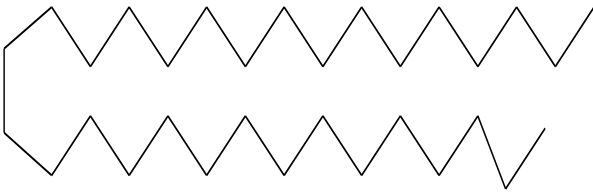
		
Compound	Species	Reference
Oleanolic acid	<i>P. daemia</i>	[37]

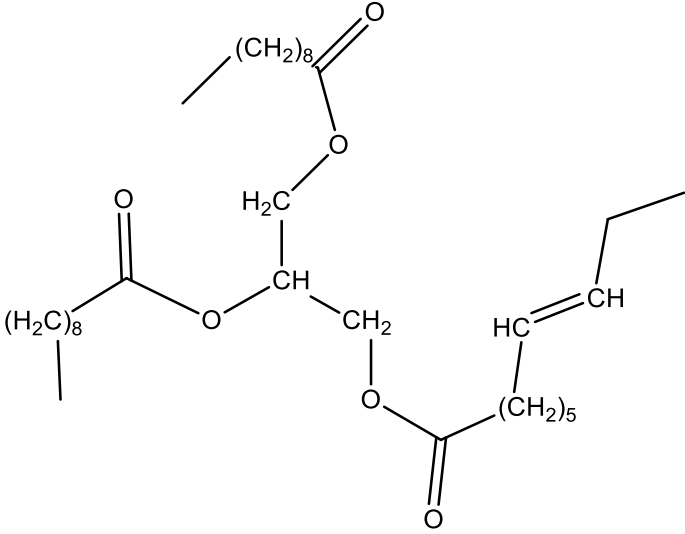
Table I-A-04: Structures of other compounds isolated from genus of *Pergularia*

			
Compound	Species		Reference
Oleic acid	<i>P. tomentosa</i>		[38]
			
Compound	R	Species	Reference

Theoretical Part : Botanical Presentation

(9Z; 12Z)-octadecadienoic acid	H	<i>P. tomentosa</i>	[38]
(9Z; 12Z)-octadecadienoic acid glucosid	Glu	<i>P. tomentosa</i>	
			
Compound	Species		Reference
6-(4,7-dihydroxyheptyl) cyclohex-2,5-diene-1,4-dione	<i>P. daemia</i>		[40]
			
Compound	Species		Reference
Betaine	<i>P. daemia</i>		[37]
			
Compound	Species		Reference
Hentriacontane	<i>P. daemia</i>		[37]

Theoretical Part : Botanical Presentation

		
Compound	Species	Reference
Triacylglycerol	<i>P. tomentosa</i>	[39]

Chapter B: Alkaloids and cardenolides

I-B-1-Alkaloids

I-B-1-1-Definition of alkaloids

The term of alkaloid was introduced by W.Meissner at the beginning of XIXe century, to indicate natural substances reacting as bases or alkalis. There are no simple and precise definition of alkaloids and it is sometimes difficult to separate alkaloids from the other natural nitrogenous metabolites [41].

It should be noted that it is difficult to give a good definition of alkaloids, due to the many particular cases. They are defined as nitrogenous, basic, substances of natural origin, having strong biological activities and most of them are toxic [42], their atom of nitrogen is in a heterocyclic system. [41].

Alkaloids are rarely free compounds in the plant, but are in the form of glycosides or salts of malic, tartaric or citric acids [42]. Biosynthetically, alkaloids are formed by starting with an amino acid [41].

I-B-1-2-History of alkaloids

Before the discovery of alkaloids as chemical molecules, the mankind has used them in the scope of medicinal and pharmaceutical importance. *Myrrh, Opium, Cannabis, Aloes, Cassia, and Hemlock* are the most prominent examples of medicinal plants which used from peoples based on the earlier beliefs and knowledge. For example, native people of America and tribes in the Amazon used the alkaloid quinine in herbal before its official use in the cure of uncomplicated malaria in 1638.

In the late 1700s, chemists tried to isolate the active ingredients in plants due to the new developments of Lavoisier and others in chemistry. Actual studies on isolation of alkaloids as pure compounds from plants are occurred only in the beginning of the 1800, despite the fact that they have been in use for ages [43].

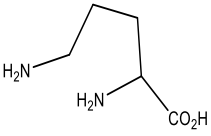
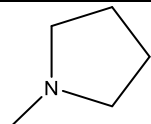
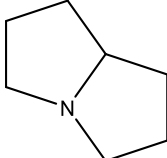
In 1803, DEROSENE was extracting a mixture of narcotic and morphine from opium, thus, he was the first one who isolated a vegetable alkali. In 1806, SERTURNER realized the alkalizing nature of the anesthetic principle of opium, a principle that would be called morphine a decade later and which MERCK would market shortly thereafter [41].

I-B-1-3-Classification of alkaloids

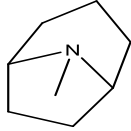
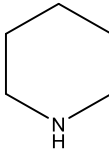
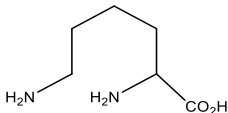
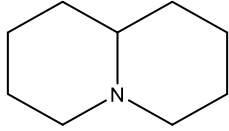
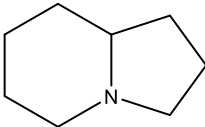
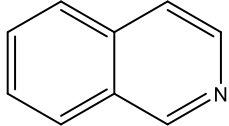
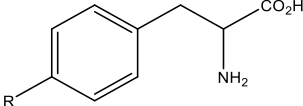
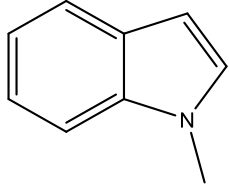
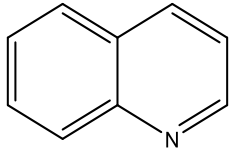
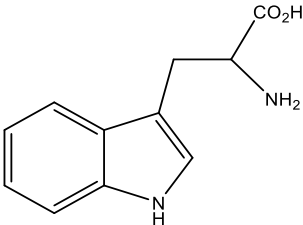
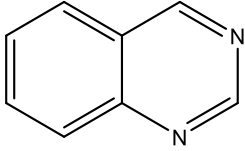
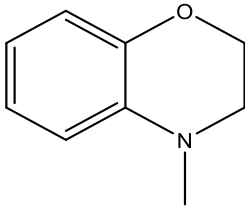
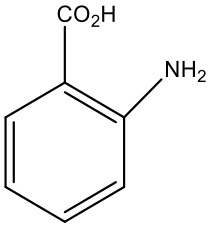
Many methods have been proposed for the classification of alkaloids such as pharmacological, taxonomical, chemical, and biosynthetic classification [43], the biosynthetic classification is generally the accepted one. They are generally classified by their common molecular precursors, based on the biological pathway employed to build the molecule. According to this classification, there are three principal types of alkaloids: true alkaloids, protoalkaloids and pseudoalkaloids [44]:

- **True alkaloids:** which represent the largest number, are biosynthesised from amino acids. These alkaloids are highly reactive substances. They are all basic and their alkalinity is due to an atom of nitrogen present in the heterocycle (except for colchicine) [42].
- **Proto-alkaloids:** They are simple amines, in which the nitrogen atom is not present in the heterocyclic system [44], and are often called "biological amines", they are soluble in water [42].
- **Pseudo-alkaloids:** generally, all the characteristics of true alkaloids present in this type of alkaloids, but are not derivatives from amino acids. The majority of this type is terpene alkaloids: monoterpene, sesquiterpenes and diterpenes alkaloids, as well as heterocyclic nitrogenous substances from the metabolism of acetate [41].

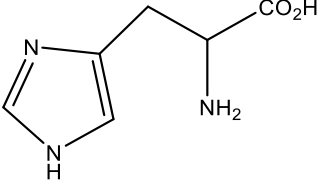
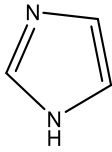
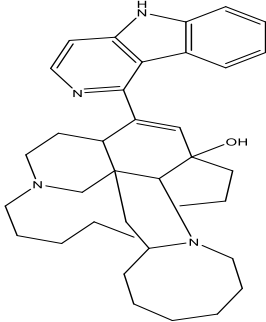
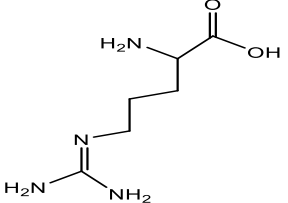
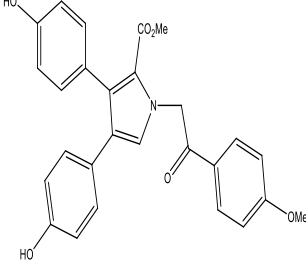
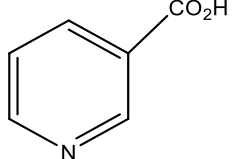
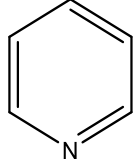
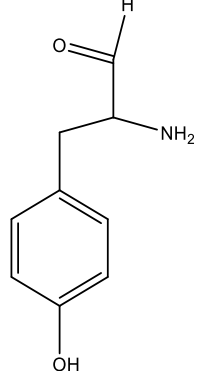
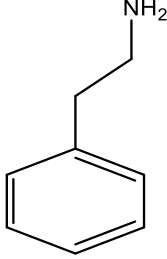
Table I-B- 01: Main types of alkaloids and their chemical groups [41, 44-46].

Alkaloid type	Precursor compound	Chemical group of alkaloids	
		Name	Basic structure
	<p>L-ornithine</p> 	Pyrrolidine alkaloid	
		Pyrrolizidine alkaloid	

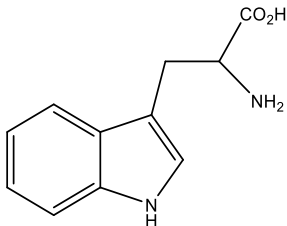
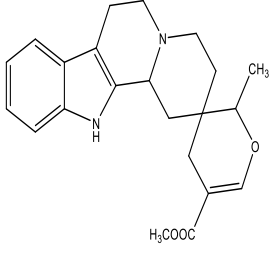
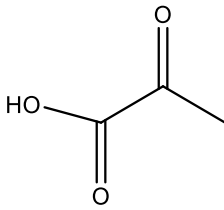
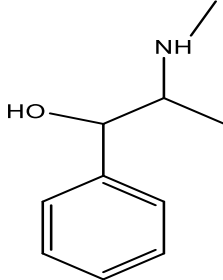
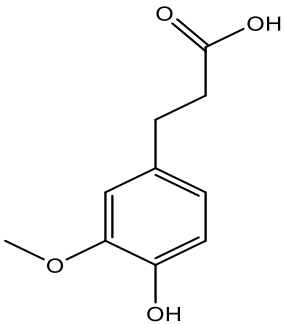
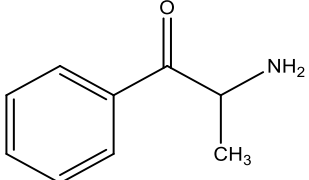
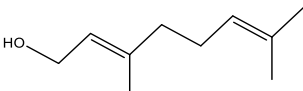
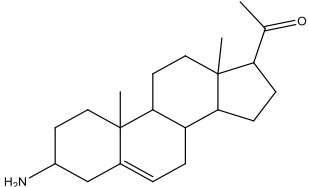
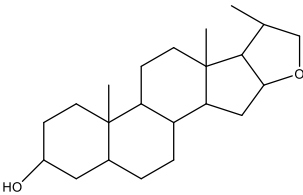
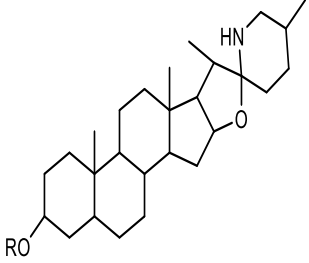
Theoretical Part: Alkaloids and Cardenolides

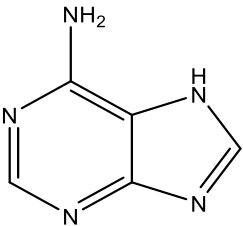
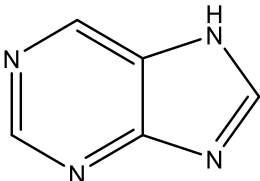
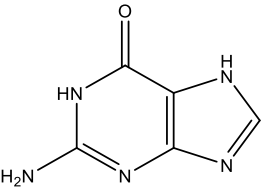
True alkaloid		Tropane alkaloid	
	L-lysine	Piperidine alkaloid	
		Quinolizidine alkaloid	
		Indolizine alkaloid	
	L-tyrosine or L-phenylalanine	Isoquinoline alkaloid	
		Indole alkaloid	
	L-tryptophan	Quinoline alkaloid	
		Quinazoline alkaloid	
	Anthranilic acid	Benzoxazine alkaloid	
			

Theoretical Part: Alkaloids and Cardenolides

	<p>L-histidine</p> 	<p>Imidazole alkaloids</p>	
		<p>Manzamine alkaloid</p>	
	<p>L-arginine</p> 	<p>Marine alkaloid</p>	<p>kind of alkaloid that can be separated from marine organisms</p> 
	<p>Nicotinic acid</p> 	<p>Pyridine alkaloid</p>	
<p>Protoalkaloids</p>	<p>L-tyrosine</p> 	<p>Phenylethylamino alkaloid</p>	

Theoretical Part: Alkaloids and Cardenolides

	<p>L-tryptophan</p> 	<p>Terpenoid indole alkaloid (ajmalicine)</p> 
Pseudoalkaloids	<p>Pyruvic acid</p> 	<p>Ephedra alkaloid</p> 
	<p>Ferulic acid</p> 	<p>Aromatic alkaloid</p> 
	<p>Geraniol</p> 	<p>Terpenoid alkaloid</p> 
	<p>Saponin</p> 	<p>Steroid alkaloid</p> 

	<p>Adenine</p> 	Purine alkaloid	
	<p>Guanine</p> 		

I-B-1-4-Distribution of alkaloids

In the plants, certain families have a marked tendency to produce alkaloids, we mention some of them: liliopsida (Amaryllidaceae, Colchiaceae) and in the Eudicotyledons or the Magnoliidae (Annonaceae, Apocynaceae, Lauraceae, Loganiaceae, Magnoliaceae, Menispermaceae, Papaveraceae, Ranunculaceae, Rubiaceae, Rutaceae, Solanaceae). In bacteria and fungi alkaloids are found rarely [41].

I-B-1-5-Physicochemical properties of alkaloids

Alkaloids have many physicochemical properties, some of them are used in the selective isolation of alkaloids, for example we mention:

- Alkaloids have molecular masses ranging from 100 to 900.
- Deoxygenated alkaloids are liquid at normal temperature, while those that contain oxygen in their formula are usually crystallizable solids.
- Alkaloids deviate the polarized light.
- Crystallized alkaloids give sharp melting points without degradation under of 200°C [41].
- Most of alkaloids are colorless compounds, only some strongly conjugated compounds are coloured or show strong fluorescence.
- Many alkaloids crystallize as a salt because it is difficult to crystallize as free bases.

- Free bases alkaloids are soluble in organic solvents but salts alkaloids are soluble in water.
- The pKa values of alkaloids vary from about 6-12, that makes them basic compounds [47].

I-B-1-6-Extraction of alkaloids

Extraction of alkaloids is based generally on the differential solubility of bases and salts alkaloids in water and in organic solvents [41]. In general, the free base alkaloids are soluble in organic solvents. In the other hand, protonation of the tertiary nitrogen in the free base alkaloids usually results in a water-soluble compound. This characteristic is used in the selective extraction of alkaloids [47]. Two different extraction methods are possible to apply extraction in an alkaline medium and extraction in an acid medium. In some cases, this general rule does not apply (ex: in the case of extraction of caffeine) [41]. The steps of protocol of each extraction method are summarized in Figure I-B-01 and Figure I-B-02.

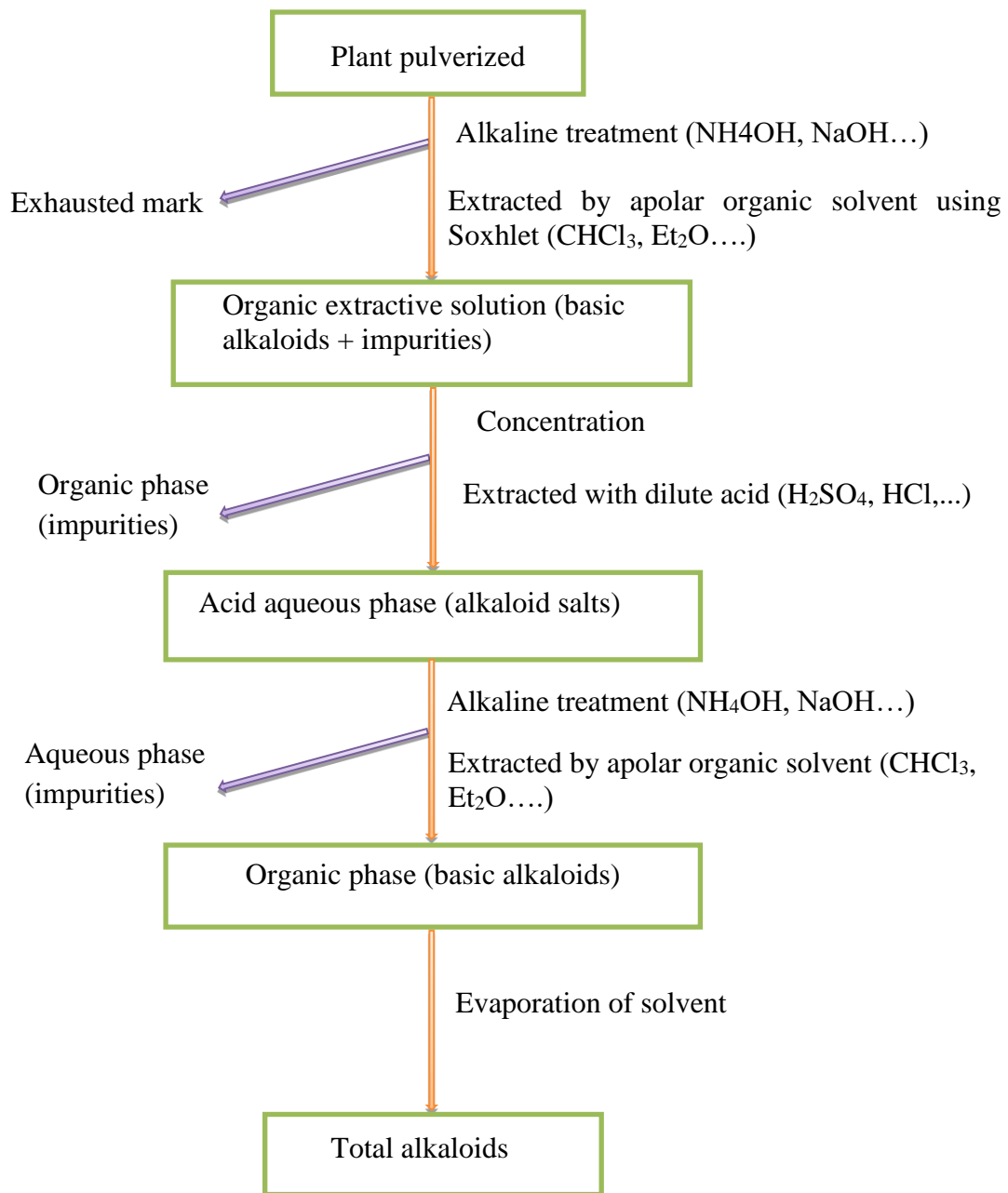


Figure I-B-01: Protocol of alkaloids extraction by apolar organic solvents in an alkaline medium [41]

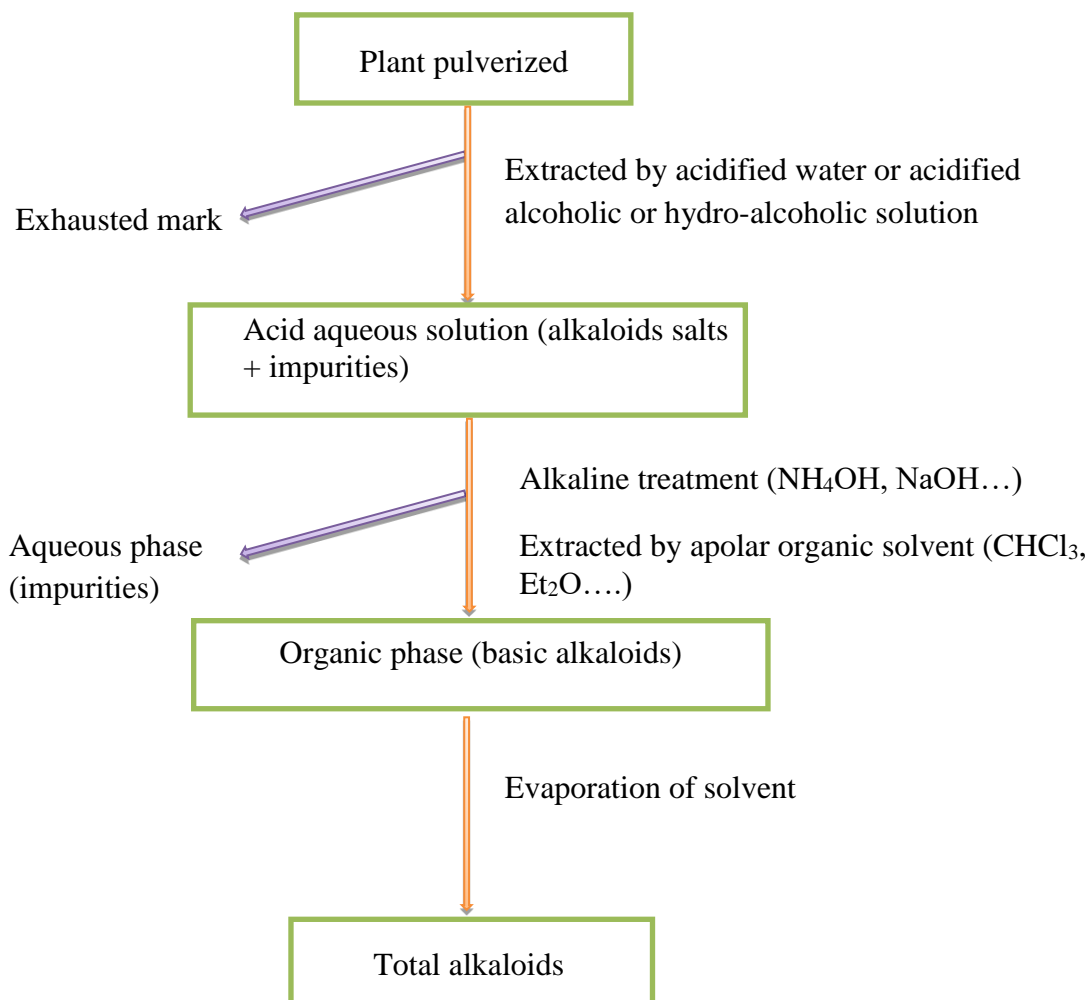


Figure I-B-02: Protocol of alkaloids extraction in an acid medium [41]

I-B-1-7-Role pharmacology of alkaloids

Most of alkaloids have an important pharmacological bioactivity in human bodies, this is why they are used as drugs. In medicine, alkaloids mainly exhibit marked pharmacological activity in some serious disorders like cardiovascular and metabolic disorders, cancer, blood pressure, inflammation, infectious diseases, neurodegenerative diseases, and miscellaneous problems [43] for examples:

- Cocaine is used in local anesthesia.
- Vinblastine, vincristine and camptothecine are used as antitumor agents [41].

- Quinidine is used as a cardiac stimulant [43] and anti fibrillants, while quinine is used as antimalarial
- Morphine and its salts are classified as narcotic analgesics [42].
- Berberine is used as an anticancer [43].

I-B-2-Cardenolides

I-B-2-1-Definition of cardenolides

Cardenolides are steroid compounds that occur naturally in plants as an ether glycosides or as an aglycon [48]. These structures comprise a steroidal part of the cardenolide (C23) or bufadienolde (C24) type, and an osidic part that most often is oligosidic [41]. The aglycon portion has a steroidal skeleton, namely: a cyclopentanoperhydrophenanthrene ring, that has a unique and structurally distinct used ring system [6]. The sequence of the four cycles of this ring system is normally of the cis-trans type or, more rarely trans-trans type [41].

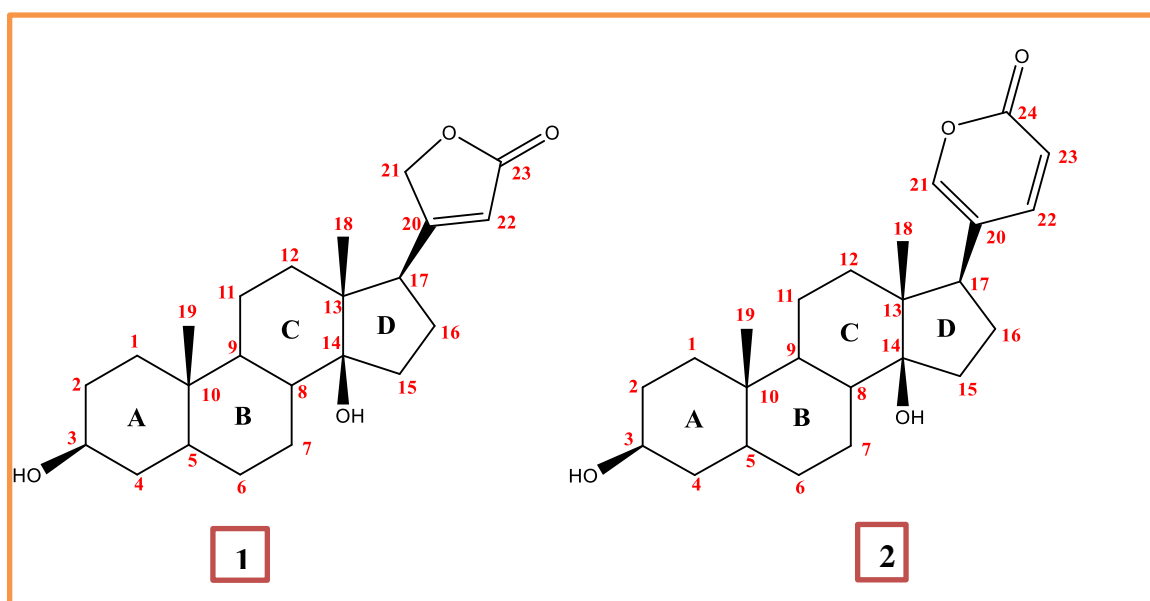


Figure I-B-03:Base structure of cardenolide (1) and bufadienolde (2) [6]

I-B-2-2-Biosynthesis of cardenolides

Production of cardenolides probably evolved from pathways for the biosynthesis of phytosterols (24 alkyl sterols) and endogenous plant steroid hormones. They are synthesized from cholesterol with progesterone as an intermediate, but, only a relatively small number of enzymes in the cardenolide biosynthesis pathway have been identified. Figure I-B-04 illustrates the predicted steps in the biosynthesis of the cardenolide aglycone [49].

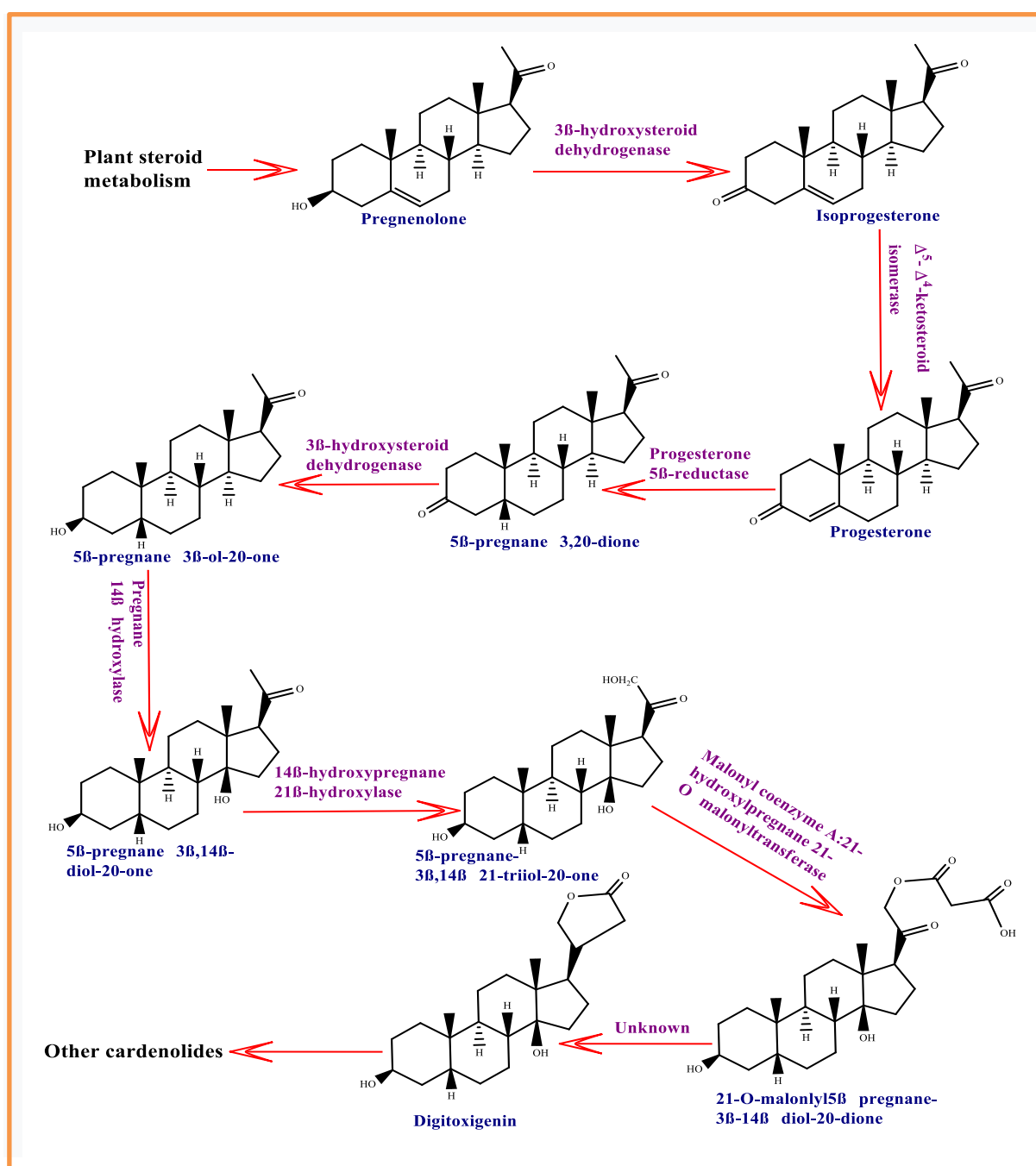


Figure I-B-04: Predicted steps of cardenolide aglycone biosynthesis pathway [49]

I-B-2-3-Structural description of cardenolide glycosides

I-B-2-3-1-Genin structure (cardenolides)

Cardenolides are always hydroxylated at C-3 β , they are characterized by a tertiary hydroxyl at C-14 β and by the substitution of the C-17 by an unsaturated lactone in orientation β [41]. Their chemical structures are quite restricted and contains the additional hydroxyl functions at: 1 β , 2 α , 3 β , 5 β , 11 α , 11 β , 12 β , 15 β , 16 β and 19 positions. These hydroxyls can be esterified, which is in rare cases [50]. Oxidation can manifest by the existence of a ketone at C-12 or by that of an epoxide, whether it is at C-11 and C-12 or C-7 and C-8. It is not uncommon for methyl at C-10 to be oxidized to hydroxymethyl or aldehyde; it can be also the cause of lactonization with the C-11 hydroxyl. Oxidation of C-13 methyl to hydroxymethyl can lead to cyclization. Exceptionally, the C ring can be unsaturated and known as: C-nor-D-homo-cardenolides [41].

I-B-2-3-2-Structure of the sugar moiety

The osidic part linked to the genin by the hydroxyl group of C-3 with single linked. It can be constituted of a single sugar or by an oligosaccharide containing of two to four sugars unit. The existence of hydroxylated group at C-2 allows the formation of a cyclic structure [41], which means that sugar moiety linked to the genin by double linkage.

The β -D-type of hexopyranose sugar ring is present in the axial orientation and the aglycone is equatorially orientated. Whereas, the α -L-type of hexopyranose sugar ring exists in equatorial orientation and the aglycone is preferentially held in the axial orientation [50].

The most frequently found sugar units that are linked to cardenolide aglycon part are: glucose, galactose, mannose, 6-desoxyhexoses as: rhamnose[51] and fucose [41], 6-desoxy-3-methylhexoses as: digitalose [51]. In addition of these sugar units, there are: 2,6-dideoxyhexoses as D-digitoxose (2,6-dideoxy-D-allose), 2,6-dideoxy-3-methylhexoses as L-oleandrose (2,6-dideoxy-3-methyl-L-mannose) and D-diginose (2,6-dideoxy-3-methyl-D-galactose), as well as, 4,6-dideoxy-2,3-methylenedioxy-D-allose[41].

Figure I-B-04 and I-B-05 illustrate the chemical structures of sugar units that are linked to cardenolides aglycone and some cardenolides and cardenolide glycosides that are isolated from different plants respectively.

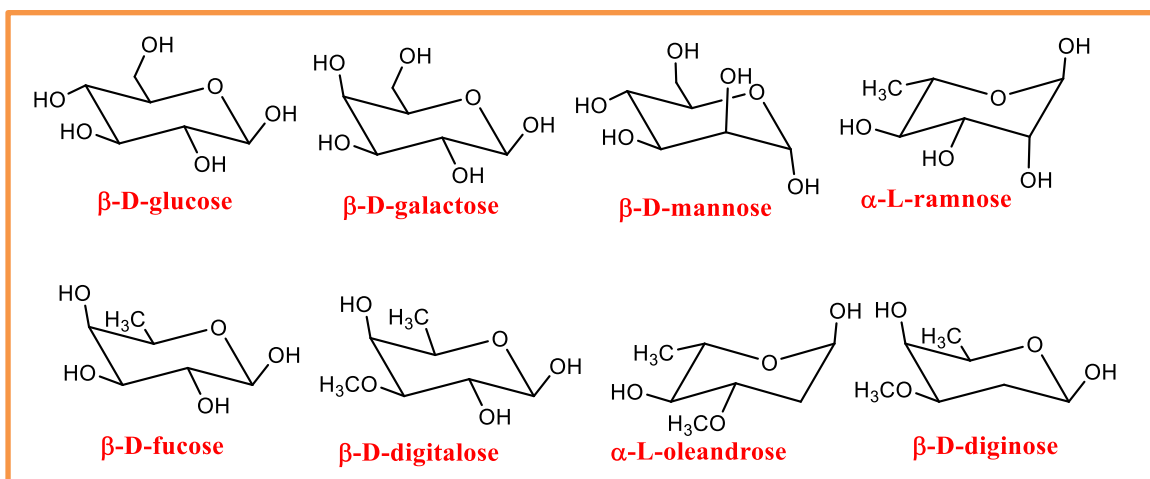


Figure I-B-05: Chemical structures of sugar units that are linked to cardenolides aglycone [41]

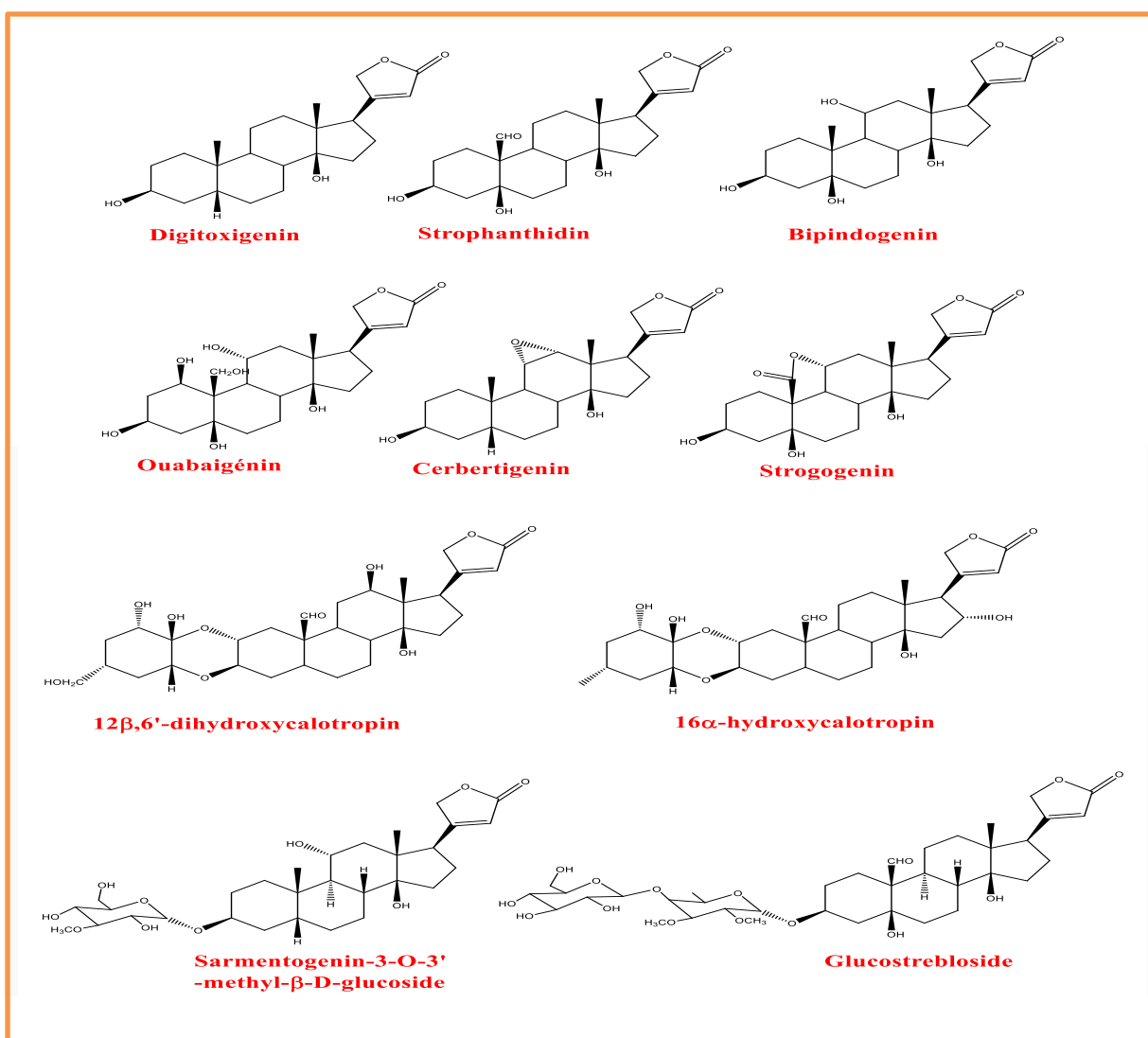


Figure I-B-06: Chemical structures of some cardenolides and cardenolide glycosides isolated from different plants [41, 49, 52, 53]

I-B-2-4-Distribution of cardenolides

In a few dozen genera, cardenolides unevenly distribute into about fifteen families, which highlight that they have a fairly restricted botanical distribution. They are represented in all subfamilies of Apocynaceae, Asclepidaceae, Periplocoideae, Rauvolfioidea and Secomonoideae. They are represented also in very limited number of genera of these families which are: Asparagaceae, Asteraceae, Brassicaceae, Celastraceae, Crassulaceae, Crossosomataceae, Fabaceae, Iridaceae, Malvaceae, Plantaginaceae, Moraceae, Ranunculaceae, Santalaceae, Solanaceae.

The presence of cardenolides in animals is exceptional, they come from food of this animals. For example, the caterpillars which feeding on Apocynaceae or Brassicaceae are containing cardenolides. however, this is not a general rule: some Coleoptera synthesize cardenolides genins from phytosterols (Chrysolinasp) [41].

I-B-2-5-Physico-chemical properties of cardenolides

Cardenolides are remarkable steroidal toxins which have these properties [54]:

- The sugars that attached to the 3β -OH group of the genin in most cardenolide glycosides are responsible for the water solubility of these compounds.
- Boiling of cardenolide glycosides in the presence of mineral acids, can easily hydrolyse their acetal linkage [6].
- The presence of the lactone ring weakens the molecule: possible opening in an alkaline medium which leading to the loss of pharmacological activity [41].

I-B-2-6-Biological activities of cardenolides

Cardenolides are naturally compounds which have a marked cytotoxic activity, which gives them an important biological activity. We summarize here the most biological activities of these compounds that have been reported:

- Cardenolide glycosides in low concentrations are used to increase the contractile force of the heart and decrease its rate of contraction by inhibiting the cellular Na⁺/K⁺-ATPase.
- Cardenolide glycosides possess anti-tumor activities against breast cancer, colon cancer, bladder cancer, liver cancer, gastric cancer, pancreatic cancer and lung cancer [6].
- Cardiac glycosides were applied for the treatment of cystic fibrosis.
- Cardenolide glycosides (digoxin, digitoxin and ouabain) were identified as the potent neuroprotective compounds.
- Cardiac glycosides are possible use in the context of ischemic stroke, this is due to their low concentrations trigger downstream signaling cascades that can prevent apoptosis and induce proliferation.
- Anti-herpes activity of glucoevatromonoside, a cardenolide isolated from a Brazilian cultivar of *Digitalis lanata*, is recently detected.
- The effectiveness of *Nerium oleander* extract (Anvirzel), which comprise primarily of Oleandrin and Oleandrigenin [55], on HIV infection of human peripheral blood mononuclear cells was studied. It is a novel candidate for anti-HIV therapeutic [56].

Chapter C: Biological activities

I-C-1-Biological activities

Biological activities of different secondary metabolites are describing the beneficial or harmful effects of them. In addition, they play an important role in highlighting the uses of the compounds in the medical applications. There are several methods to study biological activity of plants, for example: Antioxidant activity, anti-diabetic activity, antimicrobial activity, anticancer activity, anti-inflammatory activity...etc.

I-C-2-Definition of free radicals

Free radicals are chemical species (atoms or molecules) that have one or more single electrons (unpaired electron) on their outer shell and able to exist independently [57], they are therefore capable of reacting with electron donors to equilibrate its charge. Free radicals are fundamental to any biochemical process and represent an essential part of aerobic life [58]. They can be derived from oxygen (ROS) or other atoms like nitrogen (RNS) [57]. They cause many diseases like rheumatoid arthritis, hemorrhagic shock, cardiovascular disorders, metabolic disorders, neurodegenerative diseases, gastrointestinal ulcerogenesis and AIDS [59].

I-C-3-Source of reactive oxygen species (ROS)

ROS are generated as a result of partial reduction of oxygen which leads to the formation of radical oxygen species such as $O_2^{\cdot-}$ (anion superoxide), HO^{\cdot} (hydroxyl radical), NO^{\cdot} (nitric oxide), as well as RO^{\cdot} (oxyl) and ROO^{\cdot} (peroxyl) radicals that are generated during lipid peroxidation (specifically from polyunsaturated fatty acid (PUFA) oxidation) [60]. Free radicals are also generated exogenously through cigarette smoke, products of ionising UV radiation, environmental pollutants, lipid oxidation products in foods and excessive intakes of iron [58].

I-C-4-Antioxidant activity

Antioxidants or oxidation inhibitors are any compound that inhibits the production of free radicals, it prevents the damage of cellular components that arises due to chemical reactions, which yield free radicals [61]. They are a large group of highly reactive substances

that have the capability of slowing or blocking oxidant processes so as to minimize the oxidation effects of free radicals [62].

I-C-4-1-Mechanisms of scavenge free radicals by antioxidants (phenolic compounds)

Phenolic compounds have reducing character due to the substitution with electron donor groups (hydroxyl group). They exert their antioxidant activity by direct scavenging of reactive oxygen species (ROS), inhibition of enzymes involved in oxidative stress, regeneration of other antioxidant (α -tocopherol), chelation of metal ions that are responsible for ROS production and, finally, stimulation of endogenous antioxidant defense systems [60].

There are two main approaches to explain the mechanisms by which phenolic compounds act as antioxidants; hydrogen atom transfer (HAT) and single electron transfer (SET)[61].

I-C-4-1-1-Electron transfer (ET) mechanism

In the case of electron transfer (ET) (Figure I-C-01), as electron-rich aromatic compounds, phenols (ArOH) are reducing compounds that are able to transfer electrons to ROS with concomitant conversion into an aryloxy radical (ArO \cdot) which is stabilized by delocalization of the unpaired electron over the aromatic nucleus [63].

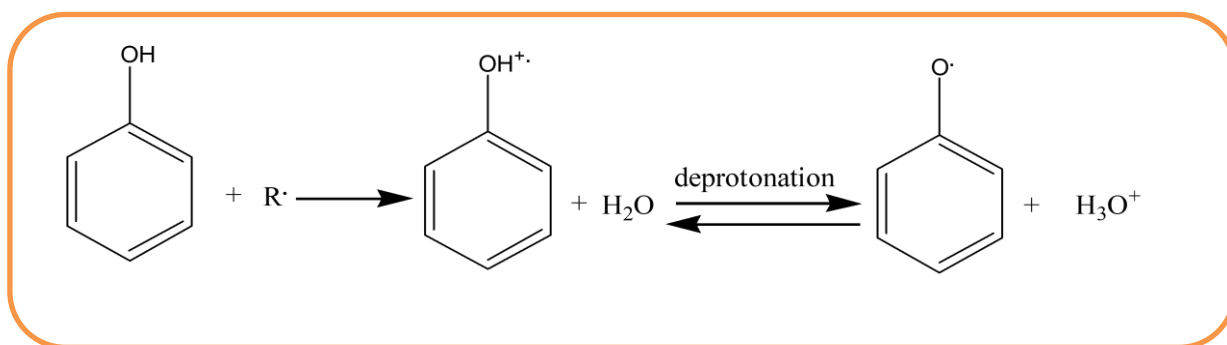


Figure I-C-01: Electron transfer (ET) mechanism of the antioxidant activity of phenolic compounds [60]

I-C-4-1-2-Hydrogen atom transfer (HAT)

In the case of H-atom transfer (HAT) (Figure I-C-02), a phenol antioxidant donates an H-atom to an unstable free radical (R \cdot) with formation of the corresponding phenoxyl radical which is stabilized by delocalization of the unpaired electron throughout the aromatic ring [60].

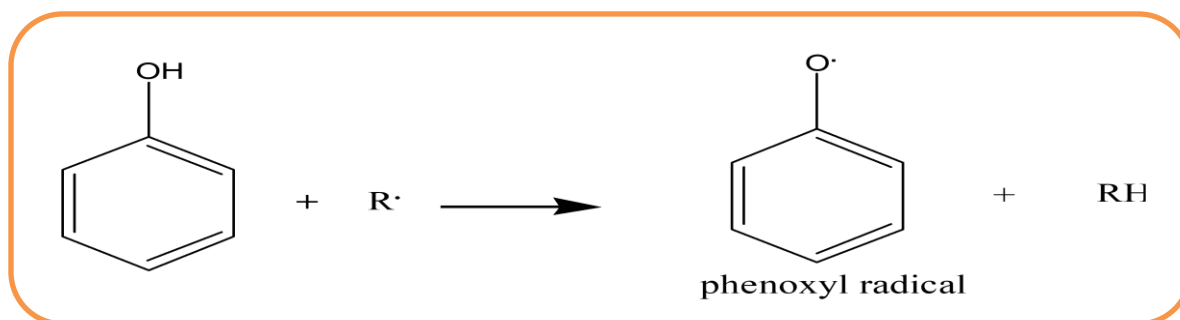


Figure I-C-02: Hydrogen-atom transfer (HAT) mechanism of the antioxidant activity of phenolic compounds [60]

The reducing effects of phenolic compounds are characterized by two important physicochemical parameters, the bond dissociation energy (BDE) of the O-H bond and the ionization potential (IP) of the phenolic compounds that quantify the HAT and ET, respectively. The lower of the BDE and the IP caused the stronger reducing activity of a phenolic compounds [60].

I-C-4-2-Methods of determination of antioxidant activity

In order to measure the antioxidant activity of biological substances many analytical methods are used. DPPH and Total antioxidant capacity (TAC) activities are among the methods used to determine the antioxidant activity of natural compounds.

I-C-4-2-1-DPPH (2,2-diphenyl-1-picrylhydrazyl) radical scavenging method

DPPH is a stable radical in solution and appears purple color absorbing at 515 nm in methanol [64]. The reaction mechanism involves the transfer of H from a phenolic compound to the DPPH radical [60]. The purple color of DPPH changes to yellow with concomitant decrease in absorbance. The color change is monitored by spectrophotometrically, it used for the determination of parameters for antioxidant properties [64].

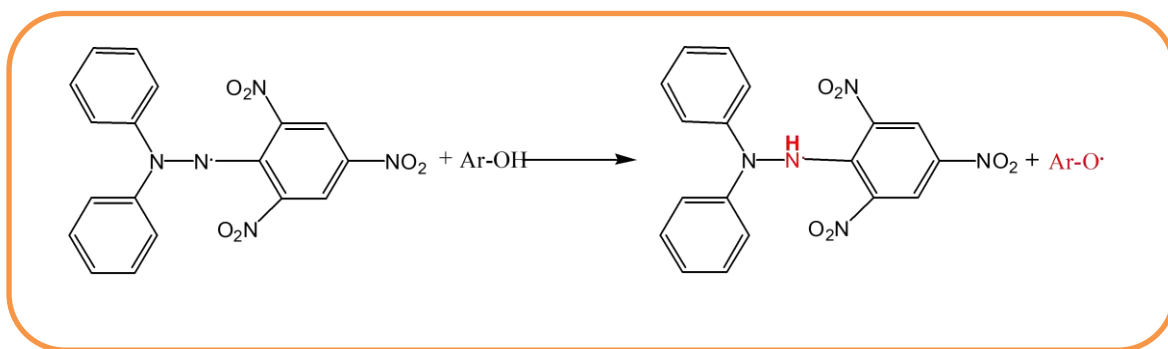


Figure I-C-03: Mechanism of inhibition of DPPH· by phenolic compounds [60]

I-C-4-2-2-Total antioxidant capacity (TAC)

Total antioxidant capacity (TAC) is the sum of antioxidant activities of nonspecific pool of antioxidants. The measuring of TAC in one single assay is much less troublesome and cheaper than determining the concentrations of numerous individual antioxidants, and does not require sophisticated equipment. The biological meaning of TAC is a parameter measuring the resultant force counteracting undesired oxidation in the material studied [65].

There are many methods to measure TAC in the extracts of plants, the reducing power of molybdenum Mo (VI) method is one of them. This technique is based on the reduction of molybdenum Mo(VI) present as molybdate ion MoO_4^{2-} to molybdenum Mo(V) present as MoO_2^{1+} in the presence of the extract to form a green phosphate complex (Mo(V)) at acidic pH [66].

I-C-5-Antidiabetic activity

I-C-5-1-Definition of diabetes

Diabetes mellitus is a metabolic disease characterized by a disorder in the regulation of carbohydrate metabolism resulting in hyperglycemia [67], it is a complex, serious chronic disease that has evolved in a very important way throughout all regions of the world. The number of people with diabetes has increased dramatically in recent years, in 2010, the number of people affected reached 221 million [68]. It is caused by inherited and/or acquired deficiency in production of insulin by the pancreas, or by the ineffectiveness of the insulin produced [69].

I-C-5-2-Classification of diabetes

The classification of diabetes has evolved over the past 50 years. In fact, in 1980, the WHO considered, like most clinicians, that there were two main classes of diabetes: insulin-dependent or type I diabetes and non-insulin-dependent or type II diabetes, diabetes of other types and gestational diabetes are also recognized [70].

I-C-5-2-1-Insulin-dependent diabetes (type I diabetes)

Insulin-dependent diabetes, also called lean diabetes because of the patient's weight loss before the age of 40 [71]. This type of diabetes called autoimmune diabetes due to destruction of β cells by the immune system, usually resulting deficiency of absolute insulin [72].

I-C-5-2-2-Non-insulin dependent (type II diabetes)

diabetes Type II is caused by a combination of genetic factors linked to insufficient insulin secretion, insulin resistance and environmental factors such as obesity, lack of exercise and stress, as well as aging [72]. This type of diabetes is most often established in adults and most of them are overweight [73].

I-C-5-2-3-Gestational diabetes

Gestational diabetes is observed in 3% of pregnant women, it can be considered transient. It is an intolerance to glucose leading to hyperglycemia of variable severity. Generally, this diabetes heals spontaneously after childbirth. It may, however, be a risk factor for later type II diabetes. The causes of its occurrence remain largely unexplained [71].

I-C-5-2-4-Other types of diabetes

The class of other special types of secondary diabetes is associated with a well-defined cause. These are pancreatic, endocrine, diabetes insipidus or corticosteroid-induced diabetes, monogenic forms of diabetes or diabetes associated with a genetic syndrome or caused by chemical agents. However, these conditions are relatively unknown [70].

I-C-5-3-Definition of α -amylase

α -Amylase as all enzymes, is a macromolecule belonging to the class globular proteins, of the endoglycanase type of the class of hydrolases which acts on α (1 \rightarrow 4) bonds of starch. It is widely represented in animals, plants and microorganisms [74]. It is an enzyme that catalyzes the degradation of carbohydrates in the small intestine. This degradation allows the

absorption of glucose and increases glycemia [75]. Therefore, the inhibition of this enzyme delays the digestion and absorption of carbohydrates and, consequently, reduces blood hyperglycemia.

I-C-6-Toxicity

I-C-6-1-Definition of toxicity

Toxicity was defined as an aspect of pharmacology which deals with the adverse effects of bioactive substances on living organisms [76]. A substance is toxic, when it causes, immediately or in the long term, transient or long-lasting disturbances of one or more functions of the body, and it may be causes their complete suppression and lead to death, after its having penetrated the body, whether at a high dose or several very close doses, or by small doses repeated for a long time [77].

In order to determine the safety and efficacy of the drugs, toxicological studies are very necessary experiment on animals such as mice, rats, guinea pigs, dogs, rabbits, monkeys, etc. because of these animals may have a similar metabolism manner and metabolites pharmacodynamics as well as human, with respect all drug conditions. Toxicological studies are divided into three types: acute, sub-acute and chronic toxicity according to the duration of drug exposure to animals [78].

I-C-6-1-1-Acute toxicity

Acute toxicity is that which causes death or very serious physiological disorders after a short time of the absorption through the different route, once or in several repetitions, of a fairly large dose of the tested substance [77]. Acute toxicity study is used to determine the Lethal Dose 50 (LD50) of a substance which is defined as the dose of a substance that can be expected to cause the death of 50% of the tested animals [76]. In this study, the animals are kept under observation for 14 days [79].

I-C-6-1-2-Sub-acute toxicity

A sub-acute toxicity study is one in which animals are given repeated doses of the tested substance in sublethal amounts for 14 to 21 days. It is used to determine the effect of the drug on the biochemical and haematological parameters of the blood as well as to identify histopathological changes [76].

I-C-6-1-3-Chronic toxicity

Chronic toxicity is the adverse effects that occur as a result of repeated daily exposure of experimental animals to the tested substance [76]. Chronic toxicity study is performed by giving the tested substance in different doses for a period of 90 days to over a year to determine carcinogenic and mutagenic potential of drug [78].

I-C-7-Anti-inflammatory activity

I-C-7-1-Definition of inflammation

Inflammation is a natural defence reaction triggered when the body is threatened by pathogens, damaged cells or irritants. This response is essential for humans to fight various infections, to promote healing and the restoration of normal function of damaged tissue [80], which means without inflammation, wounds and infections would never heal [81]. Inflammation causes four cardinal symptoms: heat, pain, redness and edema [82]. The body's inflammatory responses have variable intensities and durations. It may be fleeting; occurs immediately after pathogen invasion and lasts up to approximately 48 hours. In this case it is called acute inflammation. However, it can persist for years, hence it is called chronic inflammation [80].

I-C-7-1-1-Acute inflammation

Acute inflammation is the body's immediate response to an aggressor, it is a complex physiological response that involves the participation of two branches of the immune system: innate immunity and adaptive immunity. This short-lived response (a few days) aims to eliminate the causative agent of tissue damage and repair the affected tissue [83].

I-C-7-1-2-Chronic inflammation

Chronic inflammation is occurred when the pathogen persists because of the failure of the acute inflammatory response or an inappropriate response [80]. The persistence of inflammation is responsible for anatomical and functional consequences that make chronic inflammatory diseases are serious [84]. Chronically inflamed tissues are characterized by infiltration of mononuclear immune cells (monocytes, macrophages, lymphocytes, and

plasma cells) and tissue destruction [85] which can caused pain, ulceration, scarring and fibrosis and non-healing wounds [81].

I-C-7-2-Anti-inflammatoryagents

Anti-inflammatories are substances that act on swelling and pain. During angina, the throat is red and swollen, and during articular rheumatism, the joint is swollen and painful, the anti-inflammatory will relieve the pain and swelling. There are two types of anti-inflammatory drugs: steroidal anti-inflammatory drugs (SAIDs) which are cortisone and its derivatives and non-steroidal drugs (NSAIDs) as aspirin. Their main drawbacks are poor digestive tolerance [84].

I-C-7-2-1-Nonsteroidal anti-inflammatory drugs (NSAIDs)

Nonsteroidal anti-inflammatory drugs (NSAIDs) are used by millions of patients around the world due to their anti-inflammatory, antipyretic and analgesic properties. They are reduce the pain, fever and inflammation [83].All NSAIDs are cyclooxygenase inhibitors [84].

I-C-7-2-2-Steroidal anti-inflammatory drugs (AISDs)

Steroidal anti-inflammatory drugs are synthetic derivatives of cortisone which are powerful anti-inflammatory drugs. They are also endowed with immunomodulatory and antiallergic properties [84].They represent the most effective treatment used for chronic inflammatory diseases such as asthma, rheumatoid arthritis, inflammatory bowel disease and autoimmune diseases [83]

I-C-7-2-3-Natural anti-inflammatory drugs

Polyphenols, flavonoids, saponins, alkaloids...etc. are active substances that are supposedly responsible for the anti-inflammatory activity. Most of these metabolites act by blocking the cyclooxygenase and lipoxygenase pathways as well as through other mechanisms [83].

I-C-8-Sedative activity

I-C-8-1-Definition of pain

According to the I.A.S.P. (International Association for the Study of Pain): Pain is the expression of an unpleasant sensory and emotional experience associated with actual or potential tissue damage or described in terms of such damage. It is the first signal of a pathological phenomenon. Depending to its intensity and its duration, it can become a real syndrome, resounding on the major organic functions and it can lead to an aggravation the patient's condition [86].

I-C-8-1-1-Types of pain

Several types of pain can be distinguished, depending on the origin of the pain there are [86]:

- Psychogenic pain of somatic origin without an identifiable cause which may include neuropsychological factors.
- Nociceptive pain due to excitation by potentially dangerous factors for the organism of cutaneous or visceral nerves.
- Neuropathic pain due to primary injury, dysfunction or disturbance of nervous, peripheral or central tissue.

I-C-8-2-Definition of sedation

The term of sedation can be defined as the use of sedative medication to relieve intolerable and refractory distress by reducing patient consciousness. It includes two core factors: the presence of severe suffering refractory to standard treatment, and the use of sedative medications with the primary aim of relieving distress [87].

Based on the duration of sedation (transient, indefinite, or maintained until death) and its depth (proportionate or deep from the outset),the sedation is divided into two different types [88]:

- Proportionate sedation, meaning the depth and duration are proportionate to the relief of pain.
- Continuous deep sedation maintained until death (CDSMD); it carried out under conditions defined by law.

I-C-8-3-Sedative drugs

Sedative drugs are drugs that calms a patient, easing agitation and permitting sleep. They are generally work by modulating signals within the central nervous system. They can dangerously depress important signals that are needed to maintain heart and lung function when they are misused or accidentally combined. Most sedatives also can cause an addictive potential, they may result in slurred speech, poor judgment, slow and uncertain reflexes at higher doses. For these reasons, sedatives should be used under supervision and only as necessary [89].

Alkaloids, terpenoids, volatile oils, flavonoids, lignanoids, coumarins and saponins can have a sedative and hypnotic properties and they call natural sedative ingredients [90].

PART II: MATERIAL AND
METHOD

***ChapterA: Qualitative and Biological
study of P. tomentosa***

II-A-1-Preparation of Sample

Pergularia tomentosa was collected from the region of Zelfana (east of Ghardaia). The harvest of this plant was in morning at the beginning of November 2017. It was identified by Professor EDOUD Amor (botanist at University of Kasdi Merbah Ouargla). The voucher specimen has been deposited in the herbarium of our laboratory (Valorisation and Promotion of Saharan Ressources VPRS) under the code: 201711Zel/PerTo (Figure II-A-01). The organs of *Pergularia tomentosa* (stems and leaves) were dried in the shade and protected from moisture and light at room temperature for 15 days, then, they were cut into small pieces and stored in paper containers at room temperature and in darkness until needed.



Figure II-A-01: Herbarium specimens of *Pergularia tomentosa*

II-A-2-Phytochemical screening

10.22 g and 10.00 g of leaves and stems, respectively were macerated in a 7/3 system (MeOH / H₂O) for 24 hours, after filtration, crude extract of each organ kept for the following phytochemical tests using standard procedures to identify the various constituents described

Mtherial and Method Part: Quantitative and Biological study of P. tomentosa

by Trease and Evans [91, 92], Harborne [93], Yadav *et al* [94], Oloyede [95] and Bruneton J [41].

➤ **Flavonoids test:**

To 1 mL of crude extract, 1 mL of lead acetate (10%) was added, the formation of a yellow precipitation indicates the presence of the flavonoids.

➤ **Steroids test:**

Two tests were performed to confirm the result:

✓ **Salkowski test:**

2 mL of crude extract was mixed with 2 mL of CHCl_3 , then 2 mL of concentrated sulfuric acid (H_2SO_4) were added. The appearance of a red coloration indicated the presence of the steroids.

✓ **Librman Burchard test:**

2 mL of crude extract were dissolved in 2 mL of CHCl_3 , then, 2 mL of concentrated sulfuric acid (H_2SO_4) and 2 mL of acetic acid were added. The appearance of a greenish coloration indicated the presence of steroids.

➤ **Tannins test:**

To 1 mL of crude extract, 0.5 mL of a 1% aqueous solution of FeCl_3 was added. The presence of tannins is indicated by a greenish or blue-blackish color.

➤ **Saponin test:**

5 mL of crud extract were put into a test tube and stirred for a few seconds, tube agitation was stopped and left for 15 min. the appearance of persistent foam indicates the presence of saponins.

➤ **Terpenoids test:**

5 mL of crude extract were added to 2 mL of chloroform and 3 mL of concentrated sulfuric acid (H_2SO_4). The formation of two phases and a brown color at the interphase indicates the presence of terpenoids.

➤ **Reducing compounds test:**

2 mL of Fehling's reagent (1 mL reagent A and 1 mL reagent B) were added to 1 mL of crude extract. The mixture was incubated for 8 min in a boiling water bath. The appearance of a bricked precipitate indicates the presence of the reducing compounds.

Mtherial and Method Part: Quantitative and Biological study of P. tomentosa

➤ **Alkaloids test:**

2 mL of crude extract were divided into two equal volumes. 2 mL of concentrated HCl were added for each extract. One of them was treated with 1 mL of Mayer's reagent, and the other with 1 mL of Wagner's reagent, each mixture was heated in a water bath. The formation of a white or brown precipitate, respectively, reveals the presence of the alkaloids.

➤ **Proteins test:**

✓ **Biuret test:**

To 3 ml of crude extract, 1 mL of NaOH (4%) and 1 mL of CuSO₄ (1%) were added. The color change of the solution to purple or pink indicates the presence of the protein.

➤ **Triterpenes Test:**

✓ **Salkowaski test:**

To 2 mL of crud extract, 5 drops of concentrated sulfuric acid (H₂SO₄) were added. The appearance of a greenish color indicates the presence of triterpenoids.

✓ **Libremann burchard test:**

To 2 mL of crud extract, 10 drops of acetic anhydride were added and mixed well, then 5 mL of concentrated sulfuric acid (H₂SO₄) was added. The appearance of a greenish color indicated the presence of triterpenoids.

➤ **Free quinone test:**

A few drops of NaOH (1%) were added to 5 mL of crud extract. The color change of solution to yellow, red or purple indicates the presence of free quinones.

➤ **Cardenolides test:**

2 mL of glacial acetic acid and a drop of FeCl₃ solution was added to 5 mL of crud extract, then, 1 ml of concentrated sulfuric acid (H₂SO₄) was added. The presence of the brown ring on the interface is characteristic of deoxy sugars of cardiac glycosides (reaction of Keller-Kiliani).

II-A-3-Quantitative study

Leaves and stems extracts were prepared in order to estimate their level of total phenols, flavonoids and condensed tannins, as well as to evaluate their biological activity.

II-A-3-1-Dosage of Total Phenolic Content

Total Phenolic Content (TPC) in different extracts was determined using the Folin–Ciocalteu reagent, according to Singleton and Ross protocol [96]. The reagent consists of

Mtherial and Method Part: Quantitative and Biological study of P. tomentosa

phosphotungstic acid ($H_3PW_{12}O_{40}$) and phosphomolybdic acid ($H_3PMo_{12}O_{40}$) which are reduced during the oxidation of phenols to blue oxides of tungsten (W_8O_{23}) and molybdenum (Mo_8O_{23}), which strongly absorb at a length wave of 760 nm.

Ethanollic Gallic acid solution ($0.03-0.25\text{ g}\cdot\text{L}^{-1}$) was used as a reference standard for plotting calibration curve. 0.5 mL of Folin-Ciocalteu reagent (10%) was added to 0.1 mL of each extract, after 2 min the mixture was neutralized with 2 mL of Na_2CO_3 solution (20%, w/v) and it was kept in dark at 25°C for 30 min. The absorbance of blue color was measured by using UV/Vis spectrophotometer at fixed wavelength of 760 nm against a blank.

The TPC was calculated using linear regression equation obtained from the standard curve of gallic acid. It was calculated as $\text{mean}\pm\text{SD}$ ($n=3$) and expressed as mg gallic acid equivalent GAE ($\text{g of dry weight (DW)}^{-1}$) of plant.

II-A-3-2-Dosage of flavonoids Content

The determination of Total Flavonoids Content (TFC) in each extract was carried out using aluminum trichloride ($AlCl_3$) according to Belguidoum M. *et al.* protocol [97]. Aluminum trichloride forms a complex with phenolic compounds. This complex has yellow color and absorb at 430 nm.

Ethanollic Quercetin solution (0.003 g/L to 0.025 g/L) was used as a reference standard for plotting calibration curve. 1.5 mL of an ethanollic solution of $AlCl_3$ (2%) was added to 1.5mL of each extract. The mixture was kept in the dark for 30 minutes at room temperature. The reading of the absorbance of each solution was determined at 430 nm against a blank.

The TFC was calculated using linear regression equation obtained from the standard curve of quercetin. It was calculated as $\text{mean} \pm \text{SD}$ ($n = 3$) and expressed as mg quercetin equivalent QE ($\text{g of the dry weight}^{-1}$) of plant.

II-A-3-3-Dosage of condensed tannins Content

The determination of Total Condensed Tannins (TCT) in each extract was carried out using ethanollic vanillin solution according to Belguidoum M. *et al.* protocol [97].It has anabsorbance at a length wave of 500 nm.

Ethanollic catechin solution (0.01 g/L to 0.1 g/L) was used as a reference standard for plotting calibration curve. 3 mL of ethanollic vanillin solution (4%) was added to 0.4 mL of each extract, then, 1.5 mL of concentrated hydrochloric acid was added also. The mixture

was kept in the dark for 15 min at room temperature. The absorbance was measured at 500 nm against a blank.

The (TCT) was calculated using linear regression equation obtained from the standard curve of vanillin. It was calculated as mean \pm SD ($n=3$) and expressed as mg catechin equivalent CE (g of dry weight (DW))⁻¹ of plant.

II-A-4-Evaluation of *in vitro* biological activities

In order to evaluate the *in vitro* biological activities of *P. tomentosa* extracts, anti-radical (antioxidant) and anti-enzymatic (antidiabetic) activities were carried out.

II-A-4-1-Antioxidant activity

II-A-4-1-1-DPPH[•] radical scavenging test

➤ Principle

The scavenging of DPPH[•] (1,1-diphenyl-2-picryl-hydrazyl) method was used to study antiradical activity of different extracts of *P.tomentosa* using protocol described by Mansouri *et al.* [98] with some modifications. This method is widely used because it is quick, easy and inexpensive [99], it is based on the reduction of DPPH radical that having a purple color to a yellow compound in the presence of hydrogen which donated by antioxidants [100].

DPPH[•] has an unpaired electron on a nitrogen atom. Due to this delocalization, the molecules of the radical don't form dimers. This radical remains in its relatively stable monomeric form at ordinary temperature [99].

➤ Procedure

1.5 ml of different concentrations of each extract (diluted in water) and control solutions were added to 1.5 mL of solution of DPPH[•] (250 μ M) prepared in methanol. The mixture was left in the dark for 30 min. The disappearance of the purple color of the mixture was compared to negative control which containing 1.5 mL of DPPH[•] solution and 1.5 mL of water. The absorbance was measured at 517 nm. The Same procedure was repeated, replacing the extract of *P. tomentosa* with BHT and ascorbic acid as references.

The antiradical activity was estimated according to the equation below:

$$\text{Percentage of inhibition} = \frac{ABS\ 517_{\text{negative control}} - ABS\ 517_{\text{sample}}}{ABS\ 517_{\text{negative control}}} \times 100$$

The inhibition of DPPH• radical was calculated as mean±SD (n=3). The antioxidant capacity of the extract was expressed as an IC₅₀ value which defined as being the concentration of the substrate which causes the loss of 50% of the activity of DPPH.

II-A-4-1-2-Reducing power of molybdenum Mo (VI) test

➤ **Principle**

Total antioxidant capacity of different extracts of *P.Tomentosa* was determined using the phosphomolybdenum method which described by Prieto *et al.* [66]. This method was based on reducing of molybdenum Mo (VI) present in the form of molybdate ion MoO₄²⁻ to molybdenum Mo (V) present in the form MoO₂¹⁺ in the presence of extract to form a green phosphate complex (Mo (V)) at acidic pH.

➤ **Procedure**

0.1 mL of different concentrations of each extract and control solutions were mixed with 1 mL of reagent solution (8 mM sodium phosphate, 0.6 M sulfuric acid, and 4 mM ammonium molybdate). The mixture was kept in a water bath at 95°C for 90 min. After that, it was left to cool at 4°C. The absorbance was read at 695 nm, against a blank (containing all reagents except the test extract).

Ascorbic acid was used as a positive control. Total antioxidant capacity of different extracts was expressed as an AEAC in mM (Ascorbic acid Equivalent Antioxidant Capacity) according to the equation below

$$AEAC = K/K'$$

K: the slope of the extract curve

K': the slope of the ascorbic acid curve

II-A-4-2-Antidiabetic activity

Antidiabetic activity of *P. tomentosa* extracts using inhibition of α -amylase enzyme was reported for the first time in our study. It was determined according to the method described by Zineb *et al.* [101].

➤ Preparation of reagents

✓ Phosphate buffer solution (0.02 M, pH = 6.9)

The buffer solution was prepared by mixed a monobasic solution A (NaH_2PO_4) (0.1 M, $M_A=0.78$ g, $V_A=45$ ml of distilled water) with a dibasic solution B (Na_2HPO_4) (0.1 M, $M_B=3.5813$ g, $V_B=55$ ml of distilled water).

✓ Preparation of 3,5-Dinitrosalicylic Reagent (DNSA)

0.5 g of DNSA was dissolved in 20 ml of distilled water. Then, 15 g of double sodium and potassium tartrate was added to this solution with stirring. The obtained solution has opaque yellow. After that, its color changed to orange due to addition of 10 ml of NaOH solution (2 N). The volume of the solution obtained was adjusted to 100 ml by adding distilled water. The reagent obtained was stored away from light and at 4 °C.

✓ Preparation of Starch solution (substrate used)

1% of starch solution was prepared by dissolving 0.5 g of starch in 50 mL of phosphate buffer solution. The obtained solution was used in alpha amylase tests.

➤ Preparation of α -amylase solution

The enzyme which was used in this test is α -amylase enzyme (commercialized), which was isolated from *Aspergillus oryzae* (Enz-no:3.2.1.1). 0.04 g of α -amylase was dissolved in 100 ml of phosphate buffer solution.

➤ Procedure

0.5 mL of starch solution (1% w/v) was mixed with 0.5 ml of α -amylase enzyme (1.3 UI/ml), then, 50 μ l of each extract (0.5 mg/mL) was added. The mixture was incubated at 37°C for 30 minutes. After that, 1 mL of DNSA reagent was added to this mixture, and it was incubated for 10 min at 100°C. After cooling, it was diluted with added 10mL of distilled water.

Mtherial and Method Part: Quantitative and Biological study of P. tomentosa

Same procedure was performed on a negative control that did not contain extract. The absorbance was read at 540 nm against a blank which containing buffer solution. α -amylase inhibition was expressed as a percentage of inhibition which was calculated by the following equation:

$$I\% = \frac{ABSc - ABSs}{ABSc} \times 100$$

I%: percentage of inhibition

ABSc: the absorbance in absence of inhibitor
(extract)

ABSs: the absorbance in presence of inhibitor
(extract)

II-A-5-Evaluation of *in vivo* biological activities

In order to evaluate the *in vivo* biological activities of both the aqueous and hydroalcoholic extracts, acute toxicity, anti-inflammatory and sedative activities were carried out.

➤ Preparation of aqueous and crude extracts

✓ Aqueous extract (decoction method)

122.989 g of the aerial part of *P. tomentosa* were cut into small pieces and placed in 1000 ml of distilled water, then boiled for 30 minutes. After cooling, the mixture was filtered using vacuum filtration. After that, the mixture was dried using the freeze dryer machine.

✓ Crud extract (hydroalcoholic extract)

72.108 g of aerial part of the *P. tomentosa* were cut into small pieces and defatting using petroleum ether. Then, the mixture was filtered and dried. After that, the plant defatted was macerated in 750 ml of hydroalcoholic mixture (8/2 methanol/distilled water) and left for 24 hours. After that, the mixture was filtered using vacuum filtration, the extract was concentrated to dryness using rotavapor.

Mtherial and Method Part: Quantitative and Biological study of P. tomentosa

➤ **Preparation of animals**

The *in vivo* study of aqueous and hydrochloric extracts of *P. tomentosa* was carried out on male and female albino mice weighing between 20-25 g. These mice were provided from the Pasteur Institute of Algeria and housed at the SIDAL animal facility. They placed in plastic cages lined with a renewable litter (Figure II-A-02), each cage houses the same sex (male or female), where the average temperature varies between 20-25°C, with a photoperiodic cycle of 12 hours of light/dark.

They were fed with a complete food in the form of pellets composed of corn, soybean meal, milling liquors, limestone, phosphates, salt, amino acids, trace elements, poly-vitamins and antioxidants. They were also provided with tap water. The mice were acclimatized to the laboratory conditions for a week before starting the experiment.

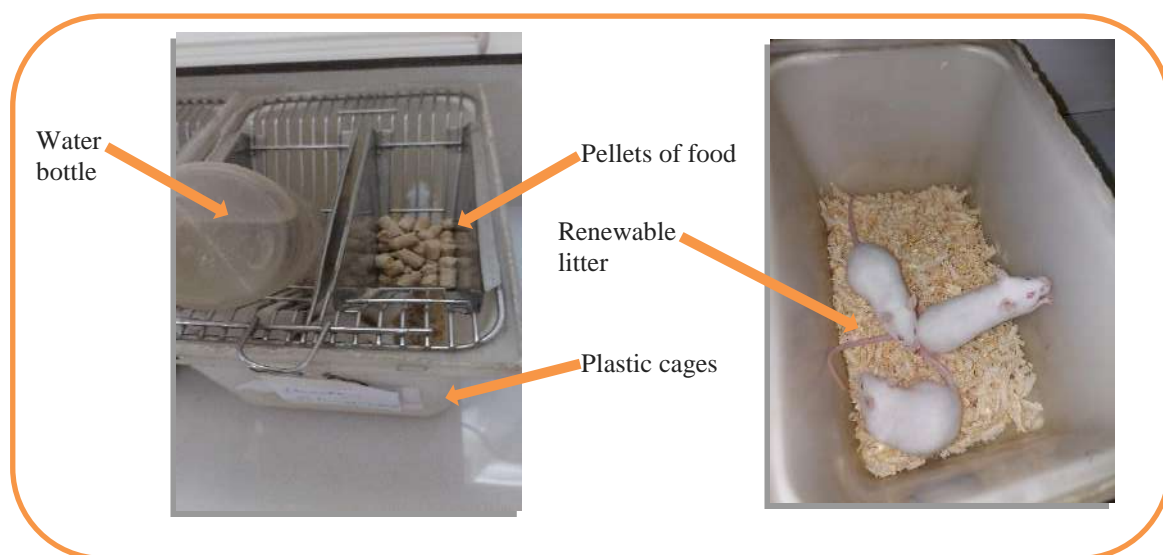


Figure II-A-02: Plastic cages of mice

II-A-5-1-Determination of acute toxicity

Determination of acute toxicity was performed on female albino mice because they are generally slightly more sensitive than male mice. This test was performed according to the Organization of Economic Co-Operation and Development (OECD) guideline 423 [102].

Mtherial and Method Part: Quantitative and Biological study of P. tomentosa

12 mice were fasted for 16 hours before the administration of extracts. After that, they were weighed and divided into two groups (according to number of the extract: aqueous and hydrochloric extracts), each group consisted of 6 female mice. 0.4 g of each extract was dissolved in 5 mL of distillate water. 0.5 mL of each extract was administered only once orally at a single dose of 2000 mg/kg to each mouse by gavage, using a suitable intubation cannula (Figure II-A-03). After the substance has been administered, food was withheld for a further 1-2 hours.

The general behaviour and mortality of mice were observed during the first 30 min after dosing, then after 2 h. They were also observed once a day during 14 days.

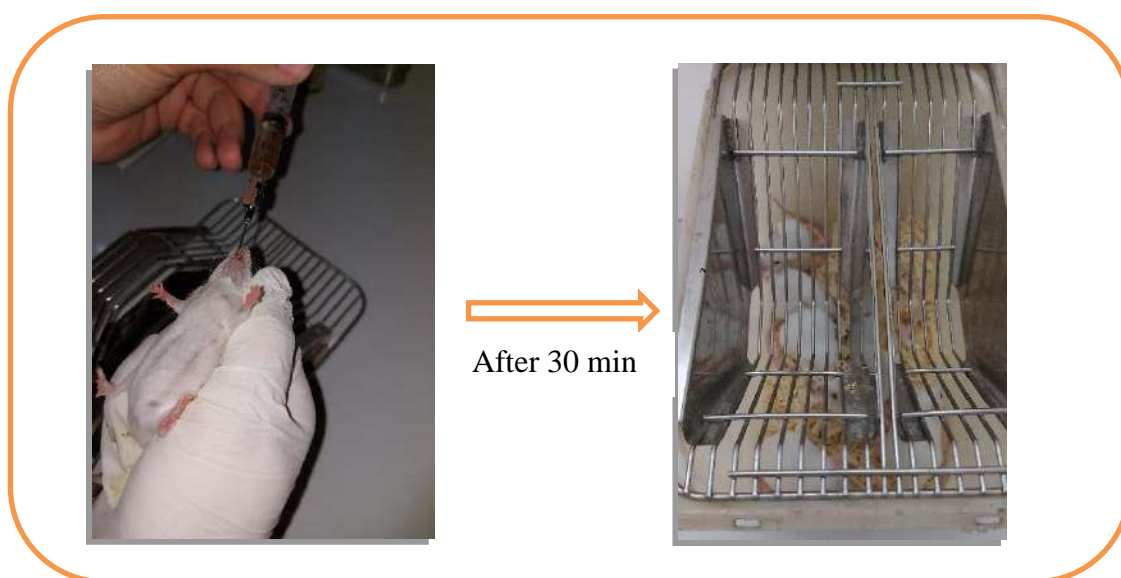


Figure II-A-03: Acute toxicity test (administration and observation of treated mice)

II-A-5-2-Anti-inflammatory test

Anti-inflammatory study of both the aqueous and hydrochloric extracts was performed on male albino mice. This test was evaluated by the carrageenin-induced edema in hind paw method according to the protocol described by SIDAL, Algiers [103].

The mice were fasted for 16 hours before the administration of extracts. Then, they were divided into four groups, each group consisted of 6 male mice (control group, reference group and two test groups). The two test groups are administered orally with 0.5 ml of each extract (0.08 g/ml) at the dose of 2000 mg/kg, while the reference and control groups are

Mtherial and Method Part: Quantitative and Biological study of P. tomentosa

administered separately with 0.5 ml of ibuprofen as a reference and distilled water, respectively.

After 30 minutes, 0.025 ml of a suspension of carrageenin (1%) was injected into the left hind paw of the mouse which causes a significant increase in the volume of the edema compared to the right paw, which is considered as a control. After 4 hours, the mice were sacrificed. Then, their legs were cut at the height of the joint and weighed on an analytical balance (Figure II-A-04).

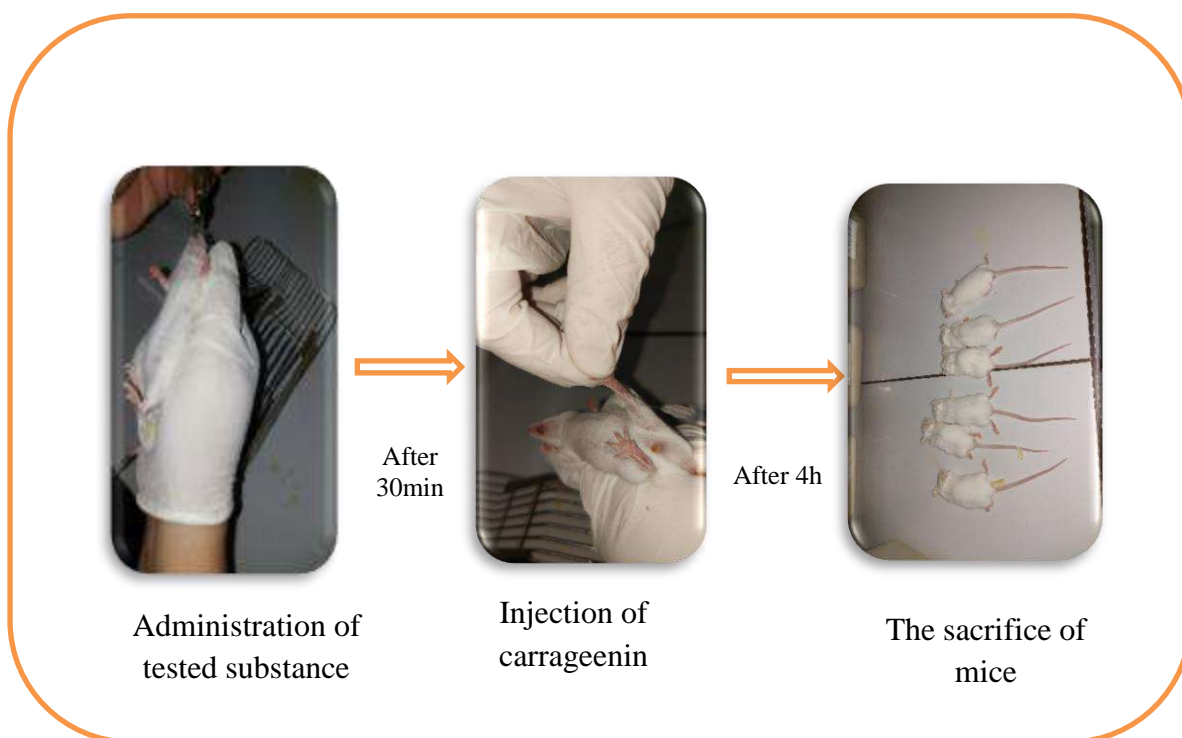


Figure II-A-04: Anti-inflammatory test

For each treated group, the arithmetic average of the weight of the left paw and the right paw were calculated in order to calculate the percentage increase in paw weights (% edema) using following formula:

$$\text{Percentage of edema} = \frac{\text{Weight average of left paw} - \text{Weight average of Right paw}}{\text{Weight average of Right paw}} \times 100$$

Mtherial and Method Part: Quantitative and Biological study of P. tomentosa

The percentage of reduction in edema of treated mice compared to control mice was also calculated using following formula:

$$\text{Percentage reduction in edema} = \frac{\% \text{ of edema of control} - \% \text{ of edema of test}}{\% \text{ of edema of control}} \times 100$$

II-A-5-3-Sedative activity

Determination of sedative activity of *P. tomentosa* was reported for the first time. Sedative test of both aqueous and hydrochloroc extracts was performed on male albino mice. It was evaluated by studying the spontaneous motility of the mice treated by the extracts, using the actimeter in cabinet of BOISSER and SIMON according to the protocol described by SIDAL, Algiers [103].

The mice were divided into four groups, each group consisted of 6 male mice. They were fasted for 16 hours before the administration of extracts. The two test groups are administered orally with 0.5 ml of each extract (0.08 g/ml) at the dose of 2000 mg/kg, while the reference and control groups are administered separately with 0.5 ml of haloperidol as a reference and distilled water respectively.

After 30 minutes, an actimeter was connected, consisting of twelve light sources which were to light up (Figure II-A-05). Then each mouse was placed in a plexiglass cage. The passage of the mouse in front of the light beam is recorded after each 5 min during 30 min (Figure II-A-06)

Mtherial and Method Part: Quantitative and Biological study of P. tomentosa

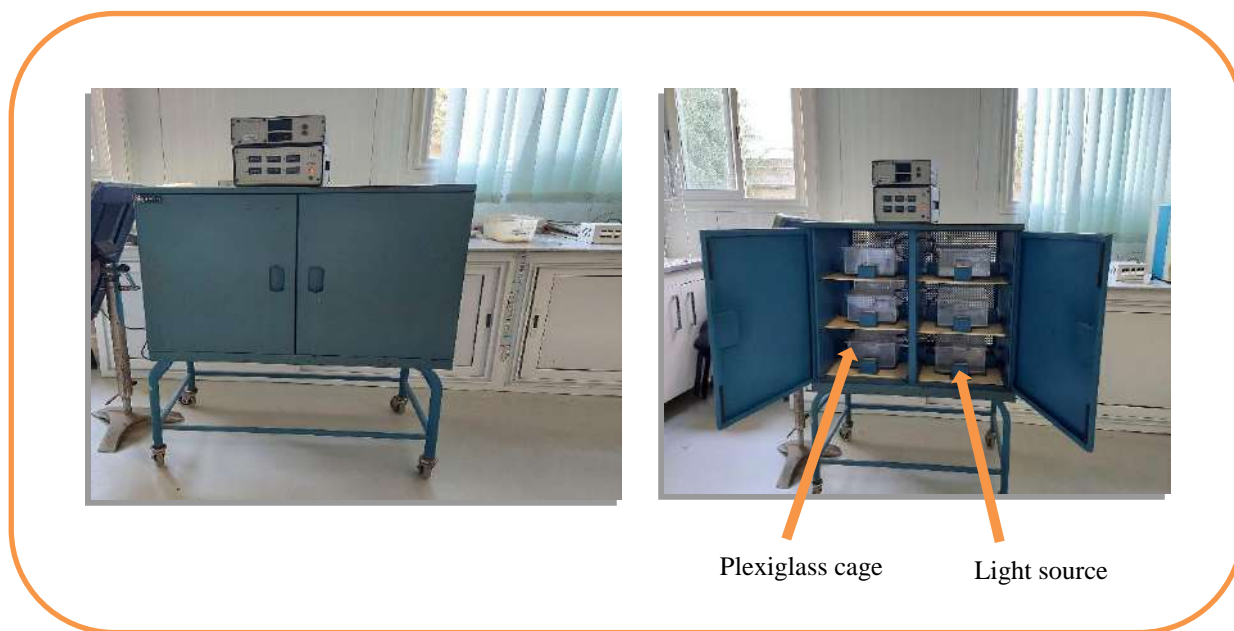


Figure II-A-05: An actimeter device

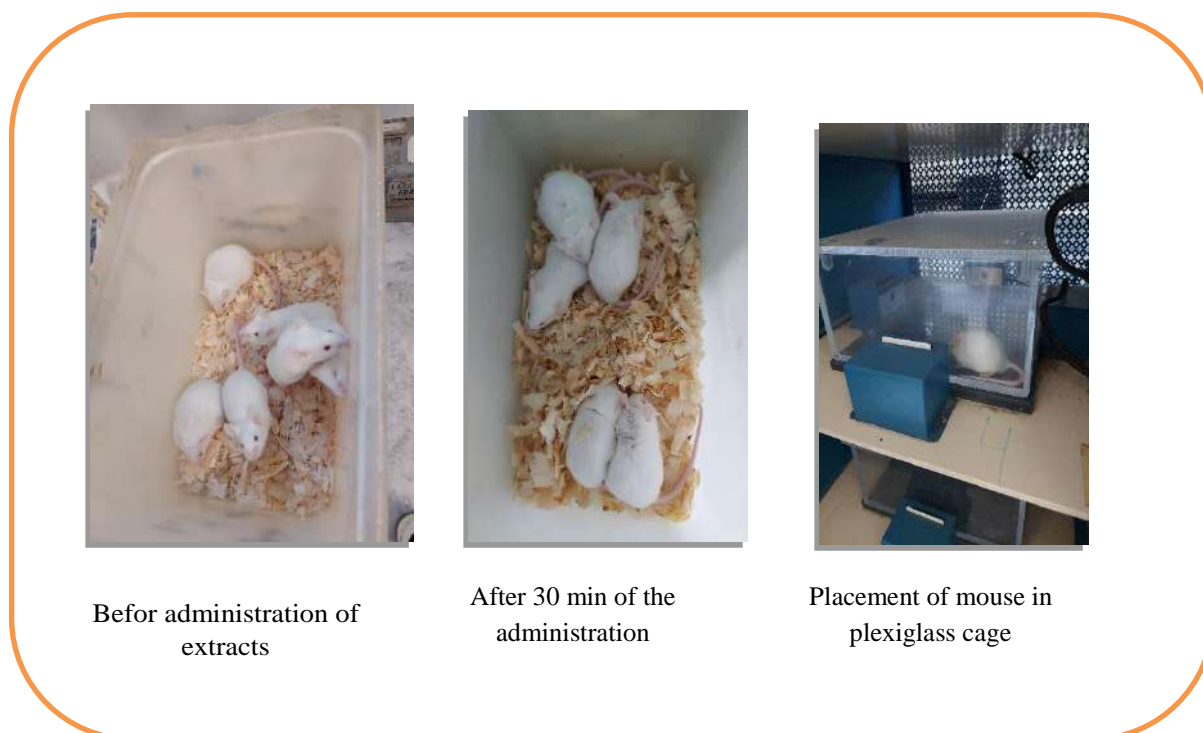


Figure II-A-06: Sedative test

Mtherial and Method Part: *Quantitative and Biological study of P. tomentosa*

For each treated group, the arithmetic average of the movement (after 30 min) of treated mice was calculated in order to calculate the percentage of reduction of movement compared to control using the following formula:

$$\text{Percentage of reduction} = \frac{\text{Movment average of control} - \text{Movment average of test}}{\text{Movment average of control}} \times 100$$

***B-Phytochemical study of P.
tomentosa***

II-B-1-Extraction, isolation and purification of alkaloids

II-B-1-1-Extraction of alkaloids

Extraction of total alkaloids from leaves of *P. tomentosa* L. was performed by using specific alkaloids extraction method, which based on difference of solubility of alkaloids in acid and alkaline medium according to BRUNETON J protocol [41].

2.337 Kg of vegetable material (the leaves) were defatted in 10 L of petroleum ether. The mixture was incubated for 48 hours in dark at ambient temperature. After filtration, the sediment was dried in the shade during a few minutes.

After drying, sediment was alkalized using a solution of ammonia (4 L; 0.5 N; pH = 10) overnight at ambient temperature, thus allowing alkaloids to pass from alkaloidal salt form to its corresponding alkaloid bases.

The alkalized sediment was placed in a cellulose cartridge (50 g), the latter was placed in an apparatus of Soxhlet (1 L) which gone up on a flask of two L, which contain dichloromethane (1.4 L). This process allowed us to extract alkaloids during 7 to 8 hours at least 7 cycles (this procedure was repeated several times using 40 L of dichloromethane). After that, the chloroform phase which contain alkaloids in base form was concentrated by evaporating the solvent. Then, it was purified by using successive liquid-liquid extraction using a solution of HCl (726 mL; 0.5 N; pH = 1). This procedure was tracked using Mayer test (alkaloids in form of salt were solubilized in aqueous phase while neutral impurities were remained in organic phase).

The aqueous phase was alkalized by using sodium hydroxide until pH = 9. Then, it was extracted again by using dichloromethane solvent (250 mL). This procedure was repeated until Mayer test of aqueous phase was negative, due to all alkaloids were passed to organic phase. The latter was concentrated to dryness. From this extraction, we obtained an alkaloid extract weighing 1.0382g (Figure II-B-01).

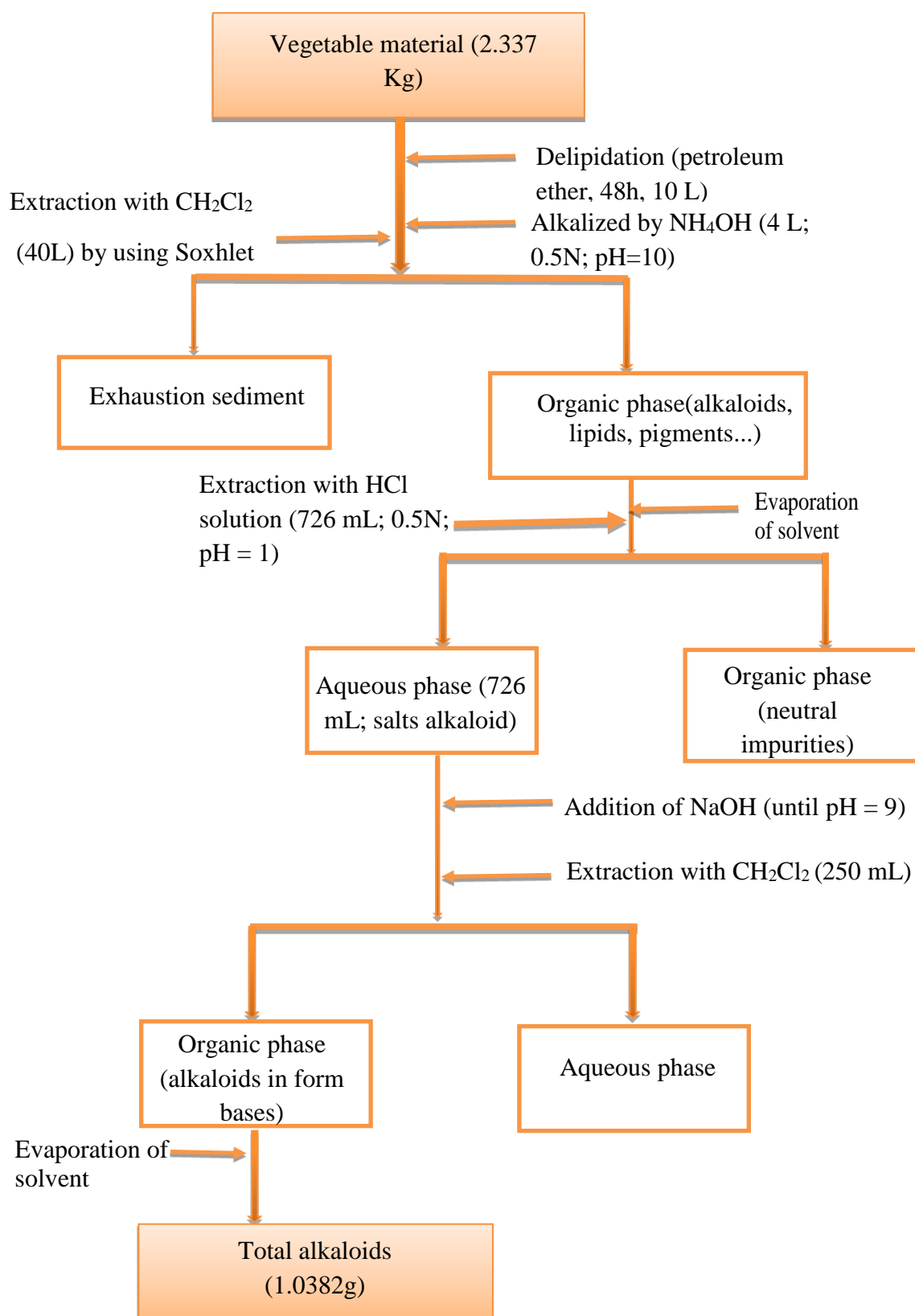


Figure II-B-01: Protocol of extraction of alkaloids

II-B-1-2-Isolation and purification of alkaloids

1.0382 g of total alkaloids extract was deposited on a column of silica gel eluting with toluene-acetone starting with toluene 100% to acetone 100%.

87 fractions of 25 mL were collected and tested using TLC plate in order to combined 7 similar sub-fractions [A-G] (Figure II-B-02).

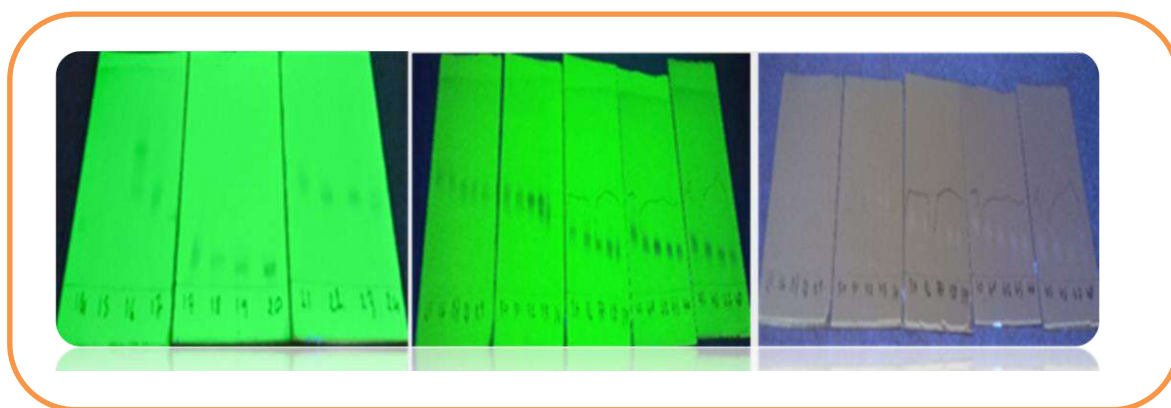


Figure II-B-02: Monitoring of fractionation of alkaloids extract

FA sub-fraction ([F22-F23]; 9.8 mg) was separated by PTLC using cyclohexane-EtOAc-NH₄OH (9:3:0.1). The band that has been scraped was washed then purified by C18 column using H₂O-MeOH (2:1) as eluent. This separation allowed us to obtain **P1** (0.4 mg).

FB sub-fraction ([F26-F28]; 7.4 mg) was chromatographed on a PTLC using the system cyclohexane-EtOAc-NH₄OH (6:3:0.1). Two bands have been scrapped and washed. The first band was rechromatographed on a PTLC, using the system cyclohexane-EtOAc-NH₄OH (7:3:0.1) to get **P2** (0.8 mg). The second band was purified by C18 column with the system
H₂O-MeOH (2:1).
Two sub-fractions that have been obtained were filtered on a column of silica gel eluting with cyclohexane-EtOAc (15:3). This separation allowed us to obtain **P3** (0.6 mg) and **P4** (0.1 mg).

FC sub-fraction ([F30-F32]; 17.3 mg) was submitted on a PTLC eluting with cyclohexane-EtOAc-NH₄OH (6:3:0.1) to obtain two bands. The first band was purified by C18 column with the system H₂O-MeOH (1:1). The first sub-fraction was purified by PTLC eluting with cyclohexane-EtOAc-NH₄OH (10.5:3:0.1) to obtain **P5** (0.1 mg). From the

second and third sub-fractions we were obtained **P6** (1.2 mg) and **P7** (0.1 mg), respectively. The second band was separated by C18 column for two time in a row using the system H₂O-MeOH (6:1/ 8:1 in each time). The second sub-fraction was purified by column of silica gel eluting with the system cyclohexane-EtOAc (15:3) then, by PTLC using the system cyclohexane-EtOAc-NH₄OH (7:3:0,1) to obtain **P8** (0.6 mg) and **P9** (0.9 mg).

FD sub-fraction ([F37-F40]; 39.2 mg) was separated by PTLC eluting with the system cyclohexane-EtOAc-NH₄OH (3:0.5:0.1), the band that has been scraped and washed was deposited on C18 column eluting with H₂O-MeOH (5:1 then 4:1). This separation allowed us to obtained two sub-fractions. The first sub-fraction was purified by C18 column with the system H₂O-MeOH (6:1) then by silica gel column using the system cyclohexane-EtOAc (10:3) to obtain **P10** (1.2 mg). From the second sub-fraction we were obtained **P11** (0.6 mg).

FE sub-fraction ([F41-F48]; 31.1 mg) was chromatographed on a PTLC using the system cyclohexane-EtOAc-NH₄OH (4:3:0.1). Two bands have been scraped and washed. The first band was purified by C18 column eluting with the system H₂O-MeOH (4:1) then by column of silica gel using the system cyclohexane-EtOAc (15:3). This separation allowed us to separate **P12** (1.3 mg), **P13** (1.7 mg) and **P14** (1.7 mg). The second band was purified by PTLC using the system cyclohexane-EtOAc-NH₄OH (1:1:0.1). **P15** (0.8 mg) was obtained.

FF sub-fraction ([F52-F57]; 52.4 mg) was submitted to a PTLC using cyclohexane-EtOAc-NH₄OH (4:3:0.1) as eluent. Six bands have been scraped and washed. The first band was purified by C18 column using the system H₂O-MeOH (1:1), then, by PTLC with the system cyclohexane-EtOAc-NH₄OH (4:3:0.1) to obtained **P16** (0.2 mg) and **P17** (0.2 mg). The second band was purified by C18 column eluting with H₂O-MeOH (1:1). Two sub-fractions have been obtained. The first sub-fraction was purified by silica gel column using the system cyclohexane-EtOAc (1:1). **P18** (1.8 mg) was obtained. The second sub-fraction was purified by PTLC with the system cyclohexane-EtOAc-NH₄OH (1:1:0.1) to obtained **P19** (0.1 mg). The third band was purified by PTLC eluting with cyclohexane-EtOAc-NH₄OH (1:2:0.1). The latter allow to separate **P20** (1 mg). The fourth, fifth and sixth bands were purified by the same latter process to give **P21** (1 mg), **P22** (1 mg) and **P23** (1.1 mg).

FG sub-fraction ([F58-F68]; 90.5 mg) was deposited on a column of silica gel using the system CH₂Cl₂- EtOAc (starting by 98% of CH₂Cl₂ to 100% of EtOAc), three sub-fractions were obtained. The first sub-fraction was purified by PTLC with the system cyclohexane-

EtOAc-NH₄OH (4:3:0.1) in order to obtain **P24** (0.1 mg). The same process was repeated to purify the second and the third sub-fractions to obtain **P25** (0.4 mg) and **P26** (0.5 mg).

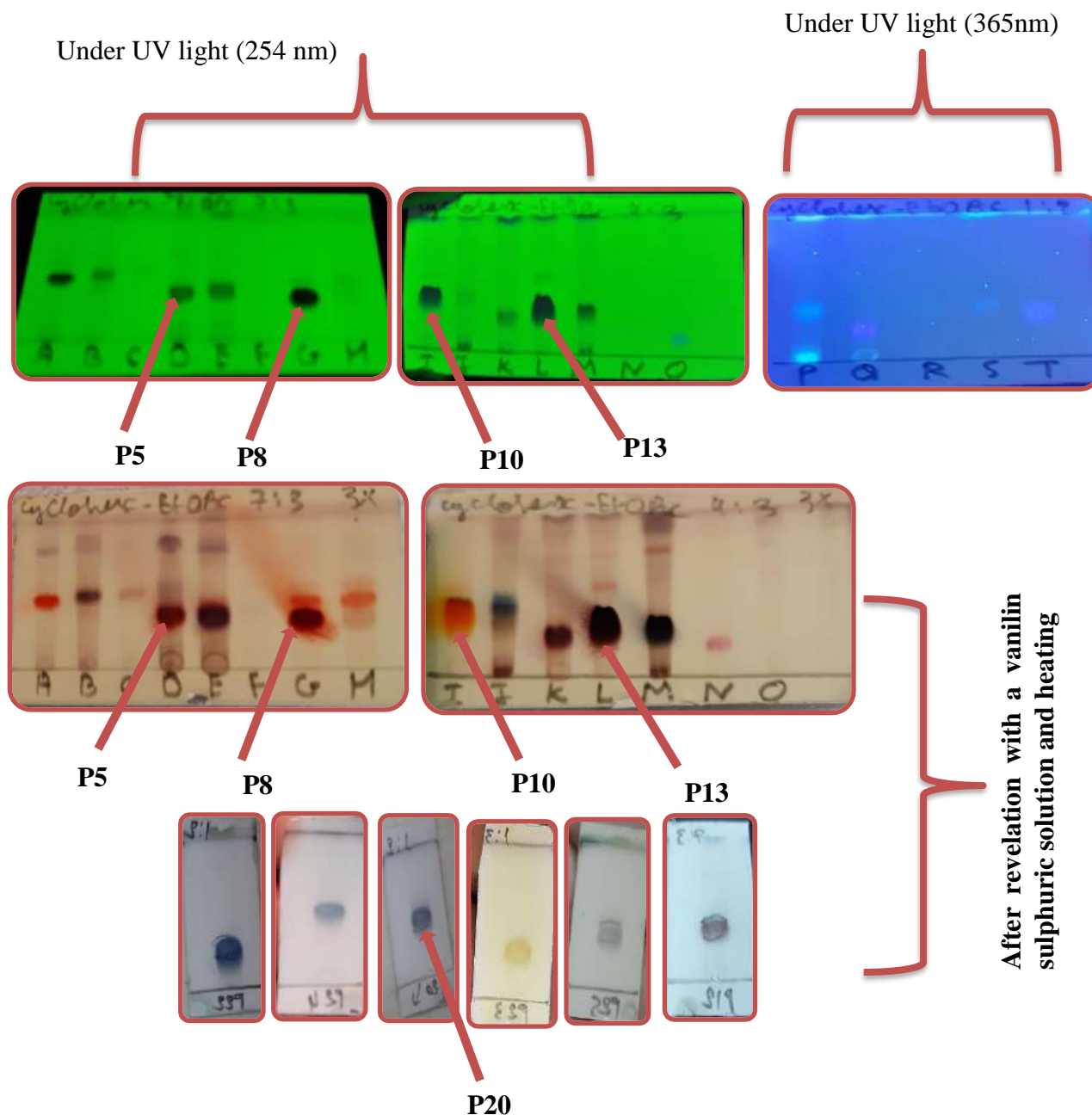
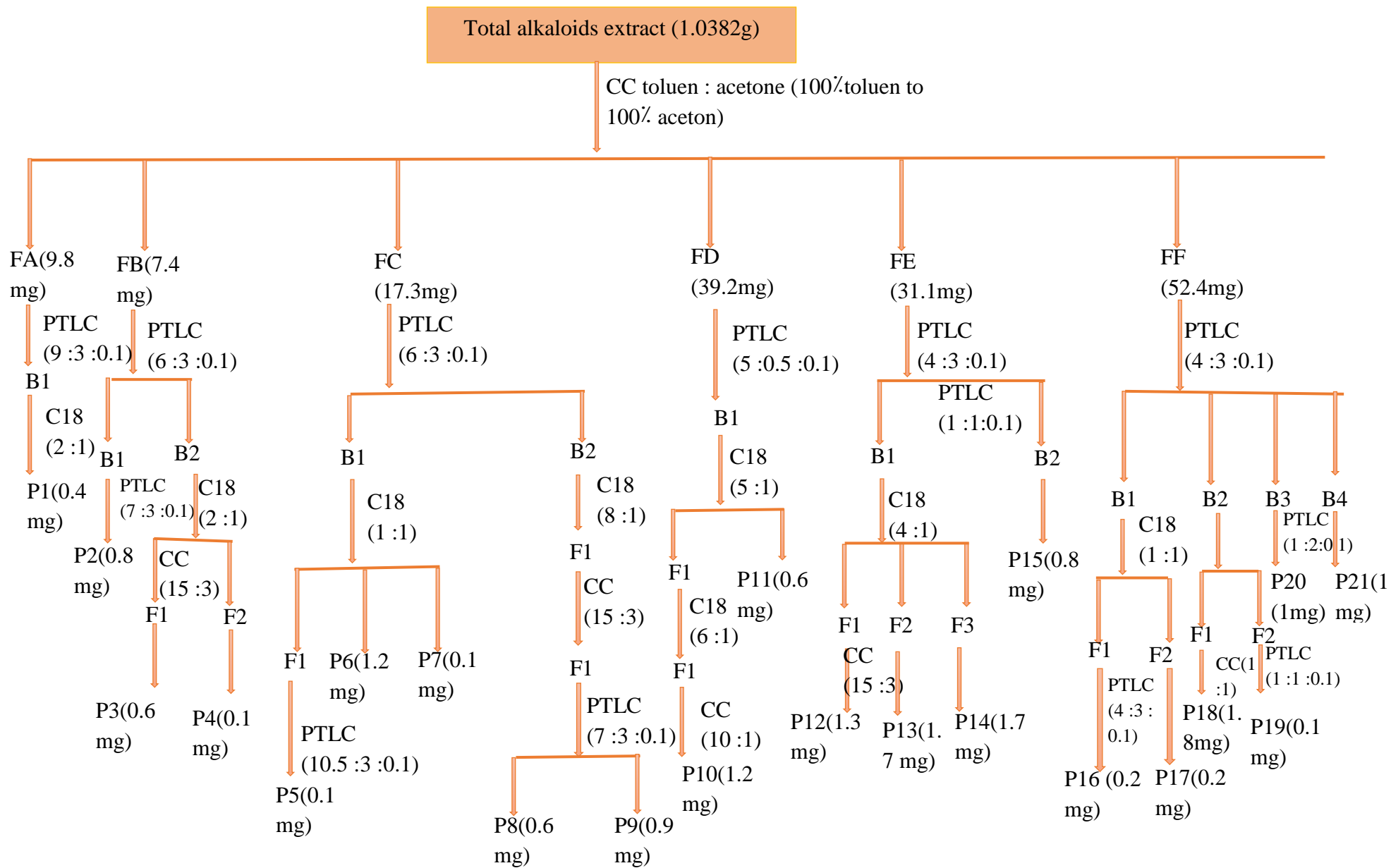


Figure II-B-03: TLC test of alkaloids isolated from *P. tomentosa*

Material and Method Part : Phytochemical Study of *P.tomentosa*



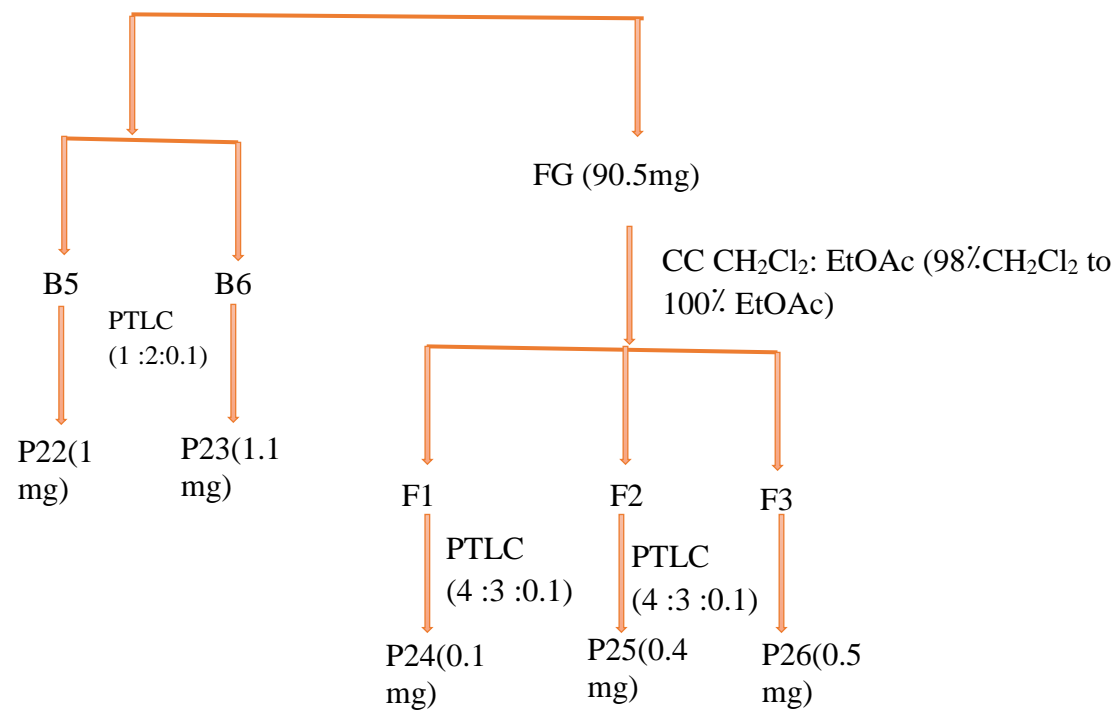


Figure II-B-04: Fractionation Scheme of alkaloid extract

II-B-2-Extraction, isolation and purification of cardenolides and phenolic compounds

II-B-2-1-Extraction of cardenolides and phenolic compounds

228.141 g of vegetable material (leaves and stems of *P. tomentosa*) was macerated in petroleum ether for 24 hours in order to eliminate fats and chlorophylls. Then, it was filtered and dried. After that, the sediment was macerated in hydroalcoholic mixture (8/2 methanol/distilled water) and left for 24 hours. The maceration procedure was repeated three times with renewing the solvent. This extractive solution was filtered and evaporated to dryness. The residue obtained was diluted with distilled water at a rate of 400-600 ml per 1 Kg of dry matter and left it to stand overnight then it was filtered.

The macerate was fractionated successively with three solvents of increasing polarity, starting with: chloroform three times, then, ethyl acetate once and finally, n-butanol six times. The three organic extracts were concentrated to dryness, then, they were weighed (Figure II-B-05).

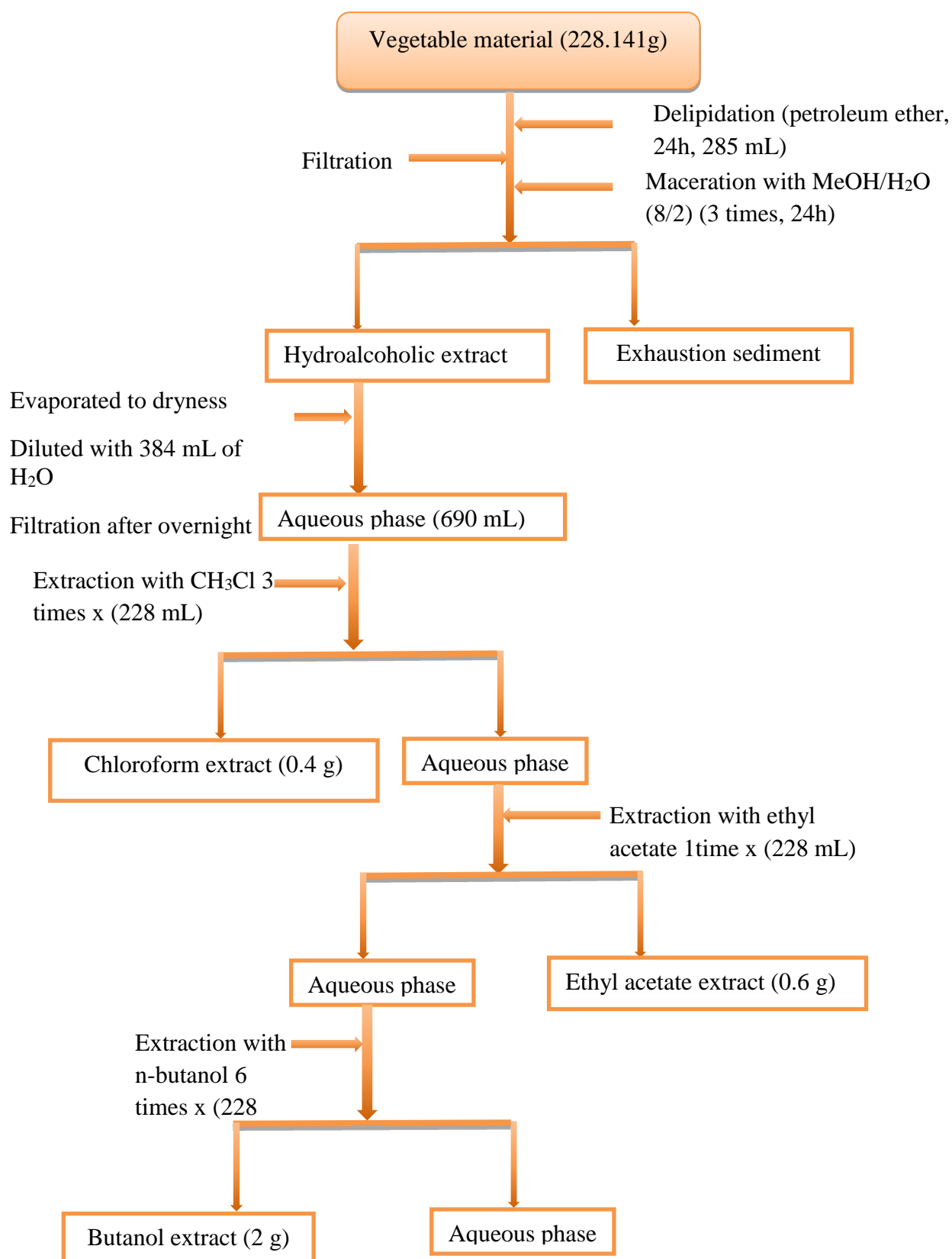


Figure II-B-05: protocol of extraction of cardenolides and phenolic compounds.

II-B-2-2-Isolation and purification of cardenolides and phenolic compounds

2,6 g of combine butanol and ethyl acetate extracts were deposited on a column of silica gel and eluted by polar gradient of system consist of: CH₂Cl₂: MeOH. The proportions used were as flows: 95:5; 90:10; 88:12; and finally, 85:15.

74 fractions of 25ml were collected and tested by using a TLC plate which visualised by using UV light (254 and 365 nm), and revealed with vanillin sulphuric and heating. This process allowed us to combin similar fractions (figure II-B-06).

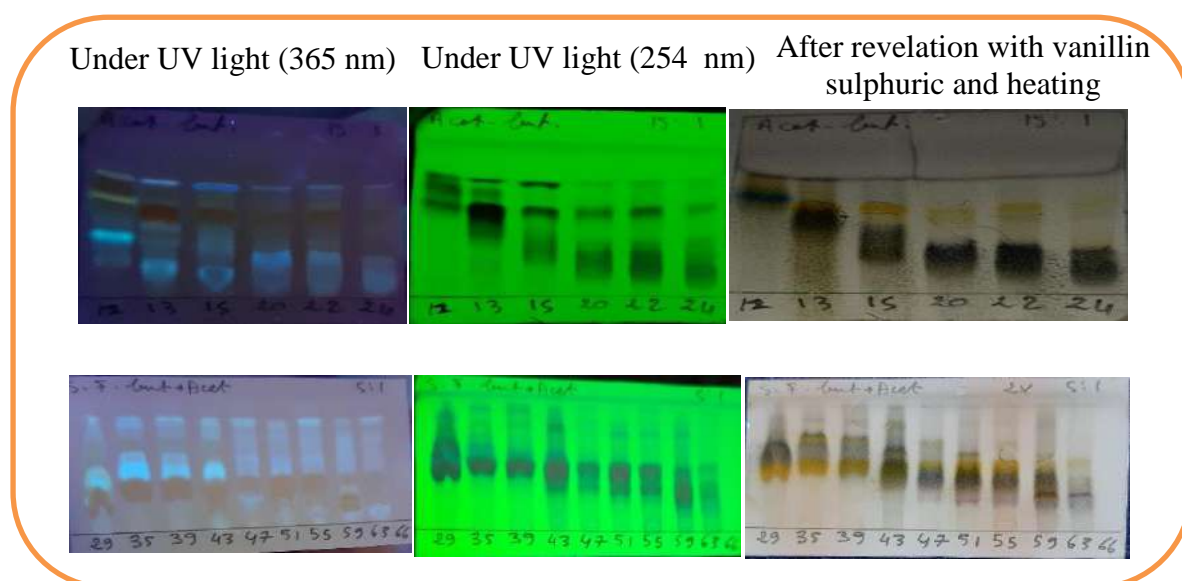


Figure II-B-06: Monitoring of fractionation of combined extracts (EtOAc and n-butanol extracts)

F13 – F26 fractions were combined and separated sequentially by using Sephadex column (LH20) using CH₂Cl₂: MeOH (4:1) as eluent. F_a1 -F_a10 sub-fractions were combined then submitted to a C18 column which eluted with the system: H₂O: MeOH (6:1 then 4:1). This separation allowed us to obtained two sub-fractions. The first sub-fraction was purified by using PLTC with the system: CH₂Cl₂: MeOH:CH₃COOH (12:1:0.1) to obtain **PN** (20.4 mg).

F_a11-F_a26 sub-fractions were purified by using PTLC successively with the system: CH₂Cl₂: MeOH:CH₃COOH (20: 1: 0.1 then 30:1: 0.1). This purification gave **PJI** (9 mg).

F27-F46 fractions (337.3 mg) were combined then rechromatographed on a column of silica gel using CH₂Cl₂: MeOH as eluent with the proportions: 15:1; 12:1; 7:1. F_a8 – F_a21

sub-fractions were combined then separated by using Sephadex column (LH-20) with the system CH_2Cl_2 : MeOH (4:1), this separation gave three sub-fractions. The first sub-fraction was purified by using C18 column using the system H_2O : MeOH (5:1 then 3:1). The latter allows to separate **PM** (4.3 mg) by recrystallization in water.

The second sub-fraction was separated by using C18 column, repeated this process four times in a row using the systems H_2O : MeOH (5:1/ 6:1/8:1/ 100% H_2O in each time). The latter was purified by using Sephadex column (LH-20) with the system: CH_2Cl_2 : MeOH (10:1) to obtain **PB** (4.5 mg).

The third sub-fraction was separated by using C18 column using the system H_2O : MeOH (5:1), then, it was purified by using PTLC with the system CH_2Cl_2 : MeOH: CH_3COOH (9:1:0.1 then 7:1:0.1). Compound **PJ** (22.8 mg) was obtained.

F_a22-F_a36 sub-fractions were combined and submitted to a C18 column for two times in a row using the systems CH_2Cl_2 : MeOH (6:1/ 8:1 in each time). The first sub-fraction resulting from this separation was separated by using PTLC with the system CH_2Cl_2 : MeOH: CH_3COOH (15:1:0.1 then 9:1:0.1). The band that has been scraped was washed then rechromatographed on a C18 column which eluted with 100% H_2O . The latter was purified by using PTLC with the system CH_2Cl_2 : MeOH: CH_3COOH (12:1: 0.1) then by using Sephadex column (LH-20) for two times in a row using the systems CH_2Cl_2 : MeOH (10:1). This separation allowed us to obtained **PVe** (6 mg).

F47-F74 were combined and separated by using C18 column using the system H_2O : MeOH (6:1). From this separation we obtained two sub-fractions. F_a1-F_a2 sub-fractions were combined and chromatographed on PTLC with the system CH_2Cl_2 : MeOH: CH_3COOH (10:1:0.1 then 8:1:0.1). The band that has been scraped was washed then purified by using Sephadex column (LH-20) for four times in a row using the same system CH_2Cl_2 : MeOH (10:1). This separation gave **PR** (6 mg).

F_a8-F_a30 sub-fractions were combined then separated by using PTLC with the system CH_2Cl_2 : MeOH: CH_3COOH (15:1:0.1). The band that has been scraped was washed then purified by using C18 column with the system H_2O : MeOH (9:1) to obtain **PV** (13.1mg).

Material and Method Part: Phytochemical Study of *P.tomentosa*

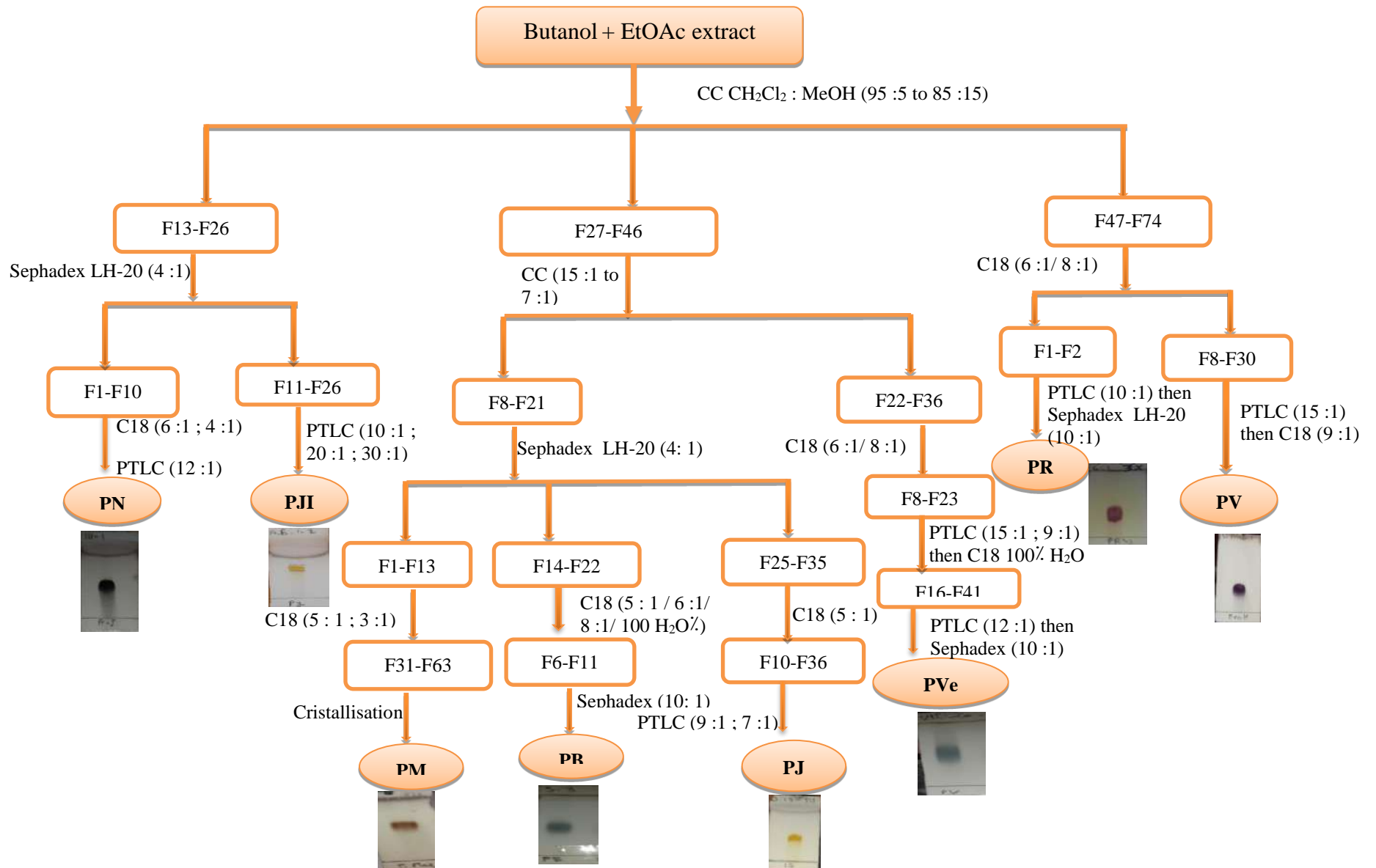


Figure II-B-07: Fractionation of combined extracts (EtOAc and butanol extracts)

PART III: RESULTS AND
DISCUSSION

***Chapter A: Qualitative and Biological
study of P. tomentosa***

III-A-1-Phytochemical tests

Phytochemical tests of stems and leaves extracts of *P. tomentosa* showed that this plant is rich of various secondary metabolites. The results obtained were illustrated in Table III-A-01:

Table III-A-01: Chemical screening of *Pergularia tomentosa*

Secondary metabolites	Stems	Leaves
Flavonoids	+	++
Alkaloids	+	++
Tannins	+	++
Reducing compounds	+	+
Cardionolides	+++	+++
Terpenoids	+++	++
Triterpenoids	+++	+++
Steroids	+++	++
Saponins	-	++
Free quinones	+	++
Proteins	+	-

-: Absence, +: Indicates the degree of presence

The results of phytochemical tests revealed that both leaves and stems extracts are rich in cardenolides, terpenoids, steroids, and triterpenoids. Flavonoids, alkaloids, free quinones and tannins were detected in high amounts in leaves extract compared to stems extract. Saponins was detected only in leaves extract, while proteins were detected only in stems extract.

The richness of *P. tomentosa* extracts in cardenolides explains the toxicity of this plant which certainly explains their use in the treatment of diseases at low concentrations.

III-A-2-Quantitative study

III-A-2-1-Total Phenolic Content (TPC)

TPC contents of different extracts is expressed in mg EAG /g of plant dry weight which calculated using linear regression equation of calibration curve plotted of gallic acid (Figure III-A-01).

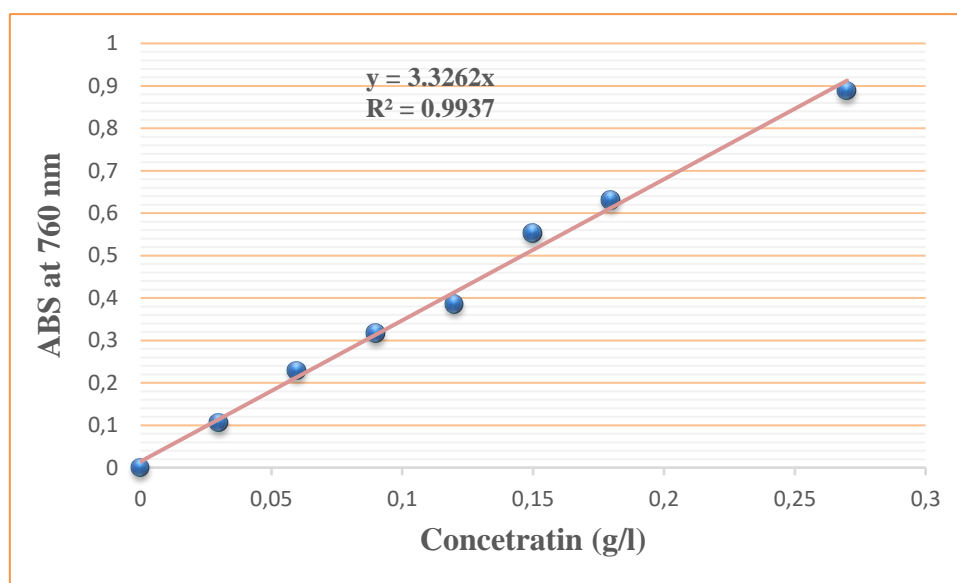


Figure III-A-01: Gallic acid calibration curve

Table III-A-02: Total phenolic content (TPC) of different stems and leaves extracts of *P. tomentosa*

Extract	Stems (mg EAG /g of plant dry weight)	Leaves (mg EAG /g of plant dry weight)
Crude	0.101 ± 0	0.1766 ± 0.0047
Chloroform	0.2246 ± 0.002	0.1336 ± 0.0035
Ethyl acetate	0.2093 ± 0.018	0.3446 ± 0.0087
n-Butanol	0.1553 ± 0.0074	0.5343 ± 0.045
Aqueous	-	0.321 ± 0.047

TableIII-A-02 present a comparison of the phenolic content between stems and leaves extracts of *P. tomentosa*.

The results showed that leaves extracts are richer in phenolic compounds compared to stems extracts (except chloroform extract).

In stems extracts, TPC varied from 0.101 ± 0 mg GAE/g of plant dry weight to 0.2246 ± 0.002 mg GAE/g of plant dry weight. The highest phenolic content is recorded in chloroform extract, in the other hand, the lower phenolic content is recorded in crude extract.

In leaves extracts, TPC varied from 0.1336 ± 0.0035 mg GAE/g of plant dry weight to 0.5343 ± 0.045 mg GAE/g of plant dry weight. The highest phenolic content is recorded in butanol extract, while, the lower phenolic content is recorded in chloroform extract.

Total phenolic content of different leaves extracts is classified according to the following decreasing order: Butanol extract > Ethyl acetate extract > Aqueous extract > Crude extract > Chloroform extract.

Total phenolic content of different stems extracts is classified according to the following decreasing order: Chloroform extract > Ethyl acetate extract > Butanol extract > Crud extract.

We observed that the increase in phenolic content of stems and leaves extracts is not related to the increase in polarity of solvents due to determination of total phenolic content by Folin-Ciocalteu reagent is a non-selective assay, there are interference of nonpolyphenol compounds such as reduced sugars and vitamin C with this reagent [104].

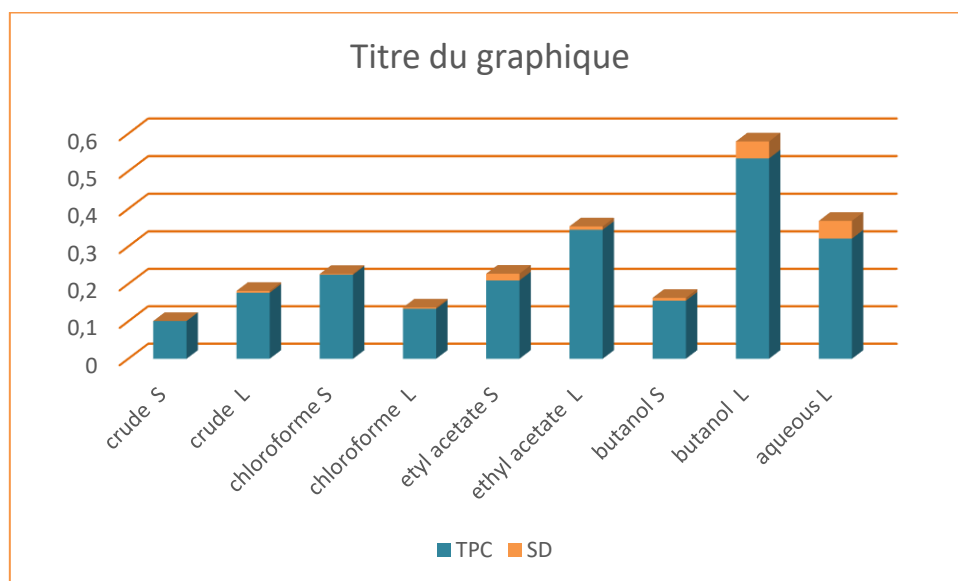


Figure III-A-02: Total phenolic content (TPC)

III-B-2-2-Total flavonoids content (TFC)

A calibration curve of quercetin was drawn in order to determine TFC of different extracts of *P. tomentosa* which expressed in mg QE /g of plant dry weight using linear regression equation of this curve (Figure III-A-03).

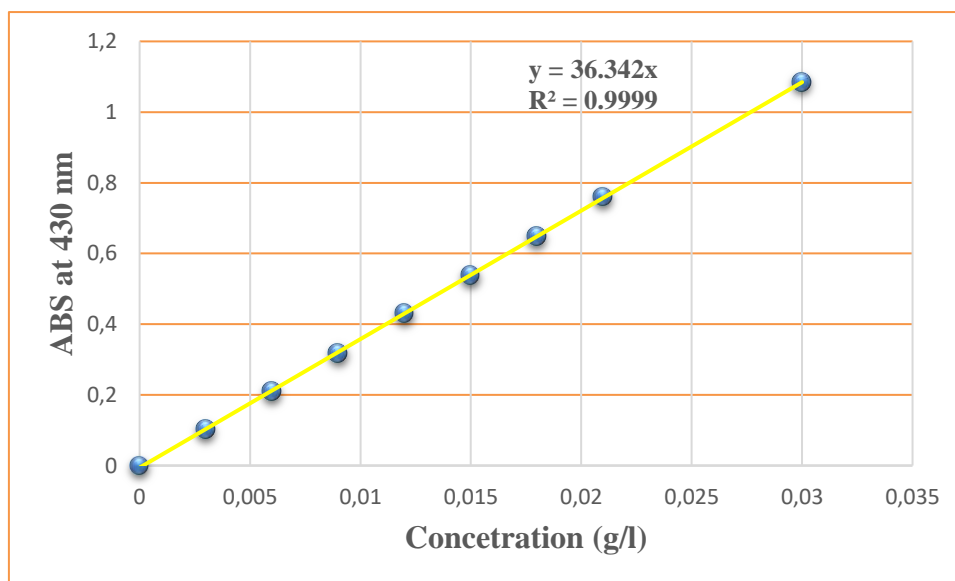


Figure III-A-03: Quercetin calibration curve

Table III-A-03: Total flavonoid content (TFC) of different stems and leaves extracts of *P. tomentosa*.

Extract	Stems (mg QE /g of plant dry weight)	Leaves (mg QE /g of plant dry weight)
Crude	0.071 ± 0.0046	0.066 ± 0.00028
Chloroform	0.00586 ± 0.0012	0.0253 ± 0.0016
Ethyl acetate	0.0444 ± 0.00079	0.043 ± 0.00077
Butanol	0.1249 ± 0.00127	0.486 ± 0.014
Aqueous	-	0.205 ± 0.0034

Table III-A-03 illustrate a comparison of flavonoid content between stems and leaves extracts of *P.tomentosa*.

The results showed that total flavonoid content (TFC) of both stems and leaves extracts is rather low compared to the phenolic content (TPC).

In stems extracts, TFC varied from 0.00586 ± 0.0012 mg QE/g of plant dry weight to 0.1249 ± 0.00127mg QE/g of plant dry weight. The highest flavonoid content is recorded in butanol extract, while, the lower flavonoid content is recorded in chloroform extract.

In leaves extracts, TFC varied from 0.0253 ± 0.0016 mg QE/g of plant dry weight to 0.486 ± 0.014 mg QE/g of plant dry weight. The highest phenolic content is recorded in butanol extract, while, the lower phenolic content is recorded in chloroform extract.

Total flavonoid content of different stems extracts is classified according to the following decreasing order: Butanol extract > Ethyl acetate extract> crude extract> chloroform extract.

Total flavonoid content of different leaves extracts is classified according to the following decreasing order: Butanol extract > Aqueous extract > crude extract> Ethyl acetate extract> chloroform extract.

From this results we showed that polar extracts are rich in flavonoid content compared to no-polar extracts, this can be explained by the results obtained by S.Heneidak *et al.*, which

highlight that *P. tomentosa* produce flavonol glycosides type [105] that generally soluble in polar solvent.

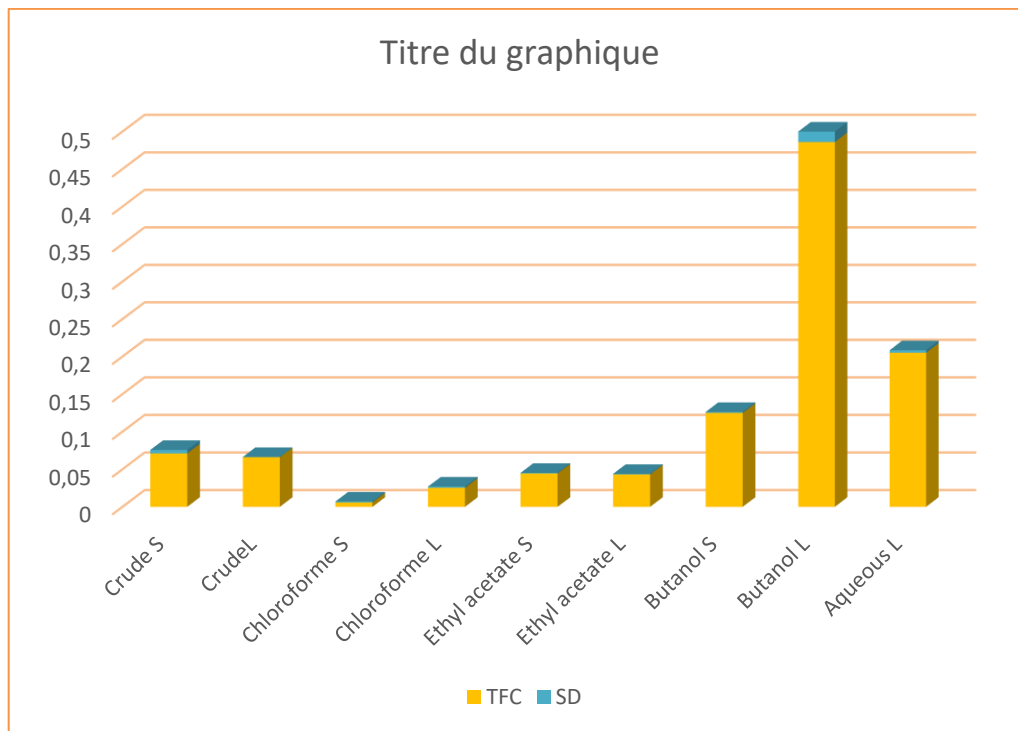


Figure III-A-04: Total flavonoid content (TFC)

III-A-2-3-Total tannins content (TTC)

A calibration curve of catechin was drawn in order to determine TTC of different stems and leaves extracts of *P. tomentosa*, which expressed in mg ECA /g of plant dry weight using linear regression equation of this curve (Figure III-A-05).

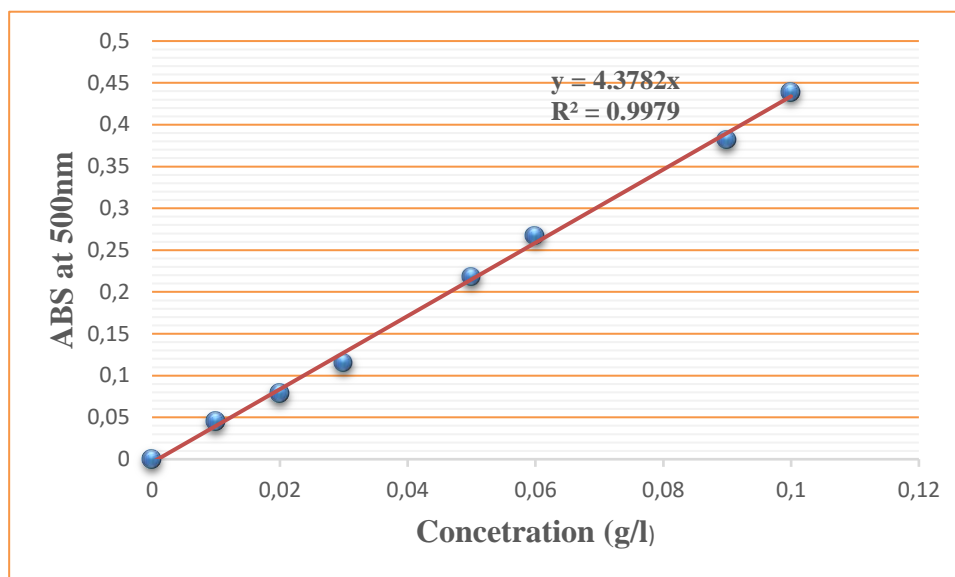


Figure III-A-05: Catechin calibration curve

Table III-A-04: Total tannins content (TTC) of different stems and leaves extracts of *P. tomentosa*.

Extract	Stems (mg ECA /g of plant dry weight)	Leaves (mg ECA /g of plant dry weight)
Crude	0.084 ± 0.0098	0.136 ± 0.0132
Chloroform	0.029 ± 0.0005	0.085 ± 0.0055
Ethyl acetate	0.061 ± 0.002	0.069 ± 0.0037
Butanol	0.133 ± 0.0211	0.149 ± 0.0159
Aqueous	-	0.436 ± 0.0046

TableIII-A-04 illustrate a comparison of tannin content between stems and leaves extracts of *P. tomentosa*.

These results show that the leaves extracts are rich in total tannins content (TTC) compared to the stems.

Results and Discussion Part: Qualitative and Biological Study of P.tomentosa

In stems extracts, TTC varied from 0.029 ± 0.0005 mg CE/g of plant dry weight to 0.133 ± 0.0211 mg CE/g of plant dry weight. The highest tannin content is recorded in butanol extract, while, the lower tannin content is recorded in chloroform extract.

In leaves extracts, TTC varied from 0.069 ± 0.0037 mg CE/g of plant dry weight to 0.436 ± 0.0046 mg CE/g of plant dry weight. The highest phenolic content is recorded in aqueous extract, while, the lower phenolic content is recorded in ethyl acetate extract.

Total tannin content of different stems extracts is classified according to the following decreasing order: Butanol extract > Crude extract > Ethyl acetate extract > Chloroform extract.

Total tannin content of different leaves extracts is classified according to the following decreasing order: Aqueous extract > Butanol extract > Crude extract > chloroform extract > Ethyl acetate extract.

The catechin used as a standard to determine the total tannin content (TTC) of different extracts, it is a condensed tannin soluble in water [106], this explains the richness of aqueous extract in tannin content compared to the other extracts.

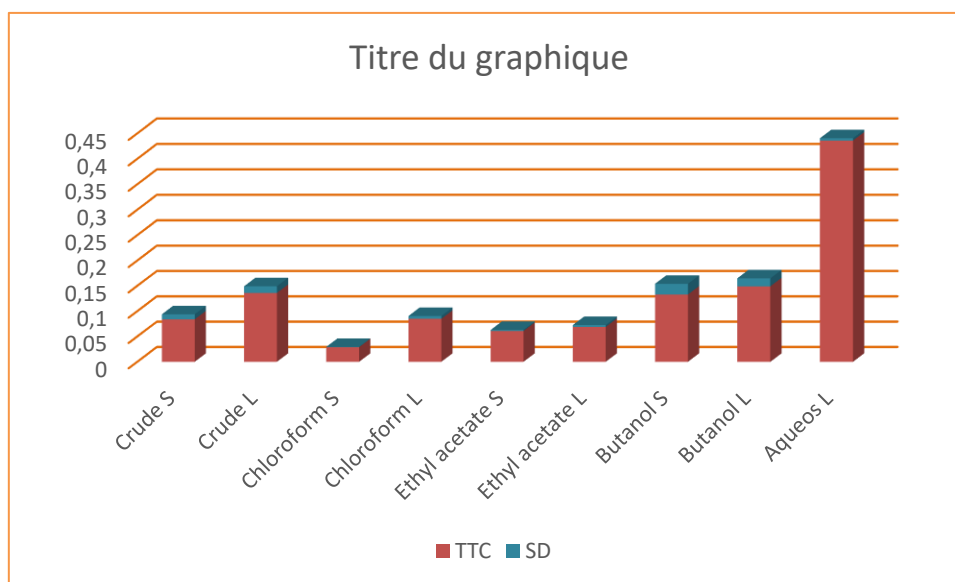


Figure III-A-06: Total tannin content (TTC)

III-A-3-Evaluation of *in vitro* biological activities

III-A-3-1-Antioxidant activity

III-A-3-1-1-DPPH• radical scavenging test

In order to illustrate the antiradical activity of different stems and leaves extracts, curves of concentration as a function of the percentage of inhibition of different extracts, have been drawn (Figure III-A-07 and III-A-08).

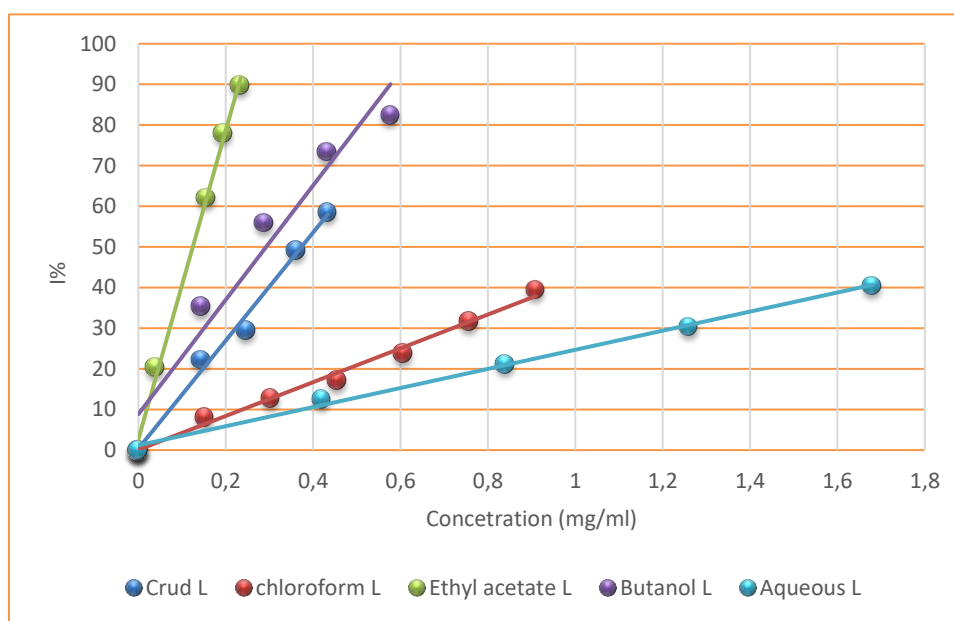


Figure III-A-07: Variation of DPPH inhibition as a function of concentration of the leaves extracts

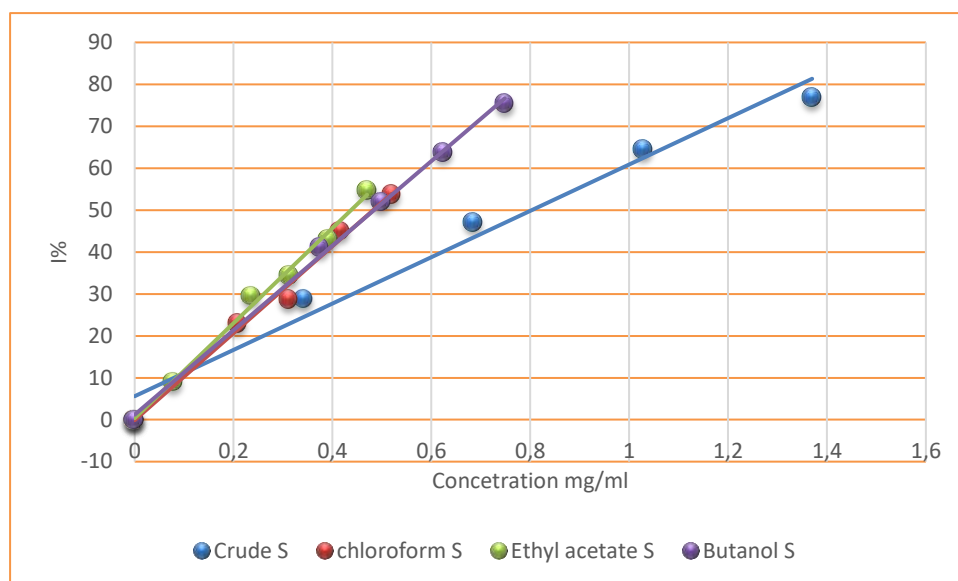


Figure III-A-08: Variation of DPPH inhibition as a function of concentration of the stems extracts

Table III-A-05: Results of the antiradical activity evaluated by the DPPH* test

Extracts	IC ₅₀ (mg/mL)
Crude S	0.4 ± 0.0
Chloroform S	0.235 ± 0.01
Ethyl acetate S	0.205 ± 0.02
n-Butanol S	0.245 ± 0.01
Crude L	0.175 ± 0.01
Chloroform L	0.605 ± 0.03
Ethyl acetate L	0.05 ± 0.02
n-Butanol L	0.07 ± 0.01
Aqueous L	0.94 ± 0.32
BHT	0.002 ± 0.0
Vitamin C	0.0045 ± 0.0

S: Stems; L: Leaves

These results show that all the extracts have an antiradical power against DPPH[•]. IC₅₀ value is inversely proportional to the antioxidant activity: the extract with the lowest value of IC₅₀, it has the highest antioxidant activity.

The IC₅₀ values of the different stems extracts of *P. tomentosa* varied from 0.4 ± 0.0 to 0.205 ± 0.02 mg/mL. The best antiradical activity of stems is recorded in the ethyl acetate stems extract, on the other hand, the minimum activity of these extracts is recorded in the crude stems extract. The IC₅₀ values are classified according to the following ascending order: Ethyl acetate extract < Chloroform extract < Butanol extract < Crude extract.

The IC₅₀ values of the different leaves extracts of *P. tomentosa* varied from 0.94 ± 0.32 to 0.05 ± 0.02 mg/mL. The best antiradical activity of leaves extracts is recorded in the ethyl acetate leaves extract, while, the minimum activity of these extracts is recorded in the aqueous leaves extract. The IC₅₀ values are classified according to the following ascending order: Ethyl acetate extract < Butanol extract < Crude extract < Chloroform extract < Aqueous extract.

For comparison, two standard antioxidants are used, BHT and ascorbic acid, they showed potent antiradical activity with IC₅₀ approximately of 0.002 ± 0.0 and 0.0045 ± 0.0 mg/ml respectively. The results showed that all stems and leaves extracts exhibit lower activity than those of BHT and ascorbic acid.

III-A-3-1-2- Reducing power of molybdenum Mo (VI) test

The curves of absorbance as a function of the inverse of the number of dilutions were plotting. They represent the variation of the reducing power of different leaves and stems extracts.

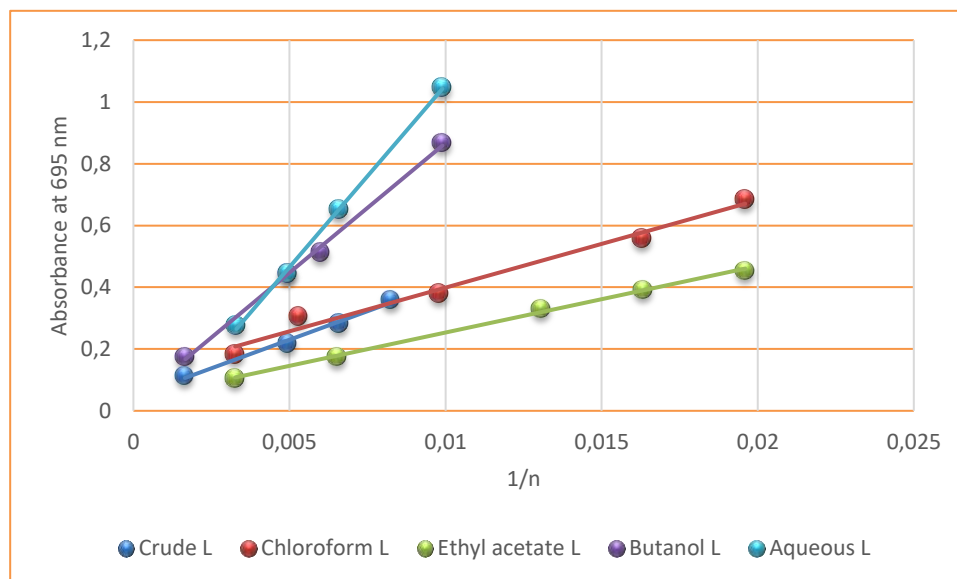


Figure III-A-09: Curves representing the reducing power of the leaves extracts.

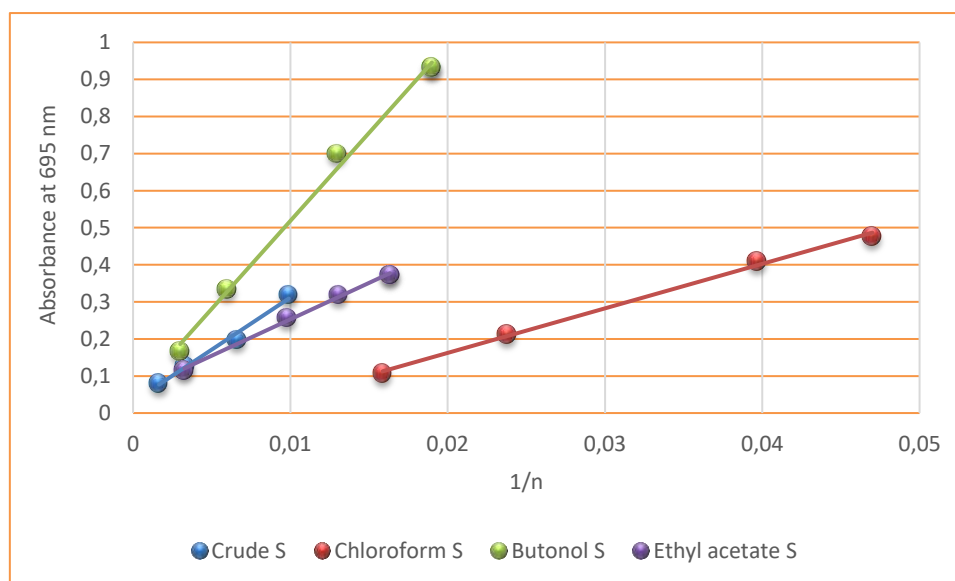


Figure III-A-10: Curves representing the reducing power of the stems extracts

Table III-A-06: Results of reducing power test (AEAC)

Extract	AEAC (mM)
Crude S	41.48 ± 1.06
Chloroform S	21.80 ± 4.28

Ethyl acetate S	42.62 ± 0.89
n-Butanol S	72.48 ± 8.62
Crude L	84.76 ± 0.05
Chloroform L	70.36 ± 7.71
Ethyl acetate L	51.45 ± 2.91
n-Butanol L	221.58 ± 7.09
Aqueous L	265.85 ± 8.09
BHT	4.96 ± 1.51
BHA	11.10 ± 7.55

S: Stems; L: Leaves

The results showed that all stems and leaves extracts have very good reducing activity, better than standards used: BHA and BHT. The reduction efficiency of molybdenum Mo (VI) is directly proportional to the value of AEAC.

The AEAC values of the different stems extracts of *P. tomentosa* varied from 72.48 ± 8.62 to 21.80 ± 4.28 mM. The best reducing capacity of stems extract is recorded in the butanol stems extract, on the other hand, the minimum activity of these extracts is recorded in the chloroform stems extract. The AEAC values are classified according to the following decreasing order: Butanol extract > Ethyl acetate extract > Crude extract > chloroform extract.

The AEAC values of the different leaves extracts varied from 265.85 ± 8.09 to 51.45 ± 2.91 mM. The best reducing capacity of leaves extract is recorded in the aqueous leaves extract, while, the minimum activity of these extracts is recorded in the ethyl acetate leaves extract. The AEAC values are classified according to the following decreasing order: Aqueous extract > Butanol extract > Crude extract > chloroform extract > Ethyl acetate extract.

The reductive capacity is based on the redox potential of antioxidants [107]. Z. Rahmani *et al.* reported that electron donor groups such as (OH, OCH₃, and alkyl) minimize the redox potential of polyphenols and increase their antioxidant capacities [57]. Therefore, the potent antioxidant activity of the stems and leaves extracts of *P. tomentosa* can be attributed mainly to the phenolic content, due to their hydroxyl groups, and / or to flavonoid

content which react with DPPH[•] giving free hydrogen atoms to the radicals [108]. For example, 3-O-galactoside and malonyl glucosides of quercetin is among the flavanols glycosides that is reported in *P. tomentosa* [20], and the oxidation potential of quercetin is around 0.25 V (Ag / AgCl) [57]. This low value of quercetin's oxidation potential greatly facilitates its electron donation.

From the evaluation of the antioxidant activity of *P. tomentosa* extracts, we show that these extracts give a good reduction of the molybdenum Mo (VI) and a weak inhibition of radical DPPH[•] compared to the standard antioxidants used. Therefore, we propose that the bioactive molecules exist in the extracts play a role of hydrogen donor more than the electrons donor.

➤ **Correlation between chemical composition and antioxidant capacity**

In order to study the relationship between the antioxidant activity of *P. tomentosa* extracts and their content in phenol, flavonoid and tannin compounds, we tried to find a linear correlation between the antioxidant capacity values calculated by the two methods (DPPH[•] and reduction of molybdenum Mo (VI) methods) and their total polyphenols, flavonoids and tannin content (Table III-A-07).

Table III-A-07-a: results of linear correlation between the IC₅₀ and AEAC values and the total polyphenols, flavonoids and tannins content of stems extracts

Correlation of stems extracts					
	TPC	TFC	TTC	IC ₅₀	AEAC
TPC	1	0.1983	0.1928	0.1319	0.1015
TFC	0.1983	1	0.9991	0.0424	0.9406
TTC	0.1928	0.9991	1	0.0530	0.9301
IC ₅₀	0.1319	0.0424	0.0530	1	0.0010
AEAC	0.1015	0.9406	0.9301	0.0010	1

Table III-A-07-b: results of linear correlation between the IC₅₀ and AEAC values and the total polyphenols, flavonoids and tannins content of leaves extracts

Correlation of leaves extracts					
	TPC	TFC	TTC	IC ₅₀	AEAC
TPC		0,79785	0,78191	0,34956	0,98632
TFC	0,79785		0,2725	-0,15937	0,75895
TTC	0,78191	0,2725		0,75631	0,82922
IC ₅₀	0,34956	-0,15937	0,75631		0,45488
AEAC	0,98632	0,75895	0,82922	0,45488	

The results showed that the TFC, TPC and TTC of the stems extracts don't correlate with the IC₅₀ values. While, TFC and TTC give excellent correlation with AEAC values with coefficient of determination (R= 0.96).

In the leaves extracts, both of TPC and TFC do not correlate with the IC₅₀ values. While, TTC give medium correlation with IC₅₀ values with coefficient of determination (R= 0.75). In the other hand, TFC and TTC give well to excellent correlation with AEAC values.

According to some studies, the antioxidant capacity depends on the structural conformation of compounds. It is generally influenced by the compounds in the samples and by the different mechanisms involved in the radical-antioxidant reactions. These compounds may have a vast set of chemical structures that could react with radicals by hydrogen donation and/or by electron transfer

There are no correlations between the two methods of antioxidant activity (AEAC and IC₅₀), these differences are attributed to a different mechanism of action of antioxidant compounds in each method. For this reason, the use of a method dependent on one mechanism may not reflect the true antioxidant capacity of compounds. Therefore, in the current research two types of antioxidant assays were performed to check the antioxidant potential of this plant.

III-A-3-2-Antidiabetic activity

III-A-3-2-1-Determination of percentage of inhibition of α -amylase activity

In order to determine the effect of stems and leaves extracts of *P.tomentosa* against activity of α -amylase enzyme; the inhibition percentage of this enzyme was calculated (Table III-A-08).

Table III-A-08: Percentage of inhibition of α -amylase

Extract	Percentage of inhibition I%
Chloroform S	23.94
Ethyl acetate S	36.44
Chloroform L	18.01
Ethyl acetate L	11.22
n-Butanol L	8.68
Aqueous L	2.74

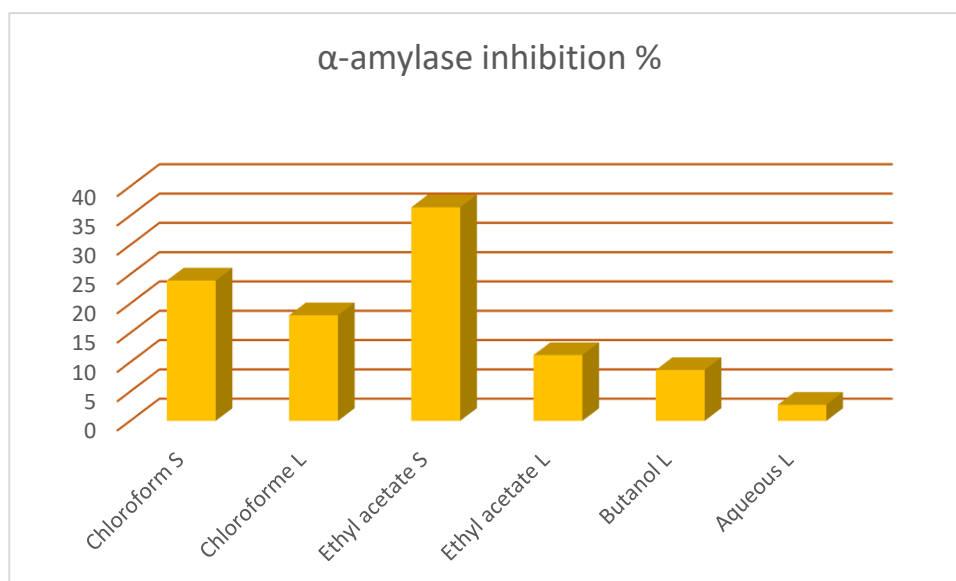


Figure III-A-11: Inhibition percentage of α -amylase activity of *P. tomentosa* extracts

The results show that extracts have different capacity to inhibit α -amylase enzyme. The highest inhibition was estimated at 36.44 and 23.94% in ethyl acetate and dichloromethane stems extract, respectively. While, the less inhibition was estimated at 8.68 and 2.74% in n-butanol and aqueous leaves extract respectively. This difference in inhibition may be due to the chemical nature of the compounds of each extract.

Phenolic compounds have height α -amylase inhibitory activity, which is confirmed by the studies of Md. Ali Asgar [109], P. Jiang *et al.* [110] and O. Oluwagunwa *et al.* [111], who were find that the inhibitory activity of α -amylase increases with an increase in the content of total phenolic compounds.

III-A-3-2-2-Determination of velocity of α -amylase activity

In order to determine the velocity of α -amylase activity in the presence and absence of inhibitory, we chose the ethyl acetate and dichloromethane stems extracts, due to their high inhibitory percentage.

Maltose standard curve was using in order to estimate concentration of reducing sugar released from starch and converted it to reaction velocities using the following equation:

$$V = C/T$$

V: α -amylase inhibition velocity

C: Concentration of reducing sugar released from starch

T: Time of incubation (30min)

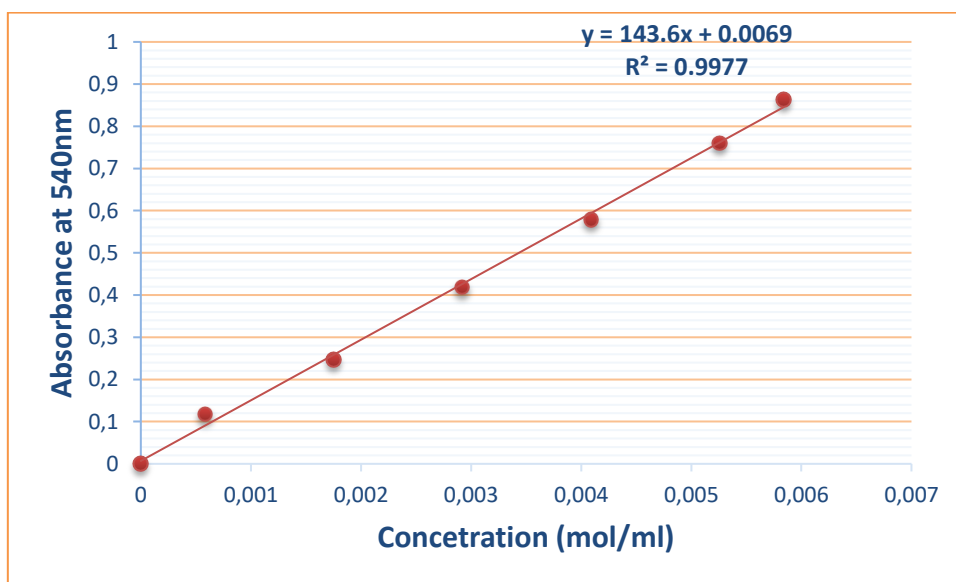


Figure III-A-12: Maltose calibration curve

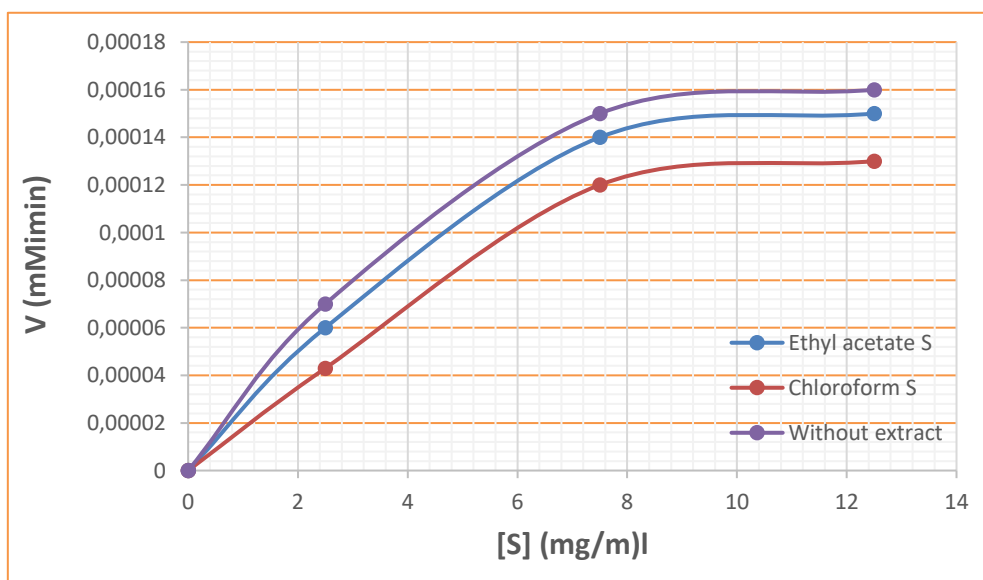


Figure III-A-13: Velocity of inhibition of α -amylase enzyme in the presence and absence of extract

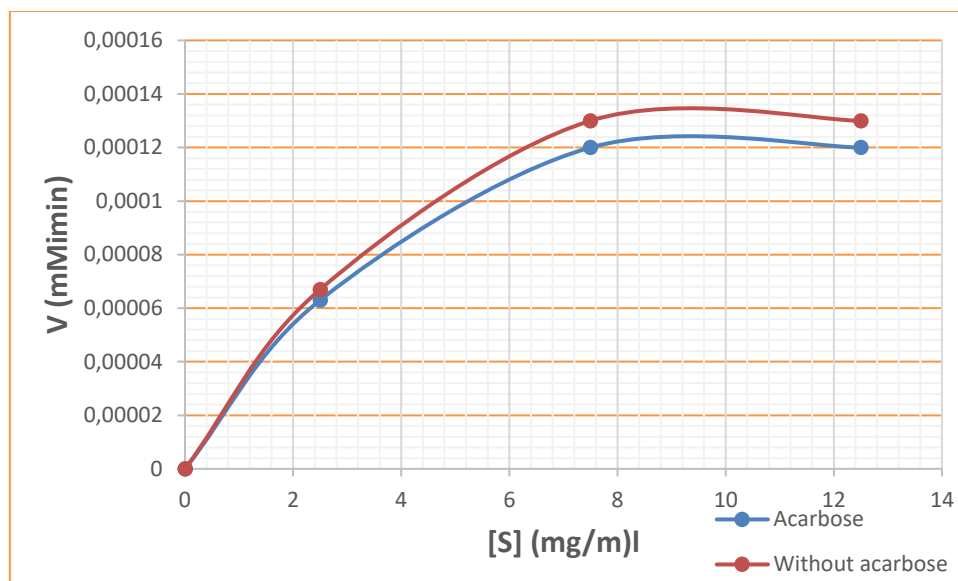


Figure III-A-14: Velocity of inhibition of α -amylase enzyme in the presence and absence of acarbose

Figure III-A-13 and III-A-14 illustrate that activity of α -amylase follows a Michaelian kinetics $V = f [S]$ [112]. According to this curve, the relationship between the concentration of starch and the enzymatic velocity is proportional in a range of linearity. We observed that the velocity has highest value at a starch concentration of 12.5 mg/mL where the curve deviates and showing a plateau, which is means that the active sites of the α -amylase enzyme are saturated.

III-A-4-Evaluation of *in vivo* biological activities

III-A-4-1-Determination of acute toxicity

Regular monitoring of mice behavior during 14 days revealed that both aqueous and crude extracts of *P. tomentosa* did not cause any signs of toxicity or mortality in any mouse at a single dose of 2000 mg/kg. There were no signs of changes were observed in skin, eyes, salivation, diarrhoea and weight loss of all mice. Therefore, the LD_{50} of these extracts is greater than 2000 mg/kg, which indicated that aqueous and crude extracts of *P. tomentosa* are considered as relatively safe according to the Globally Harmonized System (GHS) of Classification and Labelling of Chemicals [113]. This result is consistent with the results of V. K. Pothagar *et al.*, which reported that the oral administration of ethanol and chloroform

leaves extracts of *P.tomentosa* at dose of 2000g/Kg did not cause any toxicity symptoms [114].

III-A-4-2-Anti-inflammatory test

The injection of carrageenin caused edema in all treated mice. The percentage of this edema, and the percentage of its reduction using the crude extract, aqueous extract and reference ibuprofen are summarized in Table III-A-09.

Table III-A-09: Anti-inflammatory effect of the aqueous extract, the crude extract and ibuprofen on edema induced by carrageenin

Substance administered	Aqueous extract	Crude extract	Ibuprofen (reference)	Distilled water (control)
Percentage of edema (%)	9.96	24.96	7.19	43.79
Percentage reduction in edema (%)	77.25	43.00	83.58	/

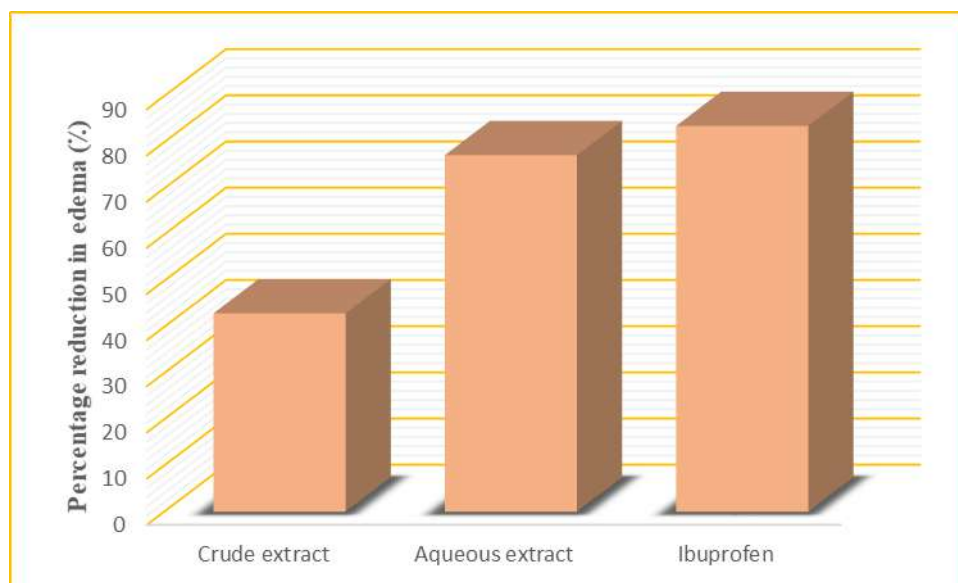


Figure III-A-15: Anti-inflammatory effect of the aqueous extract, the crude extract and ibuprofen

The results showed that the increase in paw volume (percentage of edema) in the groups treated with the extracts (9.96 % and 24.96 % for aqueous and crude extracts respectively) and ibuprofen (7.19 %) was less significant compared to the control group (43.79 %), which indicated that the oral administration of extracts and ibuprofen induce a highly significant inhibition of inflammation. The aqueous extract showed a percentage of inhibition (percentage reduction in edema) very close to that of reference ibuprofen (77.25 % and 83.58 for aqueous and ibuprofen respectively), while the crude extract showed lower percentage inhibition (43.00%) than reference ibuprofen. These results do not contradict those reported by V.L. Kumar *et al.* This study was conducted on the latex of *Calotropis procera* (Asclepiadaceae family) which has a chemotaxonomy very close to that of our plant. This study reported that the oral administration of dry latex of *Calotropis procera* at the dose of 5mg/Kg inhibited the development of paw edema in rats treated with carrageenin, with a percentage of inhibition of 71% [115].

The anti-inflammatory activity of the aqueous and crude extracts is linked to their chemical composition such as polyphenols, flavonoids, steroids, terpenoids, alkaloids. Most of these metabolites act by blocking the cyclooxygenase and lipoxygenase pathways as well as through other mechanisms [83]. The difference of anti-inflammatory activity between these extracts was probably associated with these bioactive compounds, which could be present at higher or lower concentrations depending on the solubility and affinity for the solvent used during the extraction.

III-A-4-3-Sedative activity

After 30 min of the placement of the mice (control, test and reference) in the actimeter, we recorded the numbers of displacements of each mice and calculated the average of the movement in order to calculate the percentage of reduction of movement; the results are summarized in Table III-A-10

Table III-A-10: Results of sedative activity of aqueous extract, crude extract and Haloperidol

Substance administrated	Aqueous extract	Crude extract	Haloperidol (reference)	Distilled water (control)
Average of the movement	242.16	192.83	44.5	479.16
Percentage of reduction of movement (%)	49.77	60.00	90.77	/

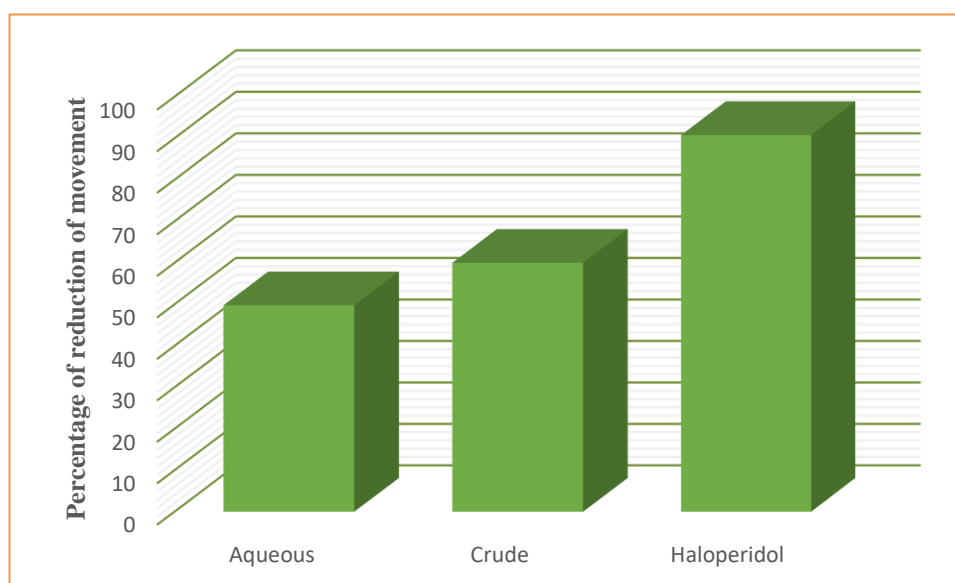


Figure III-A-16: Sedative activity of the aqueous extract, the crude extract and haloperidol

The results showed that the reduced in movement of the groups treated with the extracts (242.16 and 192 movement for aqueous and crude extracts, respectively) and haloperidol (44.5 movement) was more significant compared to the control group (479.16 movement). The oral administration of the extracts presented a percentage of reduction of movement of 49.77% and 60.00% for aqueous and crude extracts respectively, which indicated that aqueous and crude extracts of *P. tomentosa* exert a good sedative activity.

The sedative activity of aqueous and crude extracts could be related to their composition in bioactive compounds, in particular alkaloids, which have different therapeutic potential in neurological, psychiatric conditions and central nervous system inhibitions [90].

**Chapter B: Phytochemical study of P.
tomentosa**

III-B-1-Structural elucidation of alkaloids isolated from *P. tomentosa*

III-B-1-1-Compound P8

Compound P8 was obtained as colorless amorphous, it takes a red color after revelation with a vanilin sulphuric solution and heating. Its structure was characterized using NMR spectroscopic analysis methods, which are 1D: ^1H NMR and ^{13}C NMR and 2D: HSQC, HMBC and COSY. Its spectra are recorded in CDCl_3 .

- ❖ The ^1H NMR spectrum (Figure III-B- 01) of this compound showed:
 - Three doublet olefinic signals with an integration of one proton of each, at δ_{H} 6.83 and δ_{H} 6.46 with a coupling constant $J= 15.7$ Hz, corresponding to trans coupling as well as δ_{H} 5.96 with a coupling constant $J= 1.2$ Hz.
 - One doublet and one doublet of doublet signals with an integration of one proton of each, at δ_{H} 2.34 and δ_{H} 2.50 with a coupling constant $J= 17.3$ Hz and $J= 17.2$ Hz; 0.9 Hz respectively, corresponding to two no-equivalent protons of $-\text{CH}_2$ group.
 - One doublet methyl signal at δ_{H} 1.88 with a coupling constant $J= 1.4$ Hz. In addition of five singlet methyl signals at δ_{H} 1.26 (s, 3H); δ_{H} 1.10 (s, 6H), δ_{H} 1.02 (s, 3H) and δ_{H} 2.30 (s, 3H).

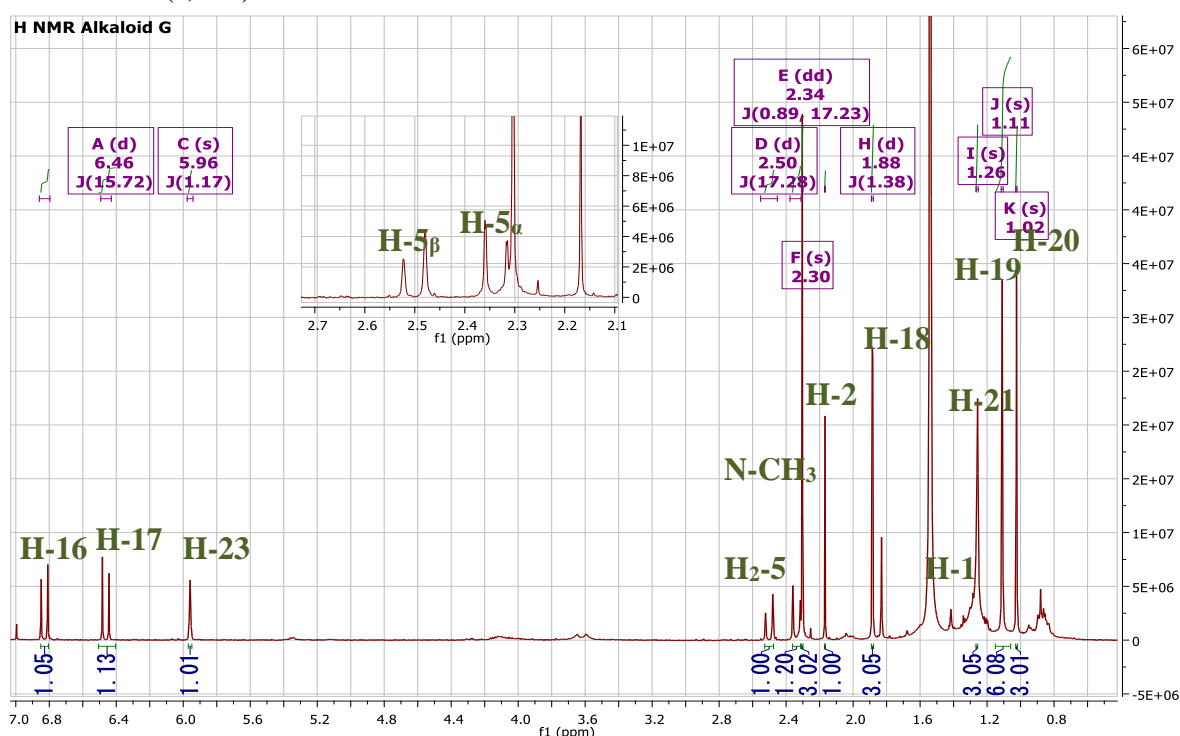


Figure III-B-01: ^1H NMR spectrum (400 MHz, CDCl_3) of compound P8

- ❖ According to ^{13}C NMR spectrum (Figure III-B- 02) there are:
 - Three olefinic signals at δ_{C} 128.00; δ_{C} 130.50 and δ_{C} 144.98.
 - Two carbonyl ester signals at δ_{C} 160.30 and δ_{C} 171.01.
 - Two carbonyl carbon signals at δ_{C} 196.99 and δ_{C} 197.73.
 - One oxygenated carbon signal at δ_{C} 79.47.
 - Three signals at δ_{C} 59.22 (deduced from HMBC spectrum), δ_{C} 49.72 and δ_{C} 41.57.
 - Six signals at δ_{C} 31.39, δ_{C} 29.86, δ_{C} 29.51, δ_{C} 24.48, δ_{C} 23.07 and δ_{C} 18.79.

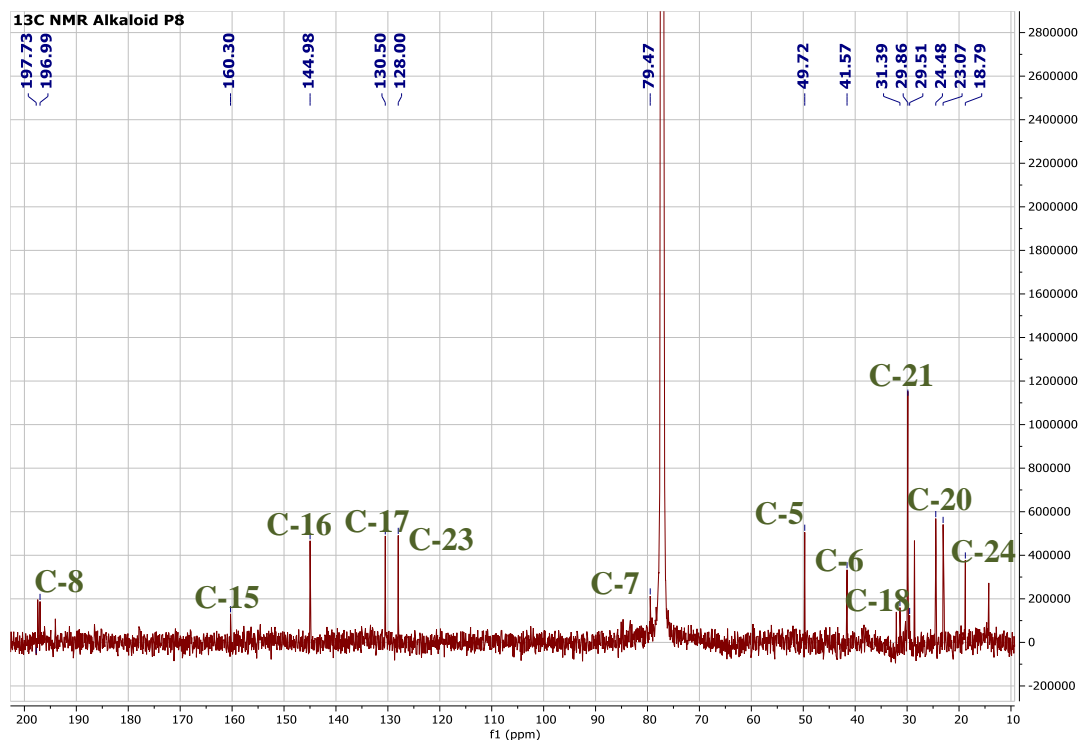


Figure III-B- 02: ^{13}C NMR spectrum (150 MHz, CDCl_3) of compound P8

- ❖ The presence of signals in [2 - 3 ppm] field in ^1H NMR spectrum and signals in [49 - 60 ppm] field in ^{13}C NMR spectrum indicate that this compound belongs to the class of pyrrolizidine alkaloid [116, 117] (Figure III-B- 03).

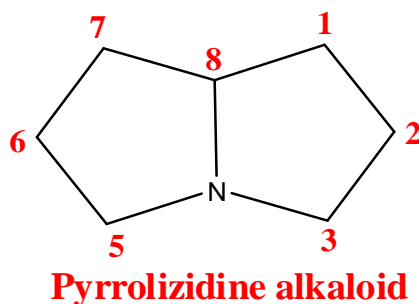


Figure III-B- 03: Basic structure of pyrrolizidine alkaloid

- ❖ Signals of C3; C5 and C8 have downfield shift compared to signals of C2; C6; C1 and C7 due to heteroatom effect which makes signals of both protons and carbons that are directly adjacent to nitrogen atom have downfield shifts [116, 117]. Thus, we conclude that:
 - Signals at: δ_H 3.67; δ_H 2.34 and δ_H 2.50 in 1H NMR spectrum attributable to H-3 and H₂-5.
 - Signals at: δ_H 2.17; δ_H 1.41 in 1H NMR spectrum attributable to H-2 and H-1.
 - Signals at: δ_C 59.22; δ_C 49.72 in ^{13}C NMR spectrum corresponding to C-3 and C-5.
 - Signals at: δ_C 38.11; δ_C 41.57 in ^{13}C NMR spectrum corresponding to C-2 and C-6.
- ❖ The presence of signals at: δ_C 160.30 and δ_C 171.01 in ^{13}C NMR spectrum indicated the presence of two carboxylic carbon linked to basic pyrrolizidine of this alkaloid which indicate that it is a macrocyclic diester alkaloid [116, 117].

Macrocyclic diester alkaloids are esters composed of amino alcohol and acid components termed the necine base and necic acid (Figure III-B- 04) [116]. They are previously isolated from Apocynaceae family from *Alafia* and *Amphineurion* genera [118].

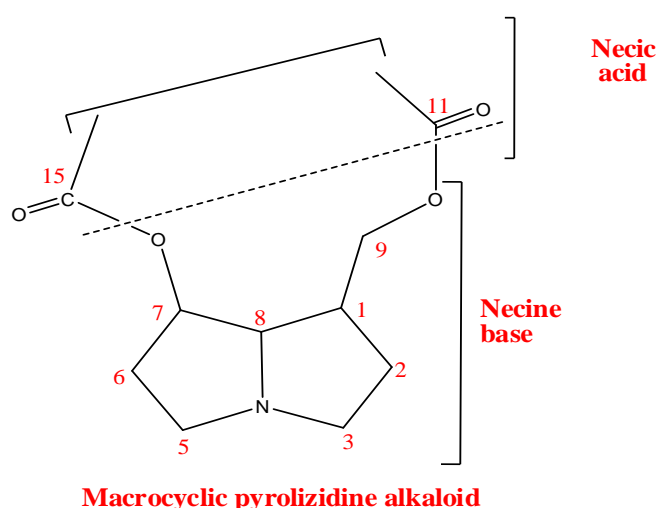
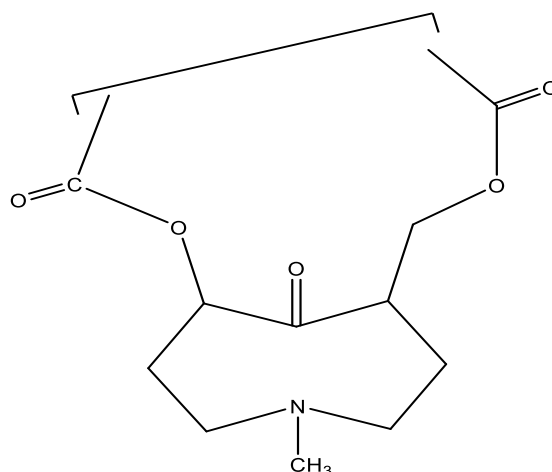


Figure III-B- 04: Basic structure of macrocyclic diester pyrrolizidine alkaloid [116]

- ❖ The presence of methyl signal at δ_H 2.30 in 1H NMR spectrum indicated that this methyl is linked to N atom which confirm that C-8 is not attached to N atom, as well as the appearance of signal at δ_C 196.99 in ^{13}C NMR spectrum indicate that this alkaloid is otonecine-type pyrrolizidine alkaloid [116]. (Figure III-B- 05).



Otonecine-type pyrrolizidine alkaloid

Figure III-B-05: Structures of otonecine-type pyrrolizidine alkaloid [116]

Chemical structure of compound P8 is confirmed using HSQC experiment, which recorded connectivity between each proton and its carbon as well as HMBC experiment that recorded long range correlations between each proton and vicinal carbons in $^2J_{H/C}$ and $^3J_{H/C}$.

Each proton is assigned to its corresponding carbon according to HSQC spectrum (Figure III-B-06 -a and III-B-06-b) which recorded:

- ❖ Typical signals of basic skeleton at:
 - δ_H 1.41 correlated with δ_C 59.49 corresponding to H-1 and C-1.
 - δ_H 2.17 correlated with δ_C 38.11 corresponding to H-2 and C-2.
 - δ_H 3.67 correlated with δ_C 59.22 corresponding to H-3 and C-3.
 - δ_H 2.34 correlated with δ_C 49.72 corresponding to H-5 $_{\alpha}$ and C-5.
 - δ_H 2.50 correlated with δ_C 49.72 corresponding to H-5 $_{\beta}$ and C-5.
 - δ_H 2.30 correlated with δ_C 28.41 corresponding to N-CH $_3$.
- ❖ Typical signals of substituents attached to basic skeleton at:
 - δ_H 6.83 correlated with δ_C 144.98.

- δ_H 6.46 correlated with δ_C 130.50.
- δ_H 1.10 correlated with δ_C 31.39.
- δ_H 1.10 correlated with δ_C 23.07.
- δ_H 1.02 correlated with δ_C 24.48.
- δ_H 1.26 correlated with δ_C 29.86.
- δ_H 5.96 correlated with δ_C 128.00.
- δ_H 1.88 correlated with δ_C 18.79.

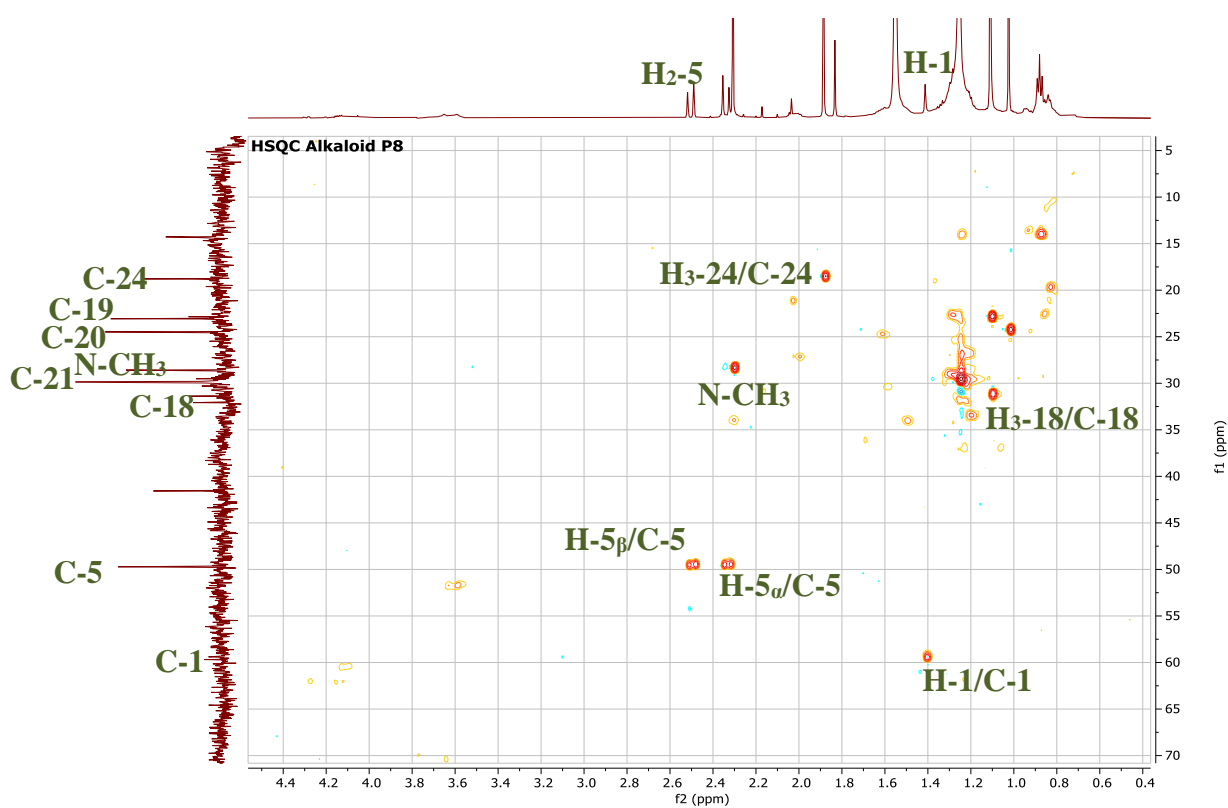


Figure III-B-06-a: HSQC expansion spectrum [4.4 - 0.6 ppm] (600 MHz, CDCl₃) of compound P8

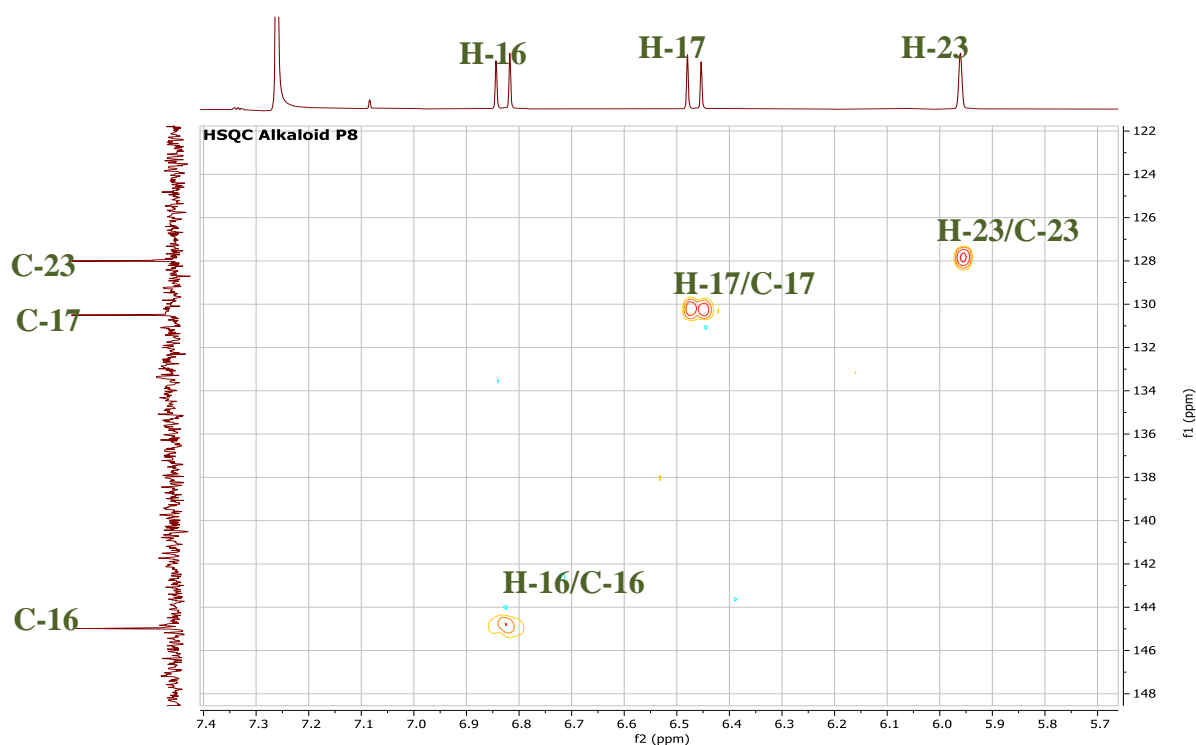


Figure III-B-06-b: HSQC expansion spectrum [7.4 - 5.7 ppm] (600 MHz, CDCl₃) of compound P8

Study of the spectrum relating to the HMBC experiment confirmed the sequence of this compound skeleton as well as attachment of the substituents on this skeleton according to correlation spots between protons and its vicinal carbons.

HMBC expansion spectrum (Figure III-B- 07) recorded correlations between:

- ❖ H-5_α (δ_{H} 2.34) has correlated with:
 - C-6 (δ_{C} 41.57).
 - C-7 (δ_{C} 79.47).
 - C-8 (δ_{C} 196.99).
- ❖ H-5_β (δ_{H} 2.50) has correlated with:
 - C-6 (δ_{C} 41.57).
 - C-7 (δ_{C} 79.47).
 - C-8 (δ_{C} 196.99).
- ❖ H-1 (δ_{H} 1.41) has correlated with:
 - C-2 (δ_{C} 38.11).
 - C-3 (δ_{C} 59.22).

These correlations confirmed the positions of geminal protons (H-5_α and H-5_β) and H-1 (δ_H 1.41) in cyclic nitrogen atom (necine base).

- ❖ N-CH₃ (δ_H 2.30) has correlated with:
 - C-8 (δ_C 196.99).

The correlation between C-8 (δ_C 196.99) and proton signal at δ 2.30 (N-CH₃) is long-range correlation indicating the formation of -O-C₈-N⁺-CH₃ linkage. This correlation is a typical correlation of otonecine-type pyrrolizidine alkaloid [116].

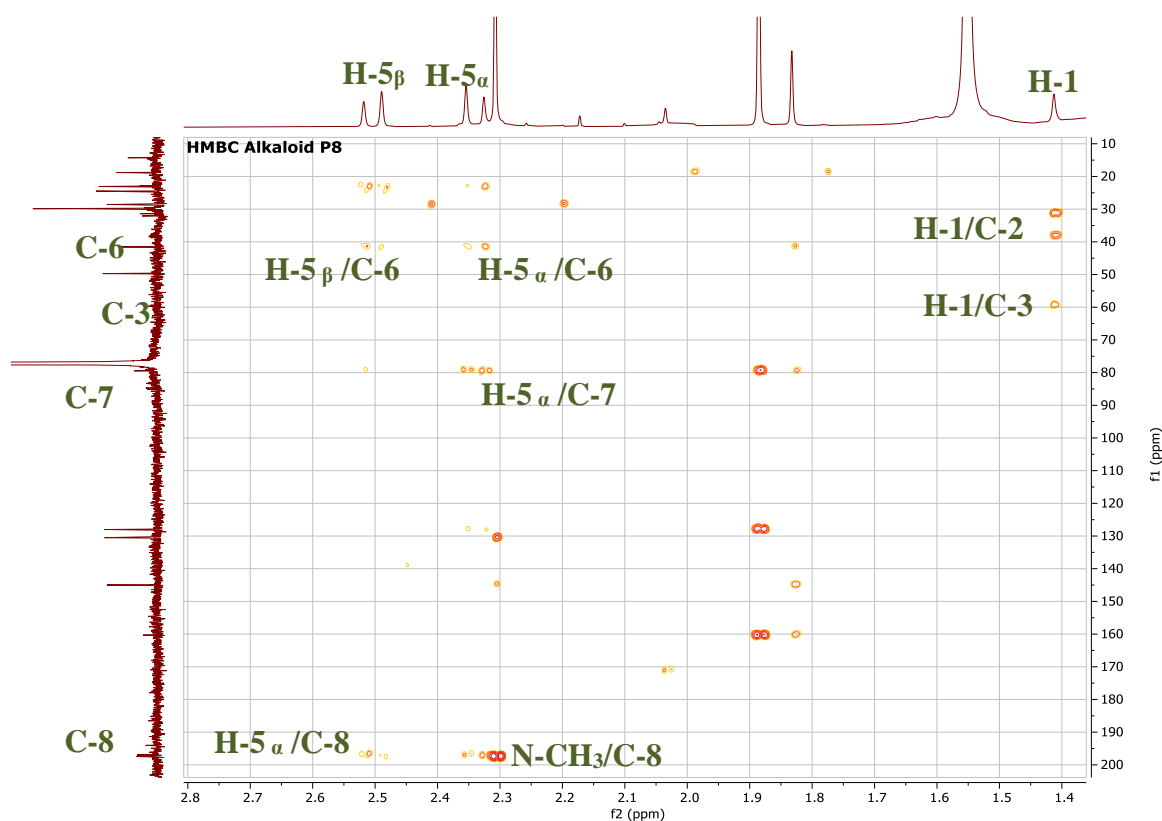


Figure III-B-07: HMBC expansion spectrum (600 MHz, CDCl₃) of compound P8 (correlation of H-1, H-5_α, H-5_β and N-CH₃)

According to the correlation of H-1, H-5_α, H-5_β and N-CH₃ group, basic skeleton of this compound has the following sequence as shown in Figure III-B-08:

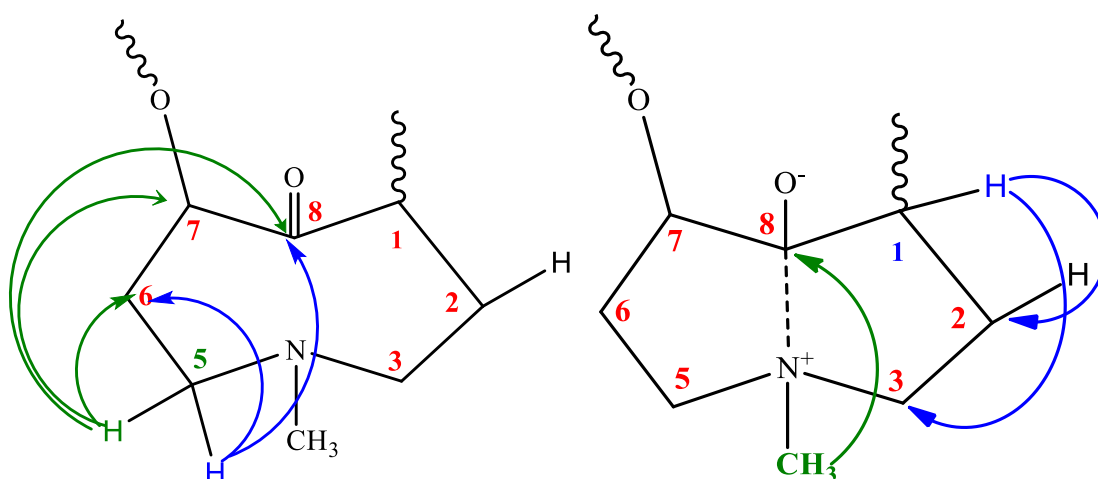


Figure III-B-08: Correlation of basic structure (correlation of H-1, H-5_α, H-5_β and N-CH₃) according to HMBC spectrum of compound P8

The presence of two methyl groups bound to quaternary carbon (C-6) is suggested by their correlation recorded from HMBC expansion spectrum (Figure III-B- 09) which are:

❖ H₃-20 (δ_{H} 1.02) has correlated with:

- C-19 (δ_{C} 23.07).
- C-6 (δ_{C} 41.57).
- C-5 (δ_{C} 49.72).
- C-7 (δ_{C} 79.47).
- C-8 (δ_{C} 196.99).

❖ H₃-19 (δ_{H} 1.10) has correlated with:

- C-20 (δ_{C} 24.48).
- C-6 (δ_{C} 41.57).
- C-5 (δ_{C} 49.72).
- C-7 (δ_{C} 79.47).

H₃-18 and H₃-19 are superimposed methylic protons, which have equivalent ¹H NMR signals while their ¹³C NMR signals are no-equivalent. The attachment of H₃-18 methyl group was confirmed by the correlation of its proton according to HMBC spectra which are:

❖ H₃-18 (δ_{H} 1.10) has correlated with:

- C-2 (δ_{C} 38.11).
- C-3 (δ_{C} 59.22).

These correlations (Figure III-B-10), as well as a correlation spot between C-18 (δ_C 31.39) and H-1 (δ_H 1.41), confirmed that this methyl group (H-18; δ_H 1.10) is attached to C-3 (δ_C 59.22).

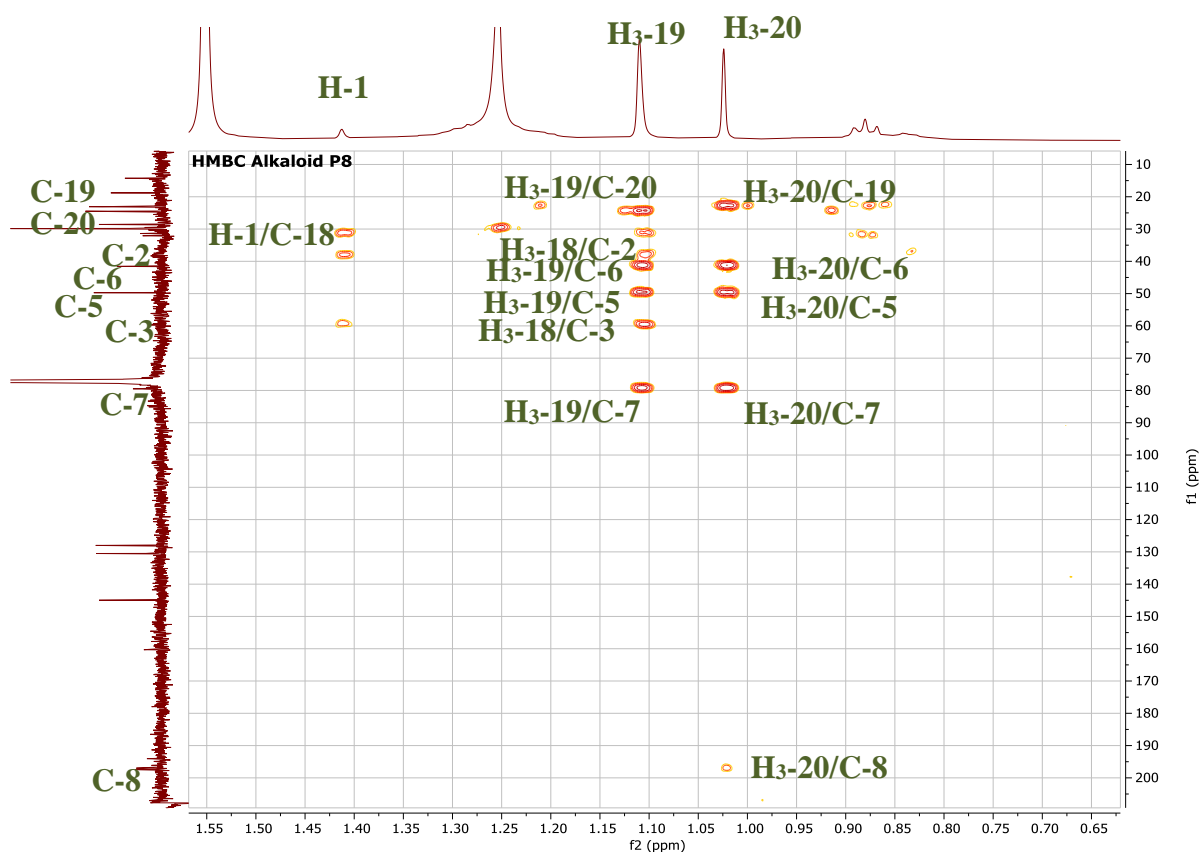


Figure III-B- 09: HMBC expansion spectrum (600 MHz, $CDCl_3$) of compound P8 (correlation of methyl groups H₃-18, H₃-19 and H₃-20)

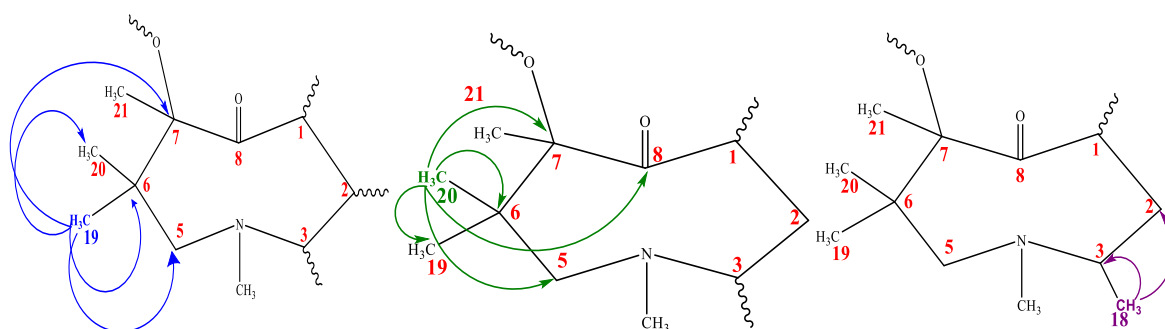


Figure III-B-10: Correlation of methyl groups (H₃-18, H₃-19 and H₃-20) according to HMBC spectrum of compound P8

❖ HMBC spectrum (Figure III-B-11-a and III-B-b) also allows to observe correlation spots between H-17 (δ_H 6.46) and corresponding to vinyl alcohol group and:

- C-8 (δ_C 196.99).

❖ In the other hand, both of C-16 (δ_C 144.98) and C-17 (δ_C 130.50) have correlated with N-CH₃ group (δ_H 2.30).

These correlations determine the connection of vinyl alcohol group (H-16 and H-17) to C-2 position.

❖ The presence of an ethylidene group attached to the necic acid moiety was determined by the correlation spots recorded from HMBC spectrum corresponding to H₃-24 (δ_H 1.88) with:

- C-15 (δ_C 160.30).
- C-23 (δ_C 128.00).

These correlations (Figure III-B-12) confirmed that ethylidene group is attached to C-14 position.

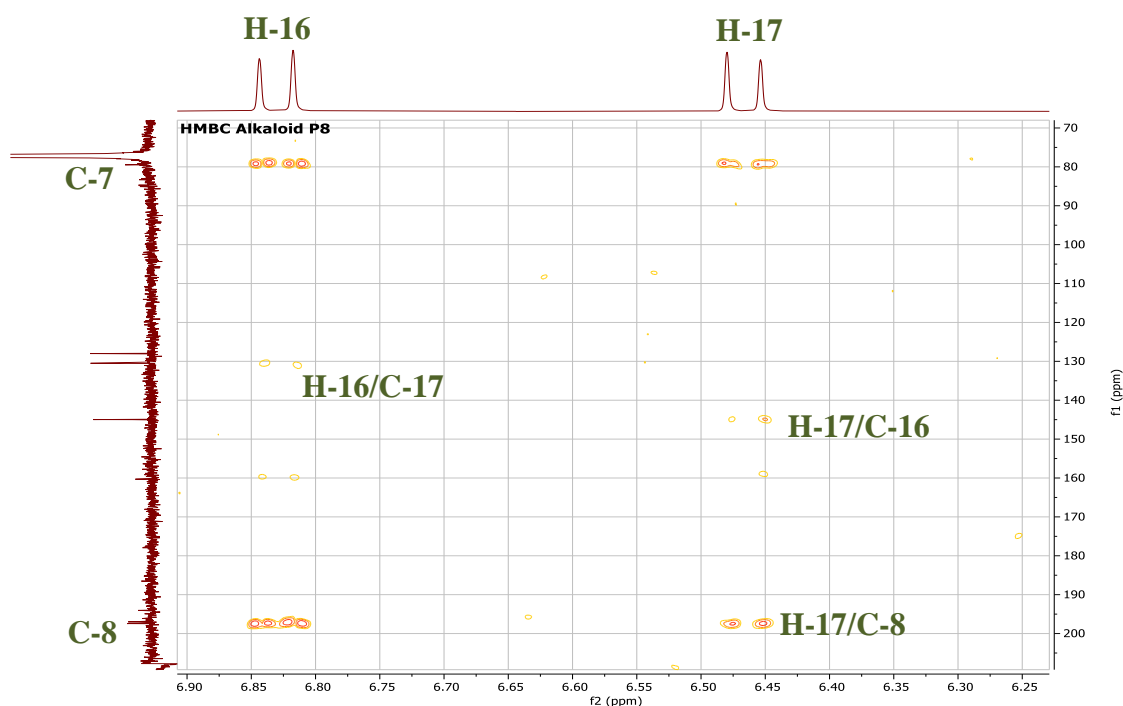


Figure III-B- 11-a: HMBC expansion spectrum (600 MHz, CDCl₃) of compound P8 (correlation H-17 and H-16)

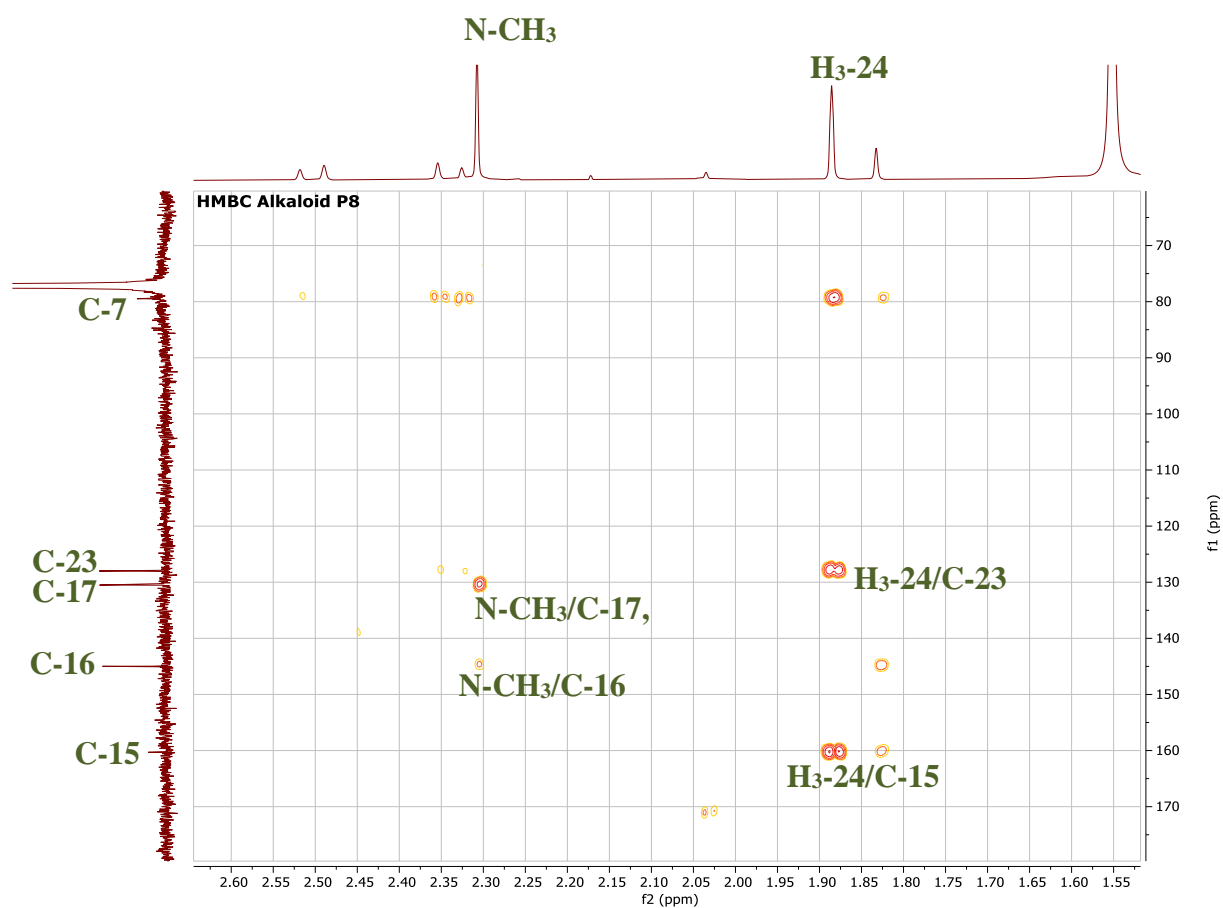


Figure III-B- 11-b: HMBC expansion spectrum (600 MHz, CDCl₃) of compound P8 (correlation H-24 and N-CH₃)

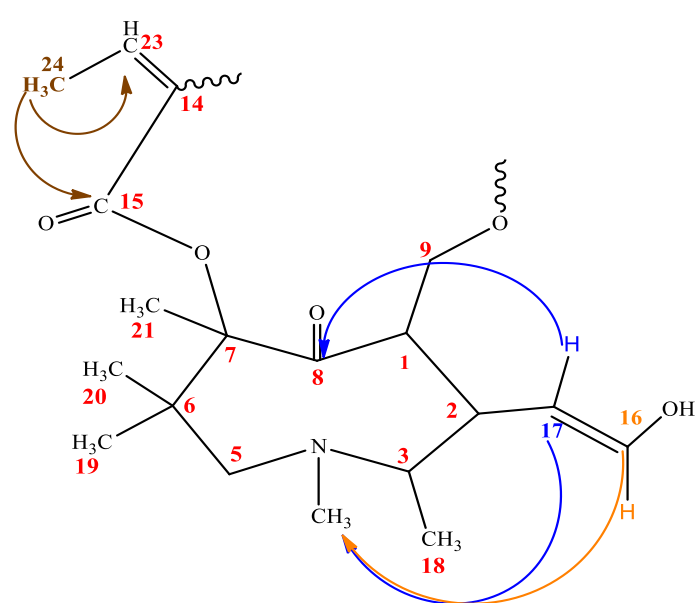


Figure III-B-12: Correlation H-17, H-16 and H-24 according to HMBC spectrum of compound P8

❖ COSY experiment (Figure III-B-13 and III-B-14) was used to confirm the sequence of some vicinal H which are:

- H-16 (δ_H 6.83) correlated with H-17 (δ_H 6.46).
- H-23 (δ_H 5.96) correlated with H₃-24 (δ_H 1.88).
- H-5 $_{\beta}$ (δ_H 2.50) correlated with H-19 (δ_H 1.10).
- H-5 $_{\alpha}$ (δ_H 2.34) correlated with H-5 $_{\beta}$ (δ_H 2.50).

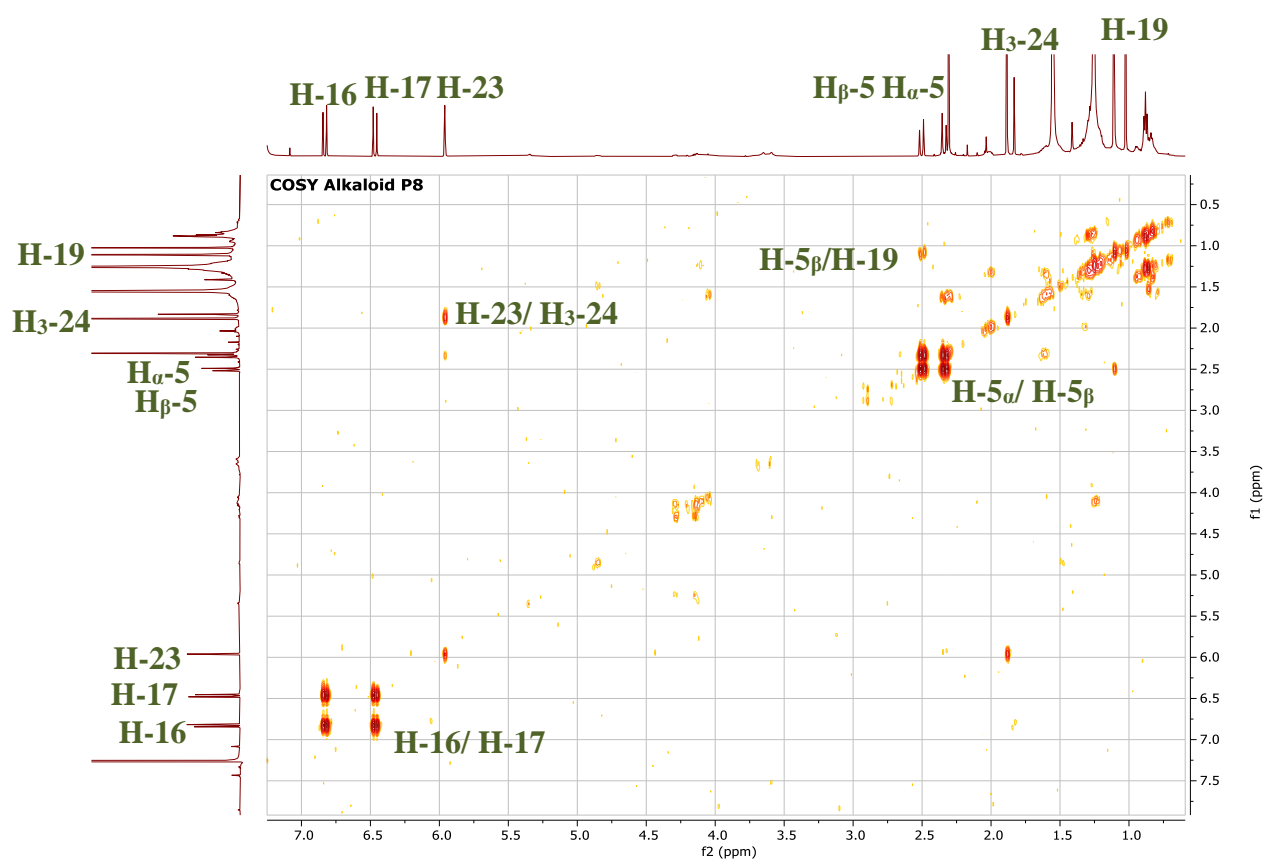


Figure III-B-13: COSY spectrum (600 MHz, CDCl₃) of compound P8

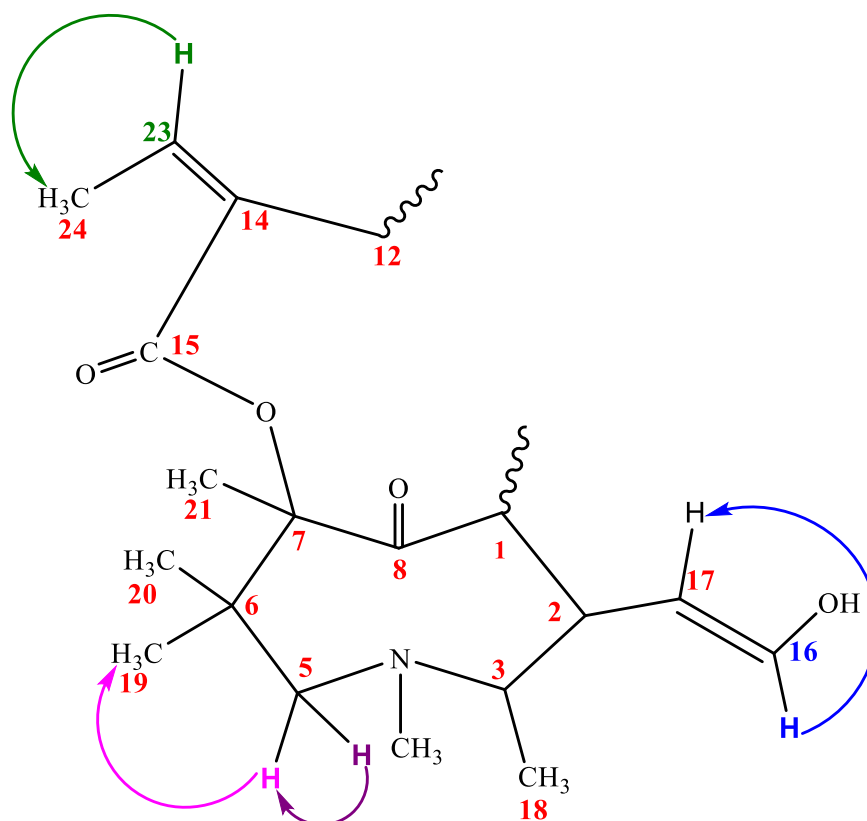


Figure III-B-14: Correlation of compound P8 according to COSY spectrum

Table III-B-01: Chemical shifts of ^1H (400 MHz) and ^{13}C (150 MHz) NMR in CDCl_3 of compound P8 (δ in ppm and J in Hz)

Compound P8		
Position	δ_{H}	δ_{C}
1	1.41 (s)	59.49
2	2.17 (s)	38.11
3	3.67 (s)	59.22
5	2.34 (dd/J=17.2/0.9 Hz)	49.72

Results and Discussion Part: Phytochemical Study of *P.tomentosa*

	2.50 (d/17.3 Hz)	
6	-	41.57
7	-	79.47
8	-	196.99
9		
11	-	171.01
12		29.51
13	-	-
14	-	138.99
15	-	160.30
16	6.83 (d/J=15.7 Hz)	144.98
17	6.46 (d/J=15.7 Hz)	130.50
18	1.10 (s)	31.39
19	1.10(s)	23.07
20	1.02(s)	24.48
21	1.26 (s)	29.86
22	-	-

23	5.96 (d/J=1.2 Hz)	128.00
24	1.88 (d/J=1.4 Hz)	18.79

On the basis of above evidence, as well as the comparison with the literature, allowed us to attribute the structure of **14-ethylidene but-11,15-dioicacid-2-hydroxyvinyl-3,N,6,6,7-pentamethyl otonecine (Tomentonecine A)** to compound P8, which is isolated for the first time as a new compound. Its structure is demonstrated in the Figure III-B-15.

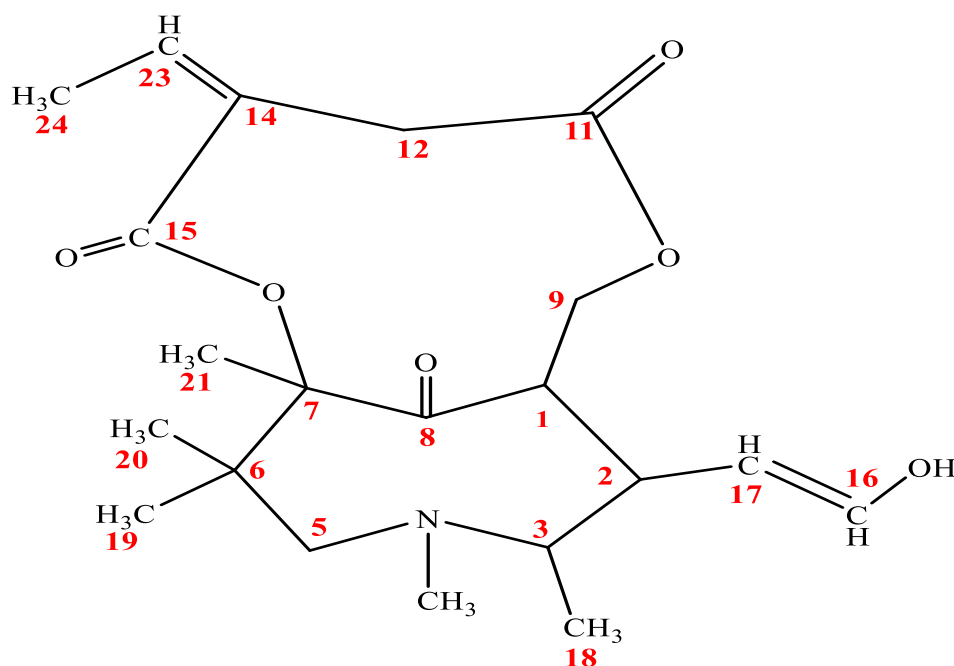


Figure III-B-15: Chemical structure of compound P8, which is an alkaloid named **Tomentonecine A**

- ❖ Tomentonecine A is an otonecine-type pyrrolizidine alkaloid composed of:
 - 2- hydroxyvinyl-3,N,6,6,7-pentamethyl otonecine.
 - 2- ethylden but-1,4-dioic acid.

III-B-1-2-Compound P13

This compound was obtained as colorless amorphous; it takes a blackish green color after revelation with a vanilin sulphuric solution and heating. Its structure was characterized using NMR spectroscopic analysis methods which are 1D: ^1H NMR and ^{13}C NMR and 2D: HSQC, HMBC and COSY. Its NMR spectra are recorded in CDCl_3 .

- ❖ The ^1H NMR spectrum (Figure III-B-16) of this compound showed:
 - Three olefinic signals with an integration of one proton for each, which are: one doublet of doublet at δ_{H} 5.88 with a coupling constant $J= 15.5$ Hz; 5.5 Hz, one doublet at δ_{H} 5.81 with a coupling constant $J= 15.7$ Hz, corresponding to trans coupling as well as one doublet at δ_{H} 5.90 with a coupling constant $J= 1.1$ Hz.
 - One doublet signal with an integration of one proton at δ_{H} 4.44 with a coupling constant $J= 2.9$ Hz.
 - Two doublet signals with an integration of one proton for each, at δ_{H} 2.25 and δ_{H} 2.45 with a coupling constant $J= 17$ Hz corresponding to two no-equivalent protons of CH_2 group.
 - Two doublet methyl signals at δ 1.96 with a coupling constant $J= 1.3$ and δ_{H} 1.30 with a coupling constant $J= 6.4$ Hz. As well as, four singlet methyl signals at δ_{H} 1.26 (s; 3H); δ_{H} 1.09 (s; 6H); δ_{H} 1.01 (s; 3H).

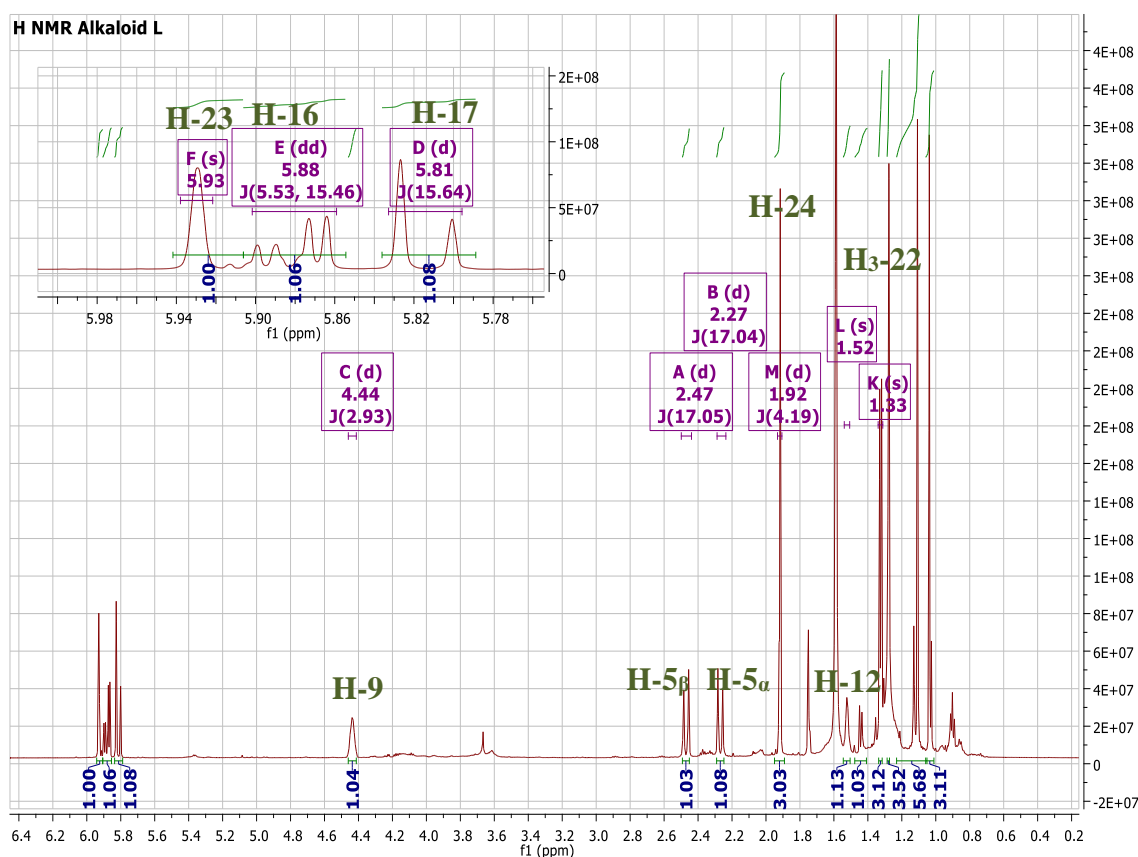


Figure III-B-16: ^1H NMR spectrum (600 MHz, CDCl_3) of compound P13

- ❖ According to ^{13}C NMR spectrum (Figure III-B-17) there are:
- Three olefinic signals at δ_{C} 127.00; δ_{C} 129.24 and δ_{C} 135.88.
 - Two carbonyl ester signals at δ_{C} 162.52 and δ_{C} 174.58.
 - One carbonyl carbon signal at δ_{C} 197.71.
 - Two signals at δ_{C} 79.19 and δ_{C} 68.41 attributable to two oxygenated carbons.
 - Two signals at δ_{C} 59.63 and δ_{C} 49.67.
 - One signal at δ_{C} 41.45 as well as six methyl signals at: δ_{C} 31.17; δ_{C} 29.40; δ_{C} 24.05; δ_{C} 23.78; δ_{C} 22.90 and δ_{C} 18.83.

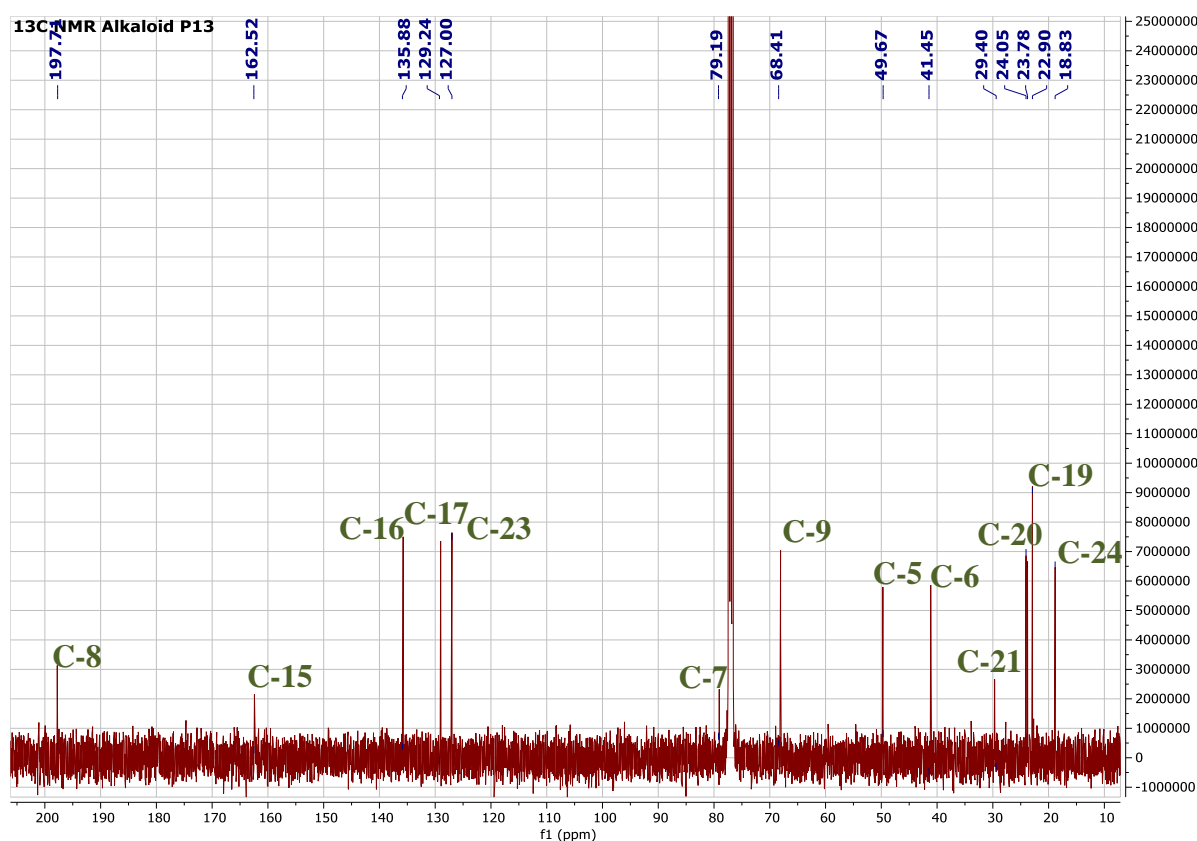


Figure III-B-17: NMR ^{13}C spectrum (100 MHz, CDCl_3) of compound P13

We observed that both ^1H and ^{13}C NMR spectra of this compound are identical with that of compound P8 with a slight difference, which indicate that compound P13 is an otonecine-type pyrrolizidine alkaloid.

The notable difference between P8 and P13 alkaloids appears clearly on the ^1H NMR spectrum of compound P13 which shows the appearance of new methyl signal at δ_{H} 1.30 as well as the disappearance of the signal attributable to the N-CH_3 . This difference is also apparent in ^{13}C NMR spectrum of this compound which shows the appearance of new signal at δ_{C} 23.78 as well as the disappearance of the signal attributable to the N-CH_3 .

❖ The proton-carbon correlation from HSQC (Figure III-B-17-a and III-B-17-b) experiment allow us to assign all protons to their corresponding carbons:

➤ Typical signals of necine base at:

- δ_{H} 1.42 correlated with δ_{C} 59.50 attributable to H-1 and C-1.
- δ_{H} 2.17 correlated with δ_{C} 38.12 attributable to H-2 and C-2.
- δ_{H} 3.67 with correlated δ_{C} 59.63 attributable to H-3 and C-3.
- δ_{H} 2.25 correlated with δ_{C} 49.67 attributable to H-5 $_{\alpha}$ and C-5.

δ_H 2.45 correlated with δ_C 49.67 attributable to H-5 β and C-5.

➤ Typical signals of necic acid at:

- δ_H 4.41 correlated with δ_C 68.41 attributable to H-9.
- δ_H 1.52 correlated with δ_C 29.40 attributable to H-12.

❖ The presence of methyl groups (H₃-18, H₃-19, H₃-20 and H₃-21), vinyl alcohol group (H-16 and H-17) and ethylidene group (H-23 and H₃-24) has also confirmed using HSQC experiment (Figure III-B-18-a and III-B-18-b) which shows the following attribution:

- δ_H 5.88 correlated with δ_C 135.88 corresponding to H-16.
- δ_H 5.81 correlated with δ_C 129.24 corresponding to H-17.
- δ_H 1.10 correlated with δ_C 31.17 corresponding to H₃-18.
- δ_H 1.09 correlated with δ_C 22.90 corresponding to H₃-19.
- δ_H 1.01 correlated with δ_C 24.05 corresponding to H₃-20.
- δ_H 1.26 correlated with δ_C 29.40 corresponding to H₃-21.
- δ_H 5.90 correlated with δ_C 127.00 corresponding to H-23.
- δ_H 1.96 correlated with δ_C 18.83 corresponding to H₃-24.

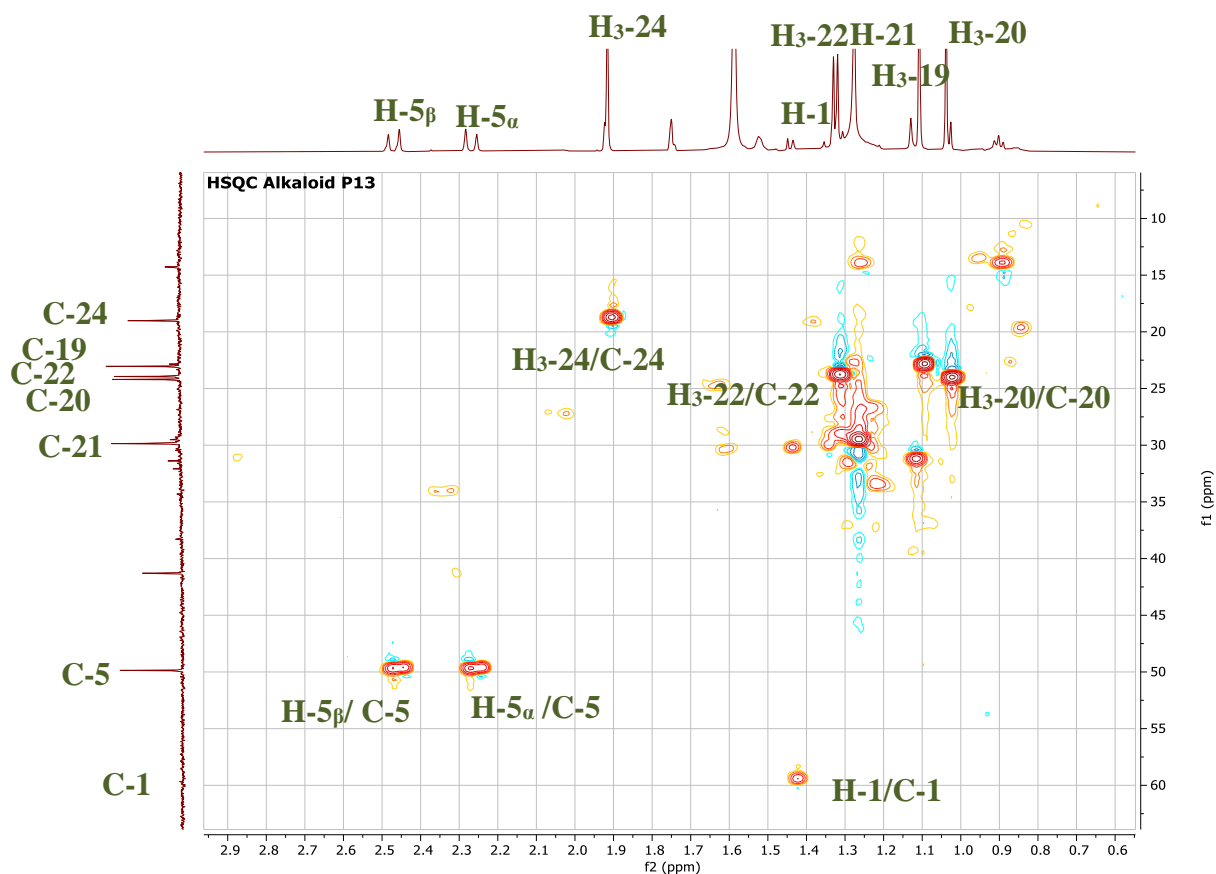


Figure III-B-18-a: HSQC expansion spectrum [2.8 - 0.7 ppm] (600 MHz, CDCl₃) of compound P13

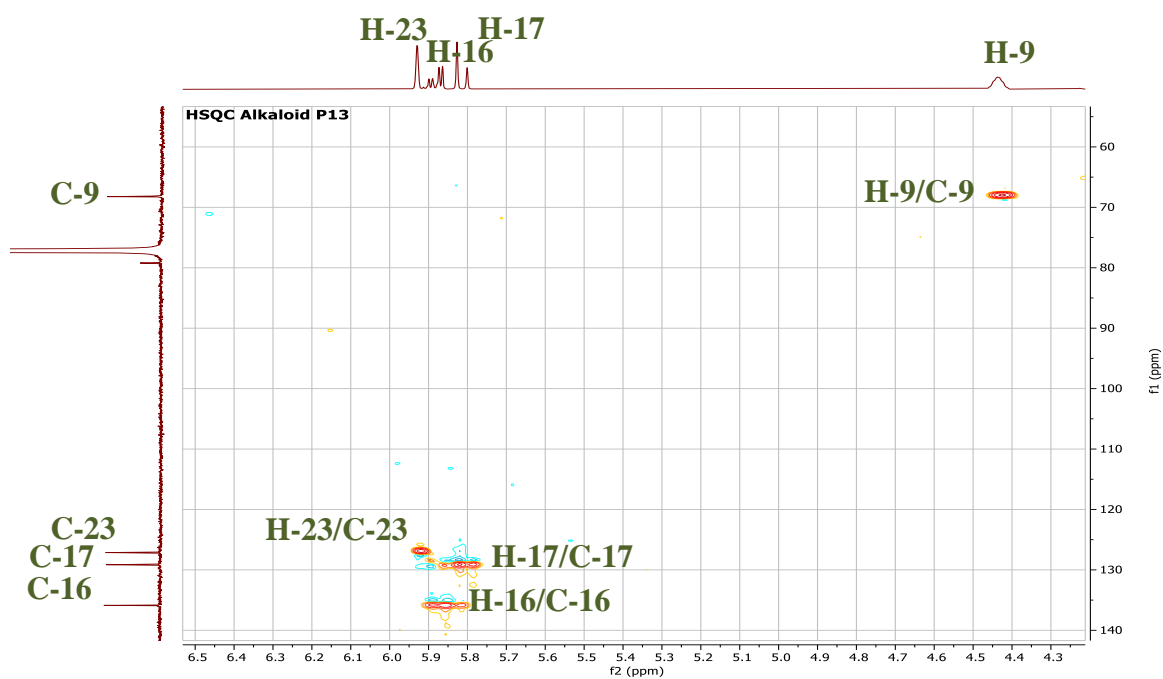


Figure III-B-18-b: HSQC expansion spectrum [6.4 - 4.3 ppm] (600 MHz, CDCl₃) of compound P13

❖ HMBC spectrum of compound P13 shows a similar correlation with the HMBC spectrum of alkaloid P8 in addition of the appearance of some new correlations, which confirm that the attachment of substituents (methyl, vinyl alcohol and ethylenic groups) in compound P13 is identical with that of alkaloid P8. HMBC spectrum allows to observe correlation spots between:

❖ H-1 (δ_H 1.42) has correlated with:

- C-2 (δ_C 38.12).
- C-3 (δ_C 59.63).
- C-18 (δ_C 31.17).
- C-16 (δ_C 135.88).

The correlation spot of H-1 with C-16 is a new correlation spot that doesn't previously shown in HMBC spectrum of alkaloid P8, its appearance allow us to confirm the attachment of ethynol group (H-16 and H-17) at C-2 position.

❖ H-5 $_{\alpha}$ (δ_H 2.25) has correlated with:

- C-19 (δ_C 22.90).
- C-6 (δ_C 41.45).
- C-7 (δ_C 79.19).
- C-8 (δ_C 197.71).

❖ H-5 $_{\beta}$ (δ_H 2.45) is correlated with:

- C-19 (δ_C 22.90).
- C-6 (δ_C 41.45).
- C-8 (δ_C 197.71).

The correlations of H-1 and H₂-5 are illustrated in HMBC expansion spectrum (Figure III-B-19 and III-B-20).

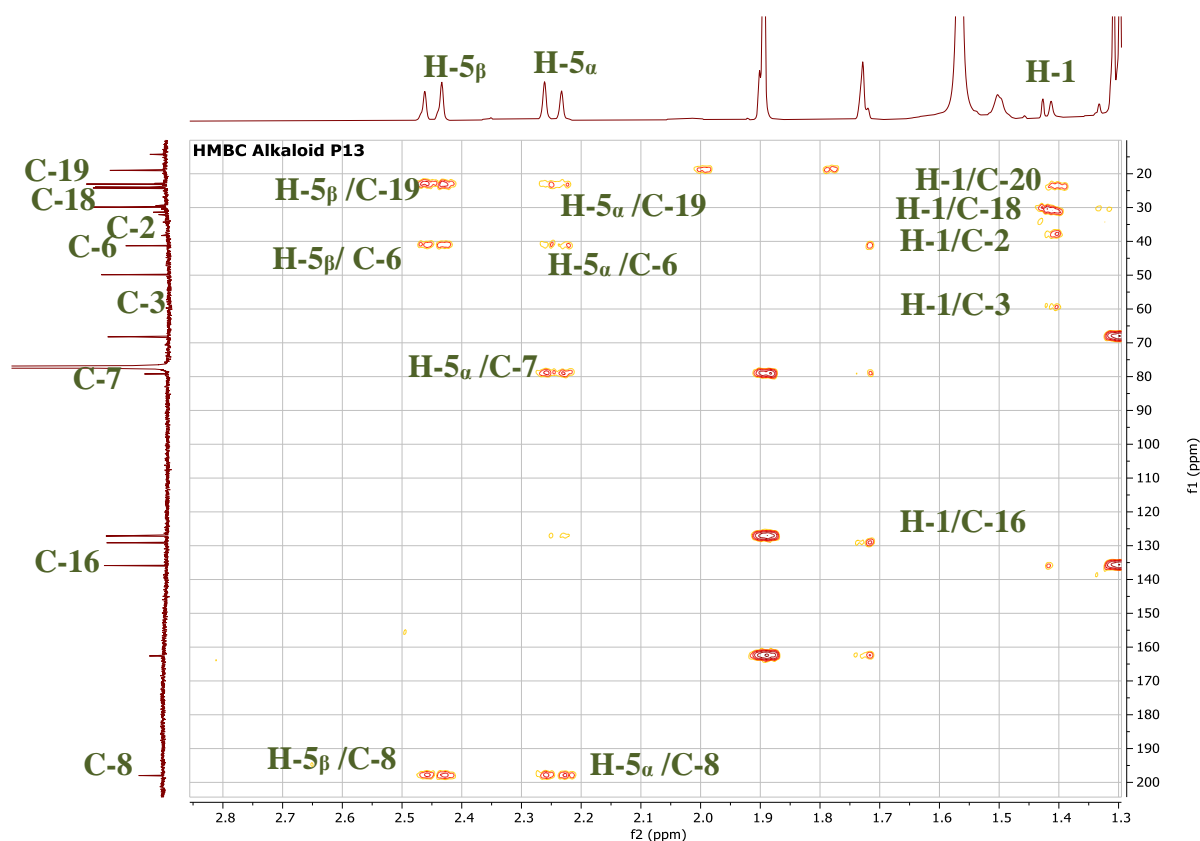


Figure III-B-19: HMBC expansion spectrum (600 MHz, CDCl₃) of compound P13 (correlation of H-1 and H₂-5)

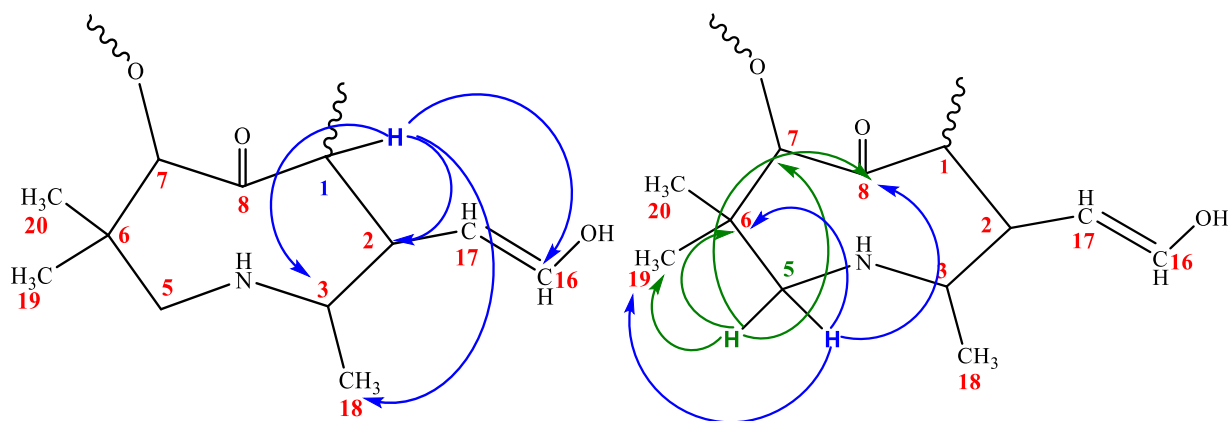


Figure III-B-20: Correlation of H-1, H-5 α and H-5 β according to HMBC spectrum of compound P13

The localisation of methyl groups (H₃-18, H₃-19 and H₃-20) is confirmed by the correlation spots observed between these protons and their vicinal carbons (Figure III-B-21) which previously appeared in HMBC spectrum of alkaloid P8 which are:

❖ H₃-20 (δ_H 1.01) has correlated with:

- C-19 (δ_C 22.90).
- C-6 (δ_C 41.45).
- C-5 (δ_C 49.67).
- C-7 (δ_C 79.19).
- C-8 (δ_C 197.71).

❖ H₃-19 (δ_H 1.09) has correlated with:

- C-20 (δ_C 24.05).
- C-6 (δ_C 41.45).
- C-5 (δ_C 49.67).
- C-7 (δ_C 79.19).

❖ H₃-18 (δ_H 1.10) is correlated with:

- C-2 (δ_C 38.12).
- C-3 (δ_C 59.63).

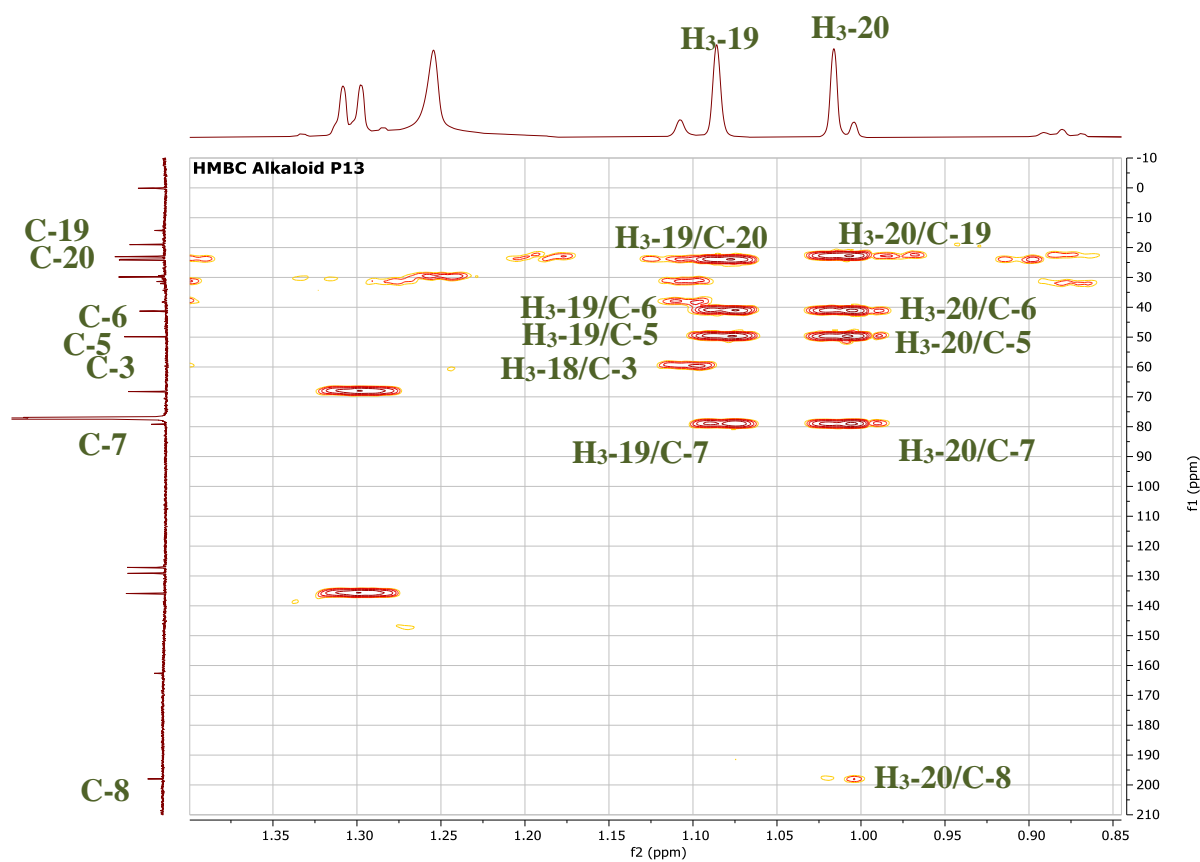


Figure III-B-21: HMBC expansions spectrum (600 MHz, CDCl₃) of compound P13 (correlation of methyl groups H-18, H-19 and H-20)

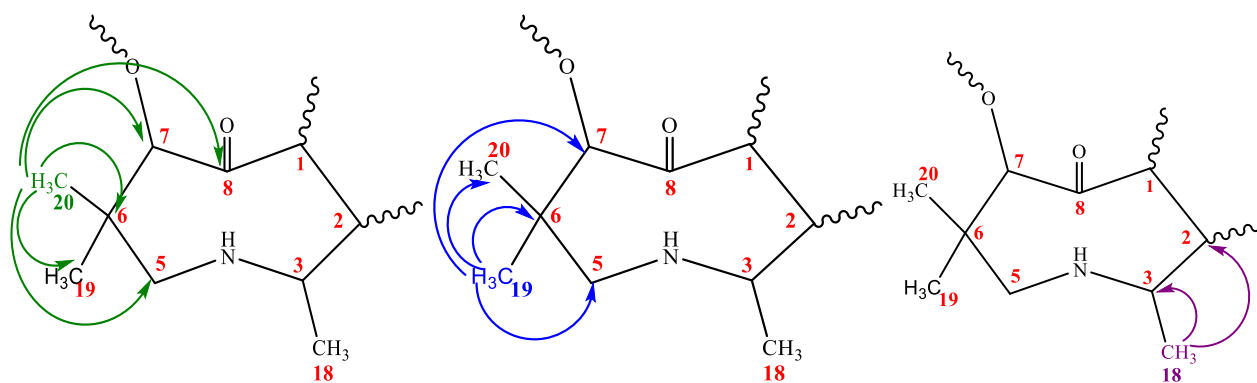


Figure III-B-22: Correlation of methyl groups H₃-18, H₃-19 and H₃-20 according to HMBC spectrum of compound P13

HMBC expansion spectrum (Figure III-B-23-a) shows also correlation spots that confirm the attachment of vinyl alcohol group (H-16 and H-17) at C-2 carbon, which are:

- ❖ H-16 (δ_{H} 5.88) has correlated with:
 - C-17 (δ_{C} 129.24).
- ❖ H-17 (δ_{H} 5.81) has correlated with:
 - C-9 (δ_{C} 68.41).
 - C-16 (δ_{C} 135.88).

The appearance of new correlation spot of H-17 with C-9, in addition of correlation spot between H-1 and C-16 (which previously mentioned), that doesn't previously shown in HMBC spectrum of alkaloid P8 allow us to confirm the attachment of vinyl alcohol group (H-16 and H-17) at C-2 position.

The ¹H NMR spectrum of compound P13 also shows an olefinic signal at δ_{H} 5.90 ($J=1.1$ Hz) which combines with the methyl group signal at δ_{H} 1.96 ($J=1.3$ Hz). That indicate the presence of ethylidene group (H-23 and H₃-24). The attachment of this group at C-14 (necic acid moiety) has been confirmed by its correlation spots in HMBC expansion spectrum (Figure III-B-23-b) which are:

- ❖ H₃-24 (δ_{H} 1.96) has correlated with:
 - C-23 (δ_{C} 127.00).
 - C-15 (δ_{C} 162.52).
- ❖ H-23 (δ_{H} 5.90) has correlated with:
 - C-24 (δ_{C} 18.83).

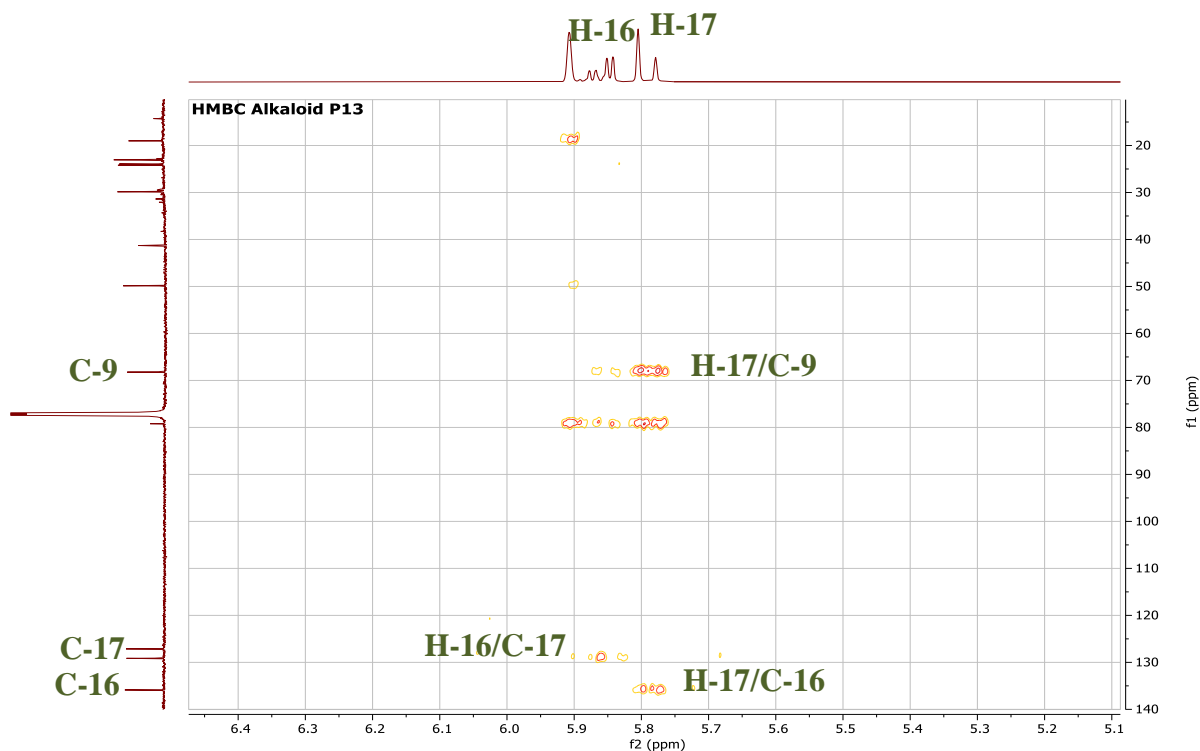


Figure III-B-23-a: HMBC expansion spectrum (600 MHz, CDCl₃) of compound P13 (correlation of H-16 and H-17)

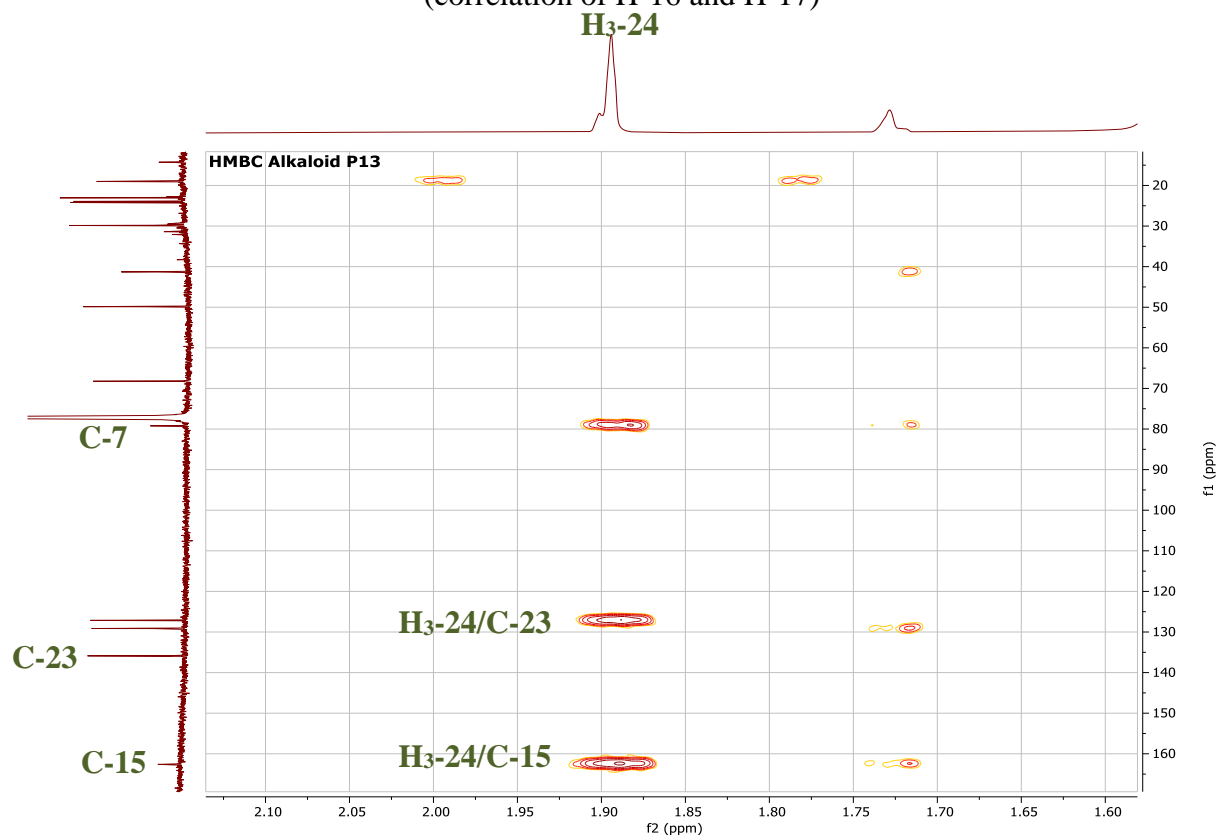


Figure III-B-23-b: HMBC expansion spectrum (600 MHz, CDCl₃) of compound P13 (correlation of H₃-24)

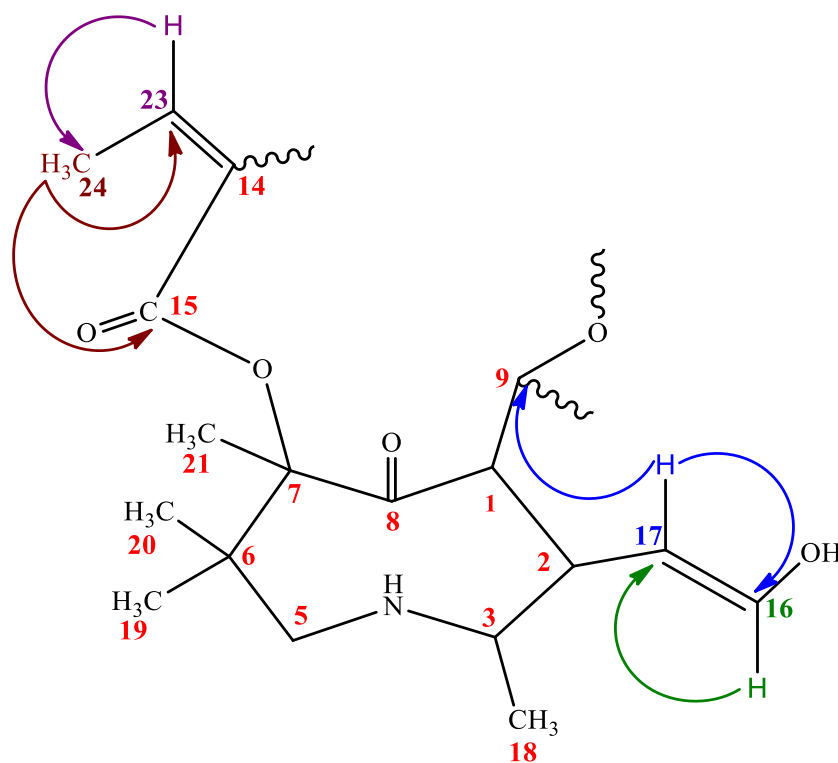


Figure III-B-24: Correlation of H-16, H-17, H-23 and H₃-24 according to HMBC spectrum of compound P13

The attachment of new methyl signal (H₃-22) at C-9 has been confirmed by its correlation spot shown in HMBC expansion spectrum (Figure III-B-25) which are:

- ❖ H₃-22 (δ_{H} 1.30) is correlated with:
 - C-9 (δ_{C} 68.41)

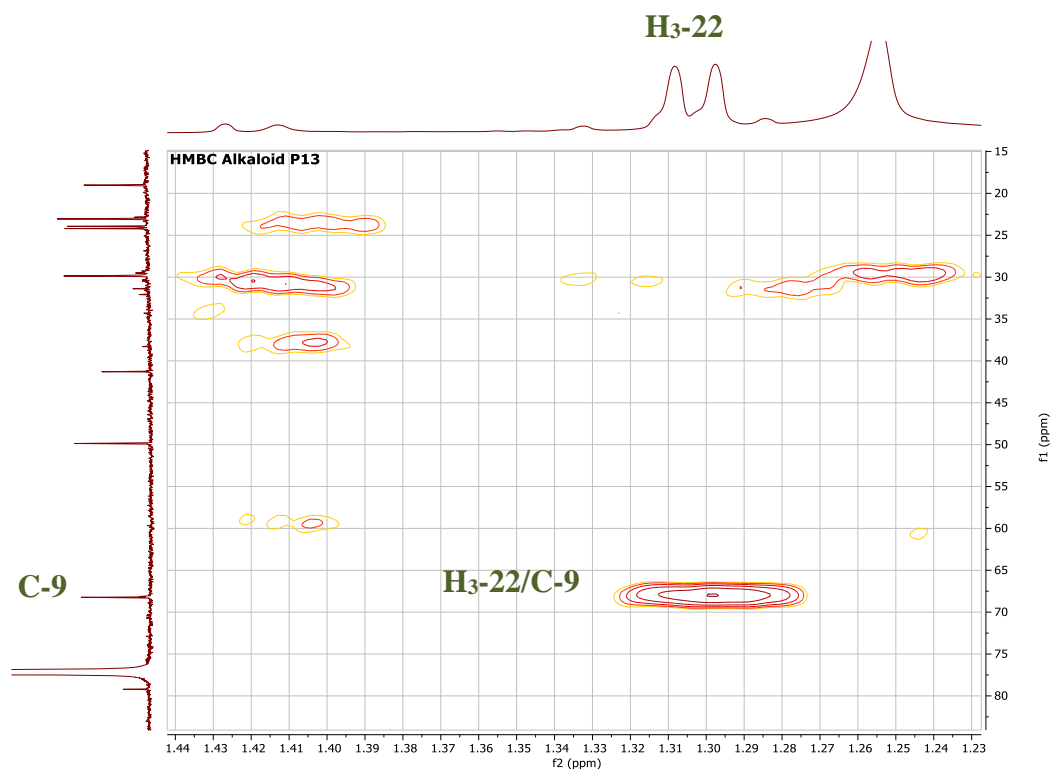


Figure III-B-25: HMBC expansion spectrum (600 MHz, CDCl₃) of compound P13 (correlation of H₃-22)

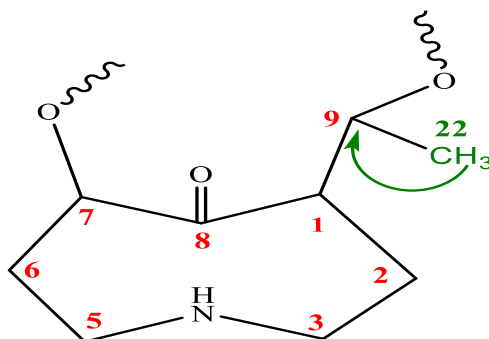


Figure III-B-26: Correlation of H₃-22 according to HMBC spectrum of compound P13

❖ COSY experiment (Figure III-B-27) show some correlation spots which confirm the sequence of some vicinal H which are:

- H-23 (δ_H 5.90) correlated with H₃-24 (δ_H 1.96).
- H₃-22 (δ_H 1.30) correlated with H-9 (δ_H 4.41).
- H-5 β (δ_H 2.45) correlated with H₃-19 (δ_H 1.09).
- H-5 α (δ_H 2.25) correlated with H-5 β (δ_H 2.45)

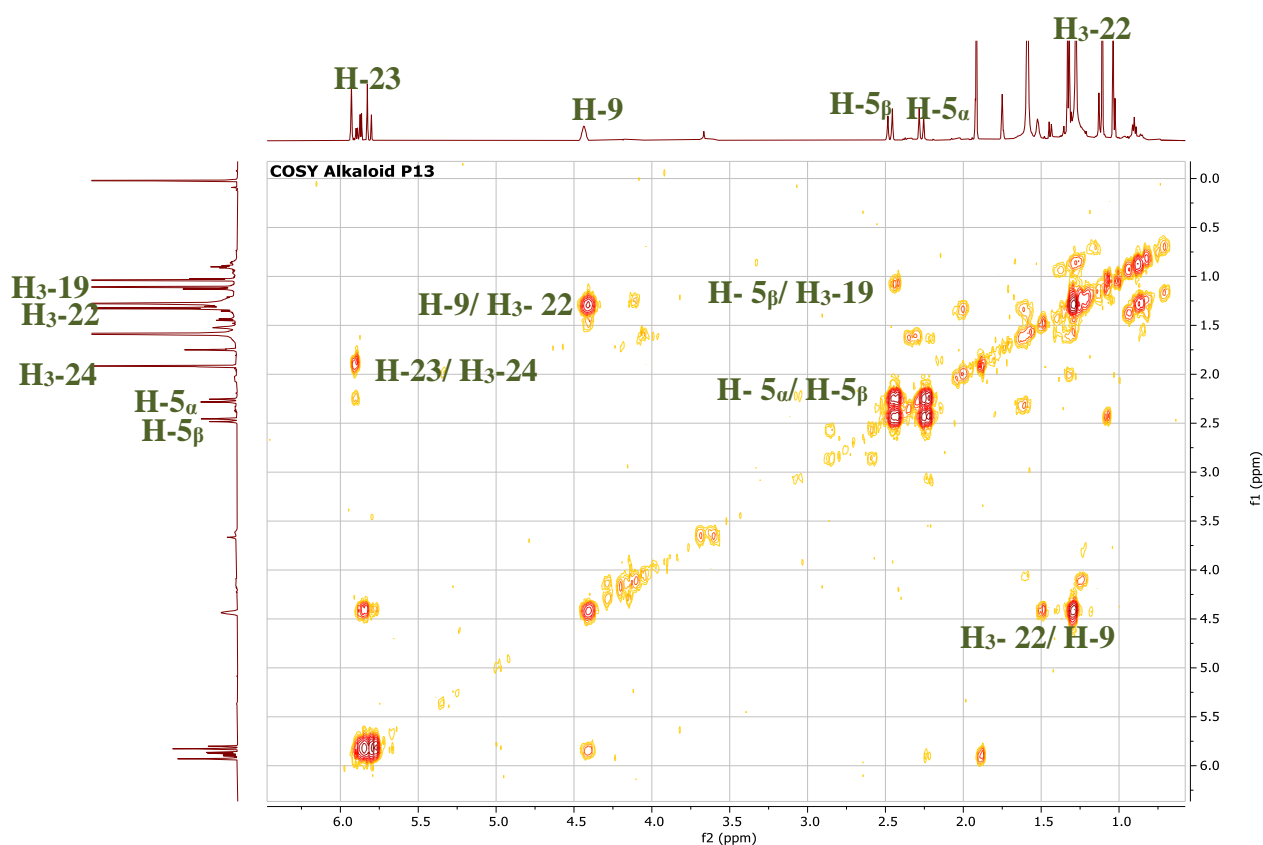


Figure III-B- 27: COSY spectrum (600 MHz, CDCl_3) of compound P13

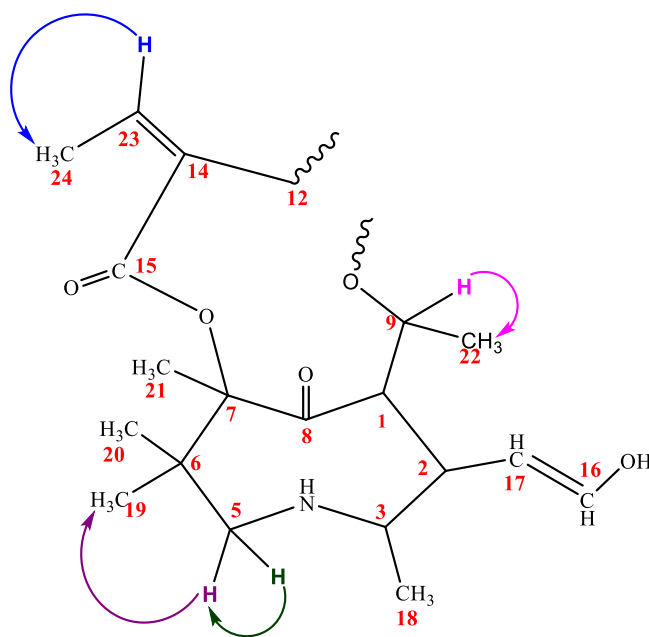


Figure III-B-28: Correlation of compound P13 according to COSY spectrum

Table III-B-02: Chemical shifts of ^1H (600 MHz) and ^{13}C (100 MHz) NMR in CDCl_3 of alkaloid P13 (δ in ppm and J in Hz)

Compound P13		
Position	δ_{H}	δ_{C}
1	1.42 (d/ J=4.6 Hz)	59.50
2	2.17 (s)	38.12
3	3.67 (s)	59.63
5	2.25 (d/ J=17.0 Hz)	49.67
	2.45 (d/ J=17.0 Hz)	
6	-	41.45
7	-	79.19
8	-	197.71
9	4.41 (d/ J=2.9 Hz)	68.41
11	-	
12	1.51 (s)	29.61
13	-	-
14	-	138.74
15	-	162.52

16	5.88 (dd/J=15.5/ 5.5 Hz)	135.88
17	5.81 (d/J=15.6 Hz)	129.24
18	1.10 (s)	31.17
19	1.09 (s)	22.90
20	1.01 (s)	24.05
21	1.26 (s)	29.40
22	1.30 (d/J=6.4 Hz)	23.78
23	5.90 (s)	127.00
24	1.96 (d/J=1.3 Hz)	18.93

The various methods of ^1H NMR, ^{13}C NMR and 2D (HSQC, HMBC, COSY) have enable us to attribute the structure of **14-ethylidene but-11,15-dioicacid -2-hydroxyvinyl,3,6,6,7,9-pentamethyl otonecine (Tomentonecine B)** to compound P13, which is isolated for the first time as a new compound. Its structure is demonstrated in the Figure III-B-29.

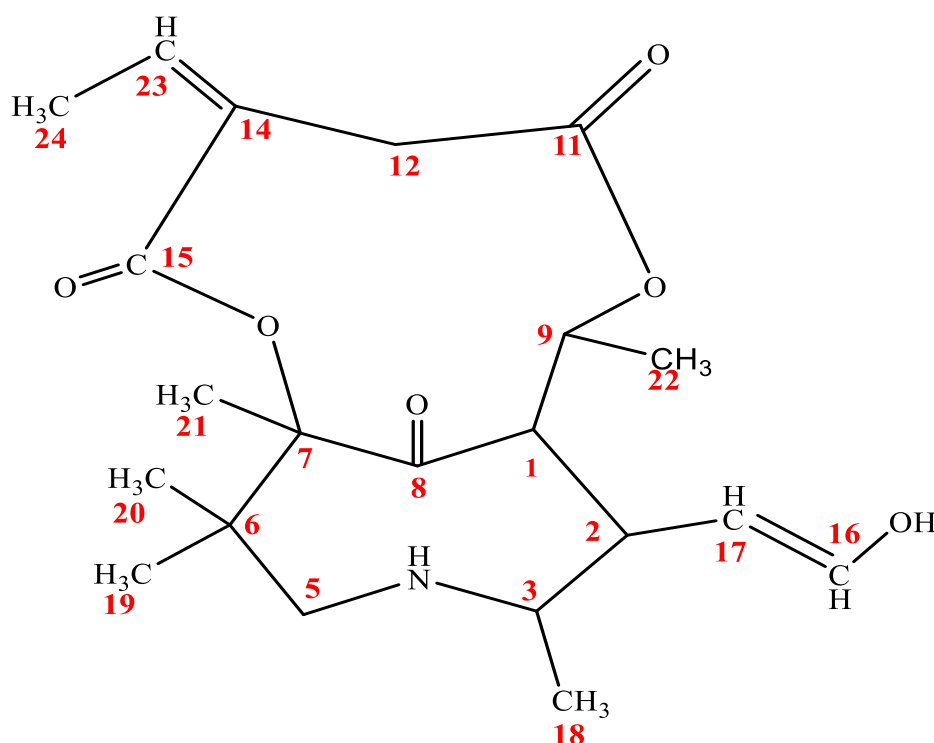


Figure III-B-29: Chemical structure of compound P13, which is an alkaloid named **Tomentonecine B**

- ❖ Tomentonecine B is an otonecine-type pyrrolizidine alkaloid composed of:
 - 2- hydroxyvinyl,3,6,6,7,9-pentamethyl otonecine.
 - 2- ethyliden but-1,4-dioic acid.

III-B-1-3-Compound P5

This compound was obtained as colorless amorphous; it takes a red color after revelation with a vanilin sulphuric solution and heating. Its structure was characterized using NMR spectroscopic analysis methods which are 1D: ^1H NMR and ^{13}C NMR and 2D: HSQC, HMBC and COSY. Its NMR spectra recorded in CDCl_3 .

- ❖ The ^1H NMR spectrum (Figure III-B-30-a and III-B-30-b) of this compound showed:

- Three doublet olefinic signals with an integration of one proton of each, at δ_H 6.83 and δ_H 6.47 with a coupling constant $J= 15.7$ Hz, corresponding to trans coupling as well as δ_H 5.96 with a coupling constant $J= 1.2$ Hz.
- One multiplet signal with an integration of one proton at δ_H 4.24.
- Two doublet signals with an integration of one proton for each, at δ_H 2.34 and δ_H 2.50 with a coupling constant $J= 17$ Hz corresponding to two no-equivalent protons of CH_2 group.
- Eight singlet methyl signals with an integration of three protons of each, at δ_H 2.31; δ_H 1.43; δ_H 1.33; δ_H 1.28; δ_H 1.25; δ_H 1.11; δ_H 1.02 and δ_H 0.88. In addition of one doublet methyl signal with an integration of three protons at δ 1.89 with a coupling constant $J= 1.4$ Hz.

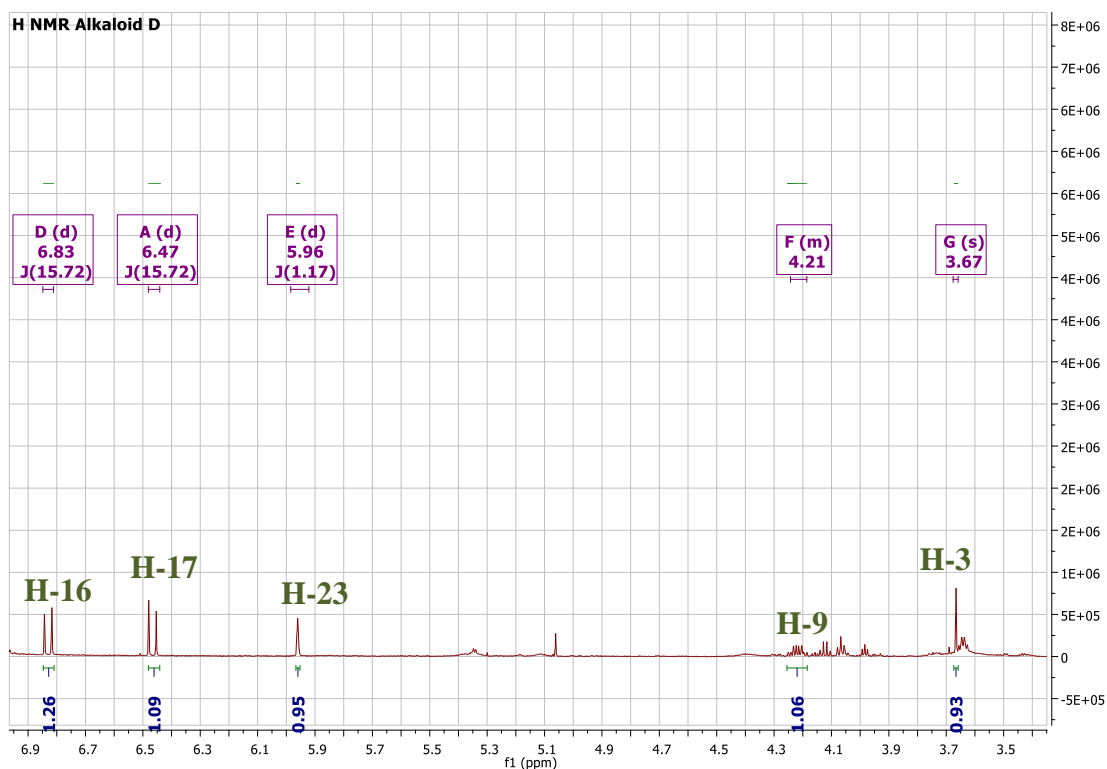


Figure III-B-30-a: ^1H NMR expansion spectrum [6.9 – 3.5 ppm] (600 MHz, CDCl_3) of compound P5

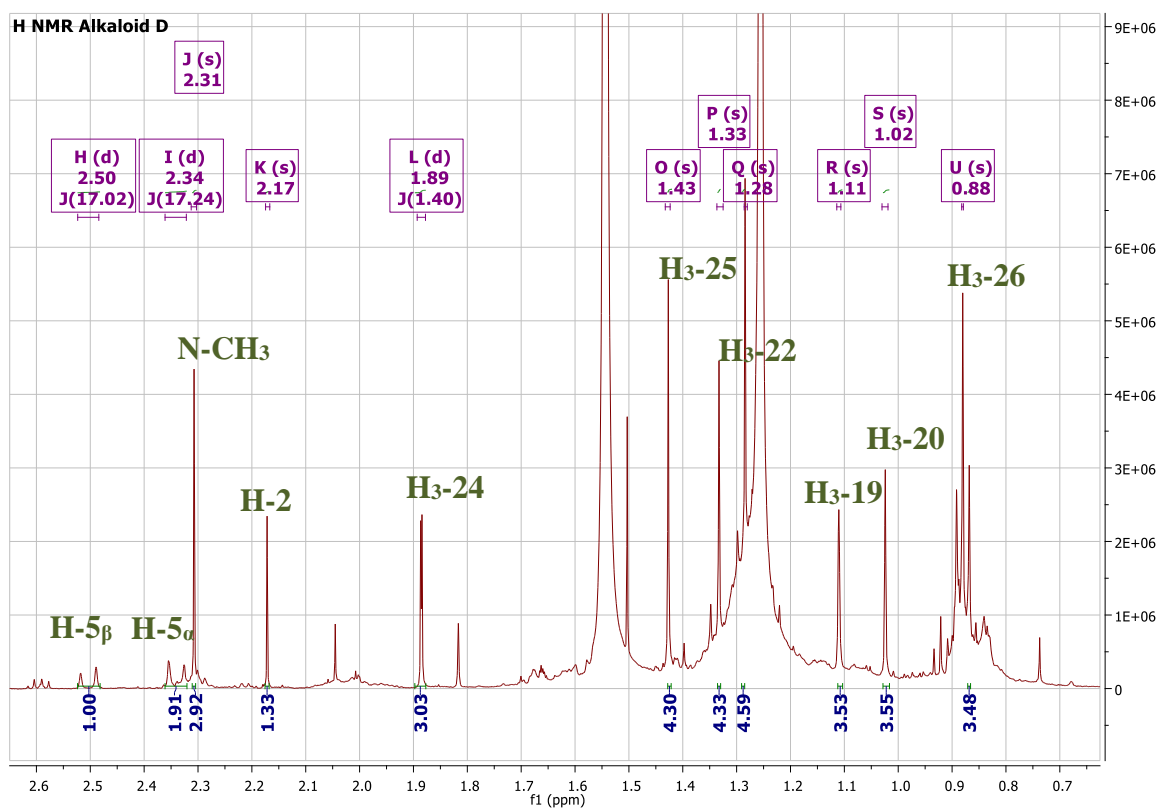


Figure III-B-30-b: ^1H NMR expansion spectrum [2.6 – 0.7 ppm] (600 MHz, CDCl_3) of compound P5

❖ According to both HSQC and HMBC spectrum:

- Three olefinic signals at δ_C 135.78; δ_C 138.64 and δ_C 147.42.
- Two carbonyl ester signals at δ_C 160.12 and δ_C 171.75.
- One carbonyl carbon signal at δ_C 197.63.
- Two signals at δ_C 79.23 and δ_C 63.49 attributable to two oxygenated carbons.
- Three signals at δ_C 59.19, δ_C 49.71 and 49.00.
- Two signals at δ_C 41.25 and δ_C 34.67.

The ^1H NMR and ^{13}C NMR spectra of compound P5 show similarities of the signals in comparison with alkaloids P8 and P13, at the level of the presence of: methyl groups (H₃-18, H₃-19, H₃-20, H₃-21, H₃-22 and N-CH₃), vinyl alcohol group (H-16 and H-17), ethylidene group (H-23 and H₃-24), carbonyl carbon (C-8), carbonyl ester (C-11 and C-15), oxygenated carbons (C-9 and C-7) and the other carbons adjacent to nitrogen atom (C-3, C-5, C-2 and C-6), which confirmed that this alkaloid has similar structure with that of P13 and P8 alkaloids which is an otonecine-type pyrrolizidine alkaloid, with a slight difference.

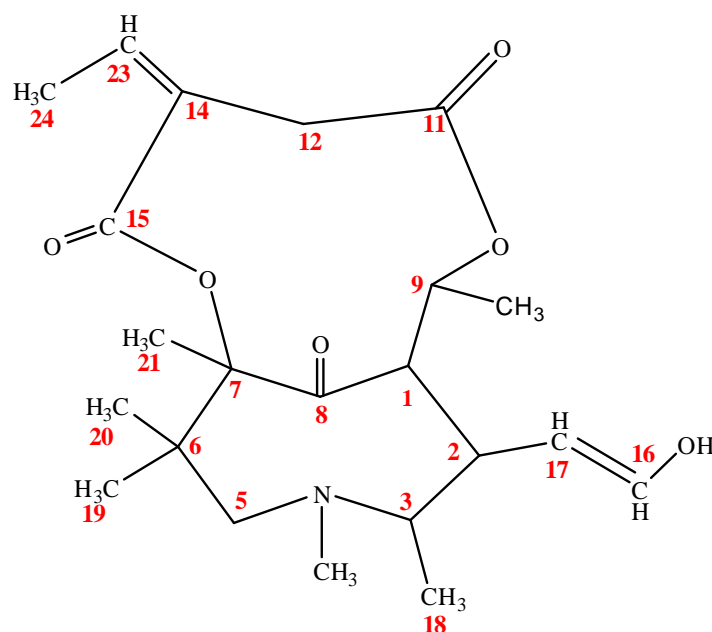


Figure III-B-31: Basic structure of compound P5

The major difference between P5, P8 and P13 alkaloids appears clearly on the ^1H NMR spectrum of P5 alkaloid, which shows the appearance of two new methyl signals at δ_{H} 1.43 and δ_{H} 0.88.

❖ The complete assignment of alkaloid P5 was established using HSQC spectrum (Figure III-B-32) of this alkaloid as well as the comparison of all ^1H NMR and ^{13}C NMR spectroscopic data of alkaloid P5 with that of both P8 and P13 alkaloids, which are:

➤ Typical signals of necine base at:

- δ_{H} 2.17 correlated with δ_{C} 34.67 attributable to H-2 and C-2.
- δ_{H} 3.67 correlated with δ_{C} 59.19 attributable to H-3 and C-3.
- δ_{H} 2.34 correlated with δ_{C} 49.71 attributable to H-5 $_{\alpha}$ and C-5.
 δ_{H} 2.50 correlated with δ_{C} 49.71 attributable to H-5 $_{\beta}$ and C-5
- δ_{C} 197.63 attributable to quaternary carbon C-8.

➤ Typical signals of necic acid at:

- δ_{H} 4.24 correlated with δ_{C} 63.49 attributable to H-9 and C-9.
- δ_{H} 1.52 correlated with δ_{C} 22.56 attributable to H-12 and C-12.
- δ_{C} 160.12 attributable to quaternary carbon C-15.
- δ_{C} 171.75 attributable to quaternary carbon C-11.

➤ Typical signals of substituents at:

- δ_{H} 6.83 correlated with δ_{C} 147.42 corresponding to H-16 and C-16.
- δ_{H} 6.47 correlated with δ_{C} 135.78 corresponding to H-17 and C-17.
- δ_{H} 1.28 correlated with δ_{C} 31.63 corresponding to H₃-18 and C-18.
- δ_{H} 2.31 correlated with δ_{C} 28.37 corresponding to N-CH₃.
- δ_{H} 1.11 correlated with δ_{C} 22.99 corresponding to H₃-19 and C-19.
- δ_{H} 1.02 correlated with δ_{C} 24.24 corresponding to H₃-20 and C-20.
- δ_{H} 1.25 correlated with δ_{C} 29.41 corresponding to H₃-21 and C-21.
- δ_{H} 5.96 correlated with δ_{C} 138.64 corresponding to H-23 and C-23.
- δ_{H} 1.89 correlated with δ_{C} 18.53 corresponding to H₃-24 and C-24.
- δ_{H} 1.33 correlated with δ_{C} 30.08 corresponding to H₃-22 and C-22.

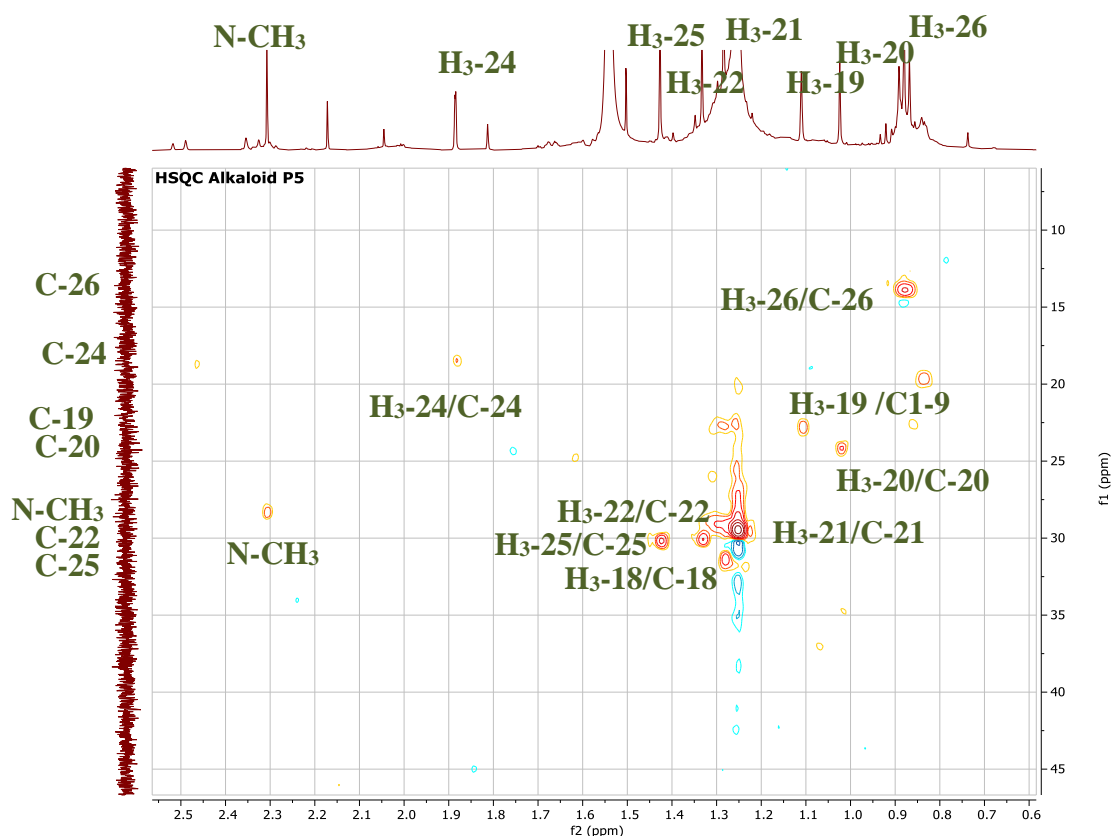


Figure III-B-32: HSQC expansion spectrum (600 MHz, CDCl_3) of compound P5

- ❖ The attachment of methyl groups ($\text{H}_3\text{-19}$ and $\text{H}_3\text{-20}$) was confirmed by appearance of correlation spots in HMBC spectrum expansion (Figure III-B-33), which are
 - ❖ $\text{H}_3\text{-20}$ (δ_{H} 1.02) has correlated with:
 - C-19 (δ_{C} 22.99).
 - C-6 (δ_{C} 41.25).
 - C-5 (δ_{C} 49.71).
 - C-7 (δ_{C} 79.23).
 - ❖ $\text{H}_3\text{-19}$ (δ_{H} 1.11) has correlated with:
 - C-20 (δ_{C} 24.24).
 - C-6 (δ_{C} 41.25).
 - C-5 (δ_{C} 49.71).
 - C-7 (δ_{C} 79.23).

The correlation mentioned above are the same of that observed in HMBC spectrum of P13 and P8 alkaloids which confirm that both CH₃-20 and CH₃-19 are linked at C- 6 position.

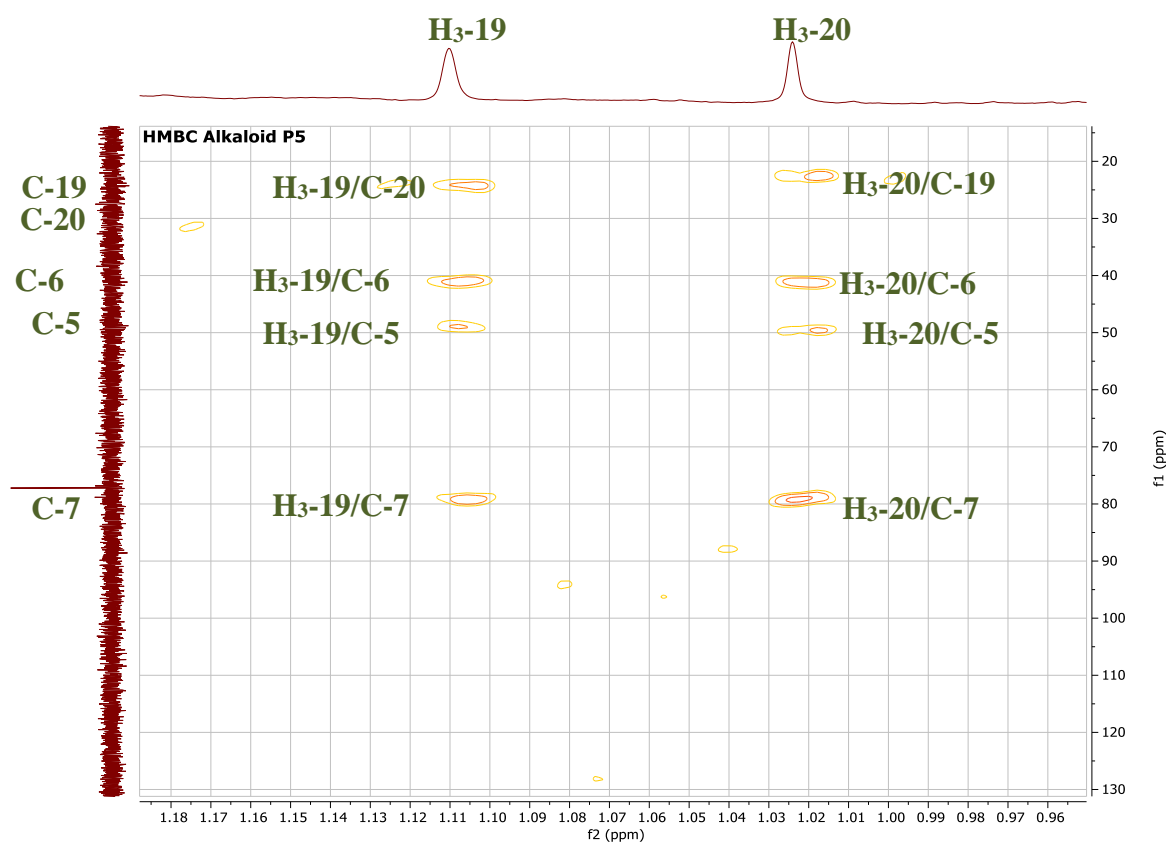


Figure III-B-33: HMBC expansion spectrum (600 MHz, CDCl₃) of compound P5 (correlation of methyl groups H-19 and H-20)

- ❖ The attachment of methyl CH₃-18 (δ_H 1.28) at C-3 (δ_C 59.19) was confirmed by its correlation spot between H₃-18 and C-2 (δ_C 34.67) which shown in HMBC expansion spectrum (Figure III-B-34-a). These correlations were previously observed in HMBC spectrum of both P8 and P13 alkaloids. In addition of that, a new correlation spot was observed between H₃-18 and C-16 (δ_C 147.42), give more evidence for attachment of CH₃-18 at C-3.
- ❖ The attachment of methyl CH₃-22 (δ_H 1.33) at C-9 (δ_C 63.49) was confirmed by its correlation spot (Figure III-B-34-a) between H₃-22 and C-2 (δ_C 34.67). This correlation spot was previously shown in HMBC spectrum of alkaloid P13.
- ❖ The attachment of new methyl corresponding to H₃-25 (δ_H 1.43 ppm) and C-25 (δ_C 30.23) at C-1 (δ_C 49), was confirmed by their correlation spots (Figure III-B-34-a)

between H₃-25 and C-2 (δ_C 34.67) and C-17 (δ_C 135.78). This attachment was confirmed also by absence of typical signal attributable to H-1 which observed in ¹H NMR of P8 and P13 alkaloids at δ_H 1.42.

The bounding of methyl substituent (H₃-25) at C-1 produced a shielding of chemical shift of: C-1 (δ_C 49.00), C-9 (δ_C 63.46) and C-2 (δ_C 34.67), due to the donating effect of methyl group.

- ❖ The attachment of new methyl corresponding to H₃-26 (δ_H 0.88) and C-26 (δ_C 13.89) at C-12 (δ_C 22.56), was confirmed by their correlation spot (Figure III-B-34-b) between H₃-26 and C-12 (δ_C 22.56).

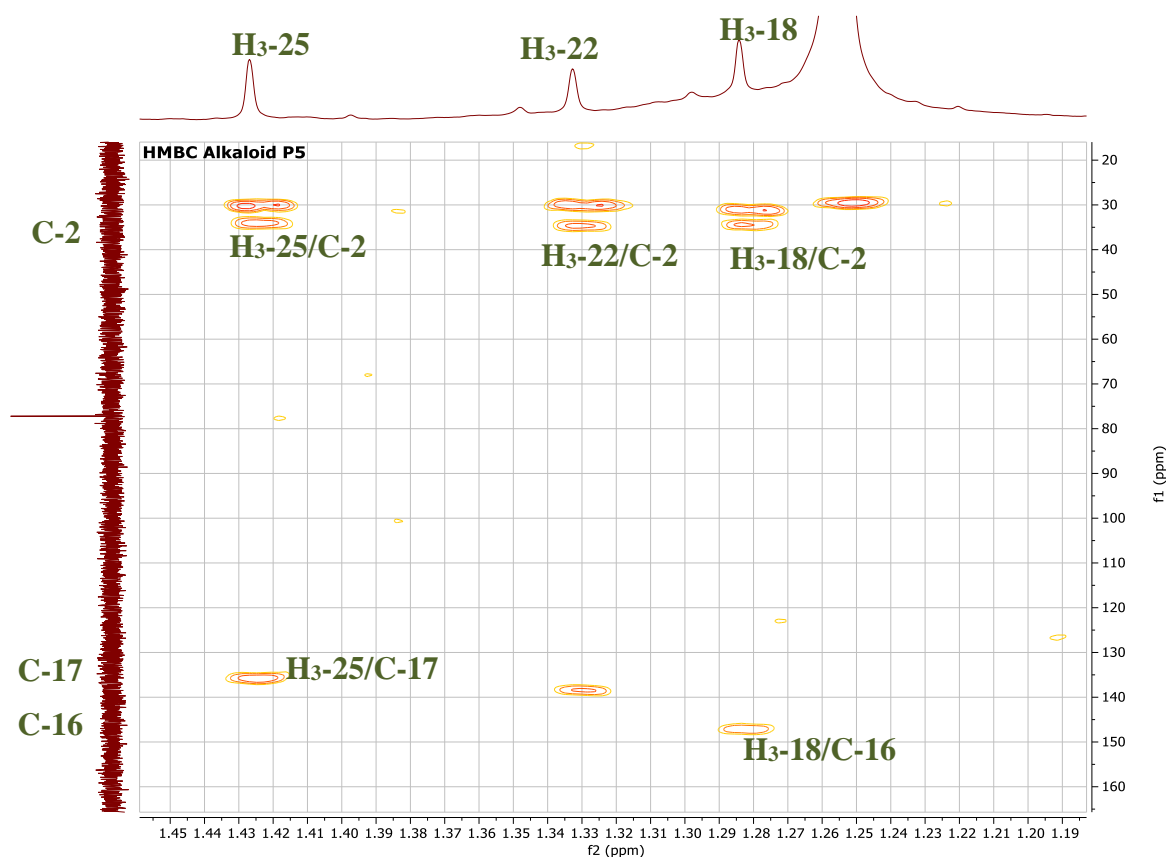


Figure III-B-34-a: HMBC expansions spectra (600 MHz, CDCl₃) of compound P5 (correlation of methyl groups H₃-18, H₃-22, H₃-25)

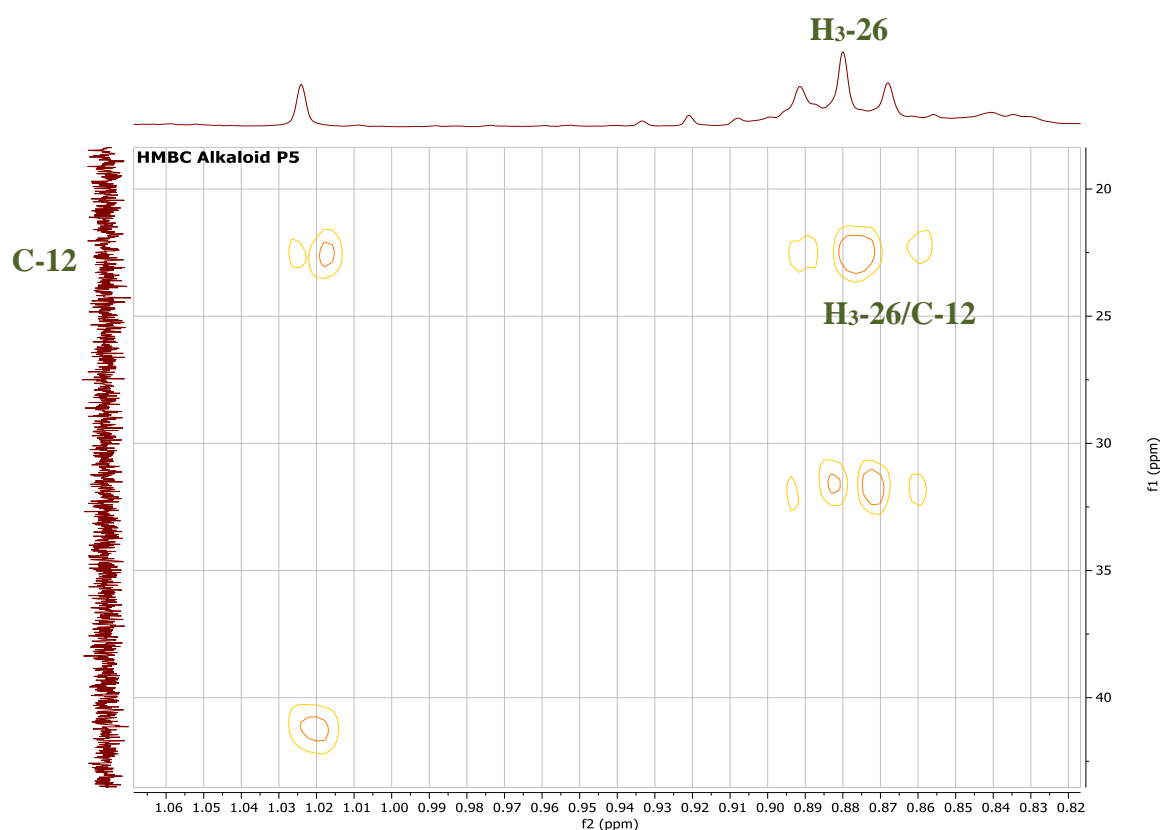


Figure III-B-34-b: HMBC expansions spectra (600 MHz, CDCl₃) of compound P5 (correlation of methyl group H₃-26)

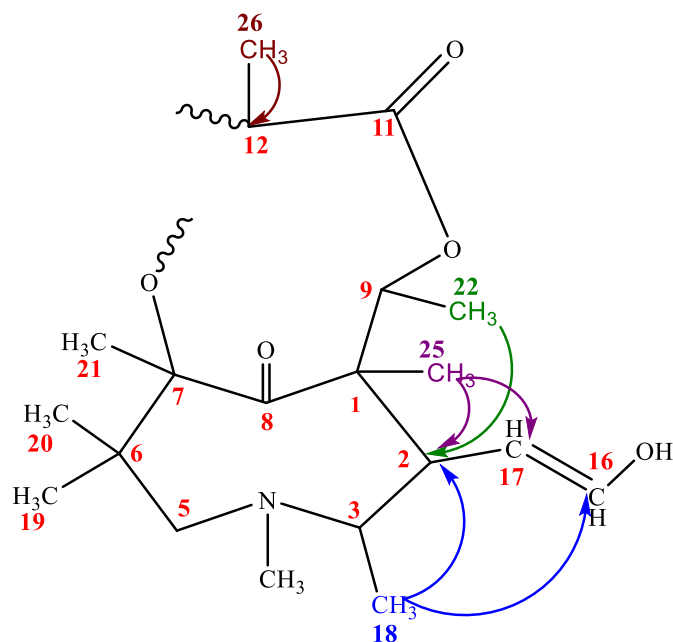


Figure III-B-35: Correlation of methyl groups (H₃-18, H₃-22, H₃-25 and H-26) according to HMBC spectrum of compound P5

Table III-B-03: Chemical shifts of ^1H (600 MHz) and ^{13}C (150 MHz) NMR in CDCl_3 of alkaloid P5 (δ in ppm and J in Hz)

Position	Compound P5	
	δ_{H}	δ_{C}
1	-	49.00
2	2.17 (s)	34.67
3	3.67 (s)	60.57
5	2.34 (d/J=17.0 Hz)	49.71
	2.50 (d/17.0 Hz)	
6	-	41.25
7	-	79.23
8	-	197.63
9	4.24 (m)	65.41
11	-	171.75
12	1.52	32.41
13	-	22.74
14	-	137.83
15	-	160.12
16	6.83 (d/J= 15.7 Hz)	147.42
17	6.47 (d/J=15.7 Hz)	135.78
18	1.28 (s)	31.63
19	1.11 (s)	22.99
20	1.02 (s)	24.24
21	1.25 (s)	29.41
22	-	-
23	5.96 (d/J=1.2 Hz)	138.64

24	1.89 (d/J=1.4 Hz)	18.53
25	1.43 (s)	30.23
26	0.88 (s)	13.89
27	1.33 (s)	30.08

According to various methods of ^1H NMR, ^{13}C NMR and 2D (HSQC and HMBC) we conclude that the structure of compound P5 is **14-ethylidene but-11,15-dioic acid- 2-hydroxyvinyl-3,N,6,6,7,1,9-heptamethyl otonecine (Tomentonecine C)**. It is isolated for the first time as a new compound. Its structure is demonstrated in the Figure III-B-36.

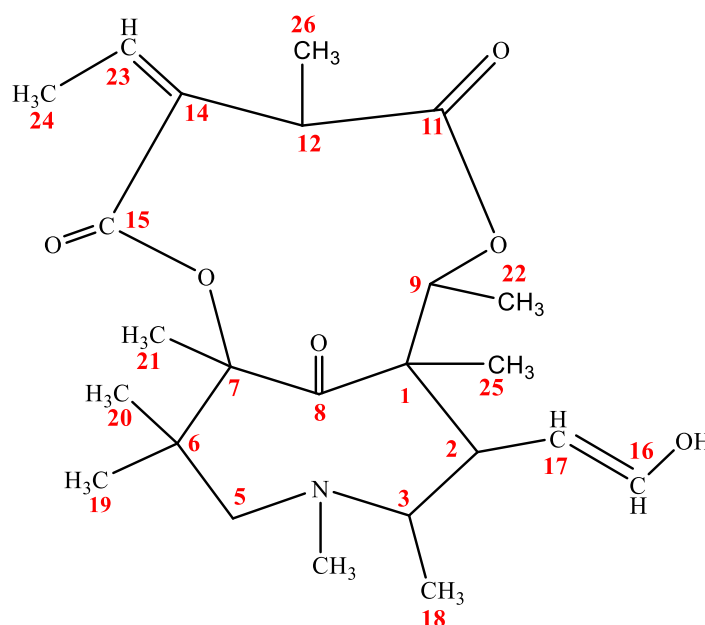


Figure III-B-36: Chemical structure of compound P5, which is an alkaloid named **Tomentonecine C**

- ❖ Tomentonecine C is an otonecine-type pyrrolizidine alkaloid composed of:
 - 2- hydroxyvinyl-3,N,6,6,7,1,9-heptamethyl otonecine.
 - 2- ethylden but-1,4-dioic acid.

III-B-1-4-Compound P20

This compound was obtained as colorless amorphous; it takes a blue color after revelation with a vanilin sulphuric solution and heating. Its structure was characterized using NMR spectroscopic analysis methods which are 1D: ^1H NMR and ^{13}C NMR and 2D: HSQC, HMBC and COSY. Its NMR spectra are recorded in CDCl_3 .

❖ The ^1H NMR spectrum (Figure III-B-37) of this compound showed:

- One singlet olefinic signal with an integration of one proton at δ_{H} 5.88.
- The signals corresponding to two no-equivalent protons of CH_2 groups which are:
 - ✓ Two doublet signals with an integration of one proton of each, at δ_{H} 4.97 and δ_{H} 4.80 with a coupling constant $J= 18$ Hz.
 - ✓ Two doublet signals with an integration of one proton of each, at δ_{H} 3.91 and δ_{H} 3.79 with a coupling constant $J= 11.3$ Hz and $J= 11.7$ Hz, respectively.
 - ✓ One doublet signal with an integration of one proton at δ_{H} 2.28 with a coupling constant $J= 15.6$ Hz, and one doublet of doublet with an integration of one proton at δ_{H} 0.80 with a coupling constant $J= 13.7; 3.5$ Hz.
 - ✓ One doublet of doublet with an integration of one proton at δ_{H} 2.15 with a coupling constant $J= 13.4; 4.6$ Hz, and one multiple signal with an integration of one proton at δ_{H} 1.85.
 - ✓ One doublet of doublet with an integration of one proton at δ_{H} 2.11 with a coupling constant $J= 13.6; 4.6$ Hz, and one doublet signal with an integration of one proton at δ_{H} 1.67 with a coupling constant $J= 13.4$ Hz.
- One doublet of doublet signal with an integration of one proton at δ_{H} 2.78 with a coupling constant $J= 9.4; 5.6$ Hz.
- One multiple signal with an integration of one proton at δ_{H} 3.67.
- One doublet signal with an integration of one proton at δ_{H} 1.70 with a coupling constant $J= 5.7$ Hz.
- One doublet signal with an integration of one proton at δ_{H} 1.15 with a coupling constant $J= 8.3$ Hz.

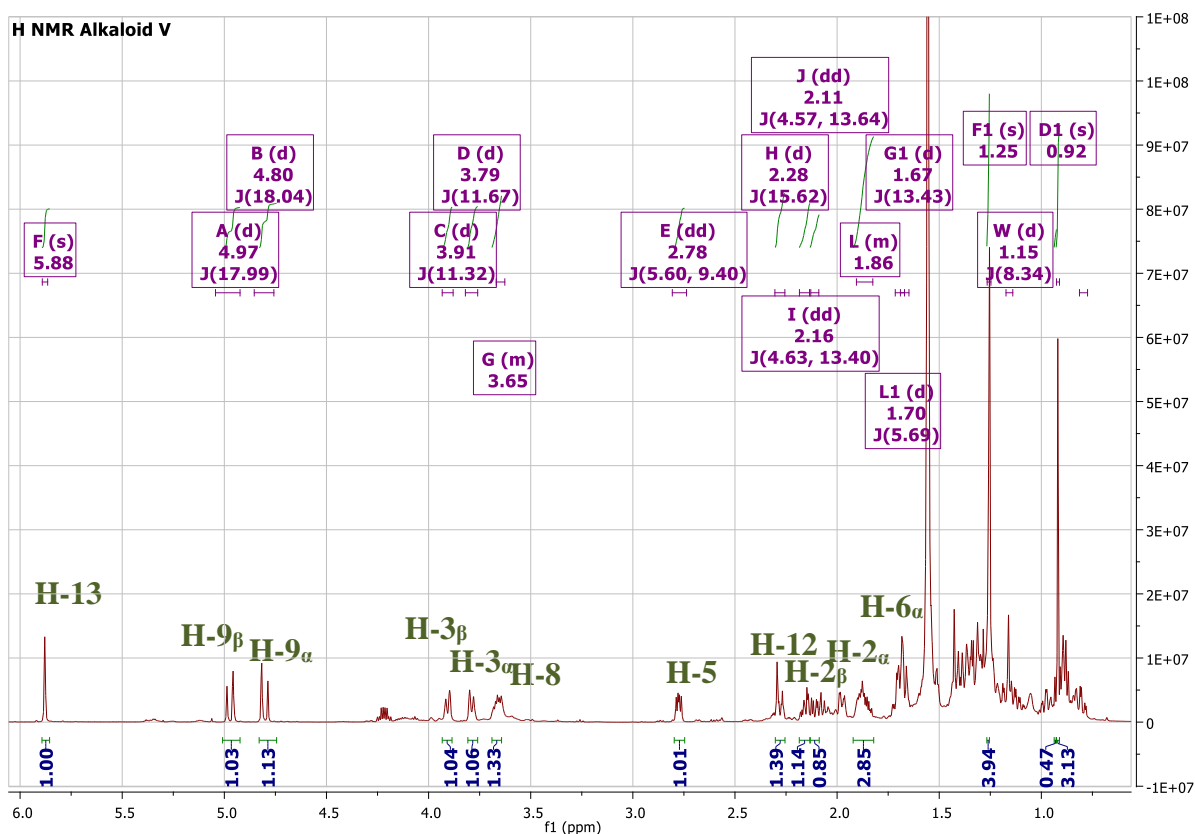


Figure III-B-37: ^1H NMR spectrum (600 MHz, CDCl_3) of Compound P20

❖ According to ^{13}C NMR spectrum (Figure III-B-38) there are:

- One olefinic signals at δ_{C} 117.90.
- Two carbonyl ester signals at δ_{C} 161.12 and δ_{C} 174.53.
- Two signals at δ_{C} 85.81 and δ_{C} 73.57 attributable to two oxygenated carbons.
- Three signals at δ_{C} 71.00; δ_{C} 60.22 and δ_{C} 50.97.
- One signal at δ_{C} 42.46.
- Three signals at δ_{C} 32.01; δ_{C} 31.47 and δ_{C} 27.05.
- Two methyl signals at δ_{C} 29.85 and δ_{C} 16.06.

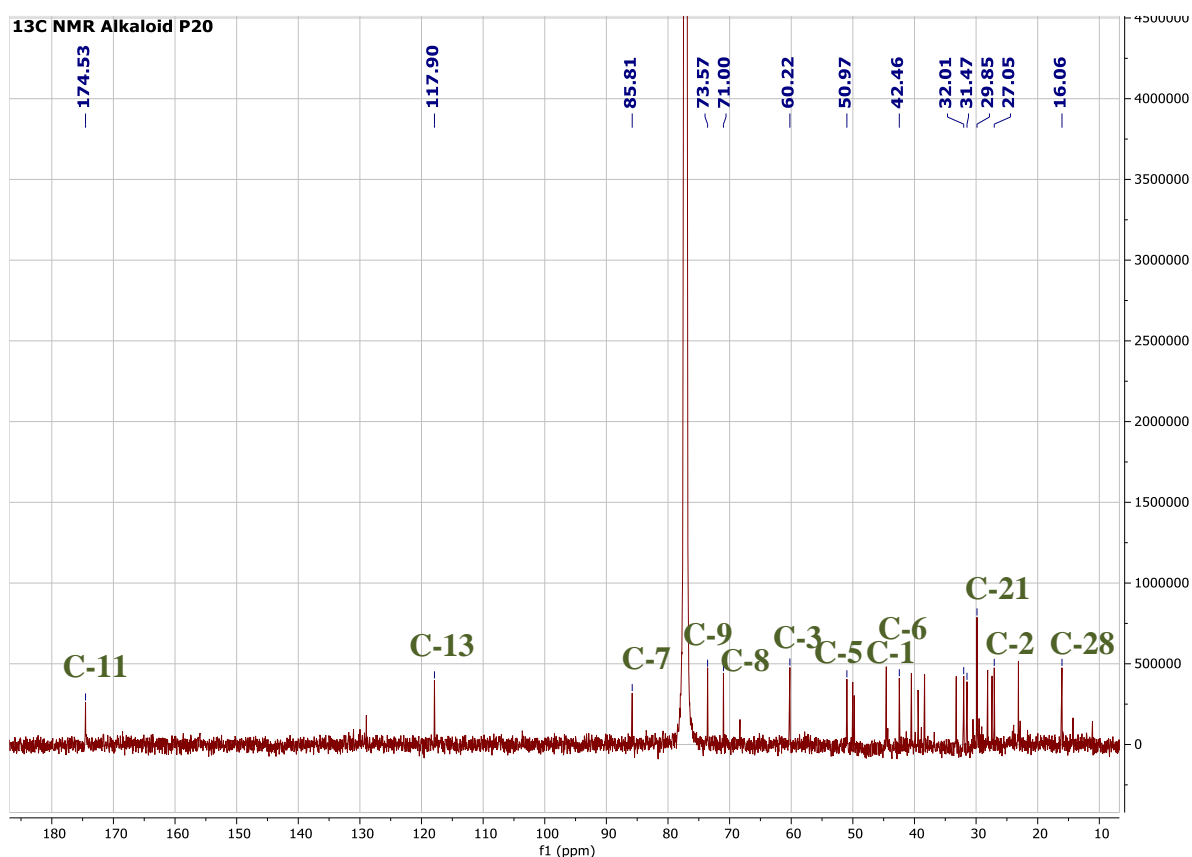


Figure III-B-38: ^{13}C NMR spectrum (150 MHz, CDCl_3) of compound P20

Both ^1H NMR and ^{13}C NMR spectra of alkaloid P20 show some similarities of signals by comparison with other alkaloids (P8, P13 and P5 alkaloids), which indicated that this compound has basic structure of macrocyclic diester pyrrolizidine alkaloid.

❖ Each proton is assigned to its corresponding carbon according to HSQC expansions spectrum (Figure III-B-39-a and III-B-39-b) which recorded:

➤ Typical signals of necine base at:

- δ_{H} 1.70 correlated with δ_{C} 42.46 attributable to H-1 and C-1.
- δ_{H} 2.15 correlated with δ_{C} 38.12 attributable to H-2 α and C-2.
 δ_{H} 1.85 correlated with δ_{C} 38.12 attributable to H-2 β and C-2.
- δ_{H} 3.91 correlated with δ_{C} 60.22 attributable to H-3 α and C-3.
 δ_{H} 3.79 correlated with δ_{C} 60.22 attributable to H-3 β and C-3.
- δ_{H} 2.25 correlated with δ_{C} 50.97 attributable to H-5 α and C-5.
- δ_{H} 2.11 correlated with δ_{C} 32.01 attributable to H-6 α and C-6.

δ_H 1.67 correlated with δ_C 32.01 attributable to H-6 β and C-6.

- δ_H 3.67 correlated with δ_C 71.00 attributable to H-8 and C-8.

➤ Typical signals of necic acid at:

- δ_H 4.94 correlated with δ_C 73.57 attributable to H-9 α and C-9.
- δ_H 4.80 correlated with δ_C 73.57 attributable to H-9 β and C-9.
- δ_H 2.28 correlated with δ_C 31.47 attributable to H-12 α and C-12.
- δ_H 0.80 correlated with δ_C 31.47 attributable to H-12 β and C-12.
- δ_H 5.88 correlated with δ_C 117.90 attributable to H-13 and C-13.

➤ Two methyl groups are attached to basic skeleton of alkaloid P20, their assignments are confirmed using HSQC experiment which shows the following attribution:

- δ_H 1.25 correlated with δ_C 29.85 attributable to H₃-21 and C-21.
- δ_H 0.92 correlated with δ_C 16.06 attributable to H₃-28 and C-28.

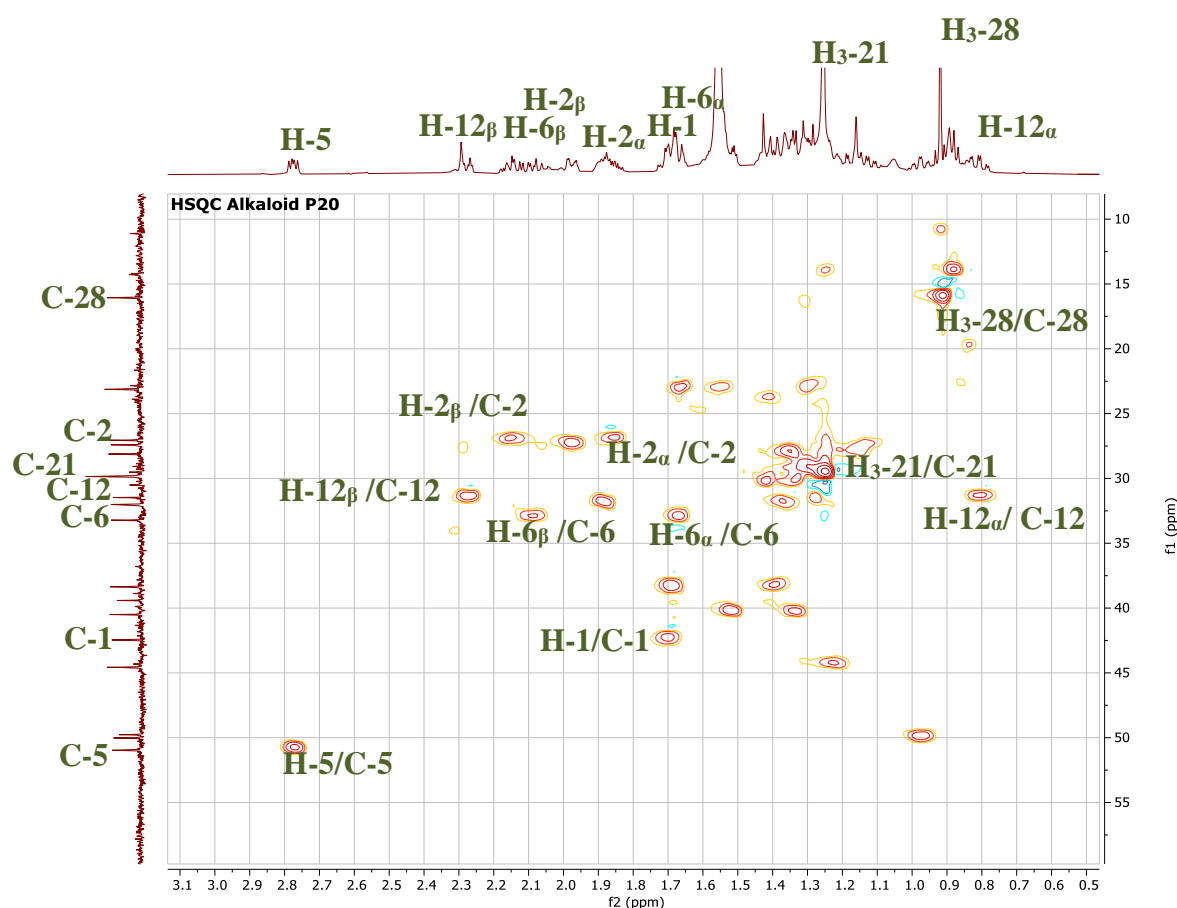


Figure III-B-39-a: HSQC expansion spectrum [3.01 – 0.6 ppm] (600 MHz, CDCl₃) of compound P20

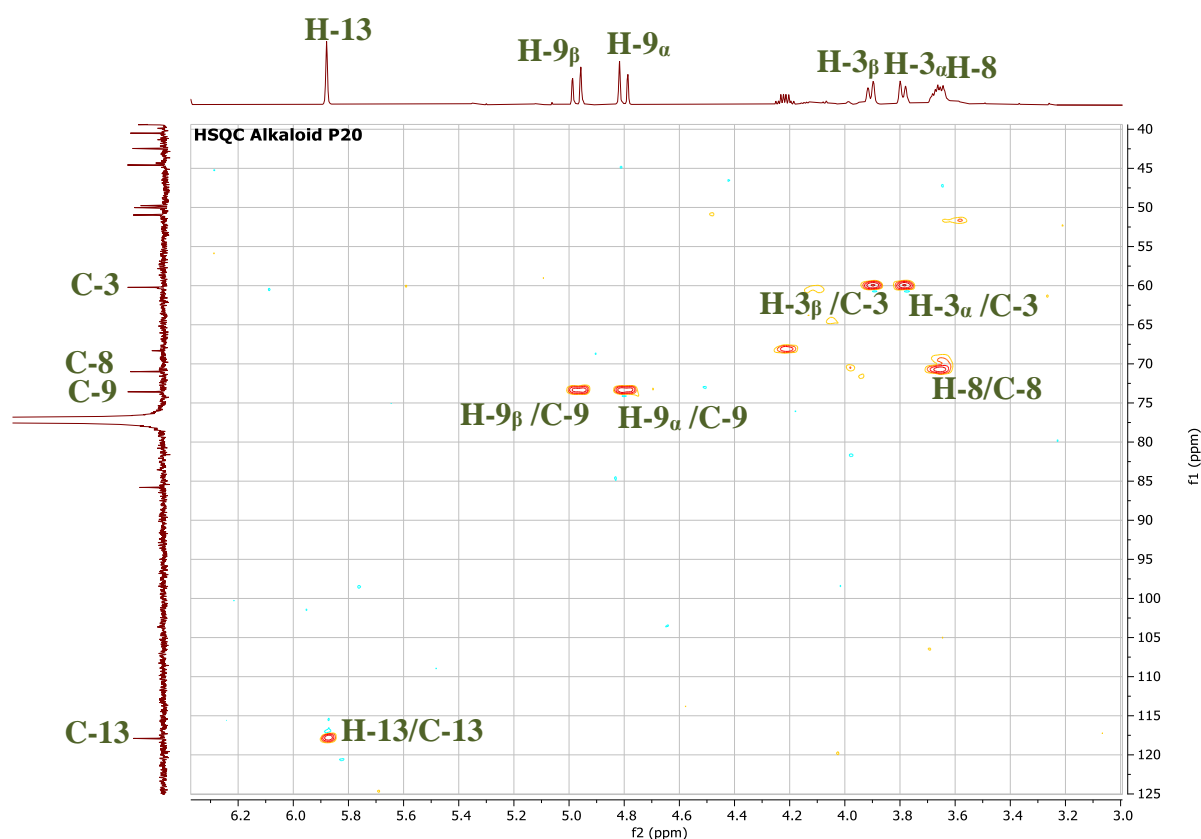
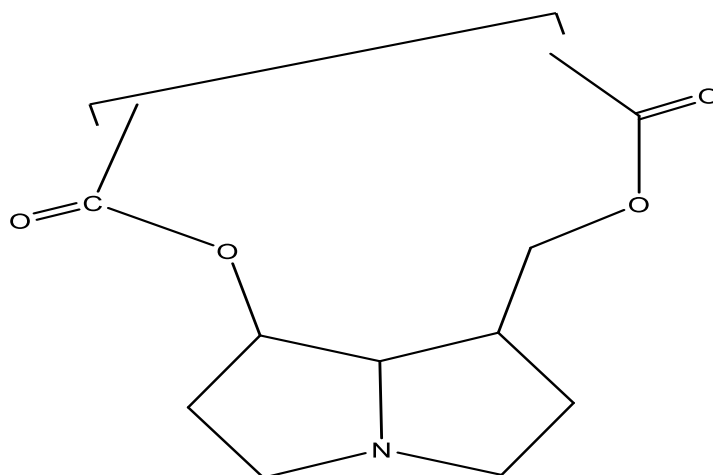


Figure III-B-39-b: HSQC expansion spectrum [6.2 – 3.2 ppm] (600 MHz, CDCl₃) of compound P20

The ¹H NMR spectrum of compound P20 shows the appearance of new proton signal at δ_{H} 3.67 that attributable to H-8, and the disappearance of methyl signal at δ_{H} 2.30 corresponding to N-CH₃ group, as well as the disappearance of signal at δ_{C} 197.58 ppm in ¹³C NMR spectrum of this compound which corresponded to a carbonyl group of a typical α,β -unsaturated ketone (C-8). These data indicate that C-8 is linked to N atom, which confirm that the type of compound P20 is retronecine-type pyrrolizidine alkaloid [116] (Figure III-B-40).



retronecine-type pyrrolizidine alkaloid

Figure III-B-40: Structures of retronecine-type pyrrolizidine alkaloid [116]

According to Catherine G. Logie *et al.*, $\Delta H-9$ value (the difference between chemical shift of the two protons of CH_2-9) is 0.14 ppm, which indicates that the size of this retronecine macrocyclic ring is 11-membered diester rings [119].

- ❖ HMBC spectrum (Figure III-B-41) of compound P20 shows some correlation spots, which confirmed the sequence of this compound skeleton as well as attachment of the methyl groups on this skeleton.
 - The attachment of methyl group CH_3-28 at C-5 was confirmed by the correlation spot between H_3-28 (δ_H 0.92) and C-5 (δ_C 50.97), as well as the correlation spot between H_3-28 and C-7 (δ_C 85.81).
 - Correlation spot was observed between H-13 (δ_H 5.88) and C-11 (δ_C 174.53); give more evidence for position of proton olifenic in necic acid.
 - Correlation spots between $H-9_\alpha$ (δ_H 4.94) and C-11 (δ_C 174.53) and $H-9_\beta$ (δ_H 4.80) and C-11 (δ_C 174.53) is appear clearly in HMBC spectrum of compound P20.

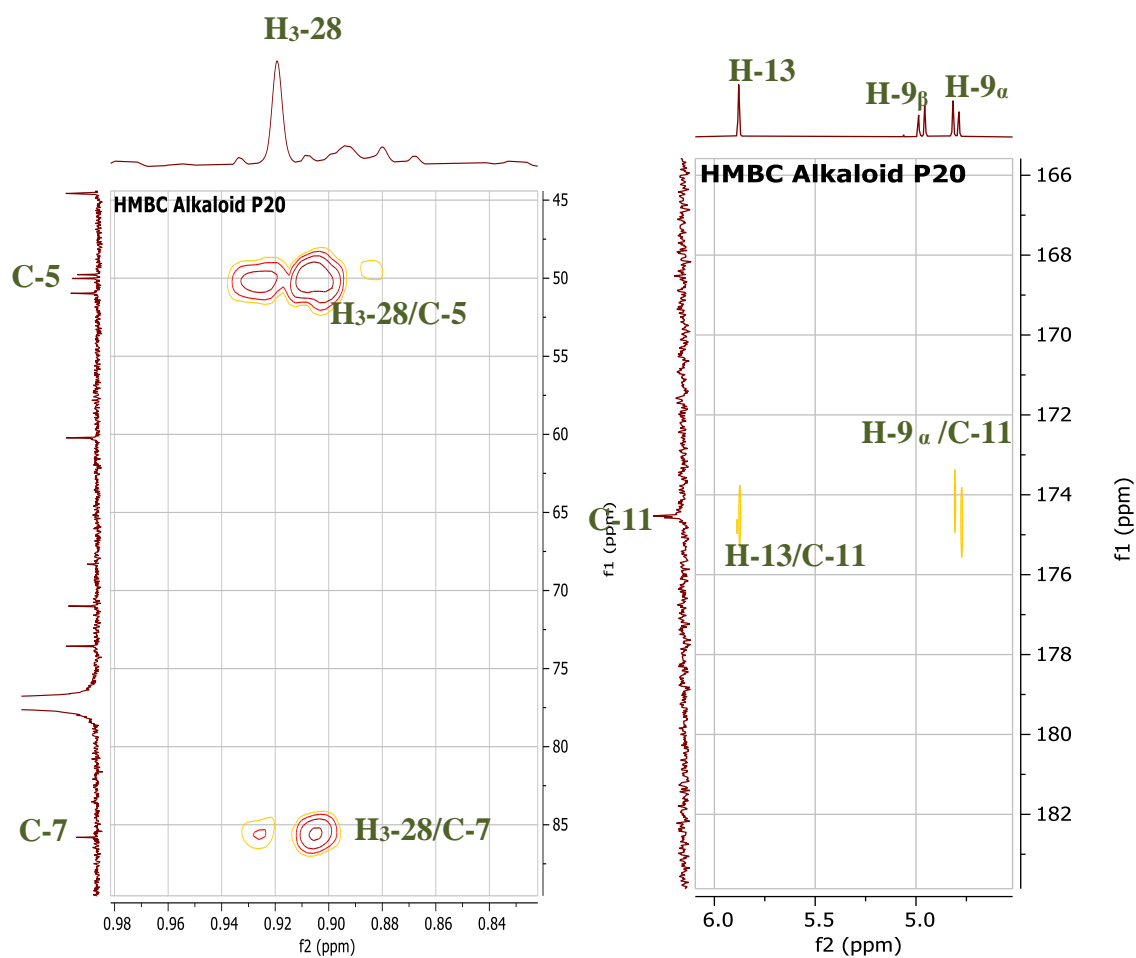


Figure III-B-41: HMBC expansions spectrum (600 MHz, CDCl₃) of compound P20 (correlation of H-9_α, H-9_β, H-13, and H₃-28)

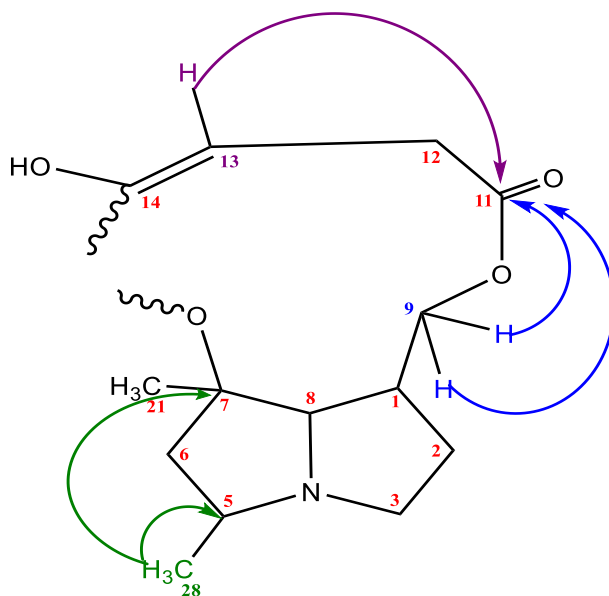


Figure III-B-42: Correlation of methyl groups (H₃-28, H-9_α, H-9_β and H-13) according to HMBC spectrum of compound P20

Table III-B-04: Chemical shifts of ^1H (600 MHz) and ^{13}C (150 MHz) NMR in CDCl_3 of alkaloid P20 (δ in ppm and J in Hz).

Compound P20		
Position	δ_{H}	δ_{C}
1	1.70 (d/J=5.7Hz)	42.46
2	2.15 (dd/J=13.4/5.3 Hz)	27.05
3	1.85 (dd/J=13.7/5.3 Hz)	60.22
	3.91 (d/J=11.3 Hz)	
5	3.79 (d/J=11.7 Hz)	50.97
	2.78 (dd/J= 9.4/5.6 Hz)	
6	2.11 (dd/J=13.6/4.6 Hz)	32.01
7	1.67 (d/J=13.4 Hz)	85.81
	-	
8	3.67 (m)	71.00
9	4.94 (d/J=18.0 Hz)	73.57
	4.80 (d/J=18.0 Hz)	
11	-	174.53
12	2.28 (d/J=15.6 Hz)	31.47
	0.80 (dd/J=13.7/3.5 Hz)	
13	5.88 (s)	117.90
14	-	137.32
15	-	
21	1.25 (s)	29.85
28	0.92 (s)	16.06

Based on all of these data, we conclude that the structure of compound P20 is **14-hydroxy-pent-13-ene-11,15-dioic acid-5,7-dimethyl retronecine (Tomentonecine D)**. It is isolated for the first time as a new compound. Its structure is demonstrated in the Figure III-B-43.

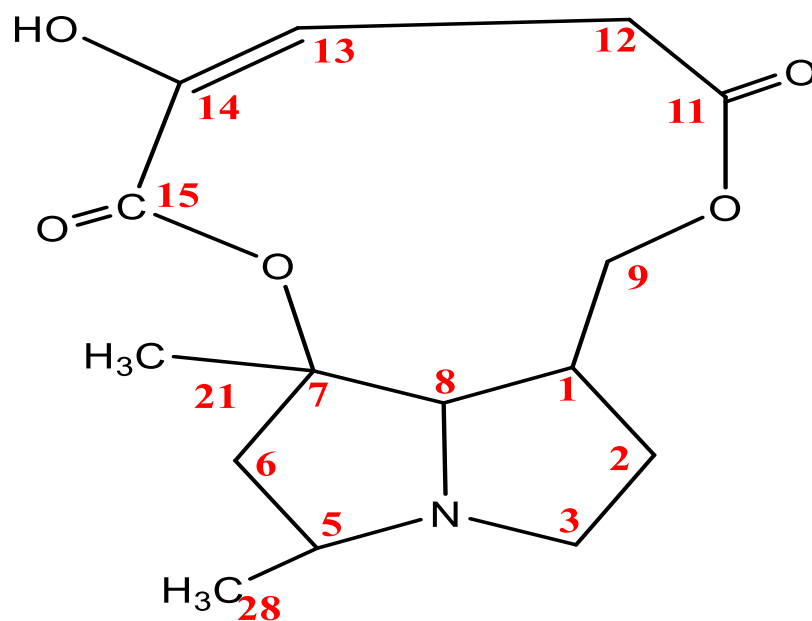


Figure III-B-43: Chemical structure of compound P20, which is an alkaloid named **Tomentonecine D**

- ❖ Tomentonecine D is a retronecine -type pyrrolizidine alkaloid composed of:
 - 5,7-dimethyl retronecine.
 - 2-hydroxy pent-2-ene-1,5-dioic acid.

III-B-1-5-Compound P10

This compound was obtained as colorless amorphous; it takes a yellow color after revelation with a vanilin sulphuric solution and heating. Its structure was characterized using NMR spectroscopic analysis methods which are 1D: ^1H NMR and ^{13}C NMR and 2D: HSQC, HMBC and COSY. Its NMR spectra are recorded in CDCl_3 .

- ❖ The ^1H NMR spectrum (Figure III-B-44) of this compound showed:
 - Two singlet olefinic signals with an integration of one proton of each, at δ_{H} 6.81 and δ_{H} 6.34.
 - Two singlet signals with an integration of one proton of each, at δ_{H} 3.78 and δ_{H} 3.79.

- One doublet signal with an integration of one proton at δ_H 2.05 with a coupling constant $J = 13.3$ Hz, and one doublet of doublet with an integration of one proton at δ_H 1.66 with a coupling constant $J = 13.3; 3.5$ Hz. These two signals corresponding to two no-equivalent protons of CH_2 group.
- One doublet signal with an integration of one proton at δ_H 2.00 with a coupling constant $J = 12.5$ Hz, and one doublet of doublet with an integration of one proton at δ_H 1.61 with a coupling constant $J = 12.4; 3.4$ Hz. These two signals corresponding to two no-equivalent protons of CH_2 group.
- Four singlet methyl signals with an integration of three protons of each, at δ_H 2.37; δ_H 1.26; δ_H 1.19 and δ_H 1.02.

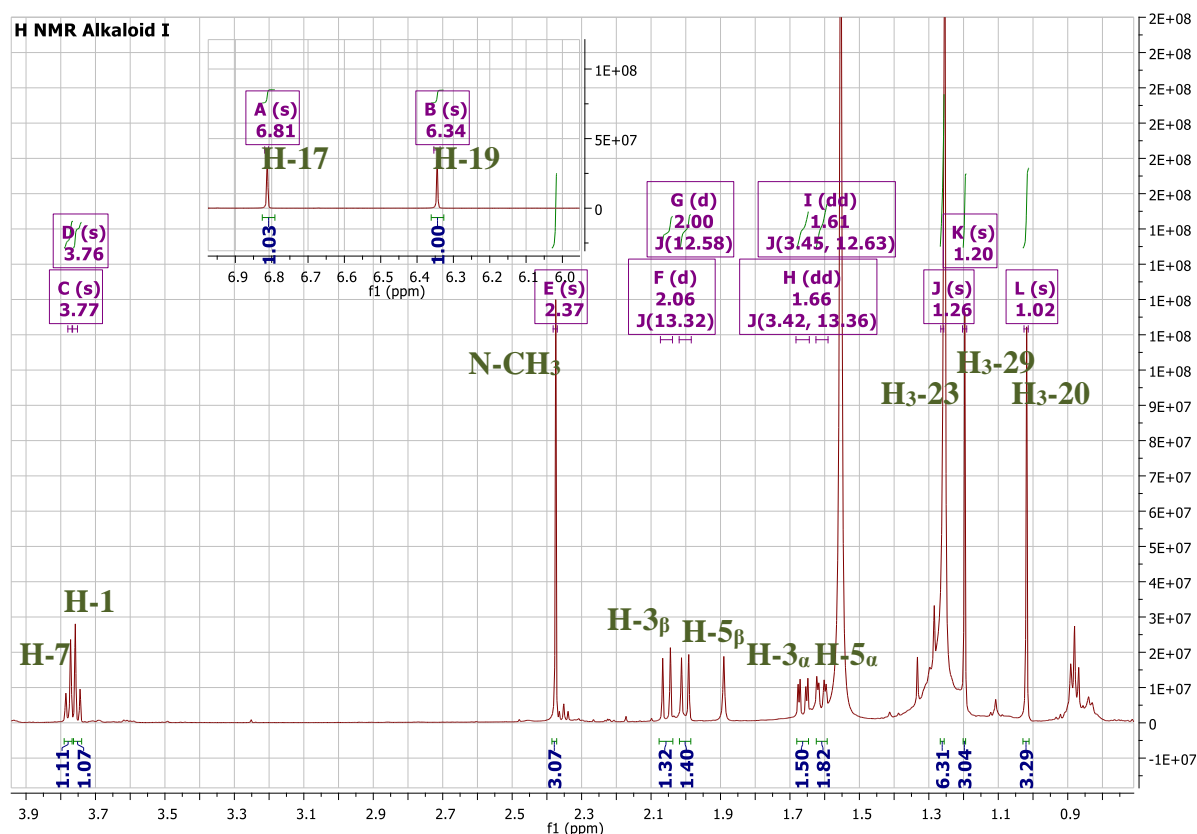


Figure III-B-44: 1H NMR spectrum (600 MHz, $CDCl_3$) of compound P10

- ❖ According to ^{13}C NMR spectrum (Figure III-B-45) there are:
- Two olefinic signals at: δ_C 138.46 and δ_C 144.43.
 - Two carbonyl ester signals at: δ_C 161.12 and δ_C 171.75.
 - One carbonyl carbon signal at: δ_C 199.65.
 - Four signals at: δ_C 85.17; δ_C 84.10; δ_C 78.47 and δ_C 71.78 attributable to four oxygenated carbons.

- Two signals at: δ_C 52.83 and δ_C 51.66.
- One signal at: δ_C 47.48.
- Four signals at: δ_C 29.85; δ_C 26.18; δ_C 22.25 and δ_C 19.49.

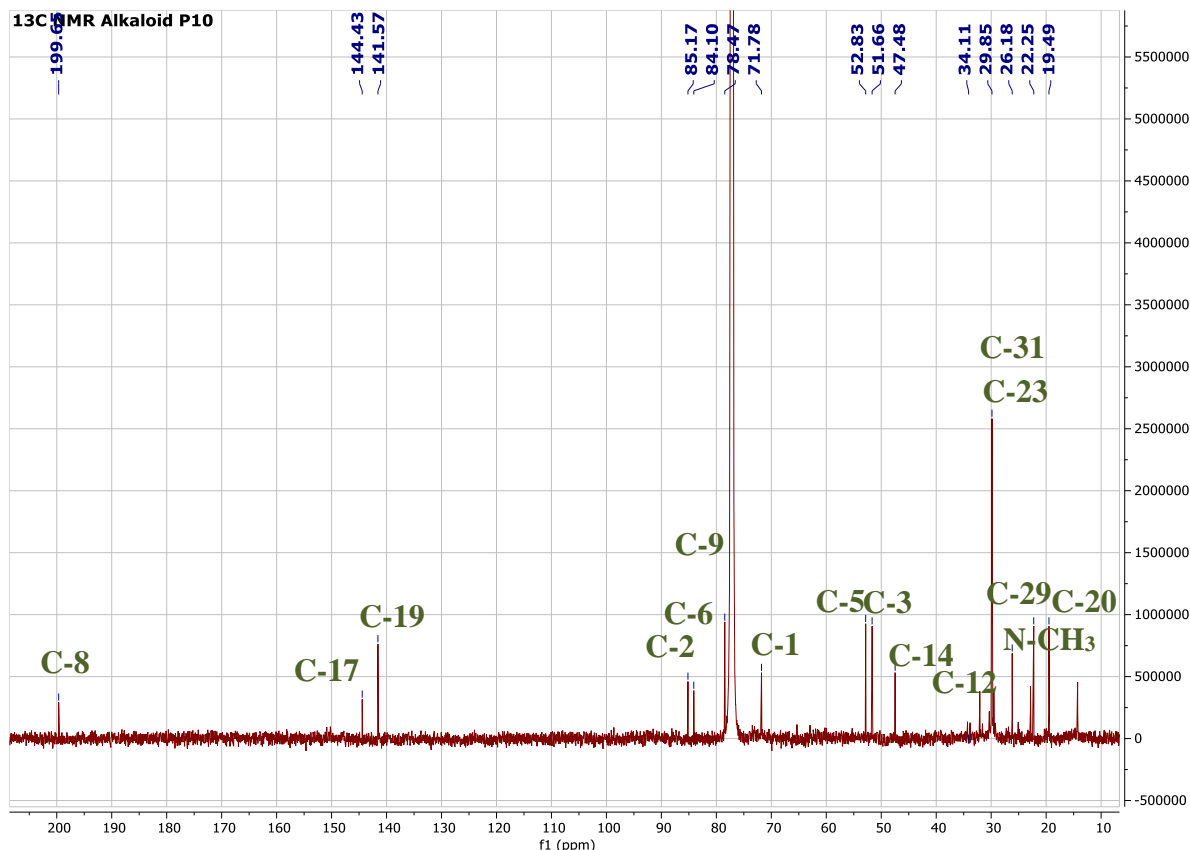


Figure III-B-45: ¹³C NMR spectrum (150 MHz, CDCl₃) of compound P10

The ¹H NMR and ¹³C NMR spectra of compound P10 shows some similarities of signals with those of P8, P13 and P5 alkaloids, which confirmed that this compound has basic structure of otonecine-type pyrrolizidine alkaloid.

The major difference between P10 and the other alkaloids (P8, P13 and P5) appears clearly on ¹H and ¹³C NMR spectra of compound P10, which show:

- ✓ The appearance of two new singlet signals at: δ_H 3.78 and δ_H 3.79.
- ✓ The appearance of new methyl signal at: δ_H 1.19.
- ✓ The disappearance of tow signals at δ_H 2.17 and δ_H 1.42 attributable to H-2 and H-1, respectively.
- ✓ The appearance of four new carbon signals at: δ_C 85.17; δ_C 84.10; δ_C 78.47 and δ_C 71.78.

❖ The proton–carbon correlation in HSQC experiment (Figure III-B-46) allowed us to assign all protons to their corresponding carbons:

➤ Typical signals of necine base at:

- δ_H 2.05 correlated with δ_C 51.66 attributable to H $_{\alpha}$ -3 and C-3.
 δ_H 1.66 correlated with δ_C 51.66 attributable to H $_{\beta}$ -3 and C-3
- δ_H 2.00 correlated with δ_C 52.83 attributable to H-5 $_{\alpha}$ and C-5.
 δ_H 1.61 correlated with δ_C 52.83 attributable to H-5 $_{\beta}$ and C-5.
- δ_H 3.76 correlated with δ_C 78.47 attributable to H-7 and C-7.

➤ Typical signals of necic acid at:

- δ_H 3.77 correlated with δ_C 78.47 attributable to H-9 and C-9.
- δ_H 2.34 correlated with δ_C 34.11 attributable to H-12 and C-12

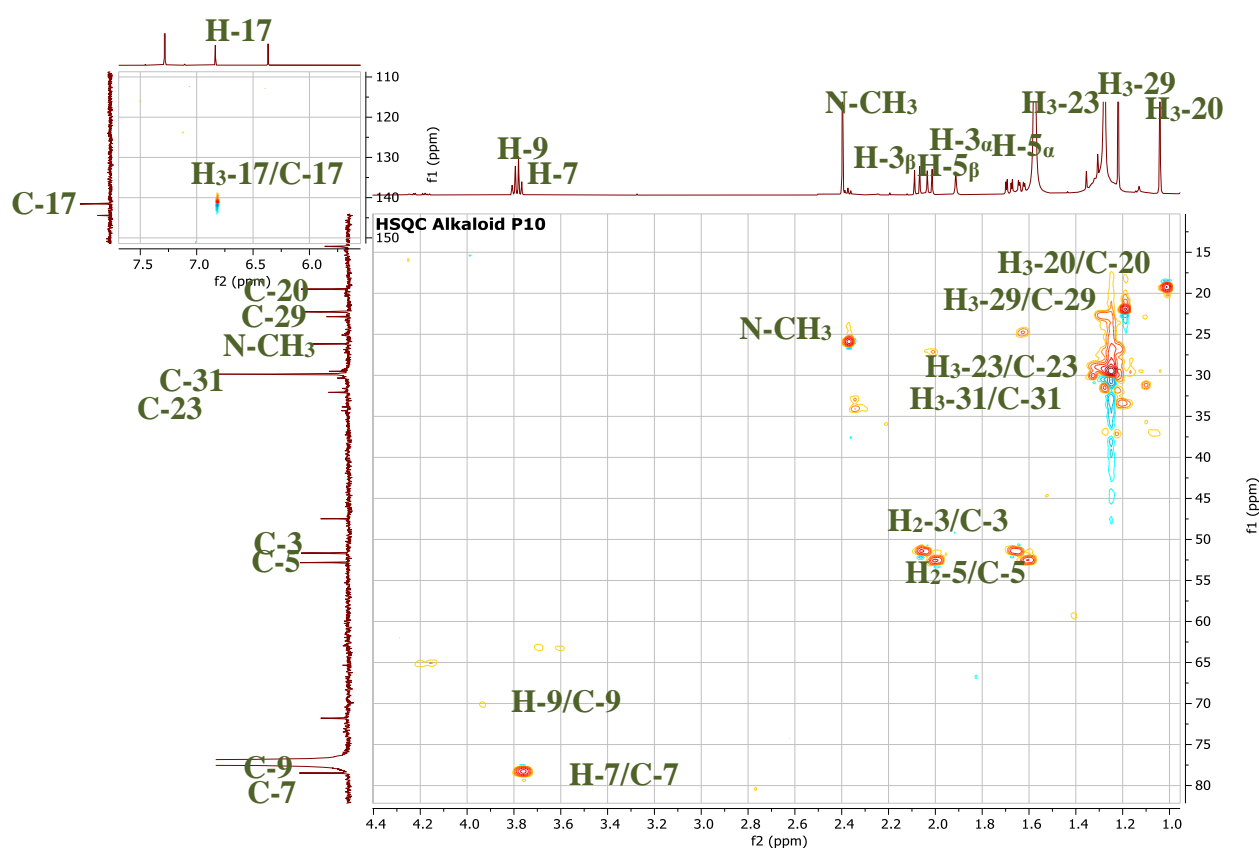


Figure III-B-46: HSQC expansion spectrum (600 MHz, CD₃Cl) of compound P10

In order to place the substituent groups on base skeleton of compound P10 we examined the HMBC spectrum, which shows a correlation spots between the protons of these substituents and their vicinal carbons.

HMBC expansion spectrum (Figure III-B-47) recorded correlation between:

❖ H-3_α (δ_H 2.05) has correlated with:

- C-5 (δ_C 52.83).
- C (δ_C 71.78).
- C (δ_C 85.17).

❖ H-3_β (δ_H 1.66) has correlated with:

- C-5 (δ_C 52.83).
- C (δ_C 71.78).
- C (δ_C 85.17).

The appearance of correlation spots between H-3_α (δ_H 2.05) and H-3_β (δ_H 1.66) and C (δ_C 85.17) and C (δ_C 71.78) (Figure III-B-47), in addition of the disappearance of the tow proton signals at δ_H 2.17 and δ_H 1.42 attributable respectively to H-2 and H-1, indicated that C (δ_C 85.17) attributable to C-2 and C (δ_C 71.78) attributable to C-1.

❖ H-5_α (δ_H 2.00) has correlated with:

- C-3 (δ_C 51.66).
- C-1 (δ_C 71.78).
- C-7 (δ_C 78.47).
- C (δ_C 84.10).

❖ H-5_β (δ_H 1.61) has correlated with:

- C-3 (δ_C 51.66).

The appearance of a correlation spot between H-5_α (δ_H 2.00) and C (δ_C 84.10) (Figure III-B-47), in addition to the disappearance of the quaternary carbon signal at δ_C 40 attributable to C-6, confirmed that C (δ_C 84.10) attributable to C-6.

❖ N-CH₃ (δ_H 2.37) has correlated with:

- C-8 (δ_C 199.65).

This long-range correlation is previously shown in HMBC spectrum of the alkaloid P8, which is a typical correlation of otonecine-type pyrrolizidine alkaloid.

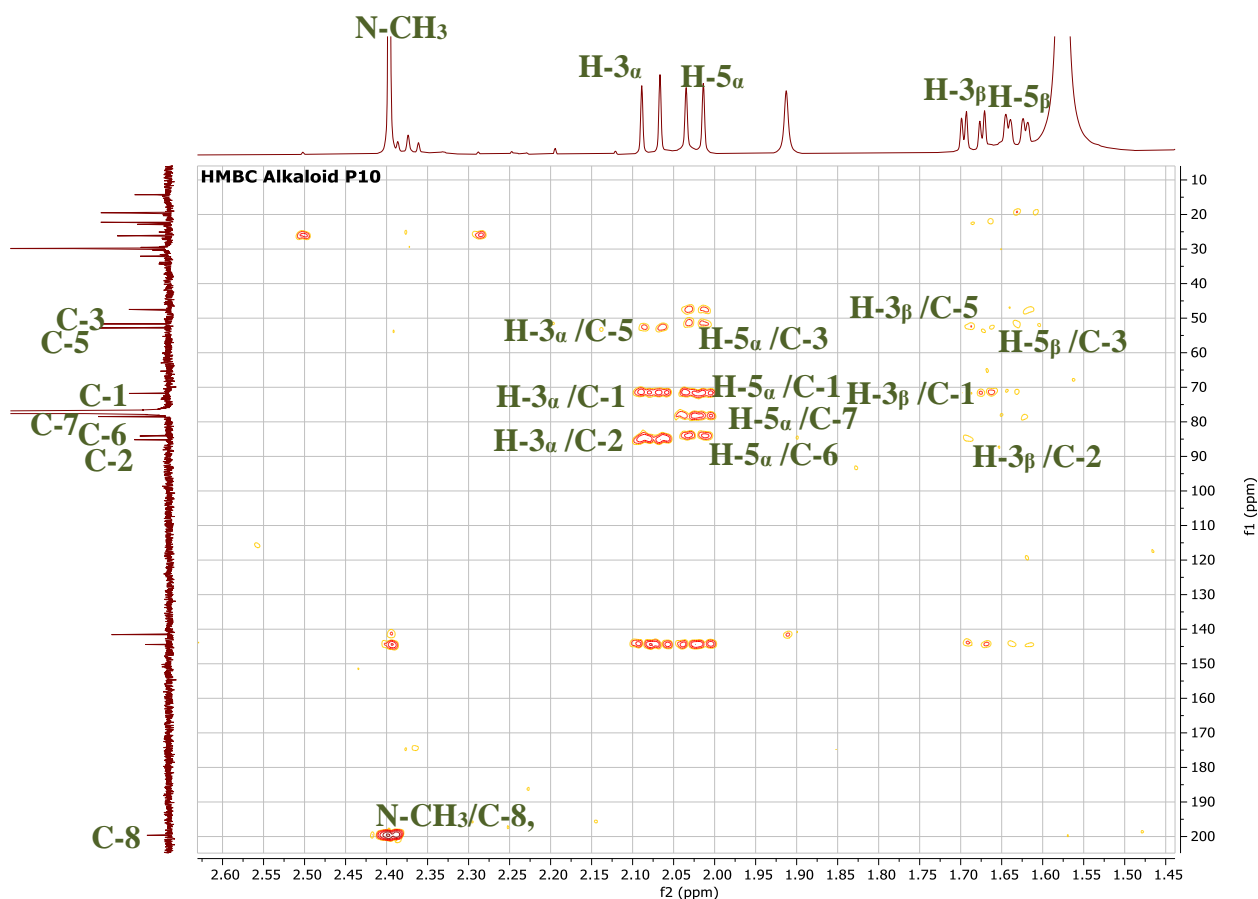


Figure III-B-47: HMBC expansion spectrum (600 MHz, CDCl_3) of compound P10 (correlation of H-3_α , H-3_β , H-5_α , H-5_β and N-CH_3)

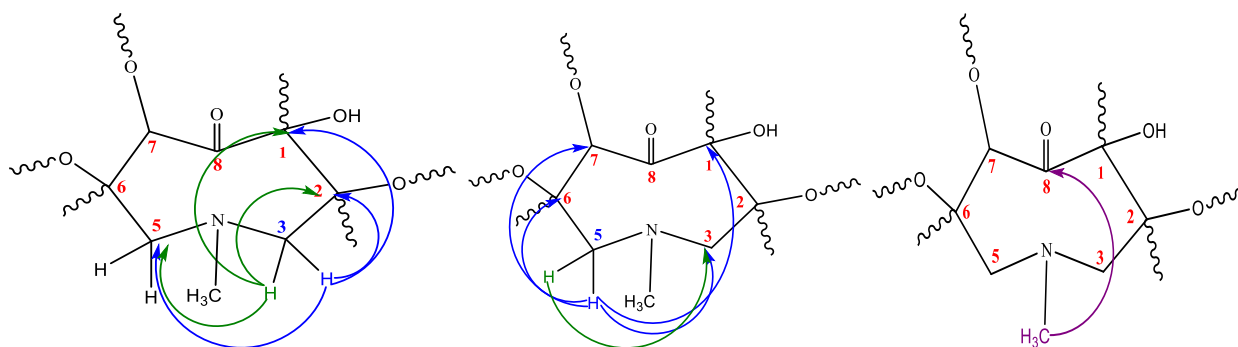


Figure III-B-48: Correlation of H-3_α , H-3_β , H-5_α , H-5_β and N-CH_3 according to HMBC spectrum of compound P10

H-7 (δ_H 3.76) and H-9 (δ_H 3.77) are two singlet protons which have almost identical chemical shift, their correlation spots were shown in the HMBC expansion spectrum (Figure III-B-49) which are:

❖ H-7 (δ_H 3.76) has correlated with:

- C-14 (δ_C 47.48).
- C-5 (δ_C 52.83).
- C-6 (δ_C 84.10).
- C-20 (δ_C 19.49).

❖ H-9 (δ_H 3.77) has correlated with:

- C-2 (δ_C 85.17).

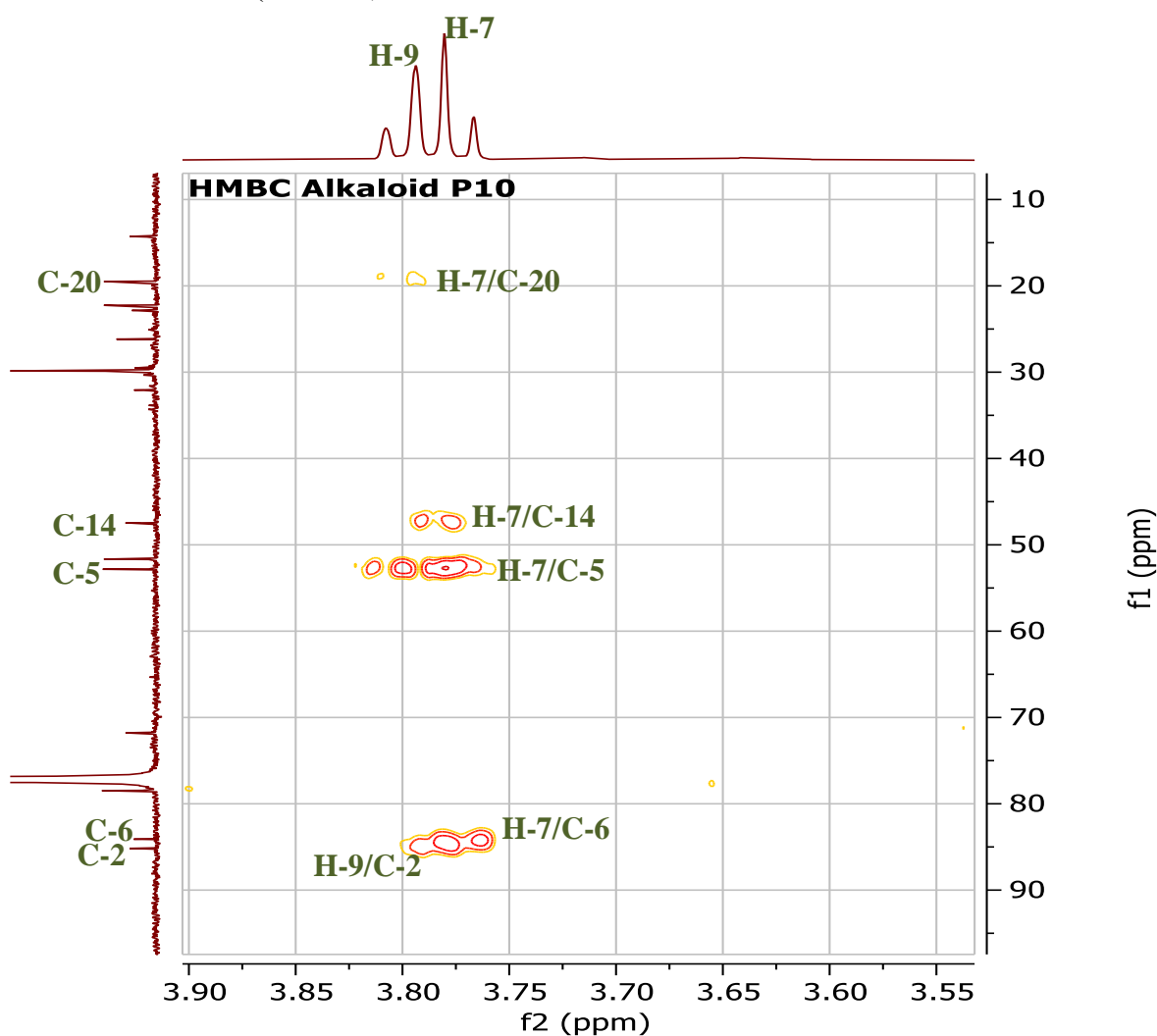


Figure III-B-49: HMBC expansion spectrum (600 MHz, $CDCl_3$) of compound P10
(correlation of H-7 and H-9)

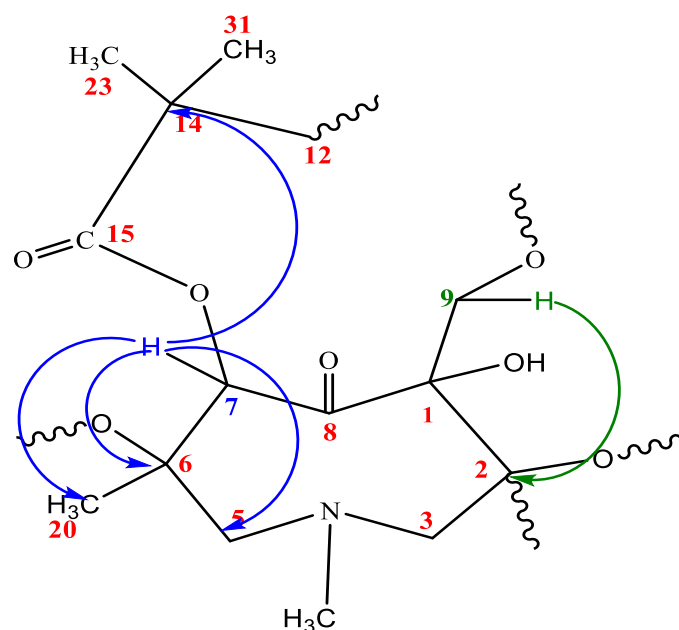


Figure III-B-50: Correlation of H-7 and H-9 according to HMBC spectrum of compound P10

The attachment of two methyl groups at two quaternary oxygenated carbon (C-2 and C-6) is suggested by their correlation spots recorded from HMBC expansion spectrum (Figure III-B-51) which are:

❖ H₃-20 (δ_{H} 1.02) has correlated with:

- C-6 (δ_{C} 84.10).
- C-7 (δ_{C} 78.47).
- C-5 (δ_{C} 52.83).

These correlation spots indicated that methyl group (CH₃-20) is attached to quaternary oxygenated carbon C-6.

❖ H₃-29 (δ_{H} 1.19) has correlated with:

- C-2 (δ_{C} 85.17).
- C-3 (δ_{C} 51.66).

These correlation spots indicated that methyl group (CH₃-29) is attached to quaternary oxygenated carbon C-2.

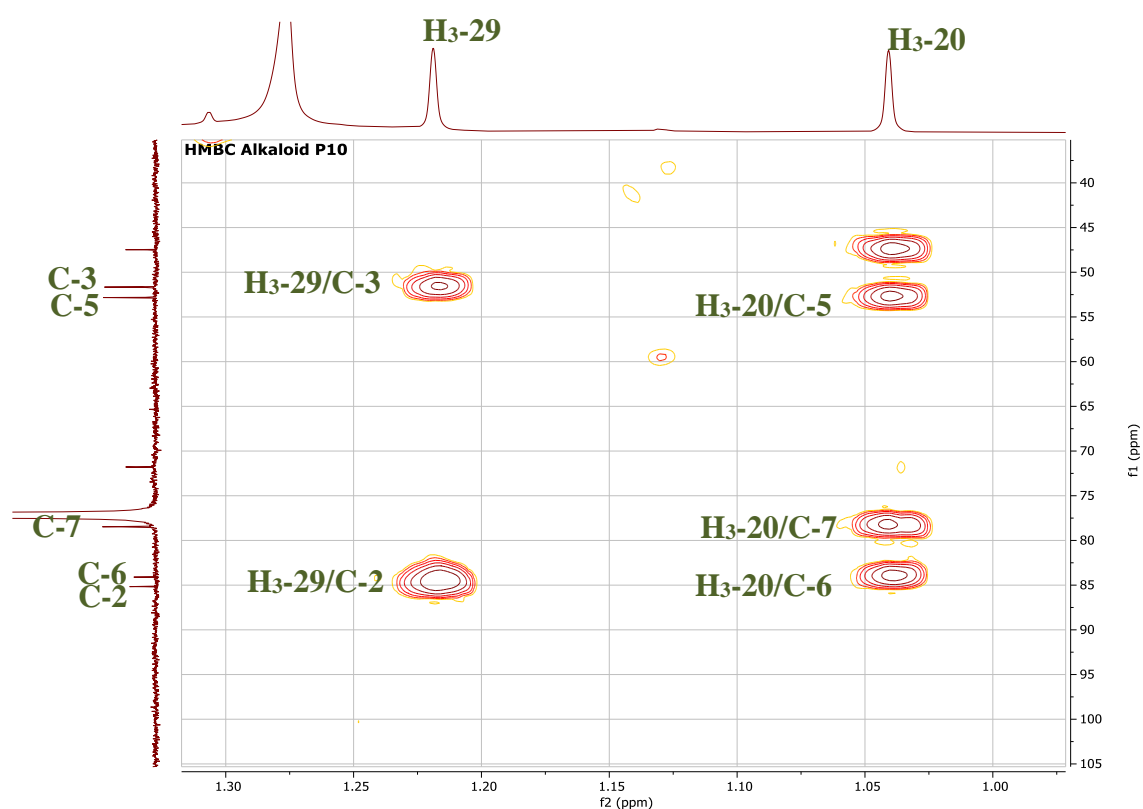


Figure III-B-51: HMBC expansion spectrum (600 MHz, CDCl₃) of compound P10 (correlation of methyl groups H₃-20 and H₃-29)

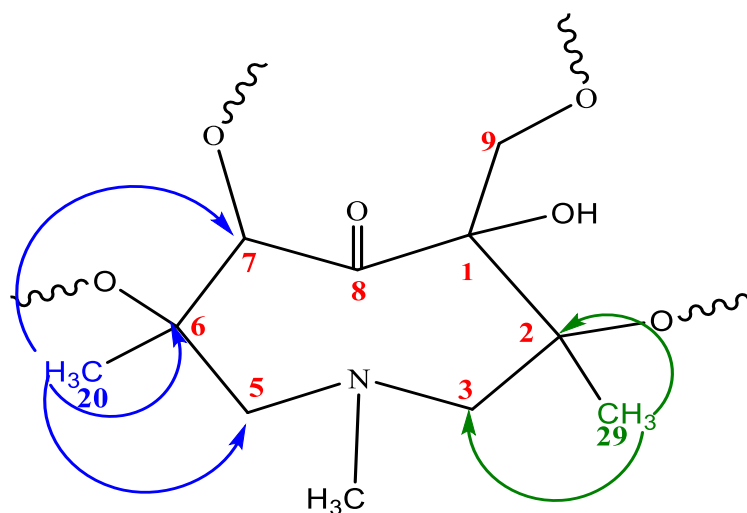


Figure III-B-52: Correlation of methyl groups H₃-20 and H₃-29 according to HMBC spectrum of compound P10

HMBC expansion spectrum (Figure III-B-53-a) shows correlation spots that indicated the attachment of 2, 2-dihydroxyvinyl group (H-17) to C-2 carbon which are:

❖ H-17 (δ_H 6.34) has correlated with:

- C-2 (δ_C 85.17).
- C-1 (δ_C 71.78).
- C-5 (δ_C 52.83).
- C-8 (δ_C 199.65).

The attachment of 2, 2-dihydroxyvinyl group (H-19) to C-6 carbon was confirmed by the correlation spots between H-19 and its vicinal carbons shown in HMBC expansion spectrum (Figure III-B-53-a) which are:

❖ H-19 (δ_H 6.81) has correlated with:

- C-5 (δ_C 52.83).
- C-30 (δ_C 144.43).

In the other hand, the attachment of 2, 2-dihydroxyvinyl (H-19) group to C-6 carbon is confirmed also by the correlation spot between H-5 $_{\alpha}$ (δ_H 2.00) and quaternary carbon C-30 (δ_C 144.43) (Figure III-B-53-b).

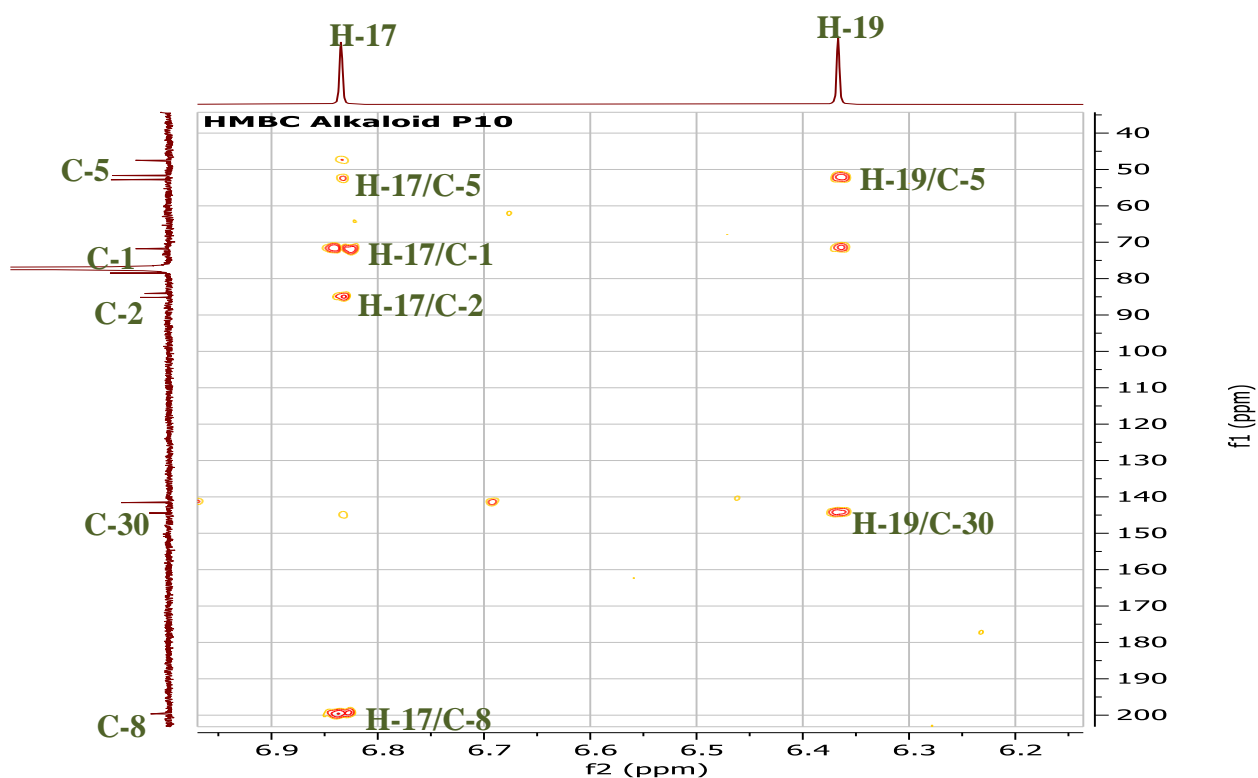


Figure III-B-53-a: HMBC expansions spectrum (600 MHz, CDCl₃) of compound P10 (correlation of dihydroxyvinyl group groups H-17 and H-19)

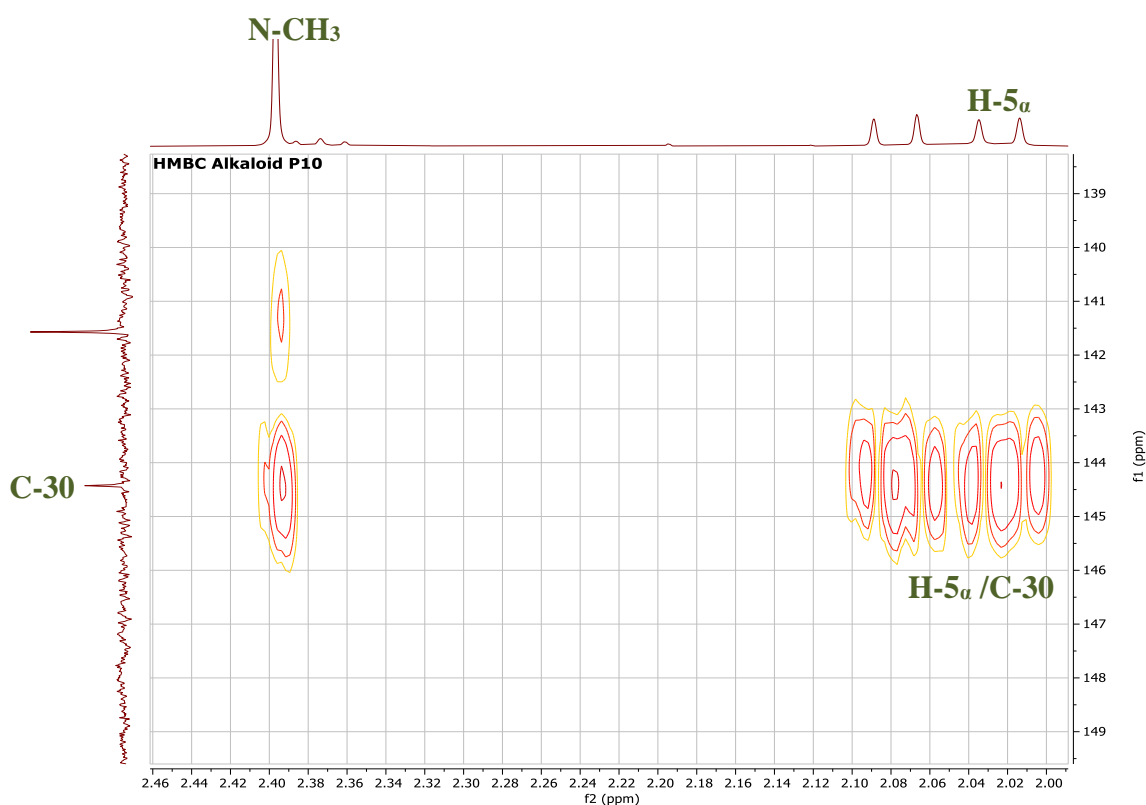


Figure III-B-53-b: HMBC expansions spectrum (600 MHz, CDCl₃) of compound P10 (correlation of N-CH₃ and H-5_α with C-30)

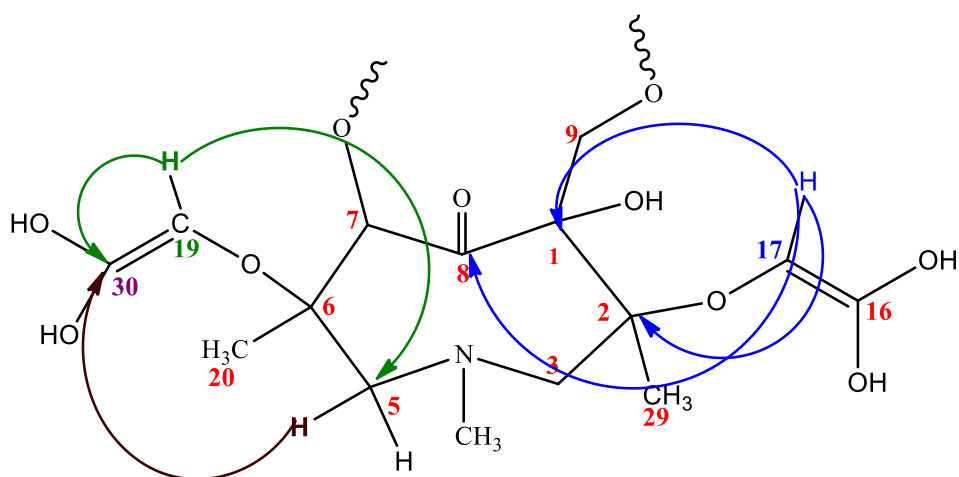


Figure III-B-54: Correlation of 2,2-dihydroxyvinyl groups (H-17, H-19 and C-30) according to HMBC spectrum of compound P10

Table III-B-05: Chemical shifts of ^1H (600 MHz) and ^{13}C (150 MHz) NMR in CDCl_3 of alkaloid P10 (δ in ppm and J in Hz)

Compound P10		
Position	δ_{H}	δ_{C}
1	-	71.78
2	-	85.17
3	2.05 (d/J=13.3 Hz)	51.66
5	1.66 (dd/J=13.3/3.5 Hz) 2.00 (d/J=12.5 Hz) 1.61 (dd/J=12.6/ 3.4 Hz)	52.83
6	-	84.10
7	3.76 (q/J=8.3 Hz)	78.47
8	-	199.65
9	3.77 (q/J=8.3 Hz)	78.47
11	-	174.38
12	2.37 (d/J=7.6 Hz)	34.11
13	-	-
14	-	47.48
15	-	161.99
16	-	147.25
17	6.34 (s)	138.46
18	-	-
19	6.81 (s)	141.57
20	1.02 (s)	19.49
23	1.26 (s)	29.85
29	1.19 (s)	22.25
30	-	144.43

31

1.26 (s)

29.85

All of these data allow us to identify the alkaloid P10 as: **14,14-dimethyl but-15,11-dioic acid-2,6-dihydroxyvinyloxy,2,6,N-trimethyl otonecine (Tomentonecine E)**. It is isolated for the first time as a new compound. Its structure is demonstrated in the Figure III-B-55.

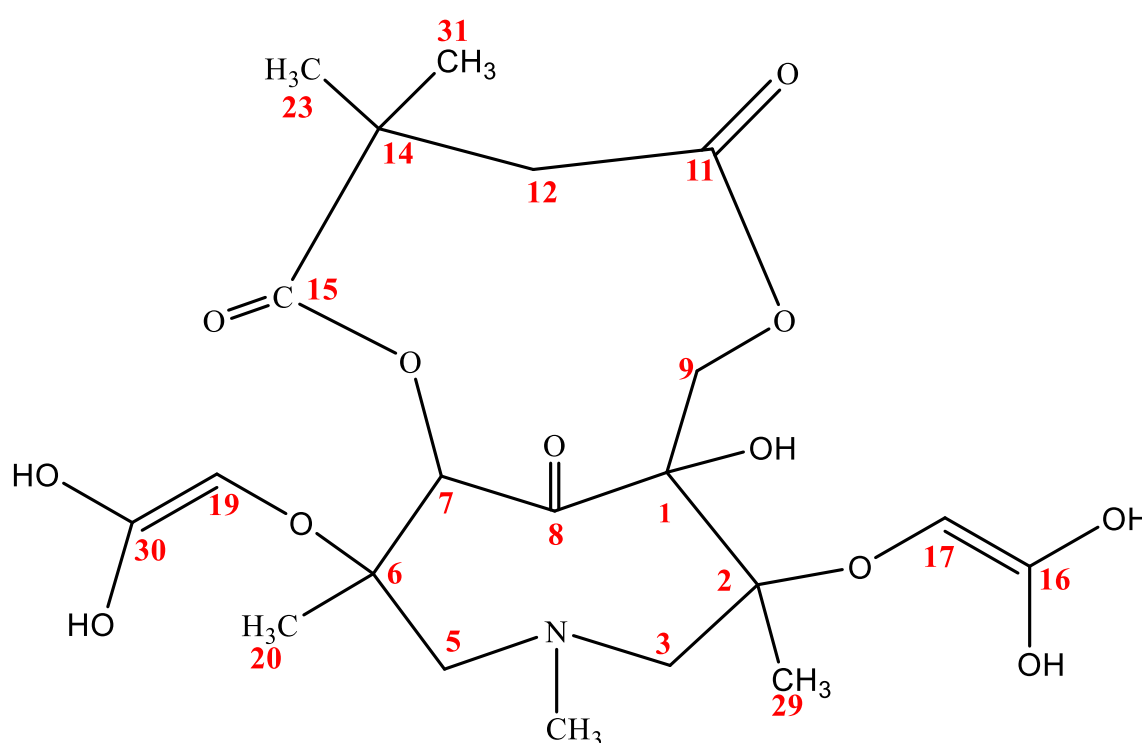


Figure III-B-55: Chemical structure of compound P10, which is an alkaloid named **Tomentonecine E**

- ❖ Tomentonecine E is an otonecine-type pyrrolizidine alkaloid composed of:
 - 2,6- di-dihydroxyvinyloxy,2,N,6-trimethyl otonecine.
 - 2,2-dimethyl but-1,4-dioic acid.

III-B-2- Structural elucidation of cardenolide glycosides isolated from *P.tomentosa*

III-B-2-1-Compound PV

Compound PV was obtained as amorphous white solid, it is invisible under UV light and it takes a violet color after revelation with a vanilin sulphuric solution and heating. Its structure was characterized using NMR spectroscopic analysis methods which are 1D: ^1H NMR and ^{13}C NMR and 2D: HSQC, HMBC and COSY. Its spectra are recorded in CD_3OD .

❖ The ^1H NMR spectrum (Figure III-B-56) of this compound showed:

➤ Typical signals of aglycon portion which are:

- One singlet olefinic signal with an integration of one proton at δ_{H} 5.81.
- The signals corresponding to two no-equivalent protons of CH_2 groups which are:

- ✓ Two doublet of doublet signals with an integration of one proton of each, at δ_{H} 4.88 and δ_{H} 4.80 with a coupling constant $J= 18.4; 1.5$ Hz and $J= 18.3; 1.6$ Hz respectively.
- ✓ One doublet and one doublet of doublet signals with an integration of one proton of each one at δ_{H} 3.78 and δ_{H} 3.52 with a coupling constant $J= 11.7$ Hz and $J= 10.7; 5.6$ Hz, respectively.
- ✓ One doublet of doublet and one triplet signals with an integration of one proton of each, at δ_{H} 2.33 and δ_{H} 0.80 with a coupling constant $J= 12.3; 3.5$ Hz and $J= 12.1$ Hz, respectively.
- ✓ Two doublet of doublet signals with an integration of one proton of each, at δ_{H} 2.03 and δ_{H} 1.83 with a coupling constant $J= 9.4; 4.0$ Hz and $J= 7.9; 4.0$ Hz, respectively.
- ✓ Two doublet of doublet signals with an integration of one proton of each, at δ_{H} 1.95 and δ_{H} 0.99 with a coupling constant $J= 12.3; 3.1$ Hz and $J= 12.0; 3.5$ Hz, respectively.
- ✓ One doublet of doublet and one doublet signals with an integration of one proton of each, at δ_{H} 1.71 and δ_{H} 1.59 with a coupling constant $J= 13.4; 3.9$ Hz and $J= 13.0$ Hz, respectively.

- ✓ One doublet of doublet and one doublet signals with an integration of one proton of each, at δ_H 1.64 and δ_H 1.45 with a coupling constant $J= 11.0$; 4.9 Hz and $J= 10.6$ Hz, respectively
- ✓ One doublet of doublet and doublet signals with an integration of one proton of each, at δ_H 1.63 and δ_H 1.43 with a coupling constant $J= 10.7$; 5.6 Hz and $J= 11.7$ Hz, respectively.
- ✓ Two doublet of doublet signals with an integration of one proton of each, at δ_H 1.28 and δ_H 1.07 with a coupling constant $J= 13.0$; 2.0 Hz and $J= 12.6$; 5.7 Hz, respectively.
- Six multiple signals with an integration of one proton of each, at δ_H 4.04, δ_H 3.90, δ_H 3.51, δ_H 1.64, δ_H 1.24 and δ_H 0.98.
- One broad signal with an integration of one proton at δ_H 3.21.
- One singlet methyl signal at δ_H 0.74.
- Typical signals of sugar portion which are:
 - One singlet anomeric signal with an integration of one proton at δ_H 4.40.
 - One multiple signal with an integration of one proton at δ_H 3.94.
 - One doublet of doublet signal with an integration of two proton at δ_H 3.49 with a coupling constant $J= 9.8$; 6.0 Hz.
 - One doublet signal with an integration of two proton at δ_H 3.17 with a coupling constant $J= 4.20$ Hz.
 - Two doublet of doublet signals with an integration of one proton of each, at δ_H 1.63 and δ_H 1.54 with a coupling constant $J= 12.0$; 4.3 Hz and $J= 10.8$; 4.3 Hz, respectively.

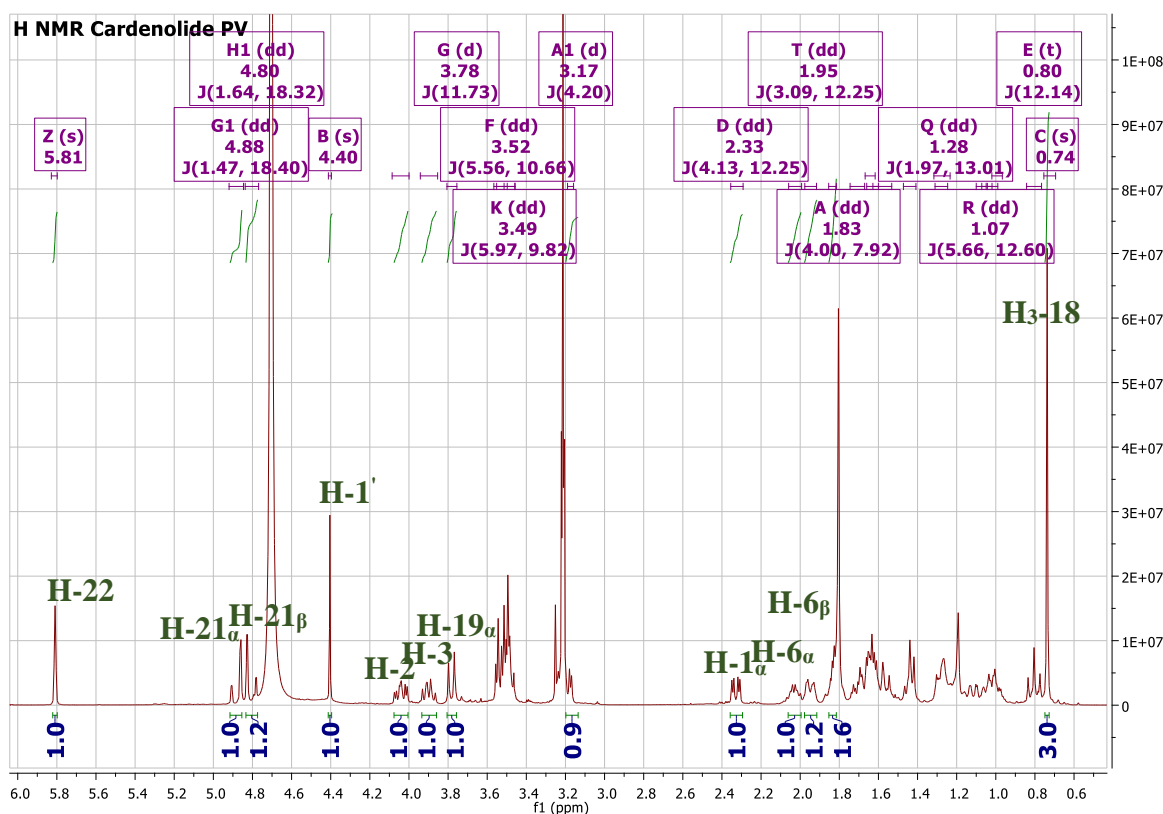


Figure III-B-56: ^1H NMR spectrum (400 MHz, CD_3OD) of compound PV

❖ The ^{13}C NMR spectrum (Figure III-B-57) of compound PV showed 29 carbon signals, of which 23 could be assigned to the aglycone moiety and six to a sugar portion. The type of each carbon was determined according to ^{13}C DEPT (135 and 90) NMR spectra (Figure III-B-58 and III-B-59). These spectra showed:

- The signals belonging to the aglycone part which are:
 - Nine methylene signals at δ_{C} 74.08, δ_{C} 58.96, δ_{C} 36.03, δ_{C} 32.40, δ_{C} 32.11, δ_{C} 31.08, δ_{C} 27.40, δ_{C} 27.06 and δ_{C} 26.91.
 - Seven methine signals at δ_{C} 72.70, δ_{C} 72.38, δ_{C} 68.57, δ_{C} 46.52, δ_{C} 45.65, δ_{C} 44.97 and δ_{C} 40.59.
 - One methyl signal at δ_{C} 8.57.
 - One olefinic methine signal at δ_{C} 116.30.
 - Five signals corresponding to quaternary carbons at δ_{C} 177.17, δ_{C} 175.97, δ_{C} 85.21, δ_{C} 55.88 and δ_{C} 40.52.
- The signals belonging to the sugar part which are:

- Two methylene signals at δ_C 64.27 and δ_C 32.75.
- Three methine signals at δ_C 96.15, δ_C 74.53 and δ_C 72.76.
- One signal corresponding to quaternary carbon at δ_C 91.57.

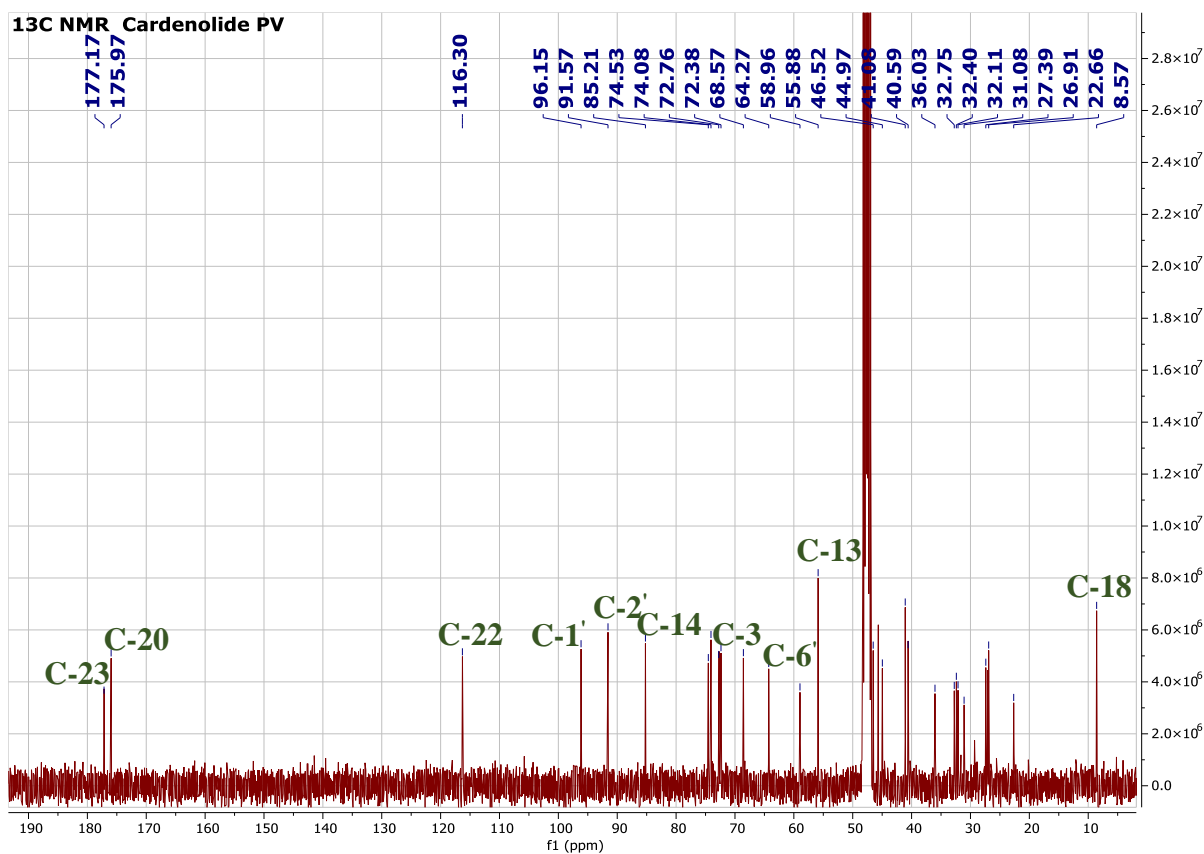


Figure III-B-57: ¹³C NMR spectrum (100 MHz, CD₃OD) of compound PV

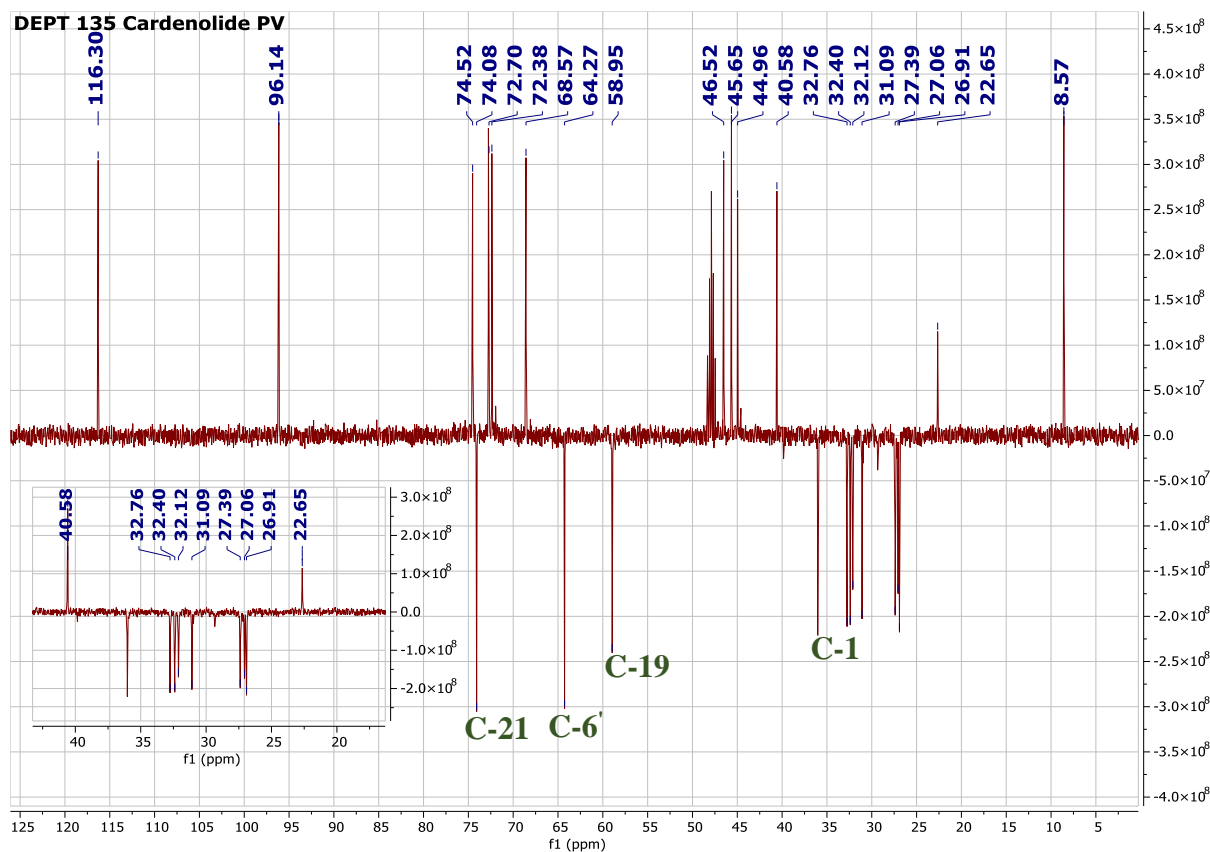


Figure III-B-58: ^{13}C NMR DEPT 135 spectrum (100 MHz, CD_3OD) of compound PV

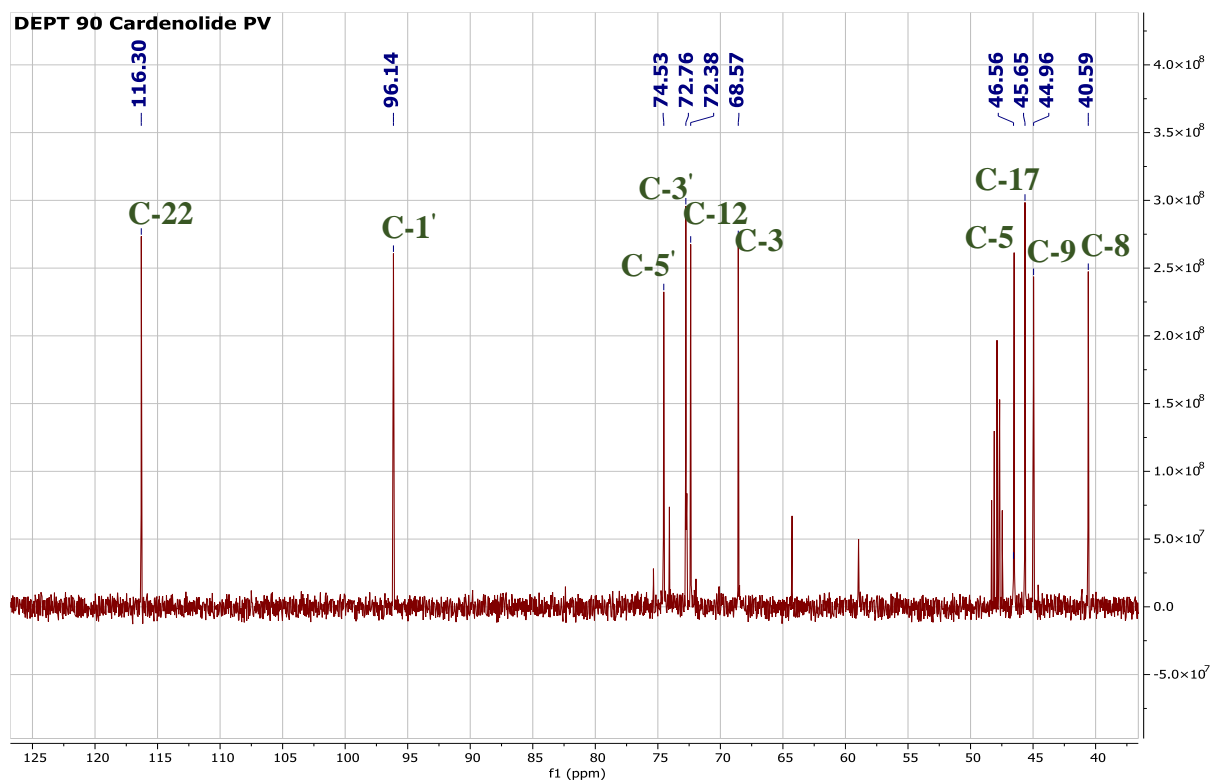


Figure III-B-59: ^{13}C NMR DEPT 90 spectrum (100 MHz, CD_3OD) of compound PV

Both of ^1H and ^{13}C NMR spectra of this compound confirmed its steroidal nature. They showed characteristic signals of α,β -unsaturated lactone (butenolactone ring) which are: singlet olefinic signal at δ_{H} 5.81 and a primary alcoholic group signal at δ_{H} 4.88; δ_{H} 4.80 as well as, an olefinic quaternary carbon signal at δ_{C} 175.97, a carbonyl carbon signals at δ_{C} 177.17 and an olefinic methine signal at δ_{C} 116.30. ^1H NMR spectrum showed also the presence of a methyl signal at δ_{H} 0.74 and a proton anomeric signal of a doubly linked sugar unit at δ_{H} 4.40. All of these data confirmed the presence of a cardenolide glycoside skeleton [34].

- ❖ Each proton is assigned to its corresponding carbon according to HSQC spectrum (Figure III-B-60). The chemical shifts of H and C of compound PV are illustrated in Table-III-B-06.

Table III-B-06: Chemical shifts of ^1H (400 MHz) and ^{13}C (100 MHz) NMR in CD_3OD of compound PV (δ in ppm and J in Hz).

Position	Compound PV	
	δ_{H}	δ_{C}
Typical signals of aglycon portion		
1	2.33 (dd; J= 12.3; 3.5 Hz)	36.03
	0.80 (t; J= 12.1 Hz)	
2	4.04 (m)	68.57
3	3.90 (m)	72.38
4	1.63 (dd; J=10.7; 5.6 Hz)	32.40
	1.43 (d; J= 11.7 Hz)	
5	0.98 (m)	46.52
6	2.03 (dd; J=9.4; 4.0 Hz)	26.91
	1.83 (dd; J=7.9; 4.0 Hz)	
7	1.28 (dd; J=13.0; 2.0 Hz)	27.06
	1.07 (dd; J=12.6; 5.7 Hz)	

8	1.64 (m)	40.59
9	1.24 (m)	44.97
10	-	40.52
11	1.64 (dd; J= 11.0; 4.9 Hz) 1.45 (d; J= 10.6 Hz)	32.11
12	3.51 (m)	72.70
13	-	55.88
14	-	85.21
15	1.71 (dd; J= 13.4; 3.9 Hz) 1.59 (d; J= 13.0 Hz)	31.08
16	1.95 (dd; J= 12.3; 3.1 Hz) 0.99 (dd; J= 12.0; 3.5 Hz)	27.39
17	3.21 (br)	45.65
18	0.74 (s)	8.57
19	3.78 (d; J= 11.7 Hz) 3.52 (dd; J= 10.7; 5.6 Hz)	58.96
20	-	175.97
21	4.88 (dd; J= 18.4; 1.5 Hz) 4.80 (dd; J= 18.3; 1.6 Hz)	74.08
22	5.81 (s)	116.30
23	-	177.17
Typical signals of sugar portion		
1'	4.40 (s)	96.15
2'	-	91.57
3'	3.94 (m)	72.76

4'	1.63 (dd; J= 12.0; 4.3 Hz)	32.75
	1.54 (dd; J= 10.8; 4.3 Hz)	
5'	3.17 (d; J= 4.20 Hz)	74.53
6'	3.49 (dd; J= 9.8; 6.0 Hz)	64.27

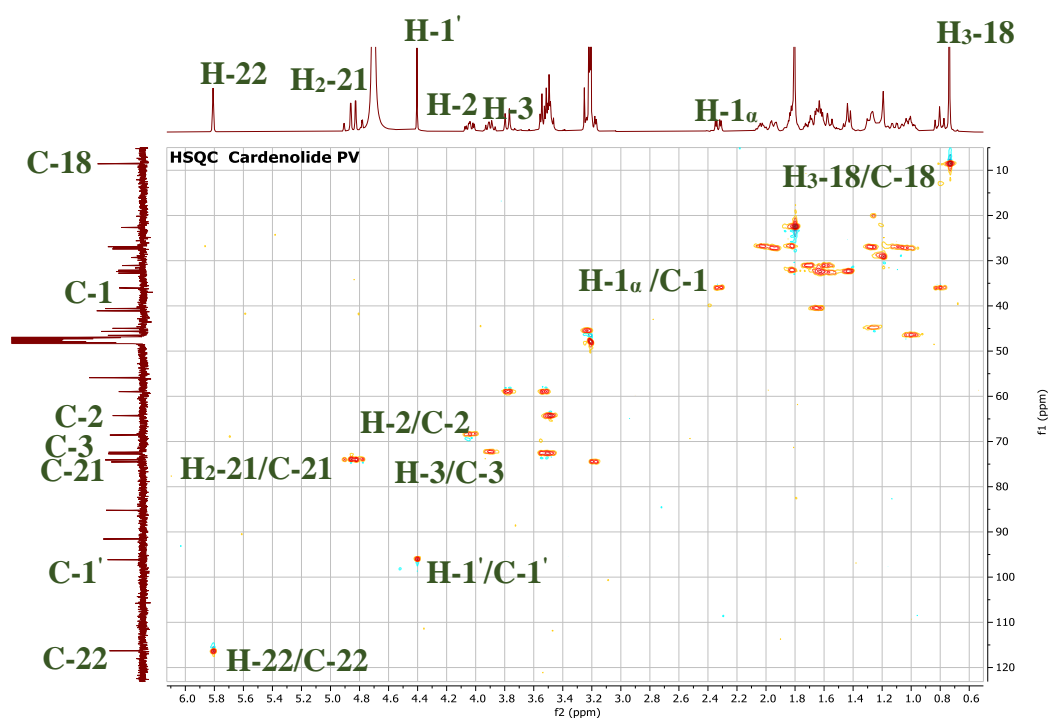


Figure III-B-60: HSQC expansions spectrum (400 MHz, CD₃OD) of compound PV

This assignment was confirmed by comparison of the ¹H and ¹³C NMR data of this compound with those of some related cardenolide glycosides [120].

The presence of four hydroxyl groups attached to this basic cardenolide glycoside skeleton is confirmed by downfield shift of: C-12 (δ_C 72.70) C-14 (δ_C 85.21), C-2' (δ_C 91.57) and C-3' (δ_C 72.76). As well as, the presence of –CH₂OH group bounded to aglycon part of this cardenolide glycoside (at C-10) is confirmed by the presence of two non-equivalent proton signals at δ_H 3.78 and δ_H 3.52. While, the presence of –CH₂OH group linked to sugar part (at C-5') is confirmed by the presence of two equivalent proton signal at δ_H 3.49 ppm.

In order to confirm the sequence of this cardenolide glycoside skeleton as well as the attachment of the substituents on this skeleton, HMBC experiment was studied. It presents correlation spots between protons and its vicinal carbons.

❖ HMBC spectrum (Figure III-B-65 and III-B-65-b) recorded correlations between:

➤ H-1_α (δ_H 2.33) has correlated with:

- C-10 (δ_C 40.52).
- C-2 (δ_C 68.57).
- C-3 (δ_C 72.38).

➤ H-1_β (δ_H 0.80) has correlated with:

- C-10 (δ_C 40.52).
- C-2 (δ_C 68.57).
- C-3 (δ_C 72.38).
- C-19 (δ_C 58.96).

➤ H-4_α (δ_H 1.63) has correlated with:

- C-2 (δ_C 68.57).

➤ H-4_β (δ_H 1.43) has correlated with:

- C-10 (δ_C 40.52).
- C-2 (δ_C 68.57).
- C-3 (δ_C 72.38).

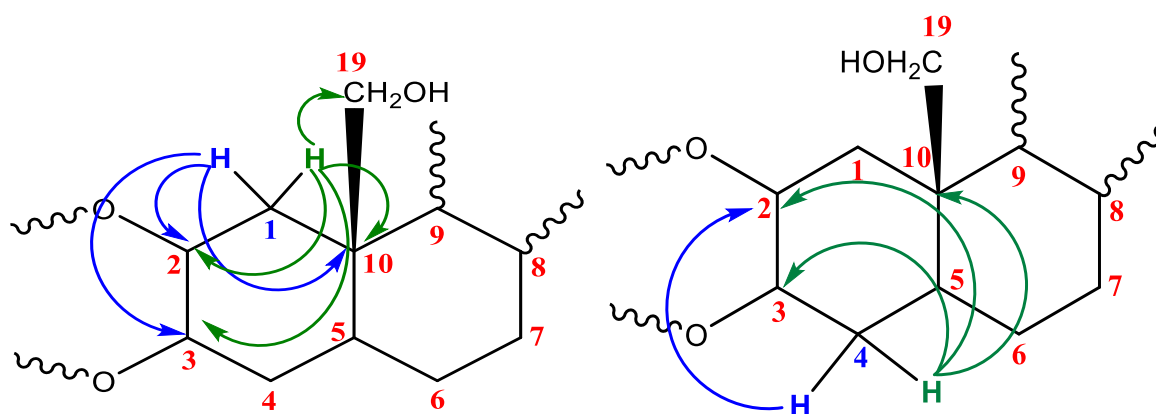


Figure III-B-61: Correlation of H-1_α, H-1_β, H-4_α and H-4_β according to HMBC spectrum of compound PV

➤ H-17 (δ_H 3.23) has correlated with:

- C-16 (δ_C 27.39).

- H₃-18 (δ_{H} 0.80) has correlated with:
 - C-17 (δ_{C} 45.65).
 - C-13 (δ_{C} 55.88).
 - C-14 (δ_{C} 85.21).
 - C-21 (δ_{C} 74.08).
- H-19 _{α} (δ_{H} 3.78) has correlated with:
 - C-5 (δ_{C} 46.52).
- H-19 _{β} (δ_{H} 3.52) has correlated with:
 - C-5 (δ_{C} 46.52).

The correlation spots of H₃-18 with C-13, C-14, C-17 and C-21 confirmed that methyl group is attached at C-13, while, the correlation of H₂-19 with C-5 confirmed that -CH₂OH group is attached at C-10.

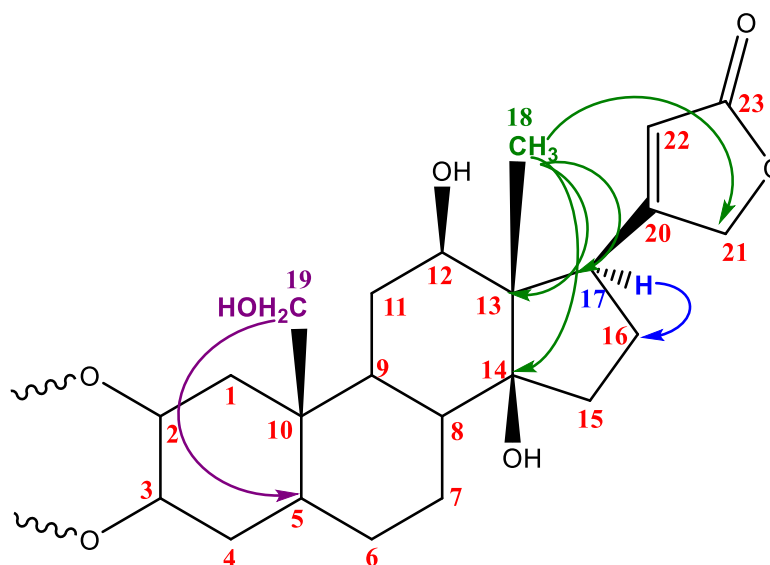


Figure III-B-62: Correlation of H-17, H₃-18 and H₂-19 according to HMBC spectrum of compound PV

- H-21 _{α} (δ_{H} 4.86) has correlated with:
 - C-22 (δ_{C} 116.30).
 - C-23 (δ_{C} 177.17).
- H-21 _{β} (δ_{H} 4.80) has correlated with:
 - C-22 (δ_{C} 116.30).
 - C-23 (δ_{C} 177.17).

➤ H-22 (δ_H 5.81) has correlated with:

- C-17 (δ_C 45.65).
- C-21 (δ_C 74.08).
- C-20 (δ_C 175.97).

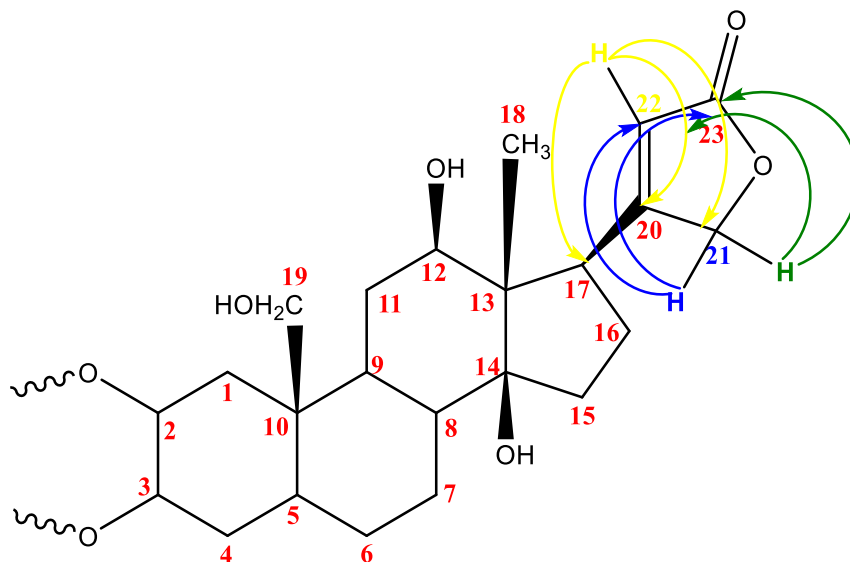


Figure III-B-63: Correlation of H-21 α , H-21 β and H-22 according to HMBC spectrum of compound PV

➤ H-1' (δ_H 4.40) has correlated with:

- C-2' (δ_C 91.57).
- C-3' (δ_C 72.76 ppm).

➤ H-4' α (δ_H 1.63) has correlated with:

- C-5' (δ_C 74.53).
- C-2' (δ_C 91.57).

➤ H-4' β (δ_H 1.54) has correlated with:

- C-3' (δ_C 72.76).

➤ H₂-6' (δ_H 3.49) has correlated with:

- C-3' (δ_C 72.76).

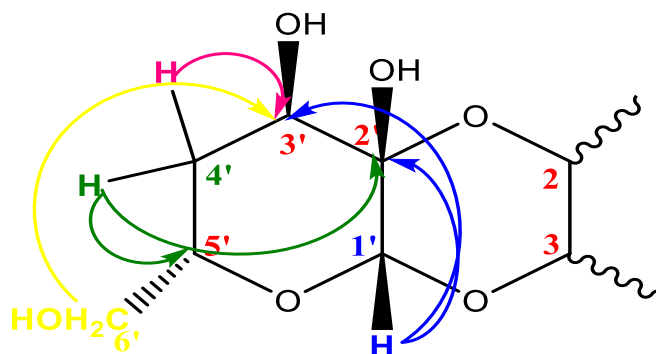


Figure III-B-64: Correlation of H-1', H-4'_α, H-4'_β and H₂-6' according to HMBC spectrum of compound PV

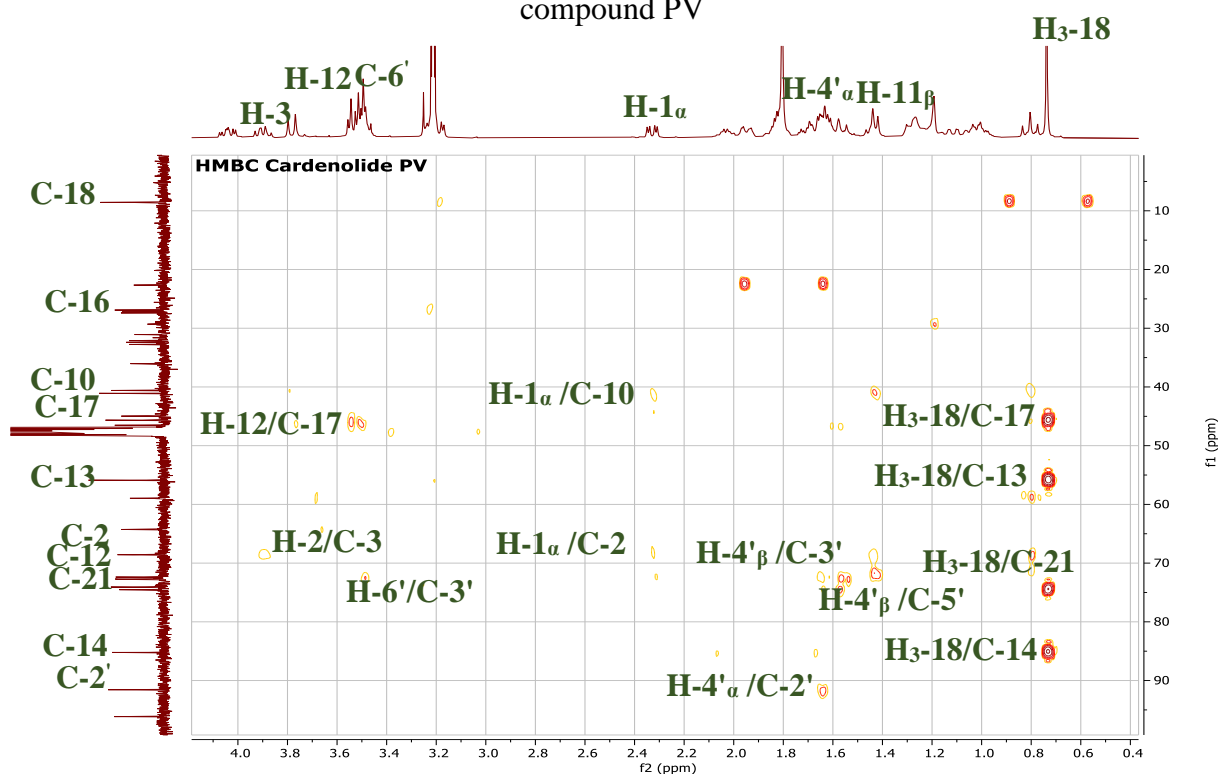


Figure III-B-65-a: HMBC expansions spectrum [4.0 – 0.4 ppm] (400 MHz, CD₃OD) of compound PV

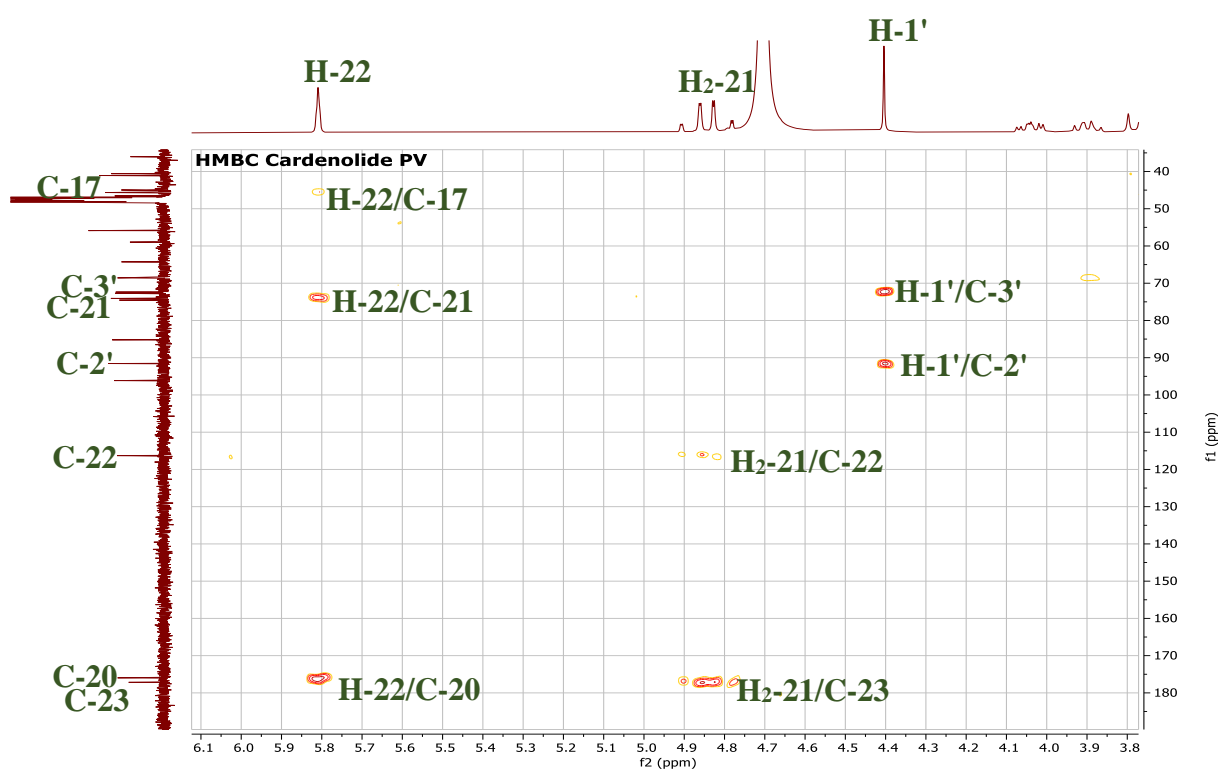


Figure III-B-65-b: HMBC expansions spectrum [6.1 – 3.8 ppm] (400 MHz, CD₃OD) of compound PV

❖ COSY experiment (Figure III-B-68) was used to confirm the sequence of sugar unit which shows the correlation spots between its vicinal H, that are:

- H-4'_α (δ_H 1.63) correlated with H-5' (δ_H 3.17).
- H-4'_β (δ_H 1.54) correlated with H-5' (δ_H 3.17).
- H-5' (δ_H 3.17) correlated with H-6' (δ_H 3.49).

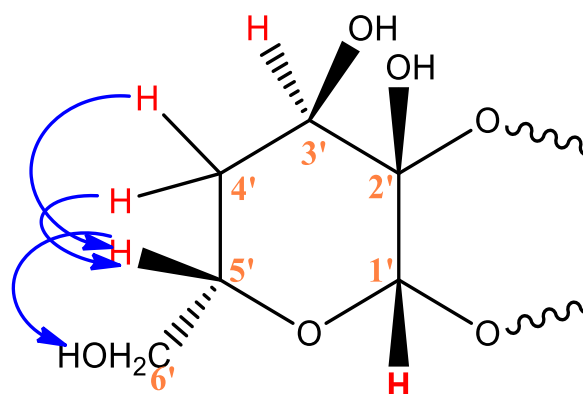


Figure III-B-66: COSY correlations of sugar part of compound PV

❖ The COSY spectrum shows also correlation spots between protons of some -CH₂ group and some vicinal H in aglycon portion, which are:

- H-1_β (δ_H 0.80) correlated with H-1_α (δ_H 2.33).
- H-1_α (δ_H 2.64) correlated with H-2 (δ_H 4.04).
- H-4_α (δ_H 1.63) correlated with H-5 (δ_H 0.98).
- H-4_β (δ_H 1.43) correlated with H-3 (δ_H 3.90).
- H-7_α (δ_H 1.28) correlated with H-7_β (δ_H 1.07).
- H-11_α (δ_H 1.64) correlated with H-12 (δ_H 3.51).
- H-15_α (δ_H 1.71) correlated with H-16_β (δ_H 0.99).
- H-16_α (δ_H 1.95) correlated with H-16_β (δ_H 0.99).
- H-21_α (δ_H 4.88) correlated with H-22 (δ_H 5.81).
- H-21_β (δ_H 4.80) correlated with H-22 (δ_H 5.81).

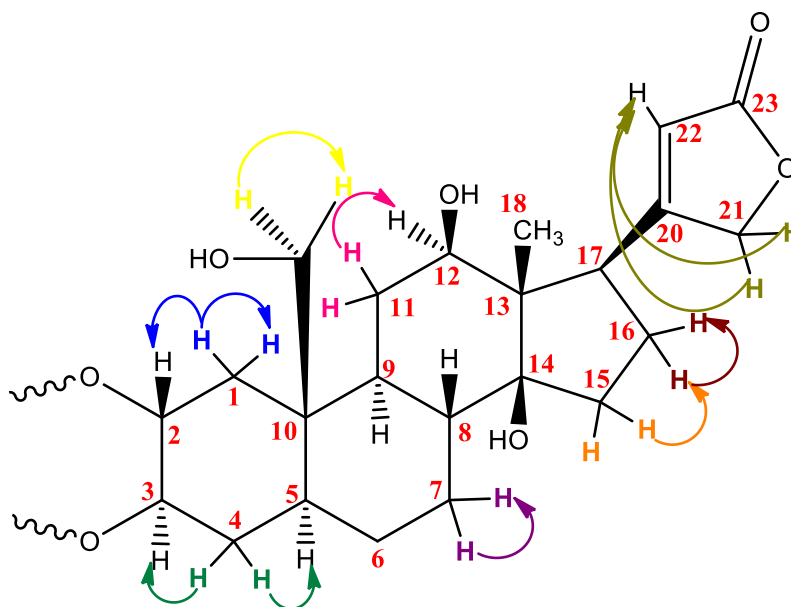


Figure III-B-67: COSY correlations of aglycon part of compound PV

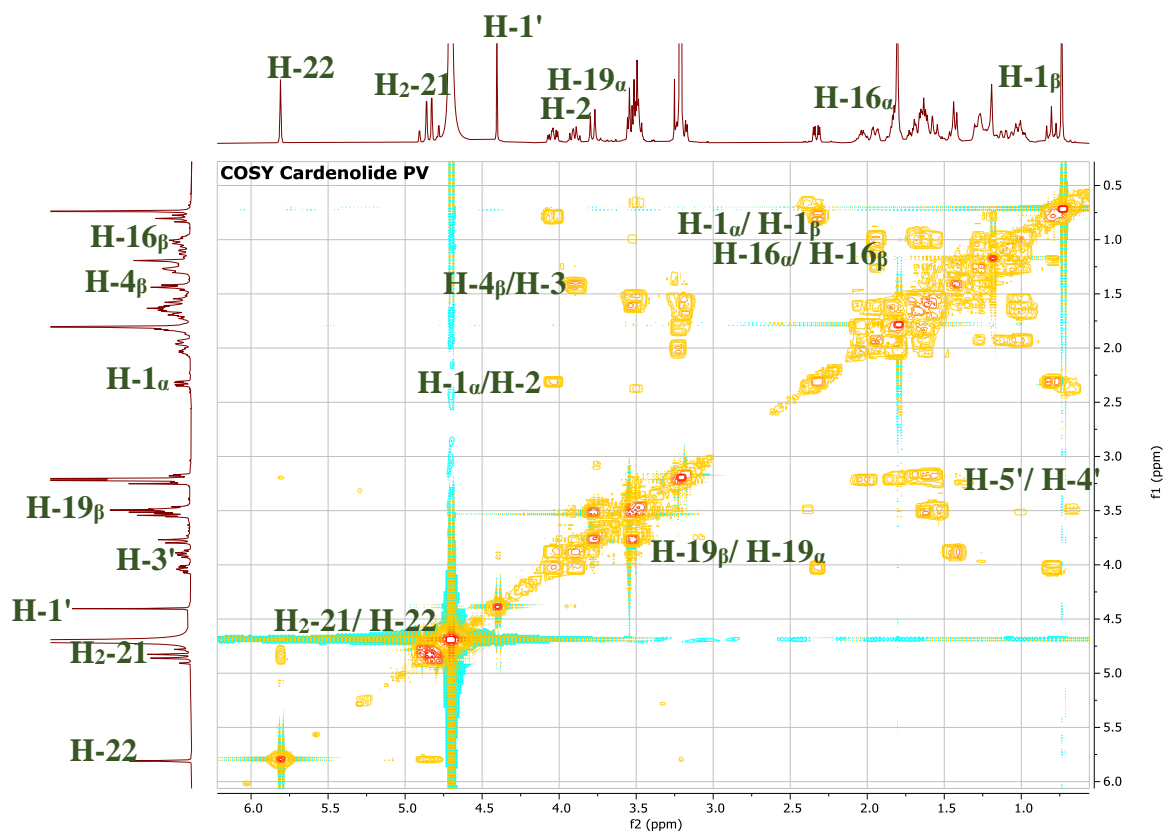


Figure III-B-68: COSY spectrum (400 MHz, CD₃OD) of compound PV

All of the NMR data are in full agreement with those of literature[120]. Therefore, chemical structure of compound PV was concluded to be **Ghalakinoside**. This compound was previously isolated from *P. tomentosa* [120]

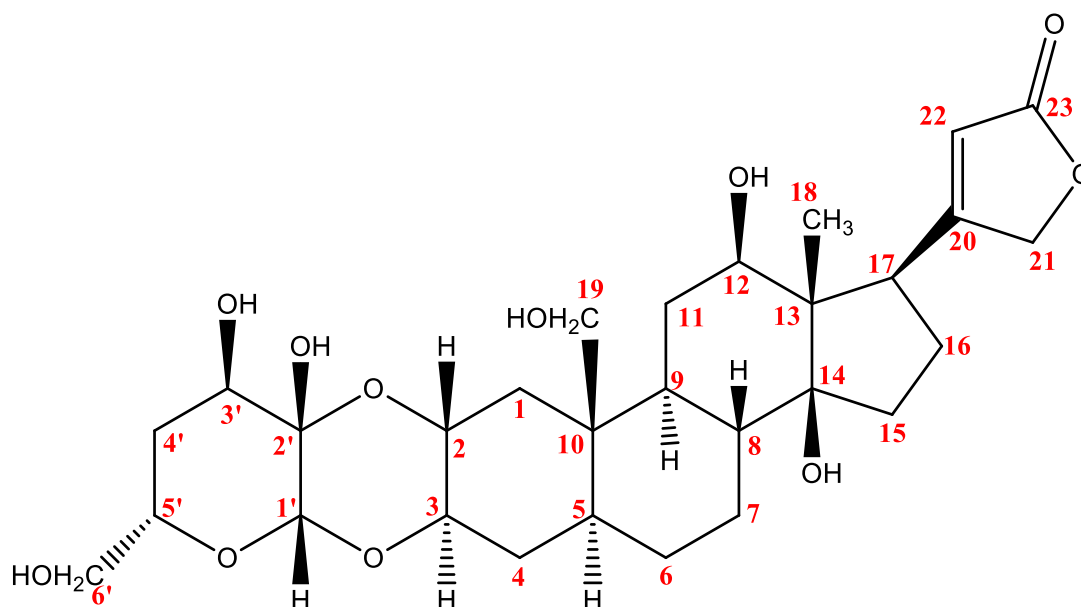


Figure III-B-69: Chemical structure of compound PV, which is a cardenolides glycoside named **Ghalakinoside**

III-B-2-2-Compound PN

Compound PN was obtained as a white amorphous, it is invisible under UV light and it takes a black color after revelation with a vanilin sulphuric solution and heating. Its structure was characterized using NMR spectroscopic analysis methods which are 1D: ^1H NMR and ^{13}C NMR and 2D: HSQC, HMBC and COSY. Its spectra are recorded in CD_3OD .

- ❖ The ^1H NMR spectrum (Figure III-B-70) of this compound showed:
 - Typical signals of aglycon portion which are:
 - One singlet signal with an integration of one proton at δ_{H} 9.93.
 - One singlet olefinic signal with an integration of one proton at δ_{H} 5.80.
 - The signals corresponding to two no-equivalent protons of CH_2 groups which are:
 - ✓ Two doublet of doublet signals with an integration of one proton of each one at δ_{H} 4.87 and δ_{H} 4.79 with a coupling constant $J= 18.8; 1.8$ Hz and $J= 18.4; 1.7$, Hz respectively.

- ✓ One doublet of doublet and one doublet signals with an integration of one proton of each, at δ_H 2.28 and δ_H 1.01 with a coupling constant $J= 12.9$; 4.2 Hz and $J= 11.9$ Hz, respectively.
- ✓ Two doublet of doublet signals with an integration of one proton of each, at δ_H 2.10 and δ_H 1.90 with a coupling constant $J= 12.7$; 2.5 Hz and $J= 13.3$; 3.8 Hz, respectively.
- ✓ Two doublet signals with an integration of one proton of each, at δ_H 2.04 and δ_H 1.83 with a coupling constant $J= 9.01$ Hz and $J= 11.5$ Hz, respectively.
- ✓ One doublet and one doublet of doublet signals with an integration of one proton of each, at δ_H 1.74 and δ_H 1.63 with a coupling constant $J= 11.4$ Hz and $J= 11.2$; 2.4 Hz, respectively.
- ✓ Two doublet of doublet signals with an integration of one proton of each, at δ_H 1.63 and δ_H 1.55 with a coupling constant $J= 11.2$; 2.4 Hz and $J= 9.5$; 2.6 Hz, respectively.
- ✓ Two doublet of doublet signals with an integration of one proton of each, at δ_H 1.55 and δ_H 1.29 with a coupling constant $J= 9.5$; 5.4 Hz and $J= 12.5$; 5.5 Hz, respectively.
- ✓ One doublet of doublet of doublet and one doublet signals with an integration of one proton of each, at δ_H 1.55 and δ_H 1.14 with a coupling constant $J= 9.5$; 5.4; 2.6 Hz and $J= 8.7$ Hz, respectively.
- One triplet signal with an integration of one proton at δ_H 3.53 with a coupling constant $J= 2.7$ Hz.
- One doublet of doublet signal with an integration of one proton at δ_H 3.27 with a coupling constant $J= 5.3$; 2.6 Hz.
- Five multiplet signals with an integration of one proton of each, at δ_H 3.74, δ_H 3.26, δ_H 1.48, δ_H 1.45 and δ_H 1.35.
- One singlet methyl signal at δ_H 0.63.
- Typical signals of sugar portion which are:
 - An anomeric singlet signal with an integration of one proton at δ_H 4.60.
 - One multiplet signal with an integration of one proton at δ_H 3.94.
 - One triplet signal with an integration of one proton at δ_H 3.47 with a coupling constant $J= 4.0$ Hz.

- Two doublet of doublet signals with an integration of one proton of each, at δ_H 1.63 and δ_H 1.56 with a coupling constant $J= 11.2; 2.4$ Hz and $J= 9.2; 1.8$ Hz, respectively.
- One doublet methyl signal at $\delta \delta_H$ 1.09 ppm with a coupling constant $J= 6.2$ Hz.

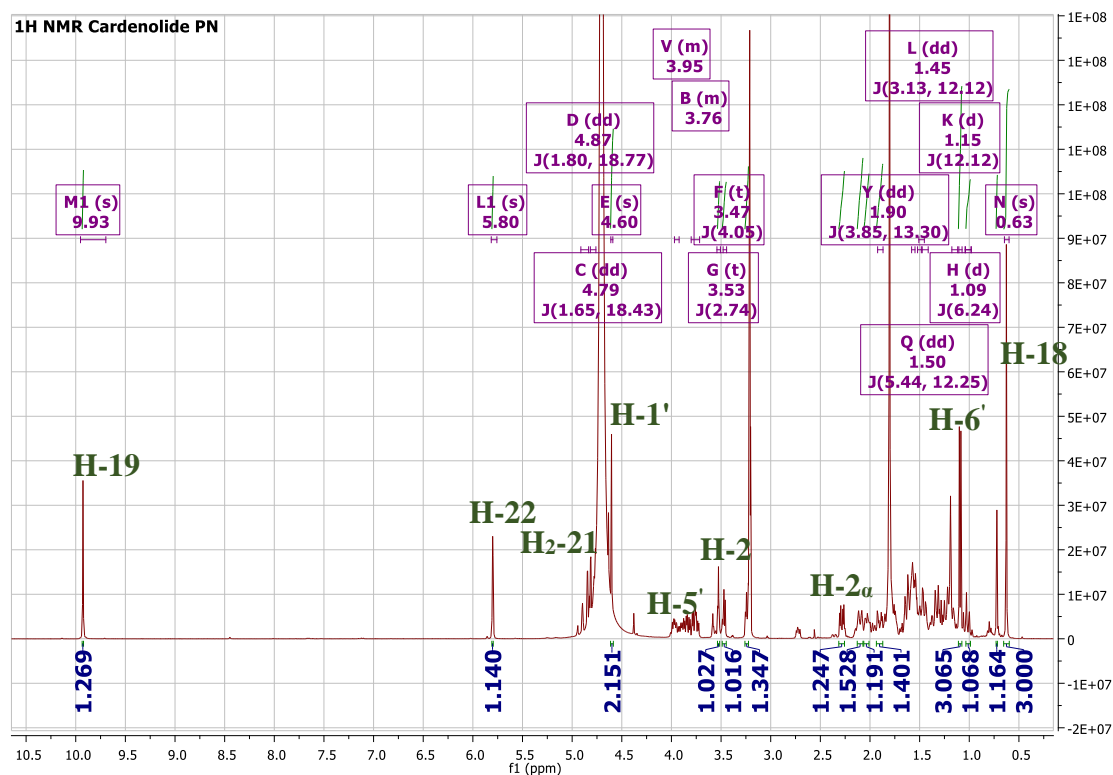


Figure III-B-70: 1H NMR spectrum (400 MHz, CD_3OD) of compound PN

- ❖ According to ^{13}C and ^{13}C DEPT (135 and 90) NMR spectra (Figure III-B-71, III-B-72 and III-B-73) there are:
 - The signals belonging to the aglycon part which are:
 - Eight methylene signals at δ_C 74.04, δ_C 35.58, δ_C 33.03, δ_C 31.60, δ_C 31.52, δ_C 27.34, δ_C 27.29 and δ_C 26.75.
 - Seven methine signals at δ_C 73.41, δ_C 70.47, δ_C 68.98, δ_C 45.45, δ_C 44.97, δ_C 43.09 and δ_C 41.54.
 - One methyl signal at δ_C 8.31.
 - One olefinic methine signal at δ_C 116.42.

- Five signals corresponding to quaternary carbons at δ_C 176.89, δ_C 175.92, δ_C 84.64, δ_C 55.55 and δ_C 52.43.
- The signals belonging to the sugar part which are:
 - One methylene signal at δ_C 36.85.
 - Three methine signals at δ_C 94.18, δ_C 70.49 and δ_C 66.02.
 - One signal corresponding to quaternary carbon at δ_C 90.58.
 - One methyl signal at δ_C 19.83.

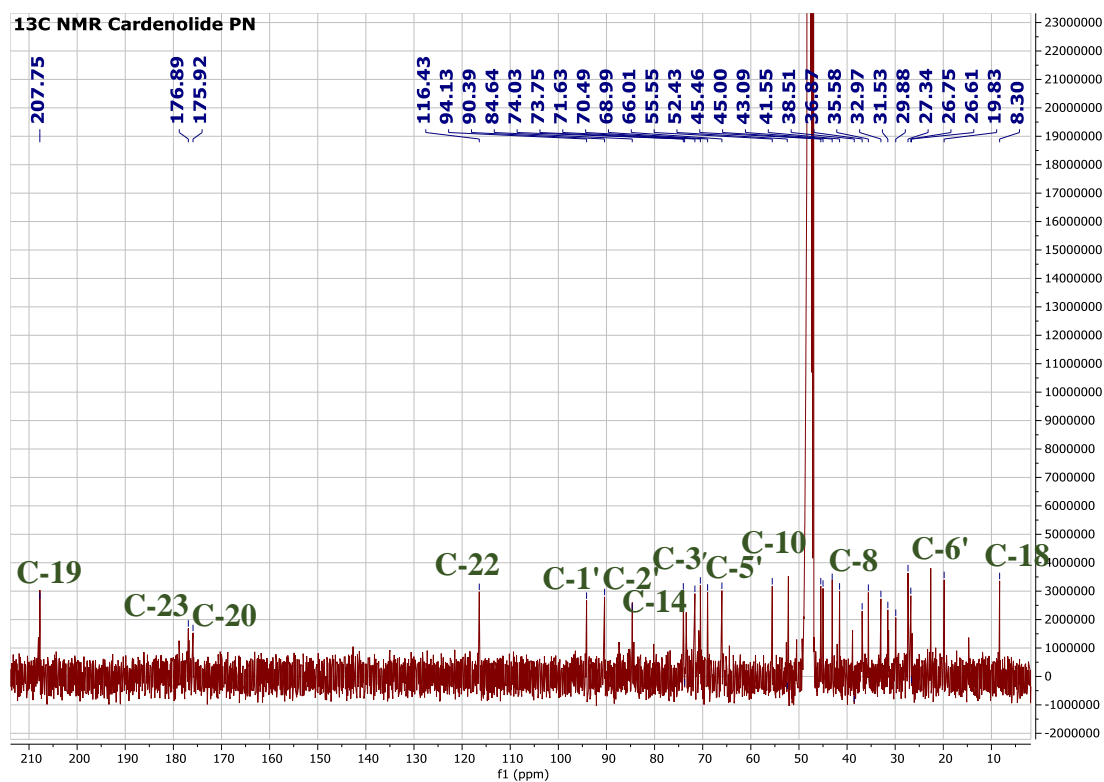


Figure III-B-71: ^{13}C NMR spectrum (100 MHz, CD_3OD) of compound PN

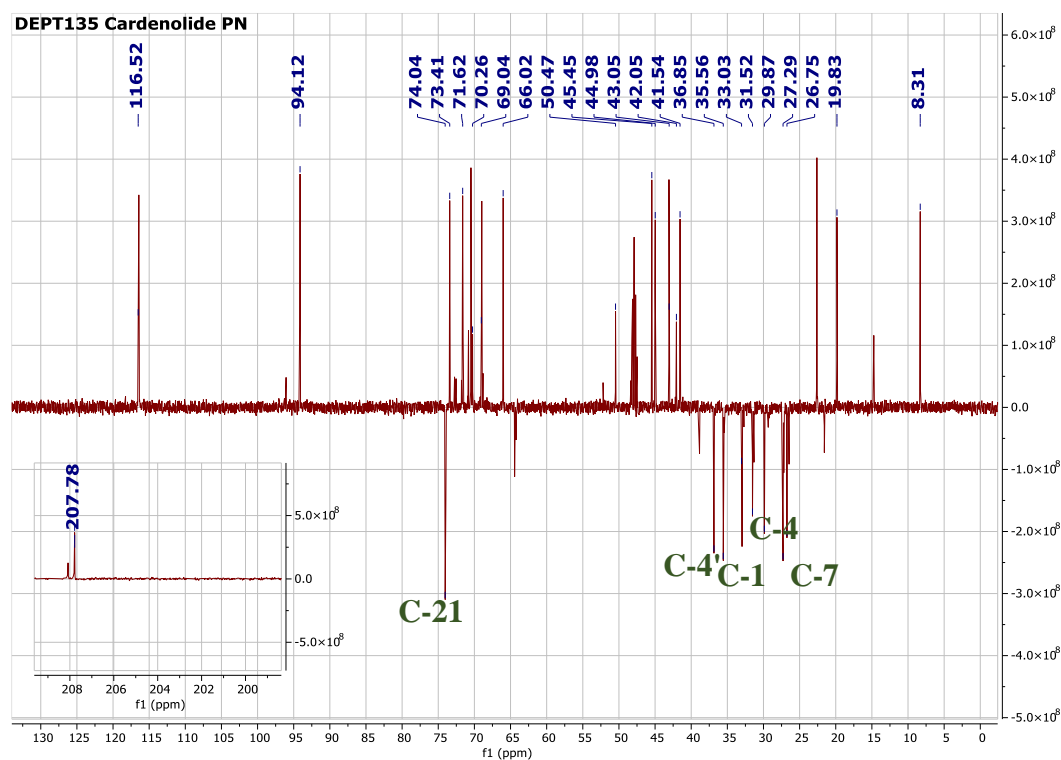


Figure III-B-72: ^{13}C NMR DEPT 135 spectrum (100 MHz, CD_3OD) of compound PN

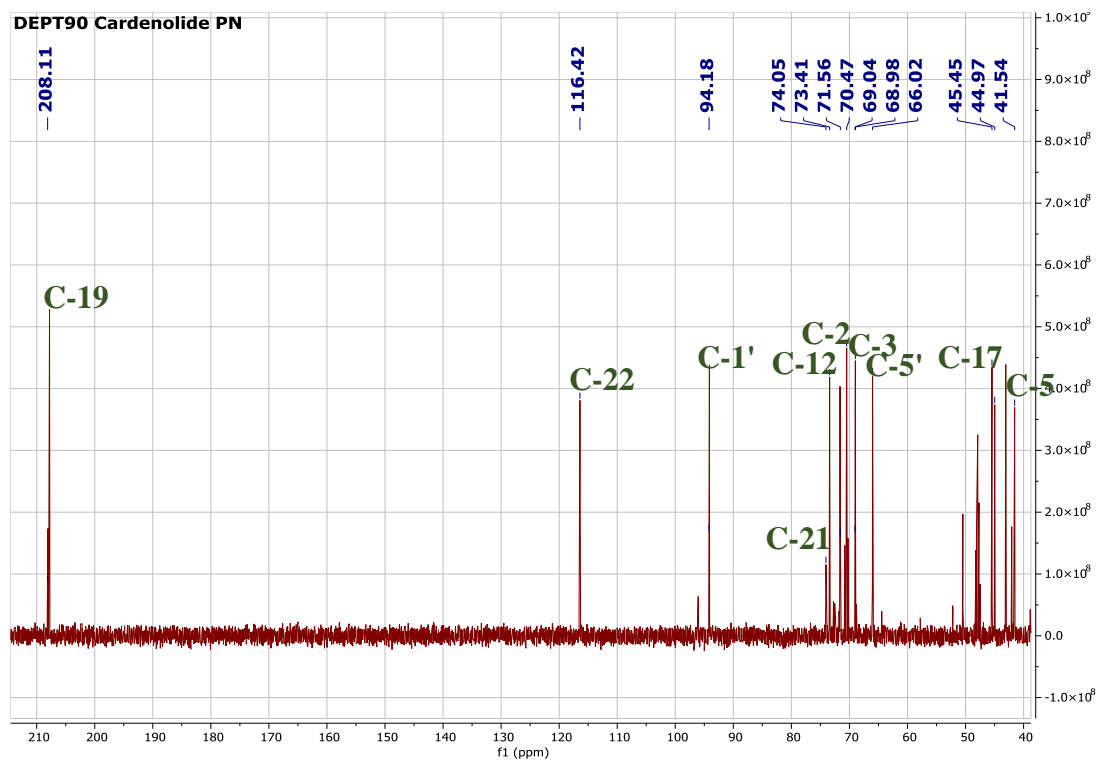


Figure III-B-73: ^{13}C NMR DEPT 90 spectrum (100 MHz, CD_3OD) of compound PN

We observed that both of ^1H and ^{13}C NMR spectra of compound PN are identical with those of compound PV with a slight difference, which indicate that this compound is a cardenolide glycoside.

The notable difference between PN and PV compound appears clearly on both ^1H and ^{13}C NMR spectra of compound PN which shows:

- ✓ The appearance of new singlet signals at δ_{H} 9.93; δ_{C} 208.11 characteristic of aldehyde group.
 - ✓ The appearance of new doublet methyl signal at δ_{H} 1.09.
 - ✓ The disappearance of tow typical signals of $-\text{CH}_2\text{OH}$ group.
- ❖ The complete assignment of compound PN was established using HSQC spectrum (Figure III-B-72) of this compound as well as the comparison of all ^1H and ^{13}C spectroscopic data of compound PN with those of literature [121]. Table III-B-07 illustrate the chemical shifts of H and C of compound PV.

Table III-B-07: Chemical shifts of ^1H (400 MHz) and ^{13}C (100 MHz) NMR in CD_3OD of compound PN (δ in ppm and J in Hz)

Position	Compound PN	
	δ_{H}	δ_{C}
Typical signals of aglycon portion		
1	2.28 (dd; J= 12.9; 4.2 Hz) 1.01 (d; J= 11.9 Hz)	35.58
2	3.53 (t; J= 2.7Hz)	70.47
3	3.74 (m)	68.98
4	1.74 (d; J= 11.4 Hz) 1.63 (dd; J= 11.2; 2.4 Hz)	31.52
5	1.45 (m)	41.54

6	2.04 (d; J= 9.01 Hz) 1.83 (d; J= 11.5 Hz)	26.75
7	1.55 (ddd; J= 9.5; 5.4; 2.6 Hz) 1.14 (d; J= 8.7 Hz)	27.29
8	1.48 (m)	43.09
9	1.35 (m)	44.97
10	-	52.43
11	1.63 (dd; J= 11.2; 2.4 Hz) 1.55 (dd;9.5; 2.6 Hz)	31.60
12	3.26	73.41
13	-	55.55
14	-	84.64
15	1.55 (dd; J= 9.5; 5.4) 1.29 (dd; J=12.5; 5.5 Hz)	33.03
16	2.10 (dd; J= 12.7; 2.5 Hz) 1.90 (dd; J= 13.3; 3.8 Hz)	27.34
17	3.27 (dd; J= 5.3; 2.6 Hz)	45.45
18	0.63 (s)	8.31
19	9.93 (s)	208.11
20	-	175.92
21	4.87 (dd; J= 18.8; 1.8 Hz) 4.79 (dd; J= 18.4; 1.7 Hz)	74.04

22	5.80 (s)	116.42
23	-	176.89
Typical signals of sugar portion		
1'	4.60 (s)	94.18
2'	-	90.39
3'	3.47 (t; J= 4.0 Hz)	70.49
4'	1.63 (dd; J= 11.2; 2.4 Hz)	36.85
	1.56 (dd; J= 9.2; 1.8 Hz)	
5'	3.94 (m)	66.02
6'	1.09 (d; J= 6.2 Hz)	19.83

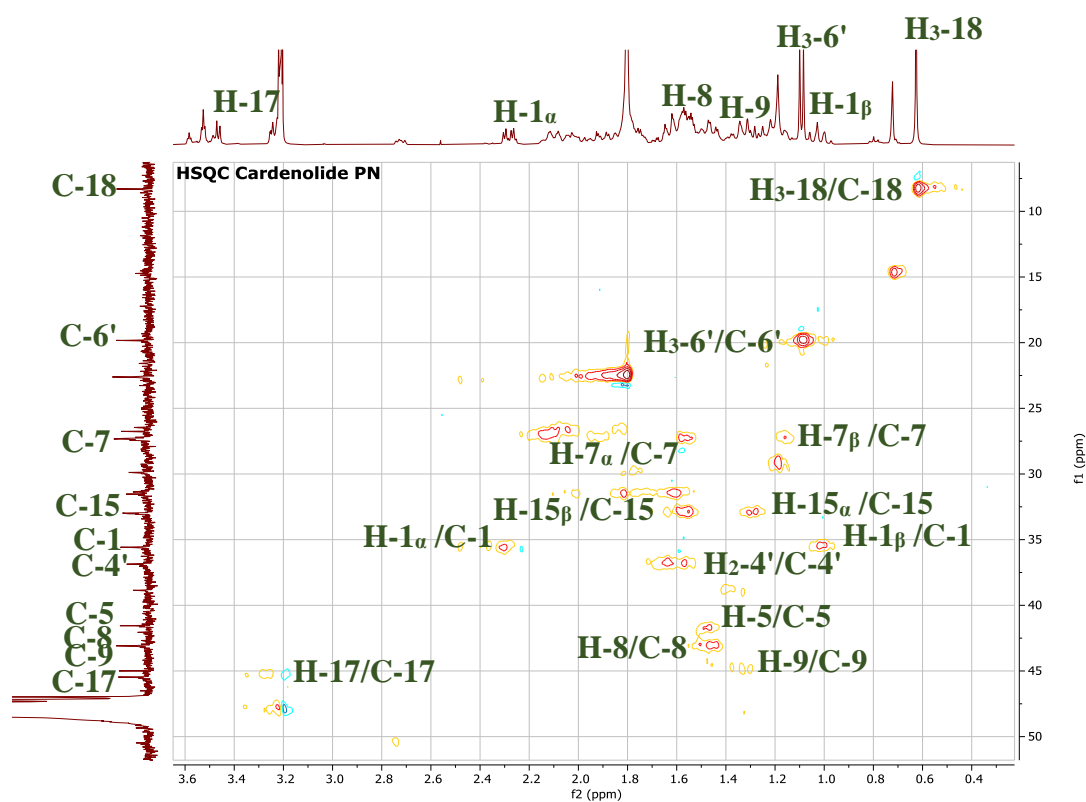


Figure III-B-74-a: HSQC expansion spectrum [3.6 – 0.4 ppm] (100 MHz, CD₃OD) of compound PN

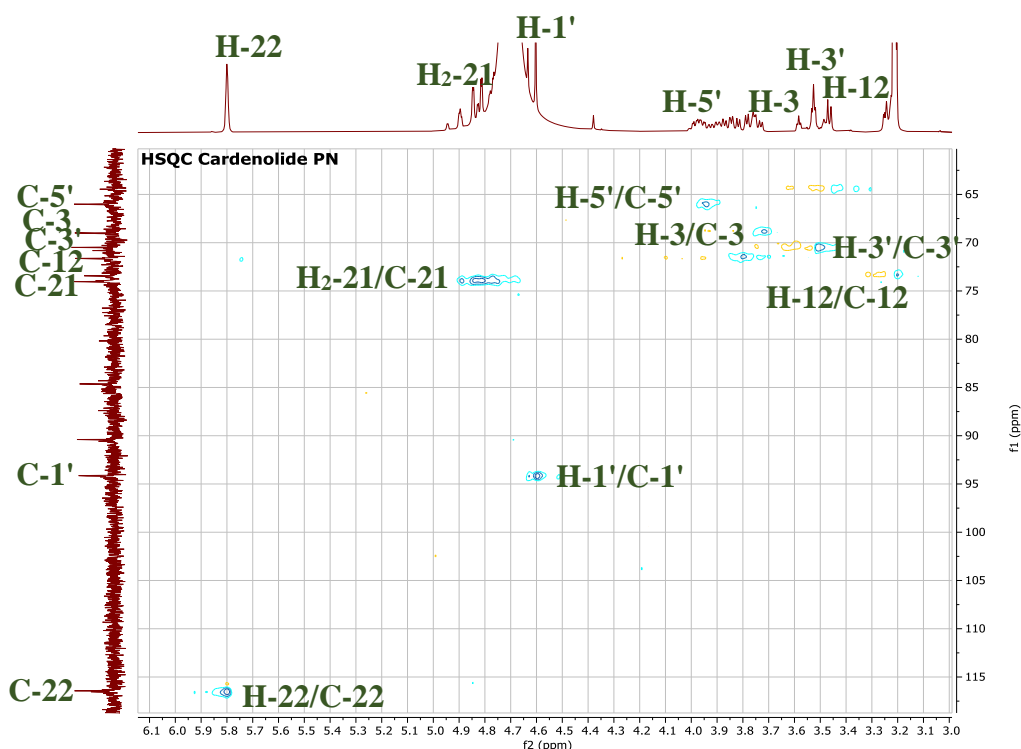


Figure III-B-74-b: HSQC expansion spectrum [6.1 – 3.0 ppm] (100 MHz, CD₃OD) of compound PN

Comparison of the spectroscopic data of PN and PV compounds, indicated that their structures were quite similar, except the –CH₂OH group (C-19) that linked at C-10 in PV compound was replaced by aldehyde group (C-19) in PN compound, as well as, –CH₂OH group (C-6') that linked at C-5' was replaced by new methyl group (C-6'). These differences confirmed by chemical shift of C-10 for compound PN was moved downfield compared to compound PV (δ_C 40.52 for PV, δ_C 52.43 for PN). Whereas, chemical shift of C-5' for compound PN was moved upfield relative to compound PV (δ_C 74.73 for PV, δ_C 66.02 for PN). These features implied the aldehyde group was linked at C-10 and new methyl group was linked at C-5' which will be confirmed by the HMBC correlations.

❖ HMBC spectrum (Figure III-B-78) allows to observe correlation spots between:

- H-1_α (δ_H 2.28) has correlated with:
 - C-2 (δ_C 70.47).
- H-1_β (δ_H 1.01) has correlated with:
 - C-3 (δ_C 68.98).
- H-2 (δ_H 3.53) has correlated with:

- C-2' (δ_C 90.39).

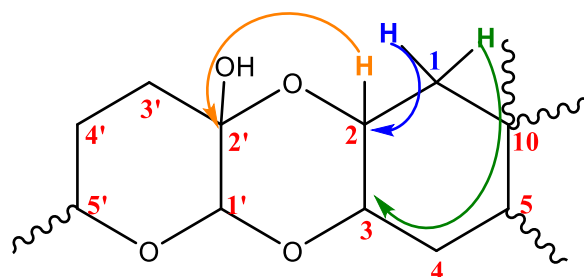


Figure III-B-75: Correlation of H-1 α , H-1 β , H-2 and H-4 α according to HMBC spectrum of compound PN

➤ H₃-18 (δ_H 0.63) has correlated with:

- C-17 (δ_C 45.45).
- C-13 (δ_C 55.55).
- C-14 (δ_C 84.64).
- C-12 (δ_C 73.41).

➤ H-21 α (δ_H 4.87) has correlated with:

- C-23 (δ_C 176.89).

➤ H-21 β (δ_H 4.79) has correlated with:

- C-23 (δ_C 176.89).

➤ H-22 (δ_H 5.80) has correlated with:

- C-21 (δ_C 74.04).
- C-20 (δ_C 175.92).

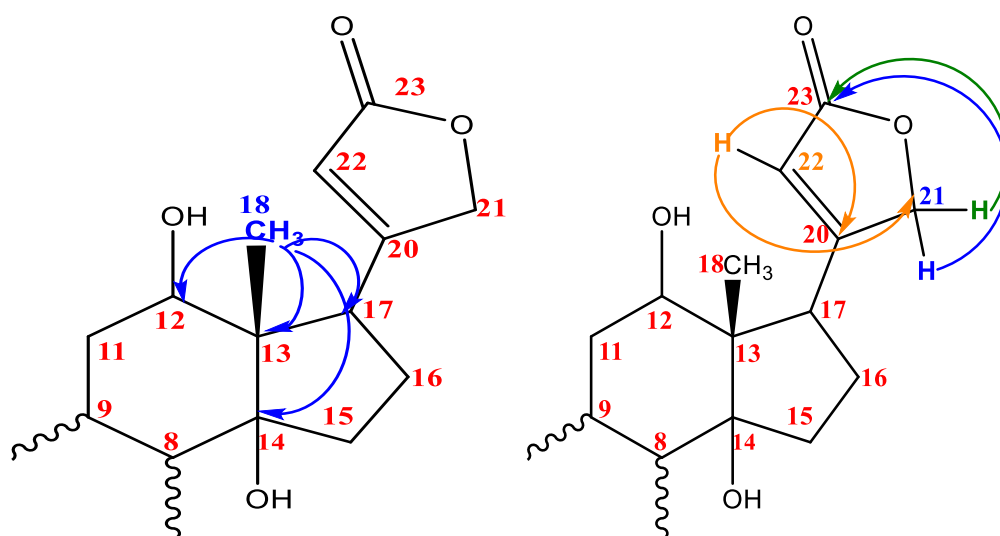


Figure III-B-76: Correlation of H₃-18, H-21 α , H-21 β and H-22 according to HMBC spectrum of compound PN

- H-1' (δ_H 4.60) has correlated with:
 - C-2' (δ_C 90.39).
 - C-3' (δ_C 70.49).
- H₃-6' (δ_H 1.09) has correlated with:
 - C-5' (δ_C 66.02).
 - C-4' (δ_C 36.85).

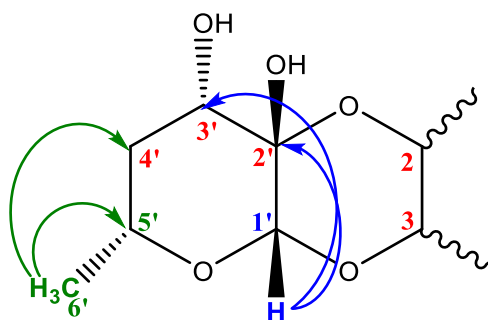


Figure III-B-77: Correlation of H-1' and H₂-6' according to HMBC spectrum of compound PN

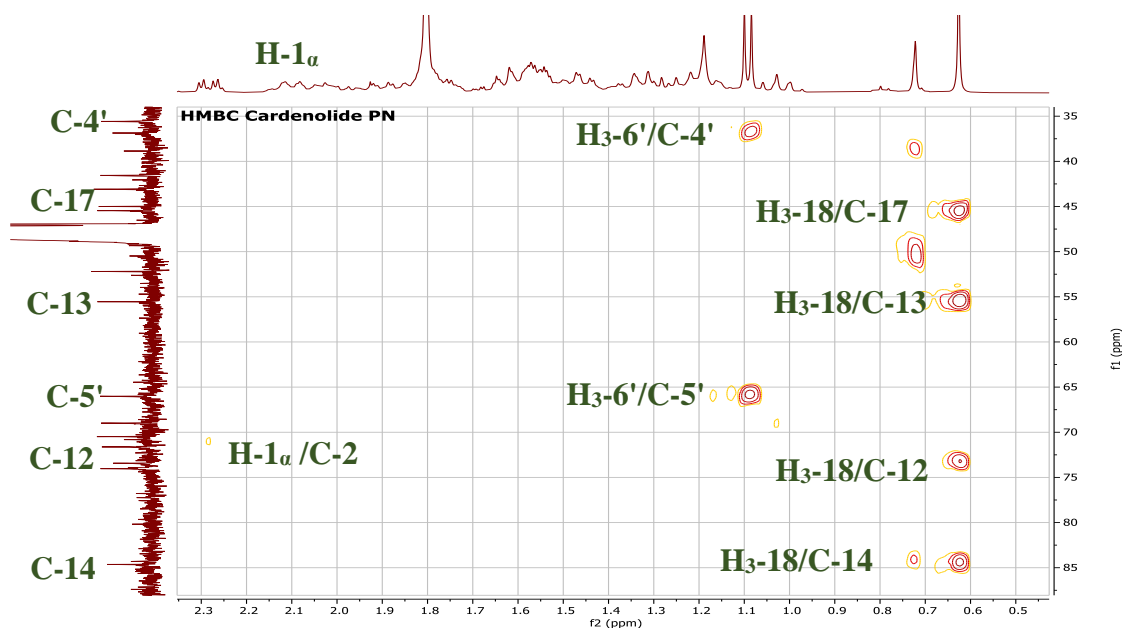


Figure III-B-78-a: HMBC expansions spectrum [3.6 – 0.4 ppm] (400 MHz, CD₃Cl) of compound PN

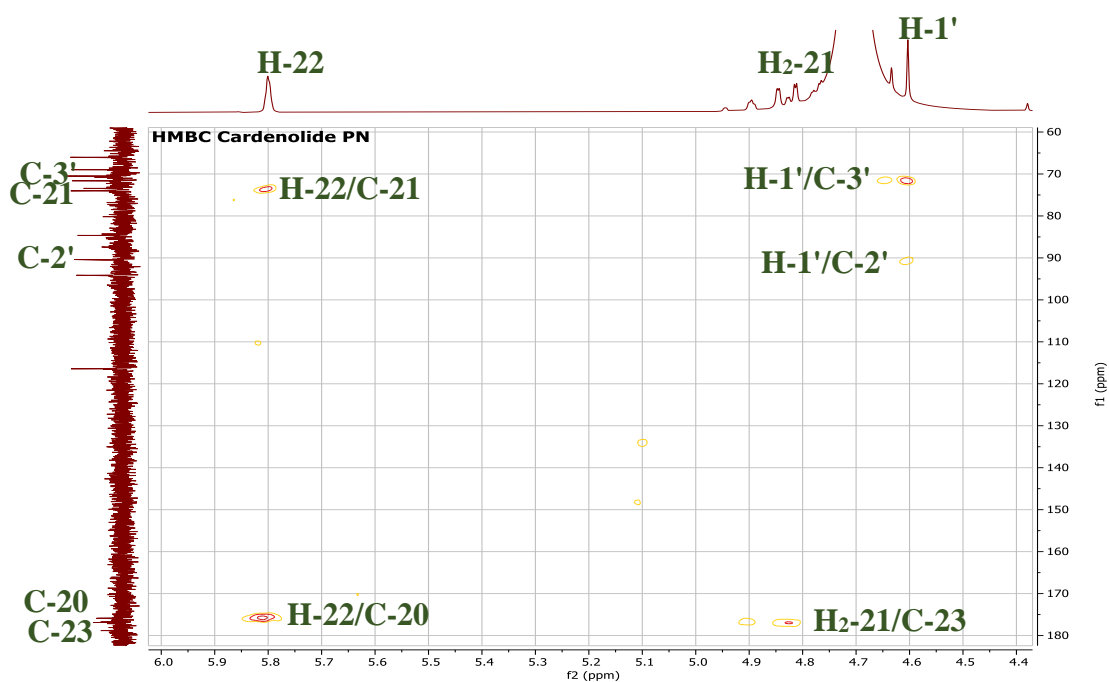


Figure III-B-78-b: HMBC expansions spectrum [3.6 – 3.0 ppm] (400 MHz, CD₃Cl) of compound PN

❖ COSY experiment (Figure III-B-81) was used to confirm the sequence of sugar unit which shows the correlation spots between its vicinal H, that are:

- H-3' (δ_H 3.47) correlated with H-4' $_{\beta}$ (δ_H 1.63).
- H-5' (δ_H 3.94) correlated with H-4' $_{\alpha}$ (δ_H 1.56).
- H-5' (δ_H 3.94) correlated with H-6' (δ_H 1.09).

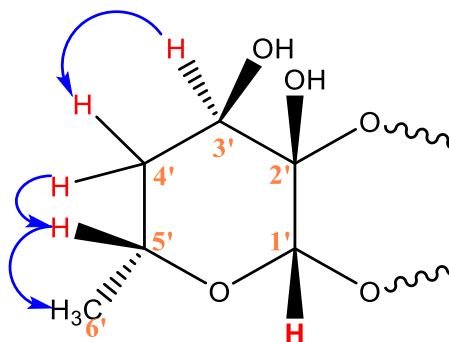


Figure III-B-79: COSY correlations of sugar part of compound PN

❖ The COSY spectrum shows also correlation spots between protons of some -CH₂ group and some vicinal H in aglycon portion, which are:

- H-1_β (δ_H 1.01) correlated with H-1_α (δ_H 2.28).
- H-1_α (δ_H 2.28) correlated with H-3 (δ_H 3.74).
- H-2 (δ_H 3.53) correlated with H-4_β (δ_H 1.63).
- H-4_α (δ_H 1.74) correlated with H-4_β (δ_H 1.63).
- H-5 (δ_H 1.45) correlated with H-6_α (δ_H 2.04).
- H-6_α (δ_H 2.04) correlated with H-6_β (δ_H 1.83).
- H-7_α (δ_H 1.55) correlated with H-7_β (δ_H 1.14).
- H-11_α (δ_H 1.63) correlated with H-12 (δ_H 3.26).
- H-15_α (δ_H 1.55) correlated with H-15_β (δ_H 1.29).
- H-16_α (δ_H 2.10) correlated with H-16_β (δ_H 1.90).
- H-19 (δ_H 9.93) correlated with H-1_β (δ_H 1.01).
- H-21_α (δ_H 4.87) correlated with H-22 (δ_H 5.80).
- H-21_β (δ_H 4.79) correlated with H-22 (δ_H 5.80).

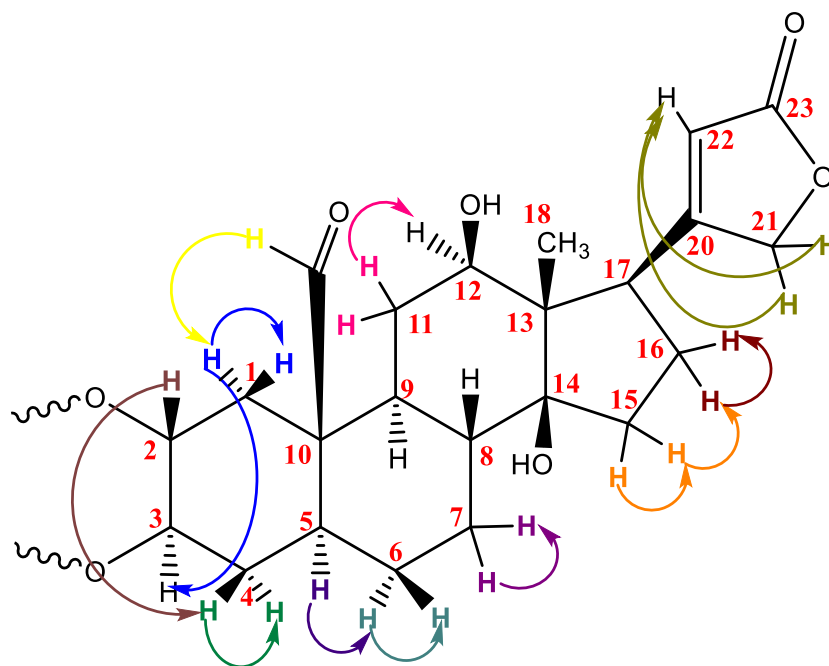


Figure III-B-80: COSY correlations of aglycon part of compound PN

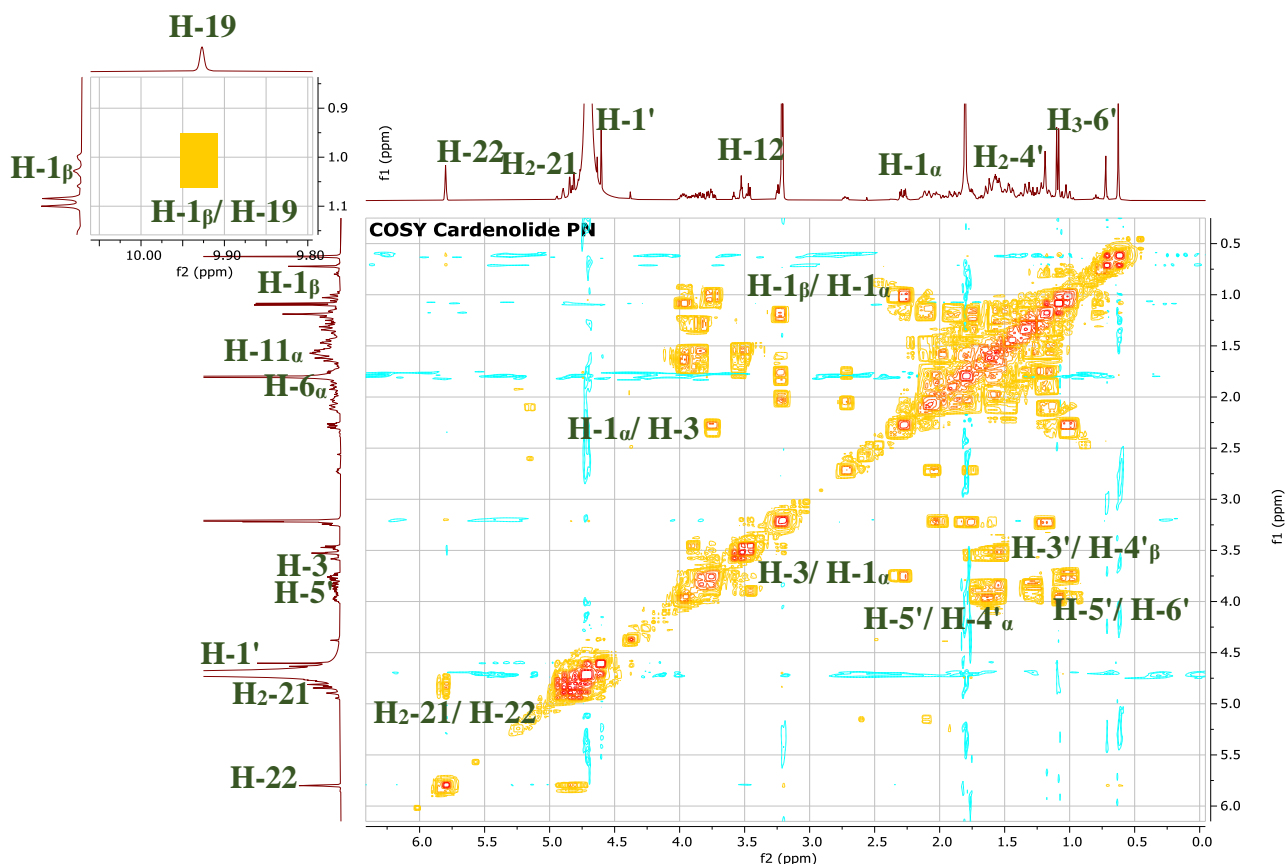


Figure III-B-81: COSY spectrum (400 MHz, CD₃OD) of compound PN

On the basis of all above evidences, compound PN was elucidated as **12 β -hydroxycalactin**. The chemical shift values of this compound are in full agreement with those of the literature [34]. This compound was isolated for the first time (as a new cardenolide glycoside) from *Pergularia tomentosa* [34]. Our study reported this compound for the second time, its structure is demonstrated in the Figure III-B-82.

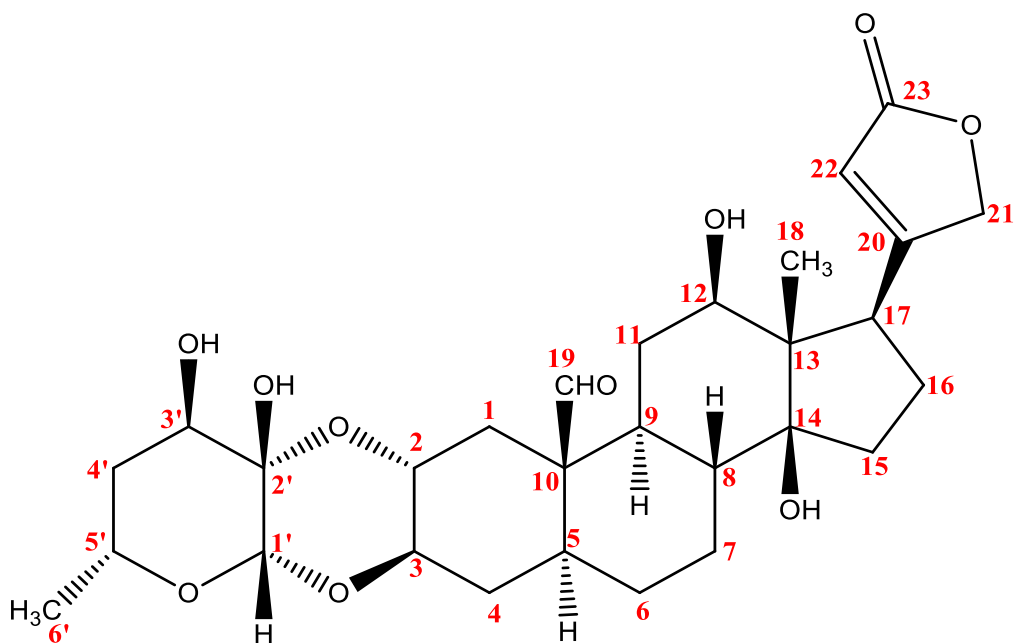


Figure III-B-82: Chemical structure of PN, which is a cardenolides glycoside named **12 β -hydroxycalactin**

III-B-2-3-Compound PVe

Compound PVe was obtained as a colorless amorphous solid, it is invisible under UV light and it takes a green color after revelation with a vanillin sulphuric solution and heating. Its structure was characterized using NMR spectroscopic analysis methods which are 1D: ^1H NMR and ^{13}C NMR and 2D: HSQC, HMBC and COSY. Its spectra are recorded in CD_3OD .

- ❖ The ^1H NMR spectrum (Figure III-B-83) of this compound showed:
 - Typical signals of steroidal aglycone portion which are:
 - One singlet signal with an integration of one proton at δ_{H} 9.94.
 - One singlet olefinic signal with an integration of one proton at δ_{H} 5.80.
 - The signals corresponding to two no-equivalent protons of CH_2 groups which are:
 - ✓ One doublet of doublet and one broad signals with an integration of one proton of each, at δ_{H} 4.92 and δ_{H} 4.82 with a coupling constant $J = 18.3; 1.4$ Hz.

- ✓ Two doublet of doublet signals with an integration of one proton for each one at: δ_H 2.48 and δ_H 0.81 with a coupling constant $J= 12.9$; 4.1 Hz and $J= 13.1$; 6.5 Hz, respectively.
- ✓ One doublet of doublet and one doublet signals with an integration of one proton of each, at δ_H 2.21 and δ_H 1.84 with a coupling constant $J= 13.5$; 6.1 Hz and $J= 12.7$ Hz, respectively.
- ✓ One doublet of doublet and one doublet signals with an integration of one proton of each, at δ_H 2.15 and δ_H 1.84 with a coupling constant $J= 12.6$; 2.9 Hz and $J= 12.7$, Hz respectively.
- ✓ One doublet and one multiplet signals with an integration of one proton of each, at δ_H 2.05 and δ_H 1.77 with a coupling constant $J= 9.6$ Hz.
- ✓ Two doublet signals with an integration of one proton of each, at δ_H 1.99 and δ_H 1.55 with a coupling constant $J= 9.5$ Hz and $J= 11.1$ Hz, respectively.
- ✓ Two doublet signals with an integration of one proton of each, at δ_H 1.84 and δ_H 1.58 with a coupling constant $J= 12.7$ Hz and $J= 12.2$ Hz, respectively.
- ✓ Two doublet of doublet signals with an integration of one proton for each, at δ_H 1.38 and δ_H 1.30 with a coupling constant $J= 12.2$; 3.1 Hz and $J= 12.6$; 3.5 Hz, respectively.
- One doublet of doublet signal with an integration of one proton at δ_H 2.73 with a coupling constant $J= 8.7$; 5.4 Hz.
- Six multiplet signals with an integration of one proton of each, at δ_H 3.43, δ_H 3.18, δ_H 1.58, δ_H 1.54, δ_H 1.38 and δ_H 1.27.
- One singlet methyl signal at δ_H 0.72.
- Typical signals of sugar portion which are:
 - An anomeric signal with an integration of one proton at δ_H 4.25 with a coupling constant $J= 7.8$ Hz.
 - Two doublet of doublet signals with an integration of one proton of each, at δ_H 3.76 and δ_H 3.54 with a coupling constant $J= 9.3$; 2.2 Hz and $J= 10.8$; 5.0 Hz, respectively.
 - Four multiplet signals with an integration of one proton of each, at δ_H 3.24, δ_H 3.18, δ_H 3.14 and δ_H 3.09

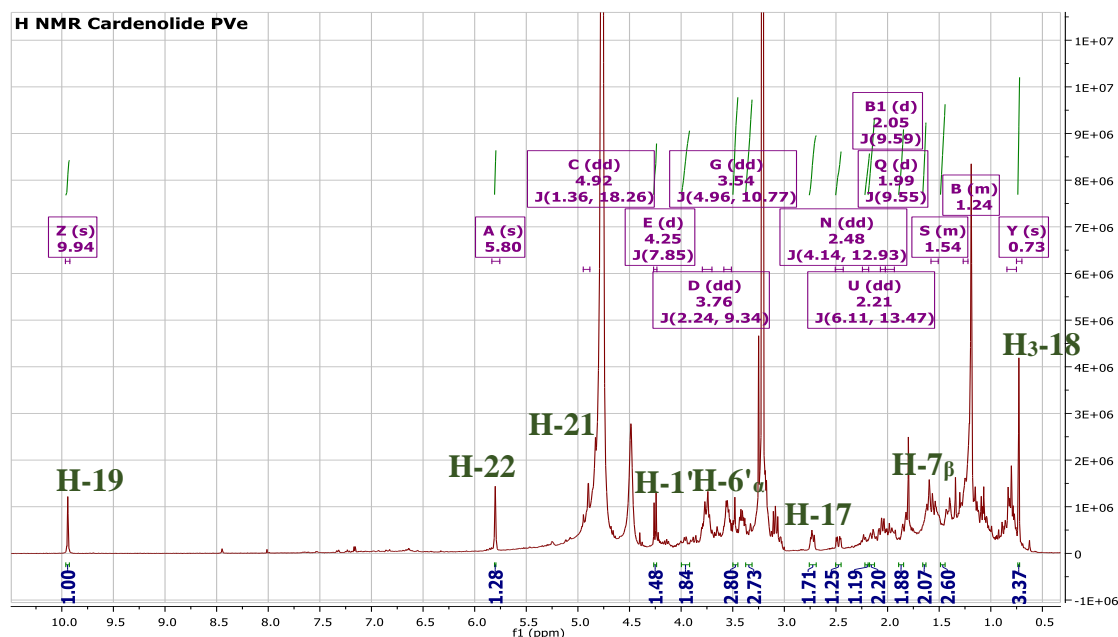


Figure III-B-83: ^1H NMR spectrum (400 MHz, CD_3OD) of compound PVe

❖ According to ^{13}C and ^{13}C DEPT (135 and 90) NMR spectra (Figure III-B-84, III-B-85 and III-B-86) there are:

➤ The signals belonging to the aglycone part which are:

- Nine methylene signals at δ_{C} 73.93, δ_{C} 38.84, δ_{C} 38.32, δ_{C} 33.69, δ_{C} 31.26, δ_{C} 27.42, δ_{C} 27.12, δ_{C} 26.47 and δ_{C} 21.70.
- Six methine signals at δ_{C} 82.84, δ_{C} 69.93, δ_{C} 50.42, δ_{C} 48.05, δ_{C} 42.37 and δ_{C} 41.98.
- One methyl signal at δ_{C} 14.74.
- One olefinic methine signal at δ_{C} 116.53.
- Five signals corresponding to quaternary carbons at δ_{C} 177.22, δ_{C} 176.77, δ_{C} 83.60, δ_{C} 52.82 and δ_{C} 49.31.

➤ The signals belonging to the sugar part which are:

- Five methine signals at δ_{C} 101.35, δ_{C} 76.55, δ_{C} 76.49, δ_{C} 73.35 and δ_{C} 70.14.
- One methylene signal at δ_{C} 61.18.

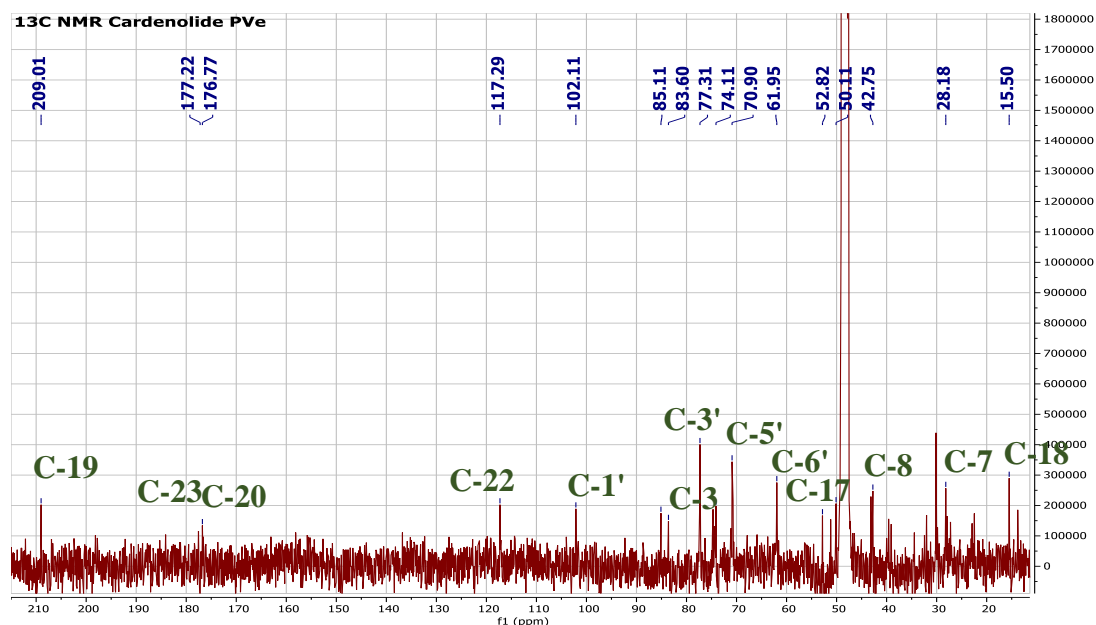


Figure III-B-84: ^{13}C NMR spectrum (100 MHz, CD_3OD) of compound PVE

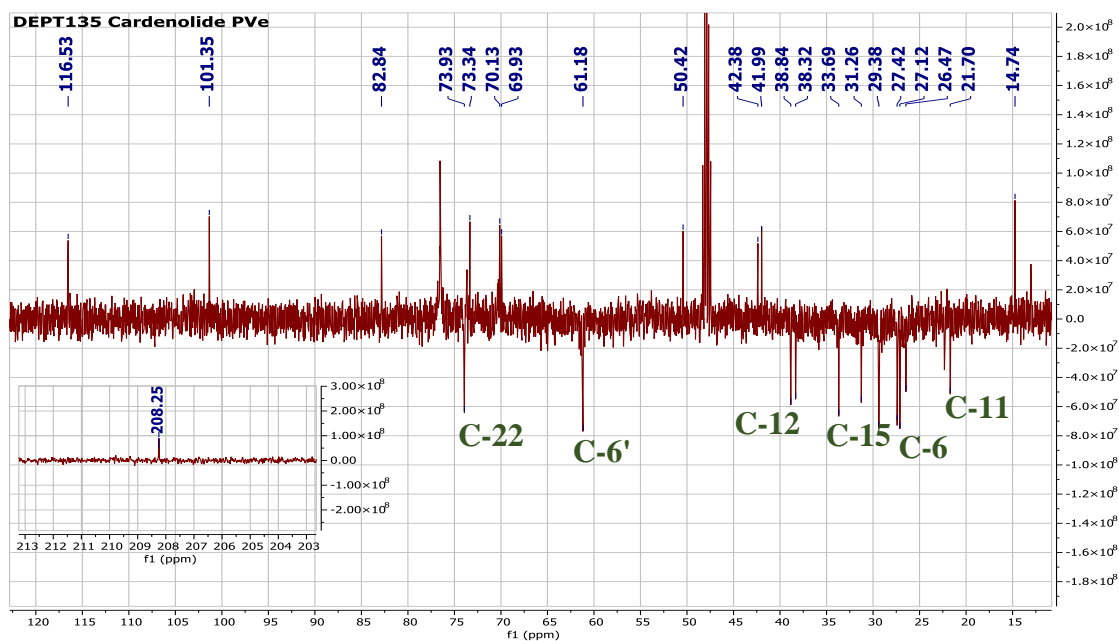


Figure III-B-85: ^{13}C NMR DEPT 135 spectrum (100 MHz, CD_3OD) of compound PVE

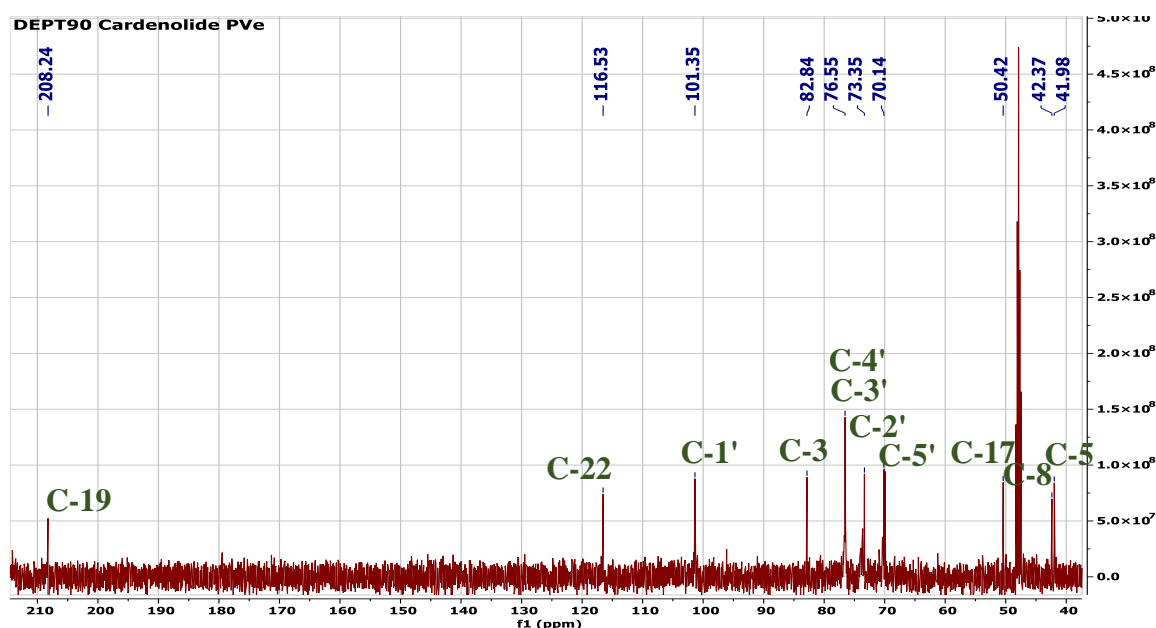


Figure III-B-86: ^{13}C NMR DEPT 90 spectrum (100 MHz, CD_3OD) of compound PVE

The coupling constant of anomeric proton ($J = 7.8$ Hz) as well as, the chemical shifts of protons and carbons of sugar unit are in full agreement with the β -D-glucopyranoside unit.

The ^1H and ^{13}C NMR spectra of compound PVE are very close to those of compound PN except the signals of sugar moiety, which indicate that this compound has a cardenolide glycoside skeleton. The major difference between the two compounds appears clearly on ^1H and ^{13}C NMR spectra of compound PVE, which show the disappearance of all signals corresponding to a doubly linked sugar unit (4'-deoxyhexosulose or 4',6'-dideoxyhexosulose), as well as, the appearance of signals corresponding to β -D-glucose unit which indicate that the sugar unit is linked to steroidal aglycon by single link.

- ❖ The proton–carbon correlation experiment (HSQC Figure III-B-87) allowed us to assign all protons to their corresponding carbons (Table III-B-08).

Table III-B-08: Chemical shifts of ^1H (400 MHz) and ^{13}C (100 MHz) NMR in CD_3OD of compound PVe (δ in ppm and J in Hz)

Position	Compound PVe	
	δ_{H}	δ_{C}
Typical signals of aglycon portion		
1	2.48 (dd; J= 12.9; 4.1 Hz)	38.32
	0.81 (dd; J= 13.1; 6.5Hz)	
2	3.40 (m)	69.93
3	3.40 (m)	82.84
4	1.99 (d; J= 9.5 Hz)	31.26
	1.55 (d; J= 11.1 Hz)	
5	1.54 (m)	41.98
6	2.15 (dd; J= 12.6; 2.9 Hz)	27.12
	1.84 (d; J= 12.7 Hz)	
7	1.84 (d; J= 12.7 Hz)	27.42
	1.58 (d; J= 12.2 Hz)	
8	1.38 (m)	42.37
9	1.27 (m)	48.05
10	-	52.82
11	1.58 (m)	21.70
12	1.38 (dd; J= 12.2; 3.1 Hz)	38.84
	1.30 (dd; J= 12.6; 3.5 Hz)	
13	-	49.31

14	-	83.60
15	2.21 03 (dd; J= 13.5; 6.1 Hz) 1.84 (d; J= 12.7 Hz)	33.69
16	2.05 (d; J= 9.6 Hz) 1.77 (m)	26.47
17	2.73 (dd; J= 8.7; 5.4 Hz)	50.42
18	0.72 (s)	14.74
19	9.94 (s)	208.24
20	-	176.77
21	4.92 (dd; J= 18.3; 1.4 Hz) 4.82 (br)	73.93
22	5.80 (s)	116.53
23	-	177.22
Typical signals of sugar portion		
1'	4.25 (d; J= 7.8 Hz)	101.35
2'	3.09 (m)	73.35
3'	3.24 (m)	76.55
4'	3.14 (m)	76.49
5'	3.18 (m)	70.14
6'	3.76 (dd; J= 9.3; 2.2 Hz) 3.54 (dd; J= 10.8; 5.0 Hz)	61.18

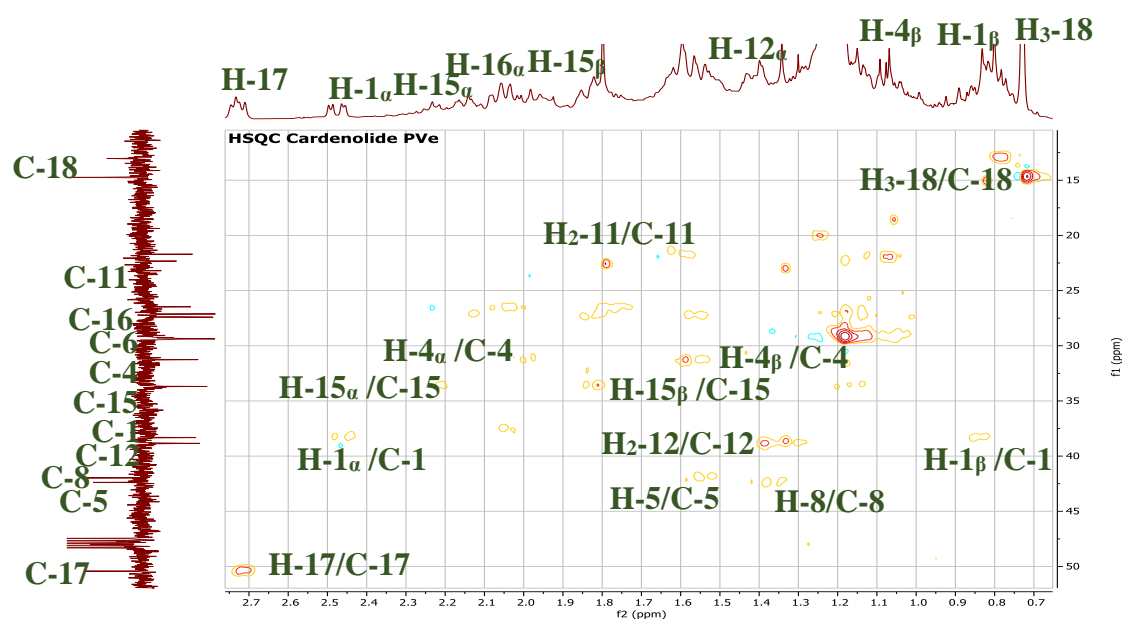


Figure III-B-87-a: HSQC expansions spectrum [2.7 - 0.7 ppm] (100 MHz, CD₃OD) of compound PVe

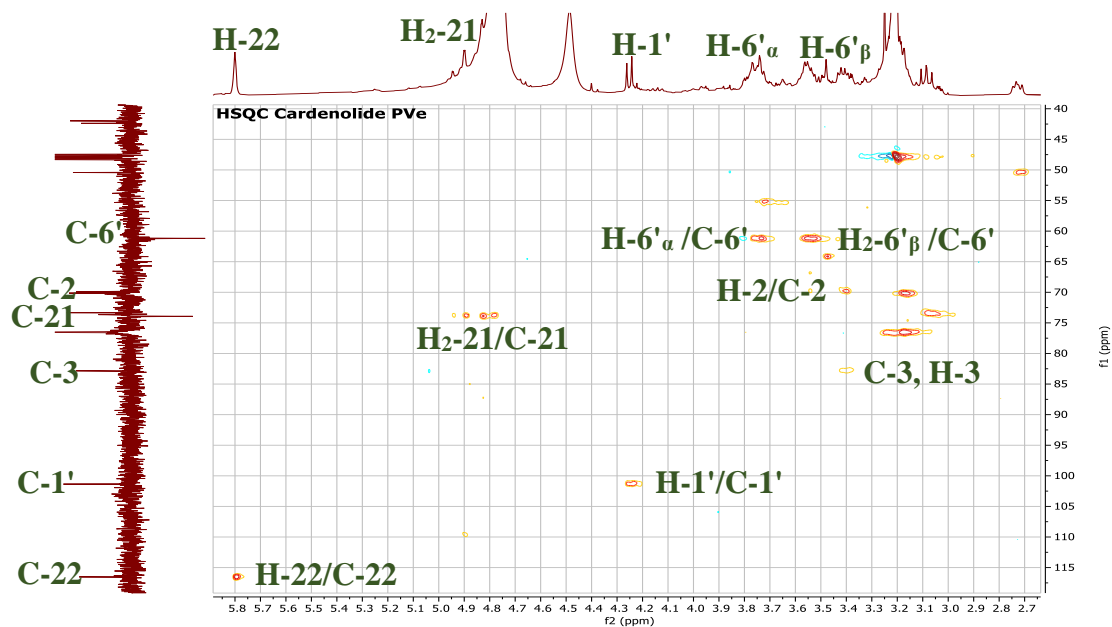


Figure III-B-87-b: HSQC expansions spectrum [5.8 – 2.7 ppm] (100 MHz, CD₃OD) of compound PVe

❖ The sequence of sugar unit is confirmed using COSY experiment (Figure III-B-88) which shows the correlation spots between its vicinal H, that are:

- H-1' (δ_H 4.25) correlated with H-2' (δ_H 3.09).
- H-2' (δ_H 3.09) correlated with H-3' (δ_H 3.24).
- H-5' (δ_H 3.18) correlated with H-6' $_{\beta}$ (δ_H 3.54).
- H-6' $_{\alpha}$ (δ_H 3.76) correlated with H-6' $_{\beta}$ (δ_H 3.54).

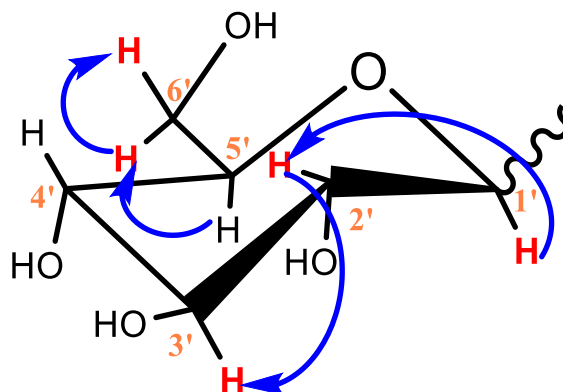


Figure III-B-88: COSY correlations of sugar part of compound PVe

❖ The COSY spectrum shows also correlation spots between protons of some -CH₂ group and some vicinal H in aglycone portion, which are:

- H-1 $_{\alpha}$ (δ_H 2.48) correlated with H-1 $_{\beta}$ (δ_H 0.81).
- H-1 $_{\alpha}$ (δ_H 2.48) correlated with H-2 (δ_H 3.43).
- H-6 $_{\alpha}$ (δ_H 2.15) correlated with H-5 (δ_H 1.54).
- H-1 $_{\beta}$ (δ_H 0.81) correlated with H-2 (δ_H 3.43).
- H-16 $_{\alpha}$ (δ_H 2.05) correlated with H-16 $_{\beta}$ (δ_H 1.77).
- H-16 $_{\alpha}$ (δ_H 2.05) correlated with H-17 (δ_H 2.73).
- H-16 $_{\beta}$ (δ_H 1.77) correlated with H-17 (δ_H 2.73).
- H-21 $_{\alpha}$ (δ_H 4.92) correlated with H-21 $_{\beta}$ (δ_H 4.82).
- H-21 $_{\alpha}$ (δ_H 4.92) correlated with H-22 (δ_H 5.80).
- H-21 $_{\beta}$ (δ_H 4.82) correlated with H-22 (δ_H 5.80).

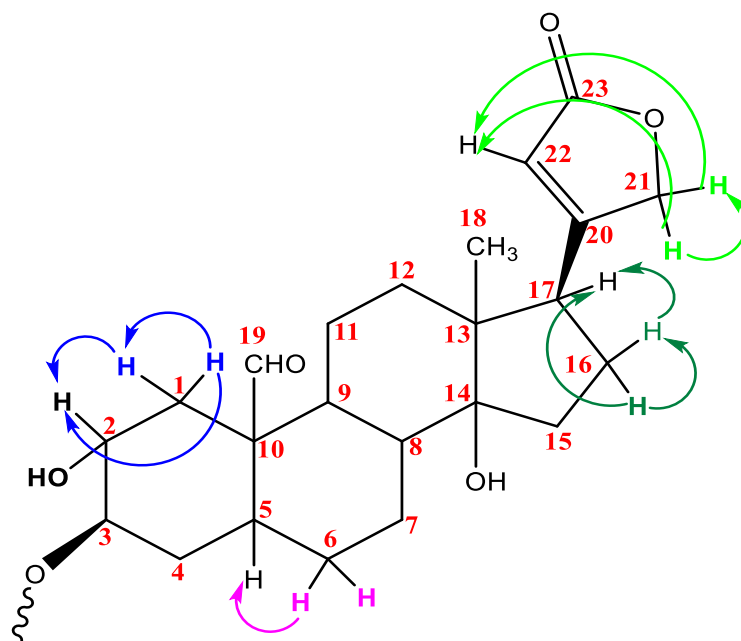


Figure III-B-89 COSY correlations of aglycone part of compound PVe

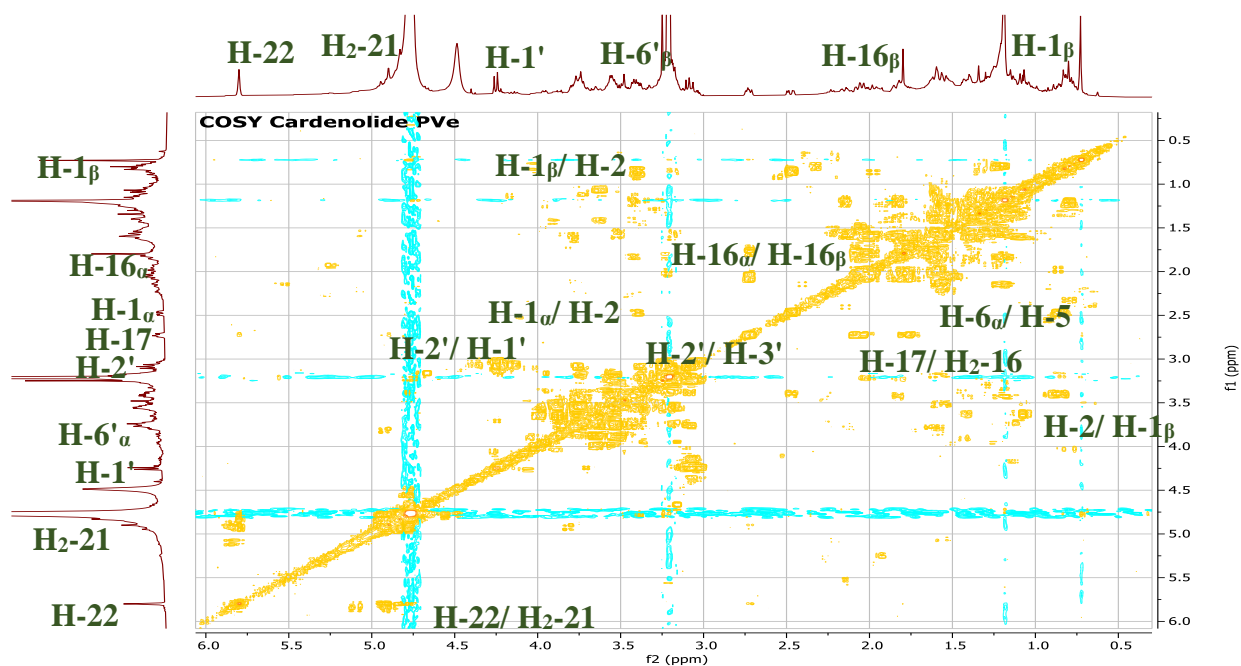


Figure III-B-90: COSY spectrum (400 MHz, CD₃OD) of compound PVe

All of the spectroscopic data of PVe compound indicate that the aglycone part of this compound is identical with that of compound PN, except that hydroxyl group (-OH) linked at

C-12 in compound PN was disappeared in compound PVe. This difference was confirmed by chemical shift of C-12, C-11 and C-13 which were shifted upfield compared to compound PN (C-12: δ_c 73.41 for PN shifted to δ_c 38.83 for PVe, C-11: δ_c 31.60 for PN shifted to δ_c 21.69 for PVe and C-13: δ_c 55.46 for PN shifted to δ_c 49.31 for PVe). This shielding effect was previously reported by S.Masour *et al.* [120].

The downfield shift of C-3 (δ_c 82.92) confirmed the linkage position of the sugar unit at this carbon. While, the chemical shift of C-2 (δ_c 69.78) confirmed that –OH group linked at C-2 is free.

All these spectral data as well as the comparison with the literature [122] allowed us to attribute the structure of **2-hydroxycorotoxigenin-3-O-glucopyranoside** to compound PVe, which is isolated for the first time as a new compound. Their chemical structure is illustrated in Figure III-B-91.

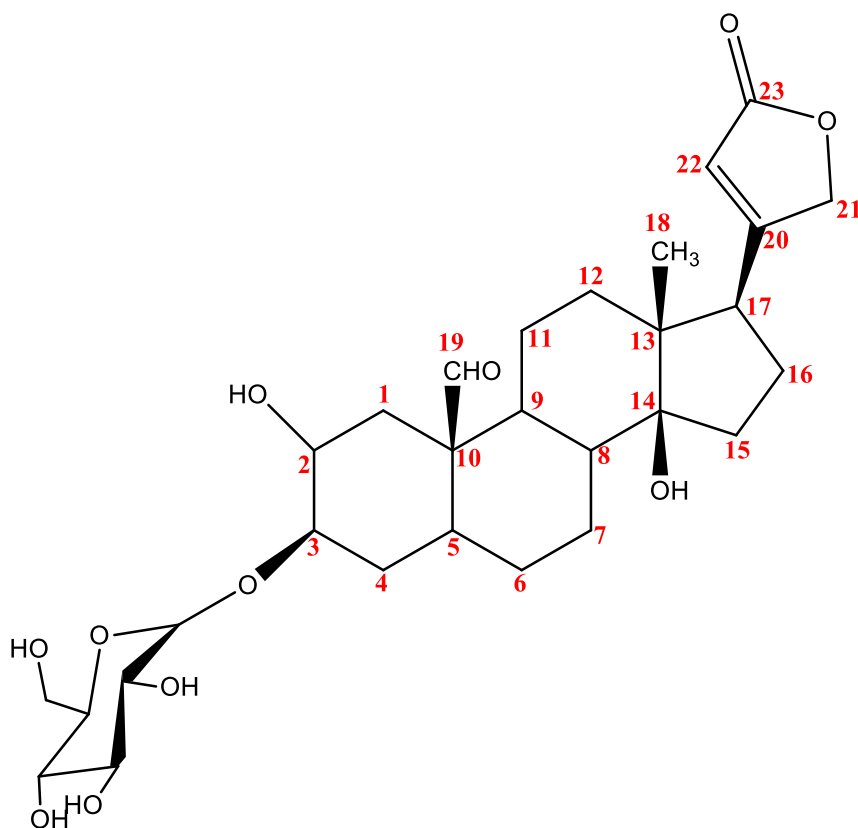


Figure III-B-91: Chemical structure of compound PVe, which is a cardenolides glycoside named **2-hydroxycorotoxigenin-3-O-glucopyranoside**

III-B-2-4-Compound M

Compound PM was obtained as a white amorphous solid, it is invisible under UV light and it takes a brown color after revelation with a vanillin sulphuric solution and heating. Its structure was characterized using NMR spectroscopic analysis methods which are 1D: ^1H NMR and ^{13}C NMR and 2D: HSQC, HMBC and COSY. Its spectra are recorded in CD_3OD .

❖ The ^1H NMR spectrum (Figure III-B-92) of this compound showed:

➤ Typical signals of steroidal aglycon portion which are:

- One doublet olefinic signal with an integration of one proton at δ_{H} 5.80 with a coupling constant $J= 1.3$ Hz.
- The signals corresponding to two no-equivalent protons of CH_2 groups which are:
 - ✓ Two doublet of doublet signals with an integration of one proton of each, at δ_{H} 4.94 and δ_{H} 4.82 with a coupling constant $J= 18.4; 1.4$ Hz and $J= 18.4; 1.7$ Hz, respectively.
 - ✓ Two doublet signals with an integration of one proton of each, at δ_{H} 4.25 and δ_{H} 3.71 with a coupling constant $J= 10.4$ Hz.
 - ✓ Two doublet of doublet signals with an integration of one proton for each, at δ_{H} 2.64 and δ_{H} 2.11 with a coupling constant $J= 13.7; 6.5$ Hz and $J= 12.4; 3.5$ Hz, respectively.
 - ✓ One multiplet and one doublet of doublet signals with an integration of one proton for each, at δ_{H} 2.56 and δ_{H} 2.02 with a coupling constant $J= 8.6; 4.0$ Hz.
 - ✓ Two doublet of doublet signals with an integration of one proton of each, at δ_{H} 2.43 δ_{H} 1.14 with a coupling constant $J= 13.1; 6.2$ Hz and $J= 13.5; 5.5$ Hz, respectively.
 - ✓ One doublet and one doublet of doublet signals with an integration of one proton of each, at δ_{H} 2.07 and δ_{H} 1.74 with a coupling constant $J= 11.5$ Hz and $J= 11.9; 3.4$ Hz, respectively.
 - ✓ Two doublet of doublet signals with an integration of one proton of each, at δ_{H} 2.03 and δ_{H} 1.61 with a coupling constant $J= 12.3; 6.9$ Hz and $J= 12.1; 8.9$ Hz, respectively.

- ✓ Two doublet of doublet signals with an integration of one proton of each, at δ_H 2.02 and δ_H 1.05 with a coupling constant $J= 8.6; 4.0$ Hz and $J= 8.6; 3.8$ Hz, respectively.
- ✓ Two multiplet signals with an integration of one proton of each, at δ_H 1.60 and δ_H 1.55.
- ✓ Two doublet of doublet signals with an integration of one proton for each at: δ_H 1.43 and δ_H 1.31 with a coupling constant $J= 10.3; 3.2$ Hz and $J= 11.4; 6.1$ Hz, respectively.
- ✓ Two doublet of doublet signals with an integration of one proton for each, at δ_H 1.34 and δ_H 1.30 with a coupling constant $J= 8.8; 4.4$ Hz and $J= 7.7; 4.8$ Hz, respectively
- One doublet of doublet signal with an integration of one proton at δ_H 2.72 with a coupling constant $J= 8.6; 5.3$ Hz.
- Three multiplet signals with an integration of one proton of each, at δ_H 1.77, δ_H 1.55 and δ_H 1.05.
- One singlet methyl signal at δ_H 0.84.
- Typical signals of sugar portion which are:
 - One doublet anomeric signal with an integration of one proton at δ_H 4.19 with a coupling constant $J= 7.8$ Hz.
 - Two doublet of doublet signals with an integration of one proton of each, at δ_H 3.79 and δ_H 3.55 with a coupling constant $J= 11.8; 2.0$ Hz and $J= 11.7; 5.8$ Hz, respectively.
 - Three multiplet signals with an integration of one proton of each, at δ_H 3.24, δ_H 3.17 and δ_H 3.09
 - One doublet of doublet signal with an integration of one proton at δ_H 3.16 with a coupling constant $J= 6.7; 2.9$ Hz.

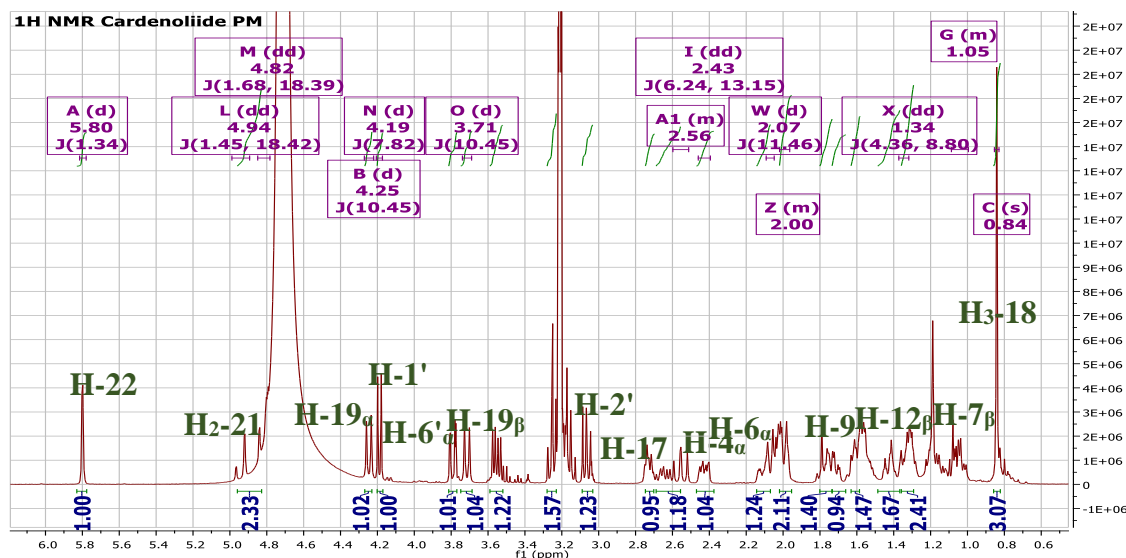


Figure III-B-92: ^1H NMR spectrum (400 MHz, CD_3OD) of compound PM

❖ 29 carbon signals were showed in the ^{13}C NMR spectrum (Figure III-B-93) of compound PM. The type of each carbon was determined according to ^{13}C DEPT (135 and 90) NMR spectra (Figure III-B-94 and III-B-95). These spectra showed:

- The signals belonging to the aglycon part which are:
 - Eleven methylene signals at δ_{C} 73.96, δ_{C} 67.31, δ_{C} 44.15, δ_{C} 39.74, δ_{C} 38.11, δ_{C} 34.02, δ_{C} 31.86, δ_{C} 28.25, δ_{C} 27.04, δ_{C} 26.58, δ_{C} 22.22.
 - Four methine signals at δ_{C} 50.70, δ_{C} 49.32, δ_{C} 46.03 and δ_{C} 41.54.
 - One methyl signal at δ_{C} 15.09.
 - One olefinic methine signal at δ_{C} 116.41.
 - Six signals corresponding to quaternary carbons at δ_{C} 177.06, δ_{C} 175.85, δ_{C} 84.93, δ_{C} 49.74, δ_{C} 38.82 and δ_{C} 214.41.
- The signals belonging to the sugar part which are:
 - Five methine signals at δ_{C} 103.18, δ_{C} 76.99, δ_{C} 76.65, δ_{C} 73.68 and δ_{C} 70.44.
 - One methylene signal at δ_{C} 61.54.

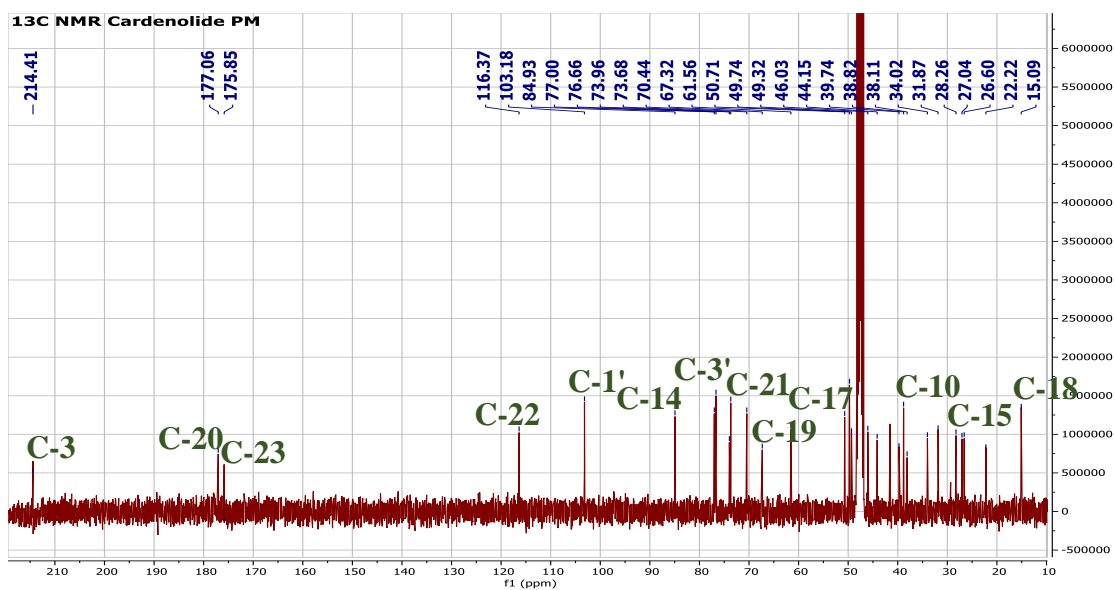


Figure III-B-93: ^{13}C NMR spectrum (100 MHz, CD_3OD) of compound PM

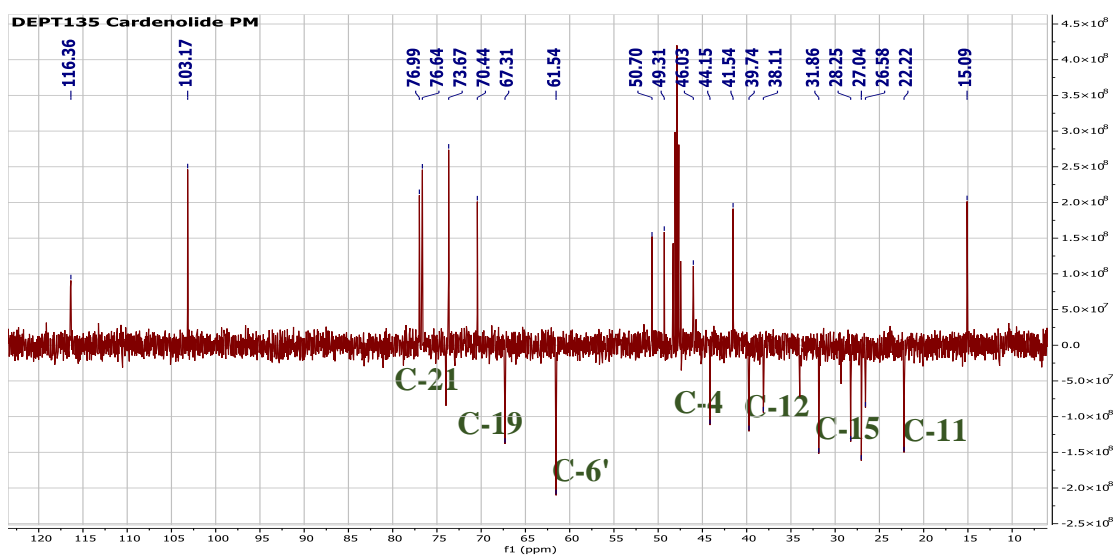


Figure III-B-94: ^{13}C NMR DEPT 135 spectrum (100 MHz, CD_3OD) of compound PM

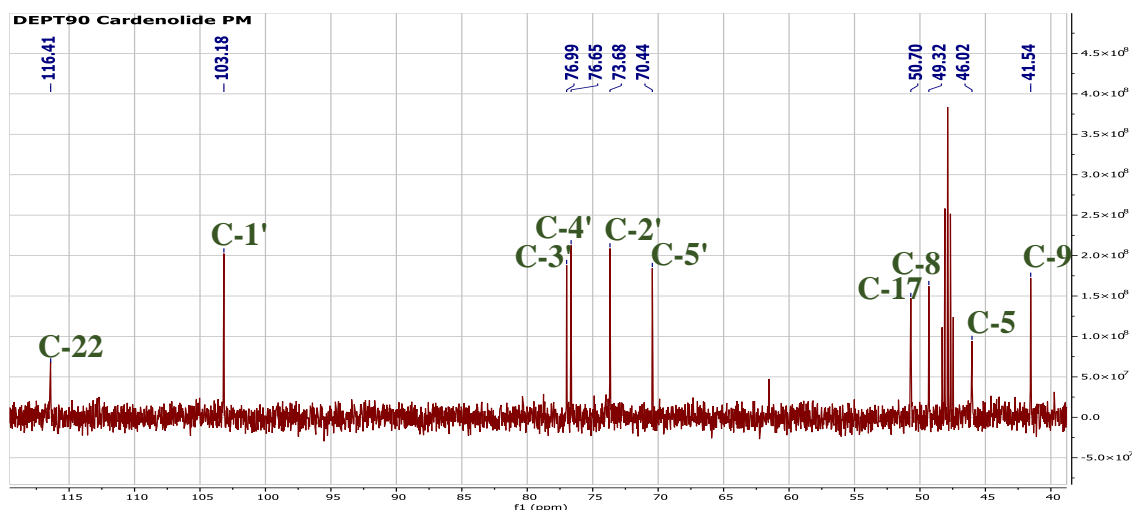


Figure III-B-95: ^{13}C NMR DEPT 90 spectrum (100 MHz, CD_3OD) of compound PM

The ^1H and ^{13}C NMR spectra of compound PM are very close to those of compound PVe which indicate that this compound has a cardenolide glycoside skeleton. Signals of sugar moiety of compound PM are identical with those of compound PVe which confirmed that the sugar unit in this compound is D- β -glucopyranosyl unit, which is linked to steroidal aglycon by a single link. The major difference between the two compounds appears clearly in ^1H and ^{13}C NMR spectra of compound PM which show:

- ✓ The disappearance of signals characteristic of aldehyde group.
 - ✓ The appearance of new typical signals of $-\text{CH}_2\text{OH}$ group at δ_{H} 4.25 and δ_{H} 3.71 and δ_{C} 67.31.
 - ✓ The appearance of new quaternary carbon signal characteristic of ketone group at δ_{C} 214.41.
- ❖ The assignment of all protons to their corresponding carbon of compound PM was established using HSQC spectrum (Figure III-B-96). Table III-B-09 illustrate the chemical shifts of H and C of compound PN.

Table III-B-09: Chemical shifts of ^1H (400 MHz) and ^{13}C (100 MHz) NMR in CD_3OD of compound PM (δ in ppm and J in Hz)

Position	Compound PM	
	δ_{H}	δ_{C}
Typical signals of aglycon part		
1	2.43 (dd; J= 13.1; 6.2 Hz)	34.02
	1.14 (dd; J= 13.5; 5.5 Hz)	
2	2.64 (dd; J= 13.7; 6.5 Hz)	38.11
	2.11 (dd; J= 12.4; 3.5 Hz)	
3	-	214.41
4	2.56 (m)	44.15
	2.02 (dd; J= 8.6; 4.0 Hz)	
5	1.55 (m)	46.03
6	2.07 (d; J= 11.5 Hz)	26.58
	1.74 (dd; J= 11.9; 3.4 Hz)	
7	2.02 (dd; J= 8.6; 4.0 Hz)	27.04
	1.05 (dd; J= 8.6; 3.8 Hz)	
8	1.05 (m)	49.32
9	1.77 (m)	41.54
10	-	38.82
11	1.60 (m)	22.22
	1.55 (m)	
12	1.43 (dd; J= 10.3; 3.2 Hz)	39.74
	1.31 (dd; J= 11.4; 6.1 Hz)	
13	-	49.74

14	-	84.93
15	2.03 (dd; J= 12.3; 6.9 Hz) 1.61 (dd; J= 12.1; 8.9 Hz)	31.86
16	1.34 (dd; J= 8.8; 4.4 Hz) 1.30 (dd; J= 7.7; 4.8 Hz)	28.25
17	2.72 (dd; J= 8.6; 5.3 Hz)	50.70
18	0.84 (s)	15.09
19	4.25 (d; J= 10.4; Hz) 3.71 (d; J= 10.4; Hz)	67.31
20	-	177.06
21	4.94 (dd; J= 18.4; 1.4 Hz) 4.82 (dd; J= 18.4; 1.7 Hz)	73.96
22	5.80 (d; J= 1.34 Hz)	116.41
23	-	175.85
Typical signals of sugar part		
1'	4.19 (d; J= 7.8; Hz)	103.18
2'	3.09 (m)	73.68
3'	3.24 (m)	76.99
4'	3.17 (m)	76.65
5'	3.16 (dd; J= 6.7; 2.9 Hz)	70.44
6'	3.79 (dd; J= 11.8; 2.0 Hz) 3.55 (dd; J= 11.7; 5.8 Hz)	61.54

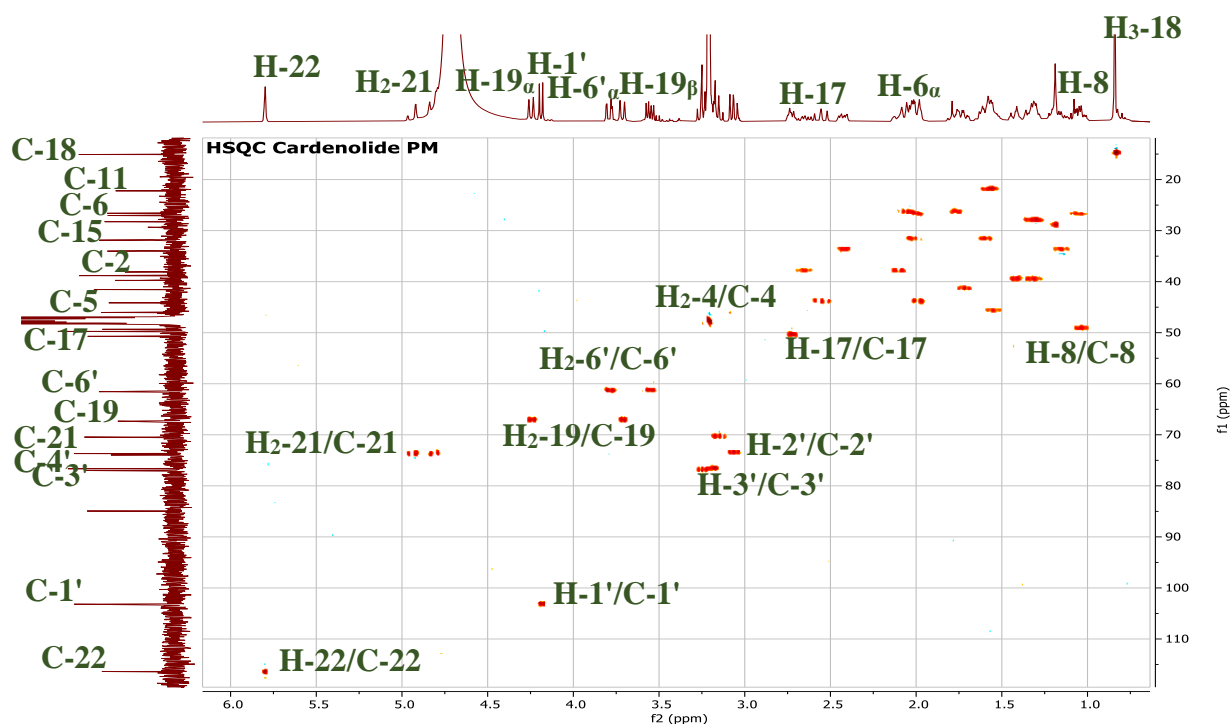


Figure III-B-96: HSQC expansions spectrum (400 MHz, CD₃OD) of compound PM

Comparison of the spectroscopic data of compound PM with those of literature, indicated that its structure was quite similar with that of **coroglaucigenin** compound, which was previously isolated from *P. tomentosa* by A. Ahmed *et al.* [3]. The major differences between the two structure compounds are:

- ✓ Hydroxyl group (-OH) that is linked at C-3 in coroglaucigenin compound was replaced by ketone group (-CO) in PM compound. This difference confirmed by chemical shift of C-3, C-2 and C-4 which were shifted downfield compared to coroglaucigenin compound (C-3: δ_C 71.70 for coroglaucigenin shifted to δ_C 214.41 for compound PM; C-2: δ_C 32.44 for coroglaucigenin shifted to δ_C 38.11 for compound PM and C-4: δ_C 39.08 for coroglaucigenin shifted to δ_C 44.15 for compound PM)
- ✓ -CH₂OH group (C-19) that linked at C-10 in compound PM was shifted downfield compared to coroglaucigenin compound (δ_C 59.9 for coroglaucigenin, δ_C 67.31 for compound PM) which indicate the presence of a linked -CH₂OH group. These

features implied the linkage position of the sugar unit at C-19, which will be confirmed by the HMBC correlations.

❖ HMBC spectrum (Figure III-B-100) allows to observe some correlation spots between:

- H-4_α (δ_H 2.56) has correlated with:
 - C-5 (δ_C 46.03).
- H-17 (δ_H 2.72) has correlated with:
 - C-20 (δ_C 177.06).
- H₃-18 (δ_H 0.84) has correlated with:
 - C-12 (δ_C 39.74).
 - C-13 (δ_C 49.74).
 - C-14 (δ_C 84.93).

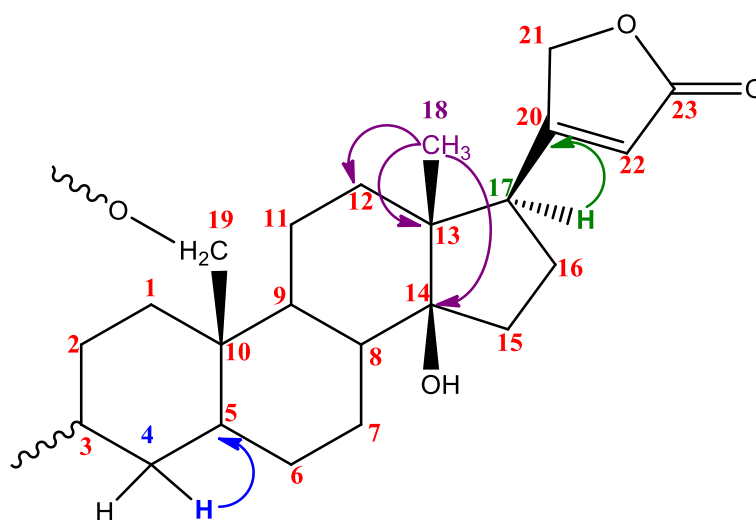


Figure III-B-97: Correlation of H-4_α, H-17 and H-18 according to HMBC spectrum of compound PM

- H-19_α (δ_H 4.25) has correlated with:
 - C-5 (δ_C 46.03).
 - C-8 (δ_C 49.31).
- H-19_β (δ_H 3.71) has correlated with:
 - C-8 (δ_C 49.31).
 - C-2 (δ_C 38.11).

- C-1 (δ_C 34.02).
- H-21 $_{\alpha}$ (δ_H 4.94) has correlated with:
 - C-22 (δ_C 116.41).
 - C-20 (δ_C 177.06).
- H-21 $_{\beta}$ (δ_H 4.82) has correlated with:
 - C-22 (δ_C 116.41).
 - C-20 (δ_C 177.06)

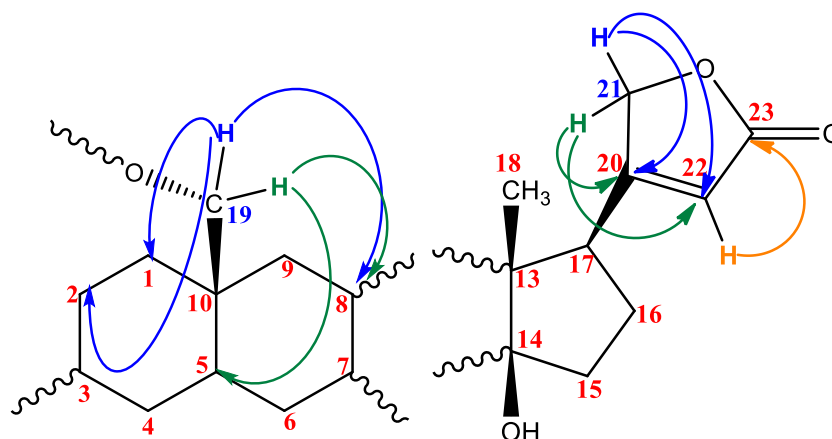


Figure III-B-98: Correlation of H-19 $_{\alpha}$, H-19 $_{\beta}$, H-21 $_{\alpha}$ and H-21 $_{\beta}$ according to HMBC spectrum of compound PM

- H-1' (δ_H 4.19) has correlated with:
 - C-19 (δ_C 67.31).
- H-2' (δ_H 3.09) has correlated with:
 - C-1' (δ_C 103.18).
 - C-3' (δ_C 76.99).
- H-3' (δ_H 3.24) has correlated with:
 - C-5' (δ_C 70.44).
- H-5' (δ_H 3.16) has correlated with:
 - C-4' (δ_C 76.65).
- H-6' $_{\beta}$ (δ_H 3.55) has correlated with:
 - C-4' (δ_C 76.65).

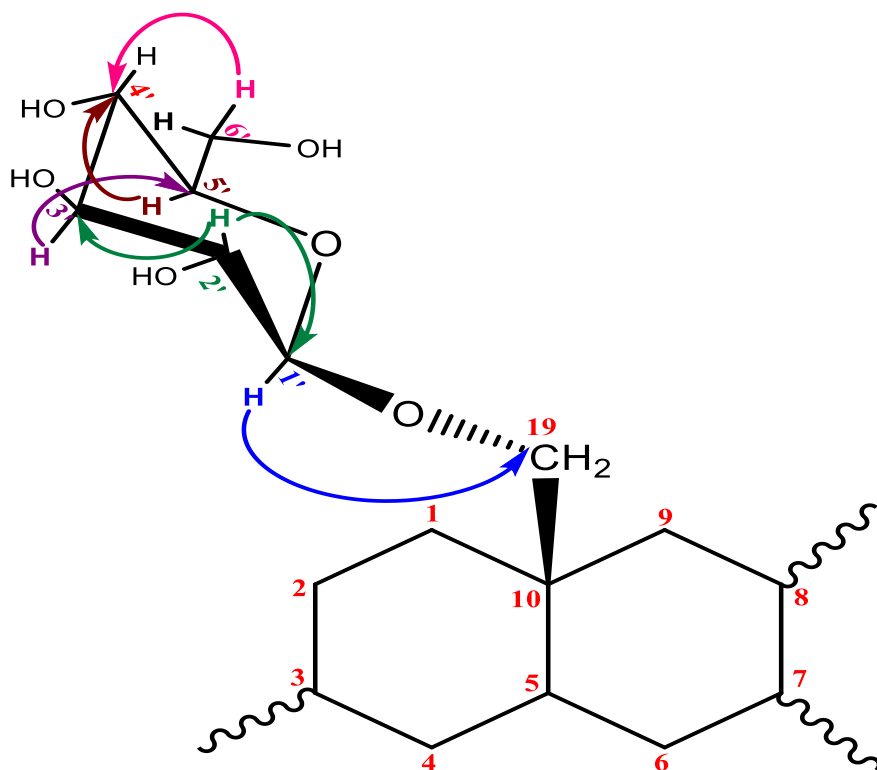


Figure III-B-99: correlation of sugar part according to HMBC spectrum of compound PM

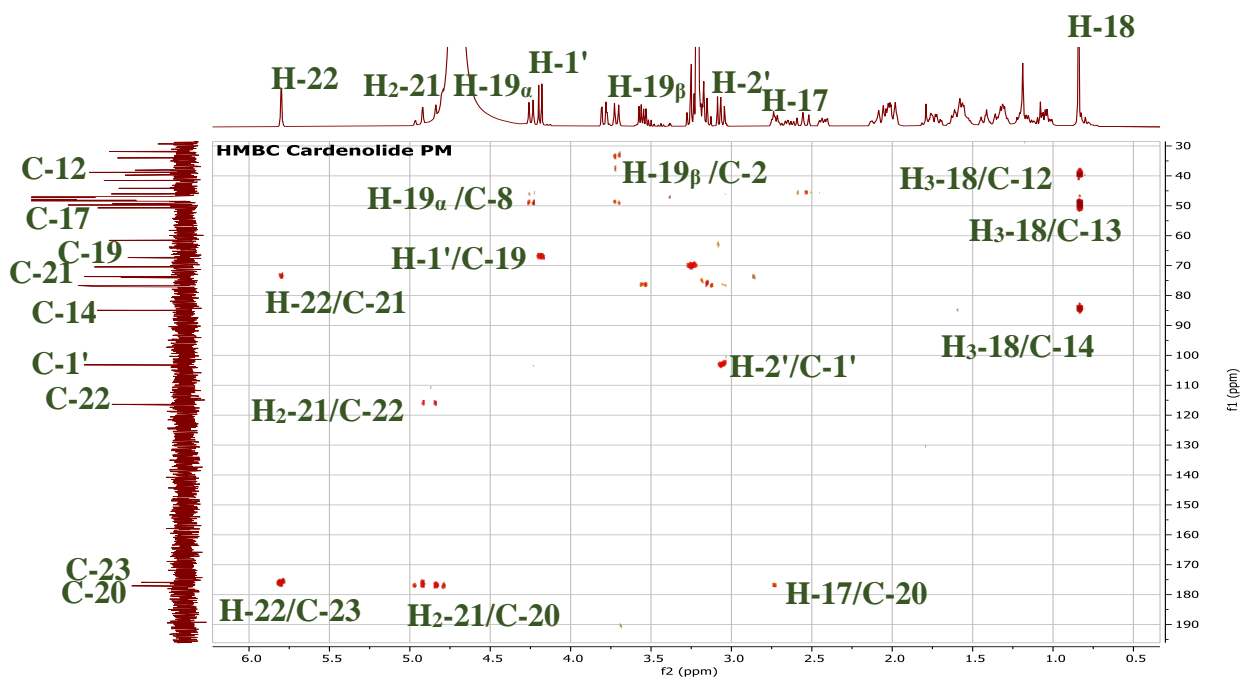


Figure III-B-100: HMBC spectrum (400 MHz, CD₃OD) of compound PM

❖ COSY experiment (Figure III-B-103) was used to confirm the sequence of sugar unit which shows the correlation spots between its vicinal H, that are:

- H-1' (δ_H 4.19) correlated with H-2' (δ_H 3.09).
- H-2' (δ_H 3.09) correlated with H-3' (δ_H 3.24).
- H-5' (δ_H 3.16) correlated with H-6' $_{\alpha}$ (δ_H 3.79).
- H-5' (δ_H 3.16) correlated with H-6' $_{\beta}$ (δ_H 3.55)
- H-6' $_{\alpha}$ (δ_H 3.79) correlated with H-6' $_{\beta}$ (δ_H 3.55).

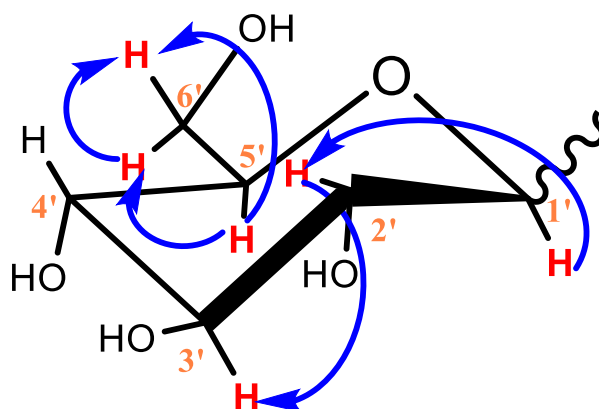


Figure III-B-101: COSY correlations of sugar part of compound PM

❖ The COSY spectrum shows also correlation spots between protons of some -CH₂ group and some vicinal H in aglycon proton, which are:

- H-1 $_{\beta}$ (δ_H 1.14) correlated with H-2 $_{\alpha}$ (δ_H 2.64).
- H-2 $_{\alpha}$ (δ_H 2.64) correlated with H-2 $_{\beta}$ (δ_H 2.11).
- H-4 $_{\alpha}$ (δ_H 2.56) correlated with H-5 (δ_H 1.55).
- H-15 $_{\alpha}$ (δ_H 2.03) correlated with H-15 $_{\beta}$ (δ_H 1.61).
- H-16 $_{\alpha}$ (δ_H 2.43) correlated with H-16 $_{\beta}$ (δ_H 1.14).
- H-19 $_{\alpha}$ (δ_H 4.25) correlated with H-19 $_{\beta}$ (δ_H 3.71).
- H-21 $_{\alpha}$ (δ_H 4.94) correlated with H-21 $_{\beta}$ (δ_H 4.82).

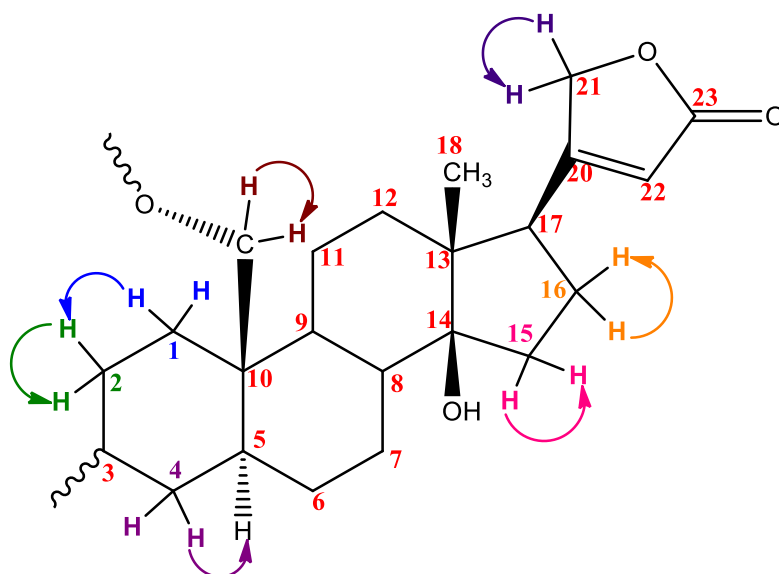


Figure III-B-102: COSY correlations of aglycon part of compound PM

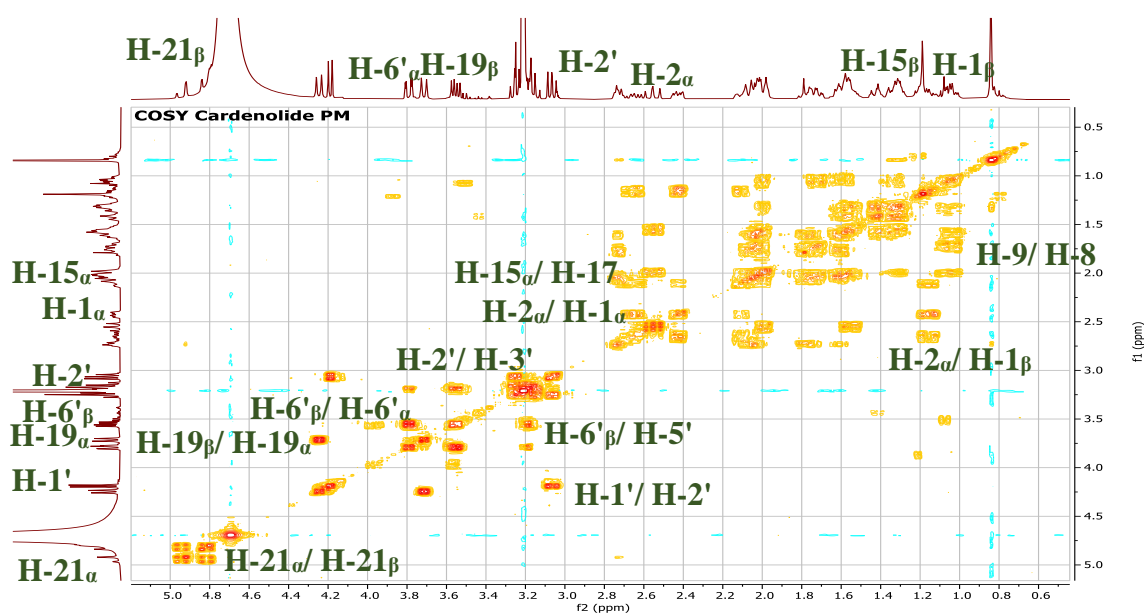


Figure III-B-103: COSY spectrum (400 MHz, CD₃OD) of compound PM

On the basis of above evidence, as well as the comparison with the literature, allowed us to attribute the structure of **3-oxo,19-O- β -D-glucopyranosylcoroglaucigenin** to compound PM, which is isolated for the first time as a new compound. Its structure is demonstrated in the Figure III-B-104:

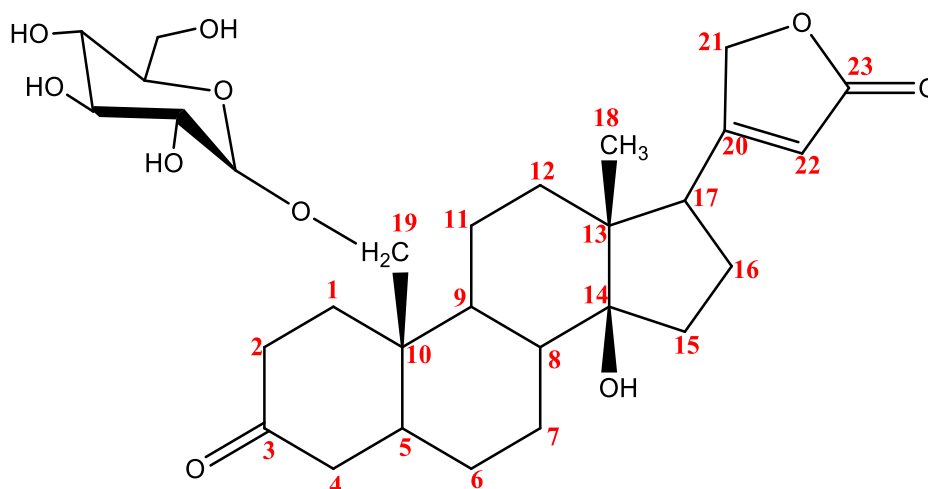


Figure III-B-104: chemical structure of compound PM which is a cardenolides glycoside named **3-oxo,19-O- β -D-glucopyranosylcoroglaucigenin**

III-B-3- Structural elucidation of phenolic compounds isolated from *P.tomentosa*

III-B-3-1-Compound PJ

Compound PJ was obtained as a yellow amorphous powder, its visible bright yellow color as well as its dark fluorescence under ultraviolet light (366 nm) suggest its flavonoid nature [123]. It takes also a yellow color after revelation with a vanillin sulphuric solution and heating. Its structure was characterized using UV-visible spectrophotometry and NMR spectroscopic analysis methods which are 1D: ^1H NMR and ^{13}C NMR and 2D: HSQC, HMBC and COSY. Its spectra are recorded in CD_3OD .

The spectral series of this compound (Figure III-B-103) was carried out by the UV-visible spectrophotometry using characteristic reagents [124], they show:

- The appearance of the band I in methanol at $\lambda_{\text{I}} = 348$ nm and the band II in methanol at $\lambda_{\text{II}} = 266$ nm indicates that this compound has a flavone or 3-substituted flavonol structure.

- A bathochromic shift of the band I of a $\Delta\lambda_I$ (NaOH/MeOH) = 53nm is observed without the decrease in the optical density, when a few drops of NaOH are added. That indicates the presence of OH group at the 4' position. As well as, the appearance of new band at $\lambda_I = 326$ nm indicates that position 7 has a free hydroxyl group. The stability of the spectrum after five minutes indicates the absence of a 3,4 dihydroxy system.
- The smaller bathochromic shift of the band I in NaOAc + H₃BO₃ spectrum compared to those in methanol spectrum [$\Delta\lambda_I$ (NaOAc + H₃BO₃ /MeOH) = 5nm] indicating the presence of ortho di OH group in A ring (6, 7 or 7, 8 di OH).
- The bathochromic shift of the band I in AlCl₃ spectrum compared to those in methanol spectrum [$\Delta\lambda_I$ (AlCl₃/MeOH) = 47nm] indicating the presence of OH group in position 5.

Table III-B-10: UV spectral series data (λ_{max} nm) of compound PJ

Reagents	Band I	Band II	New band
MeOH	348	266	/
NaOH	401	275	326
NaOH after 5 min	401	275	326
NaOAc + H ₃ BO ₃	353	266	/
AlCl ₃	395	274	/

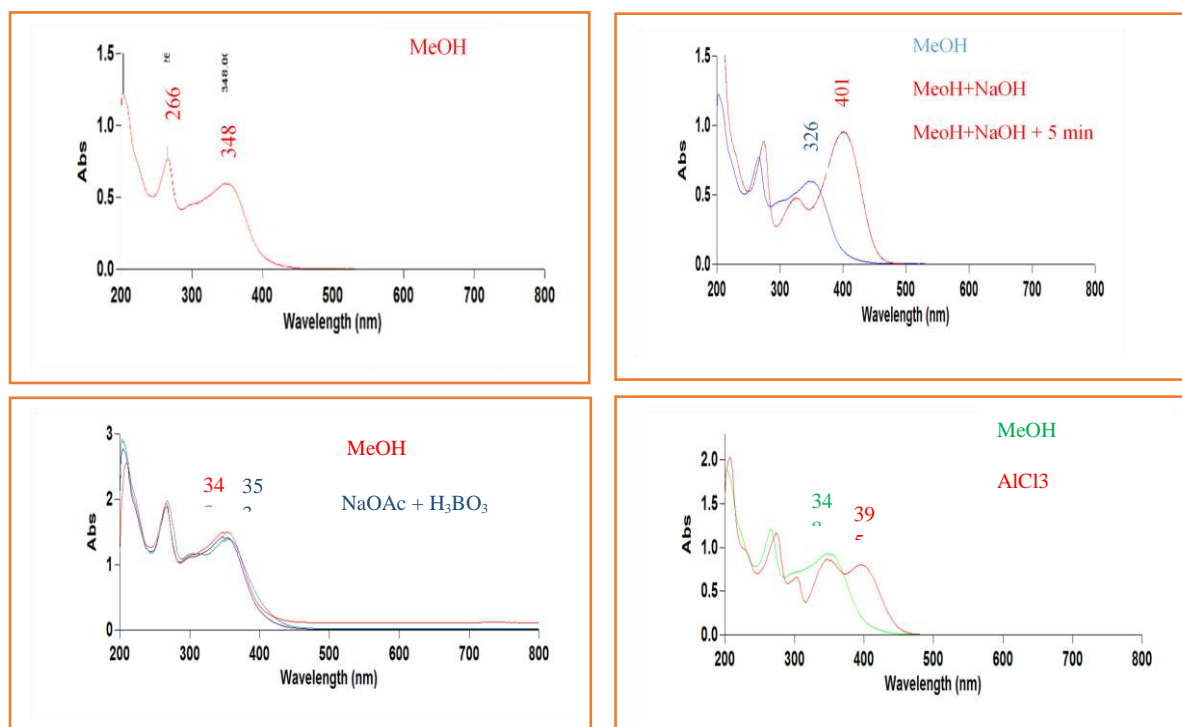


Figure III-B-105: The UV spectral series of compound PJ

- ❖ The ^1H NMR spectrum (Figure III-B-106) of compound PJ showed the presence of signals characteristic of a flavonoid glycoside skeleton which are:
 - Two doublet signals with an integration of two proton of each, at δ_{H} 8.00 and δ_{H} 6.85 with a coupling constant $J= 8.9$ Hz of each one, which assignable to four characteristic aromatic protons of a 4-monosubstituted B ring.
 - One doublet anomeric signal with an integration of one proton at δ_{H} 4.99 with a coupling constant $J= 7.5$ Hz. This coupling constant is characteristic of the β configuration.
 - Two doublet of doublet signals with an integration of one proton of each, at δ_{H} 3.67 and δ_{H} 3.54 with a coupling constant $J= 11.8; 2.4$ Hz and $J= 11.7; 5.2$ Hz, respectively.
 - One triplet signal with an integration of one proton at δ_{H} 3.41 with a coupling constant $J= 8.8$ Hz.
 - Two multiplet signals with an integration of one proton of each one at δ_{H} 3.45 and δ_{H} 3.18.

- One doublet signal with an integration of one proton at δ_{H} 3.35 with a coupling constant $J = 9.4$ Hz.

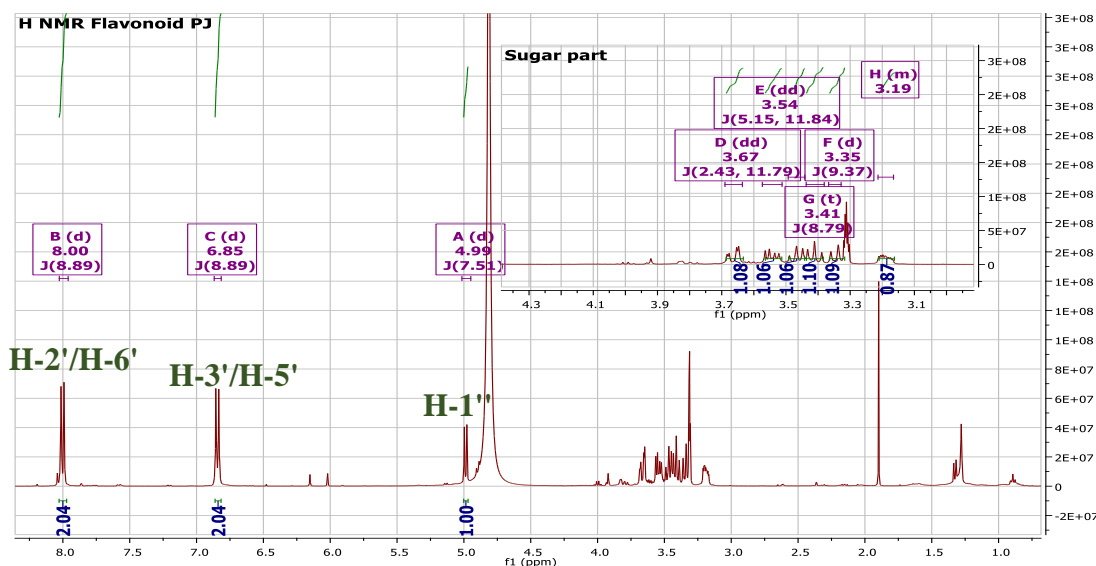


Figure II-B-106: ¹H NMR spectrum (400 MHz, CD₃OD) of compound PJ

- ❖ The ¹³C NMR spectrum (Figure III-B-107) of compound PJ showed the presence of typical signals of flavonoid aglycon part and the signals characteristic of sugar part. The type of each carbon was determined according to ¹³C DEPT (135 and 90) NMR spectra (Figure III-B-108 and III-B-109). These spectra showed:
 - Four aromatic carbon signals, each two of them are identical at δ_{C} 130.71 and δ_{C} 115.07.
 - Nine signals corresponding to quaternary carbons at δ_{C} 176.95, δ_{C} 174.71, δ_{C} 161.38, δ_{C} 160.93, δ_{C} 157.83, δ_{C} 156.55, δ_{C} 133.72, δ_{C} 120.93 and δ_{C} 101.37.
 - Five methine signals at δ_{C} 103.89, δ_{C} 76.85, δ_{C} 76.73, δ_{C} 74.22 and δ_{C} 69.90.
 - One methylene signal at δ_{C} 61.15.

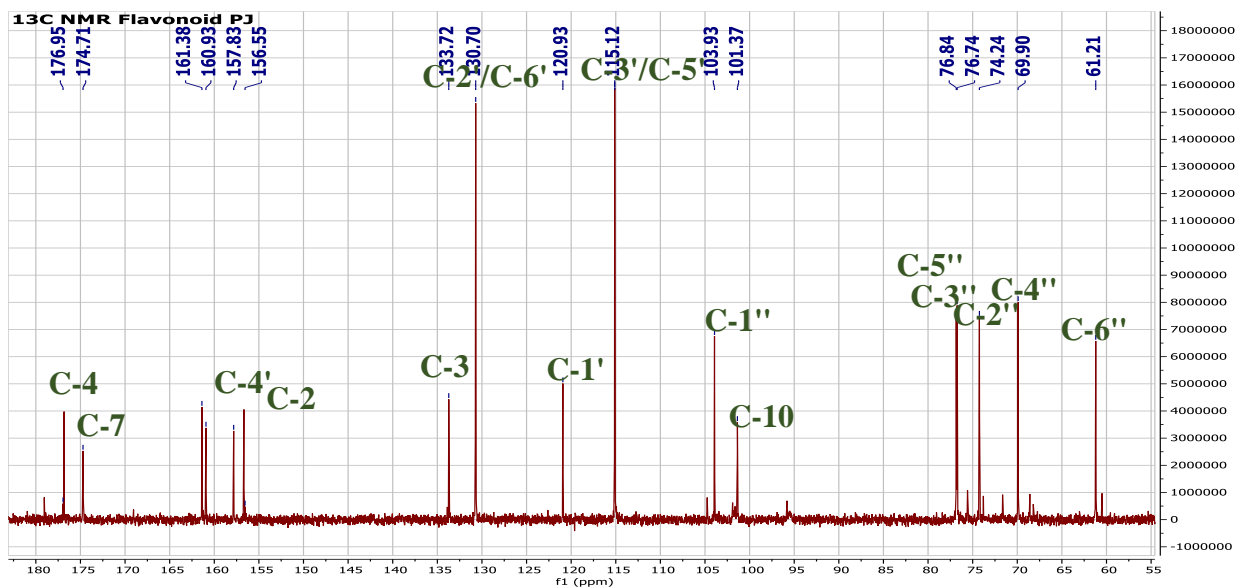


Figure III-B-107: ¹³C NMR spectrum (100 MHz, CD₃OD) of compound PJ

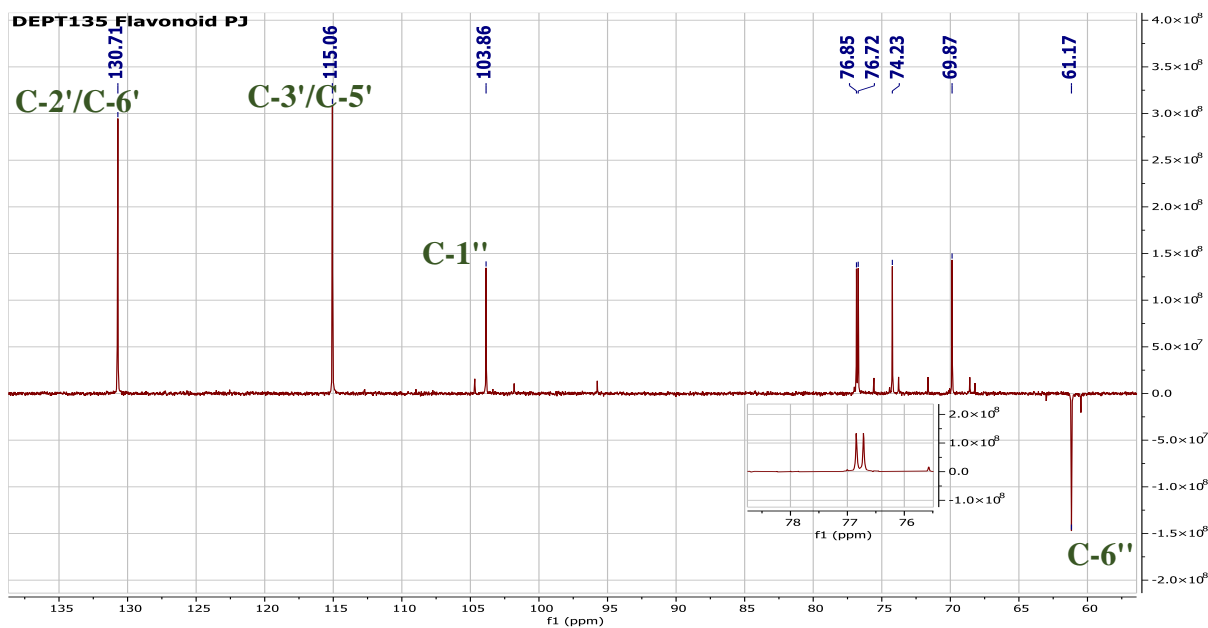


Figure III-B-108: ¹³C NMR DEPT 135 spectrum (100 MHz, CD₃OD) of compound PJ

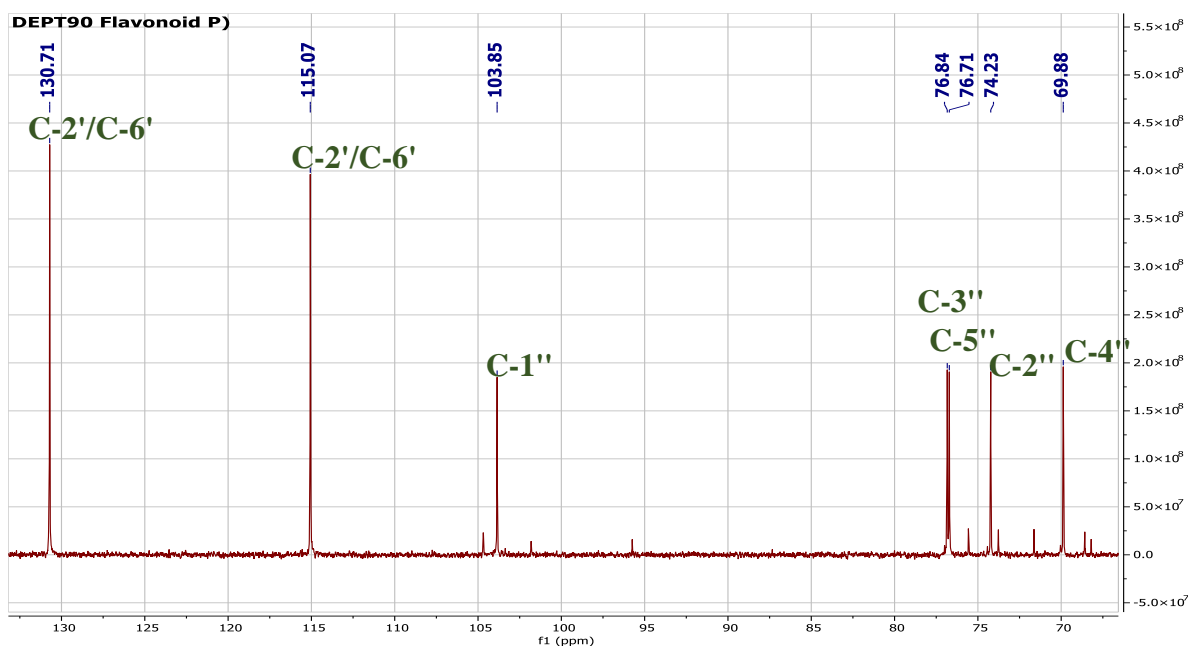


Figure III-B-109: ^{13}C NMR DEPT 90 spectrum (100 MHz, CD_3OD) of compound PJ

- ❖ Comparison of the ^1H and ^{13}C NMR spectra of compound PJ with those of literature, indicated that its structure was quite similar with that of **kaempferol-3-glucoside** compound [125]. The complete assignment of compound PJ was established using HSQC spectrum (Figure III-B-110-a and III-B-110-b) of this compound as well as the comparison of all ^1H and ^{13}C spectroscopic data of this compound with those of literature [125]. Table III-B-11 illustrate the chemical shifts of H and C of compound PJ.

Table III-B-11: Chemical shifts of ^1H (100 MHz) and ^{13}C (75 MHz) NMR in CD_3OD of compound PJ (δ in ppm and J in Hz)

Compound PJ		
Position	δ_{H}	δ_{C}
Typical signals of aglycon part		
2	-	156.55
3	-	133.72

Results and Discussion Part: Phytochemical Study of P.tomentosa

4	-	176.95
5	-	157.83
6	-	
7	-	174.71
8	-	
9	-	160.93
10	-	101.37
1'	-	120.93
2'	8 d (J 8.9 Hz)	130.71
3'	6.85 d (J 8.9 Hz)	115.07
4'	-	161.38
5'	6.85 (d; J= 8.9 Hz)	115.07
6'	8 (d; J= 8.9 Hz)	130.71
Typical signals of sugar part		
1''	4.99 (d; J= 7.5 Hz)	103.85
2''	3.45 (t; J= 8.8 Hz)	74.23
3''	3.35 (d; J= 9.4 Hz)	69.88
4''	3.18 (m)	76.84
5''	3.45 (m)	76.71
6''	3.54 (dd; J= 11.7; 5.2 Hz)	61.17
	3.67 (dd; J= 11.8; 2.4 Hz)	

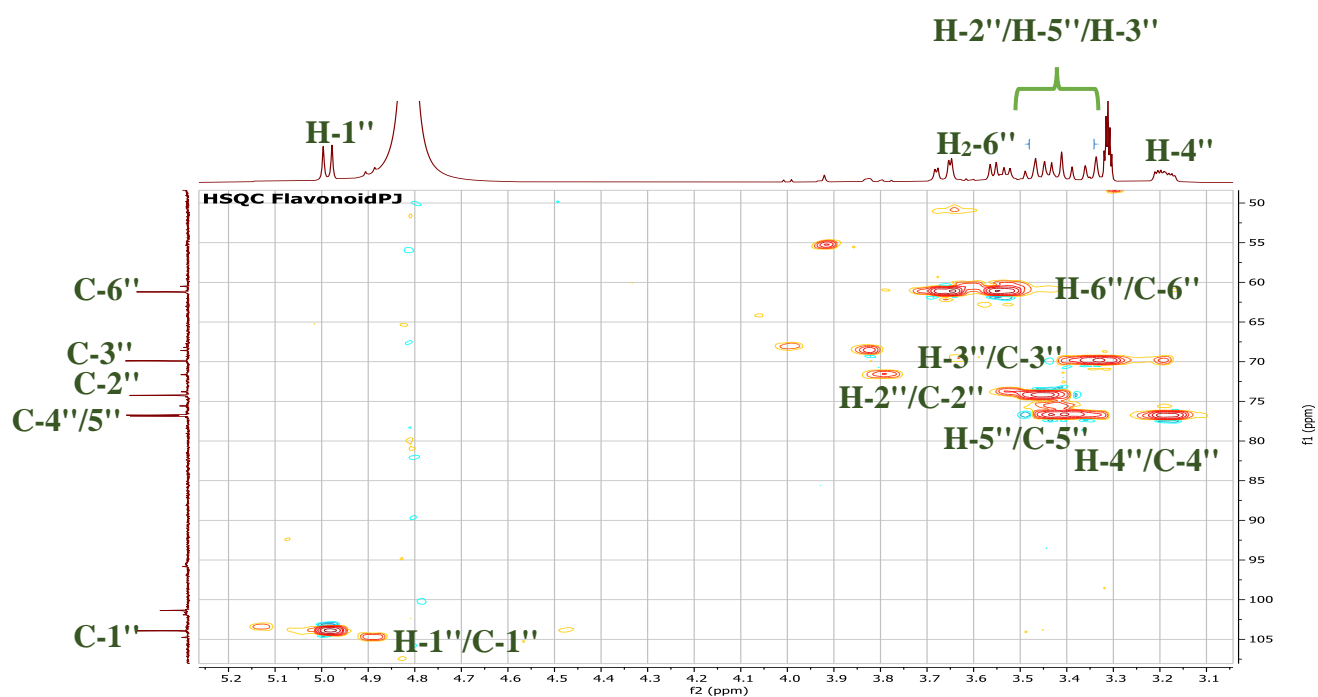


Figure III-B-110-a: HSQC expansions spectrum [5.2 – 2.1 ppm] (400 MHz, CD₃OD) of compound PJ

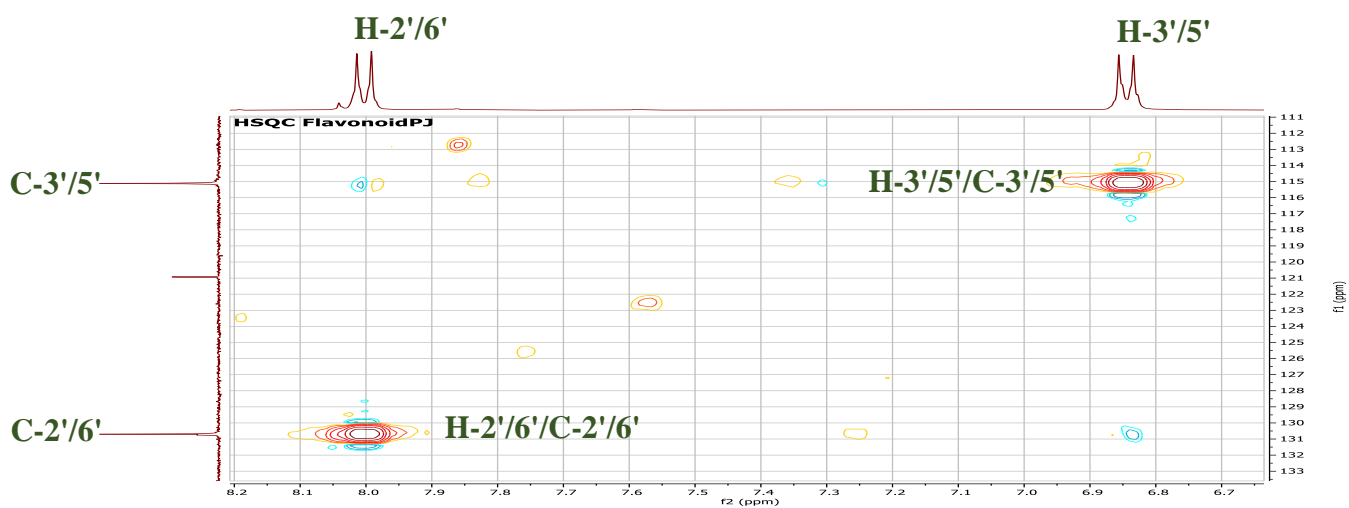


Figure III-B-110-b: HSQC expansions spectrum [8.2 – 6.7 ppm] (400 MHz, CD₃OD) of compound PJ

❖ In order to confirm the sequence of this flavonol skeleton as well as the attachment of the glucose unit at C-3 of this skeleton, HMBC experiment (Figure III-B-113) was studied. It recorded correlations between:

➤ H-2'/6' (δ_H 8.00) has correlated with:

- C-3'/5' (δ_C 115.07).
- C-2 (δ_C 156.55).
- C-4' (δ_C 161.38).

➤ H-3'/5' (δ_H 2.73) has correlated with:

- C-2'/6' (δ_C 130.71).
- C-1' (δ_C 120.93).
- C-4' (δ_C 161.38).

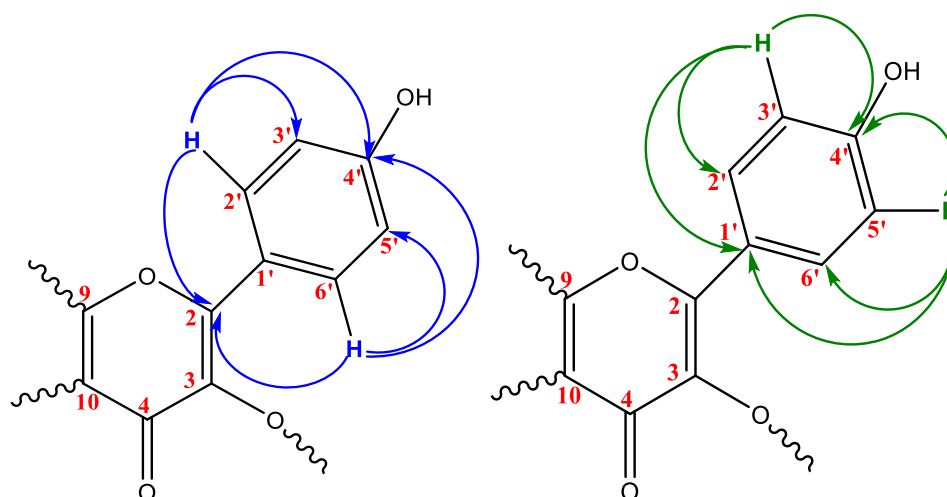


Figure III-B-111: correlation of H-2'/6' and H-3'/5' according to HMBC spectrum of compound PJ

➤ H-1'' (δ_H 4.99) has correlated with:

- C-3 (δ_C 133.72).
- C-5'' (δ_C 76.71).

➤ H-2'' (δ_H 3.45) has correlated with:

- C-1'' (δ_C 103.85).
- C-4'' (δ_C 76.84).

➤ H-4'' (δ_H 3.18) has correlated with:

- C-3'' (δ_C 69.88).
- H-3'' (δ_H 3.35) has correlated with:
 - C-5'' (δ_C 76.71).
 - C-6'' (δ_C 61.17).
- H-5'' (δ_H 3.41) has correlated with:
 - C-3'' (δ_C 69.88).
 - C-2'' (δ_C 74.23).
- H-6'' $_{\alpha}$ (δ_H 3.68) has correlated with:
 - C-3'' (δ_C 69.88).
 - C-5'' (δ_C 76.71).
- H-6'' $_{\beta}$ (δ_H 3.55) has correlated with:
 - C-3'' (δ_C 69.88).

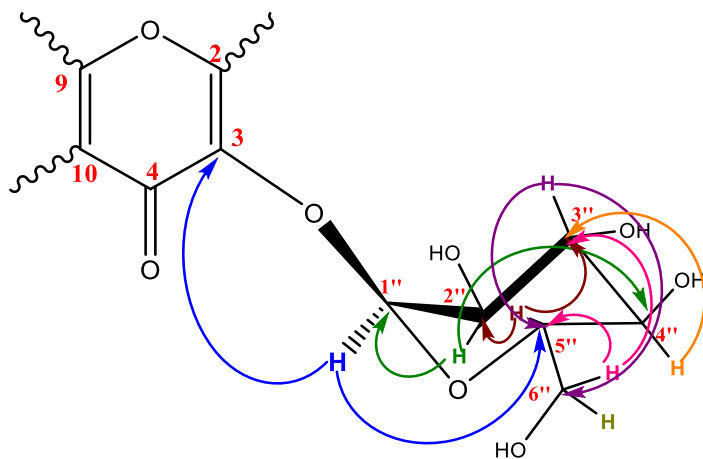


Figure III-B-112: correlation of protons of sugar part according to HMBC spectrum of compound PJ

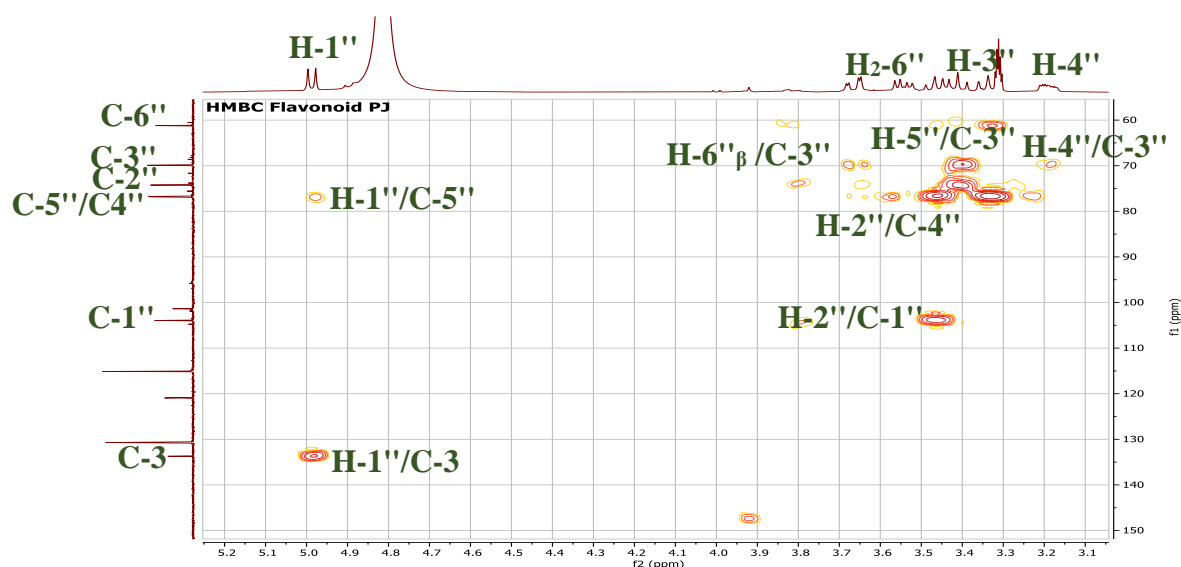


Figure III-B-113-a: HMBC spectrum [5.2 – 3.1 ppm] (400 MHz, CD₃OD) of compound PJ

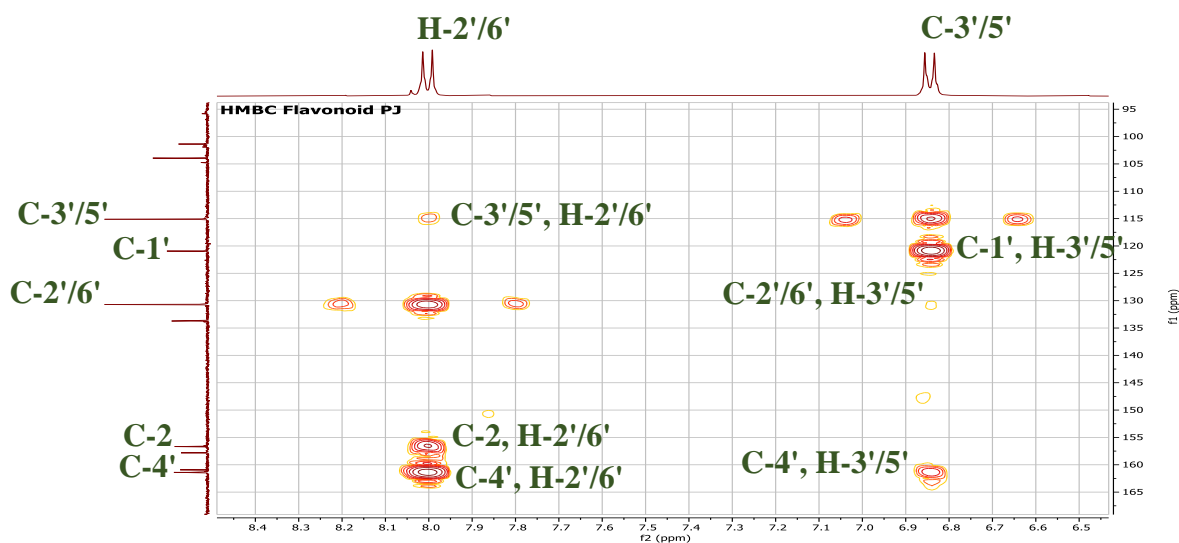


Figure III-B-113-b: HMBC spectrum [8.4 – 6.5 ppm] (400 MHz, CD₃OD) of compound PJ

❖ COSY experiment (Figure III-B-115-a and III-B-115-b) was used to confirm the sequence of sugar unit and aromatic protons, it shows the correlation spots between each vicinal H, that are:

- H-2',6' (δ_H 8.00) correlated with H-3',5' (δ_H 6.85).

- H-1'' (δ_H 4.99) correlated with H-2'' (δ_H 3.45).
- H-3'' (δ_H 3.35) correlated with H-4'' (δ_H 3.18).
- H-4'' (δ_H 3.18) correlated with H-6'' $_{\alpha}$ (δ_H 3.67).
- H-4'' (δ_H 3.18) correlated with H-6'' $_{\beta}$ (δ_H 3.54).

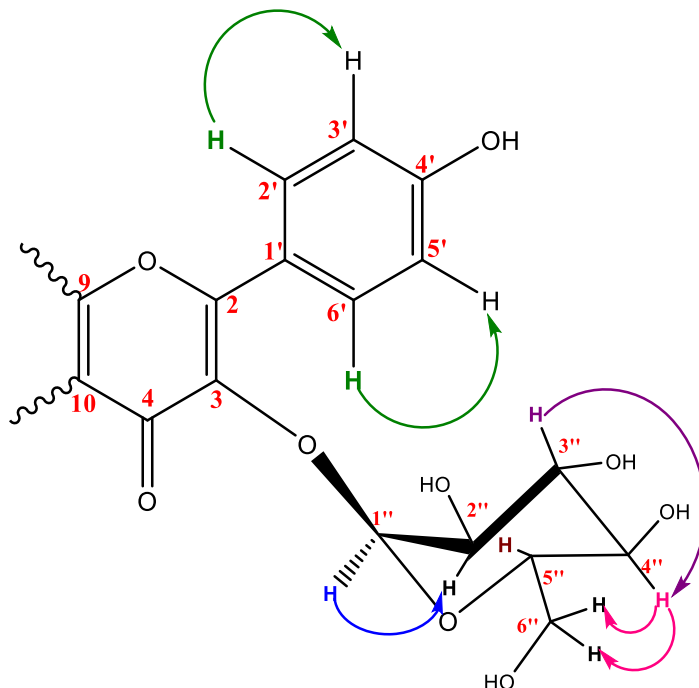


Figure III-B-114: COSY correlations of aromatic and sugar protons of compound PJ

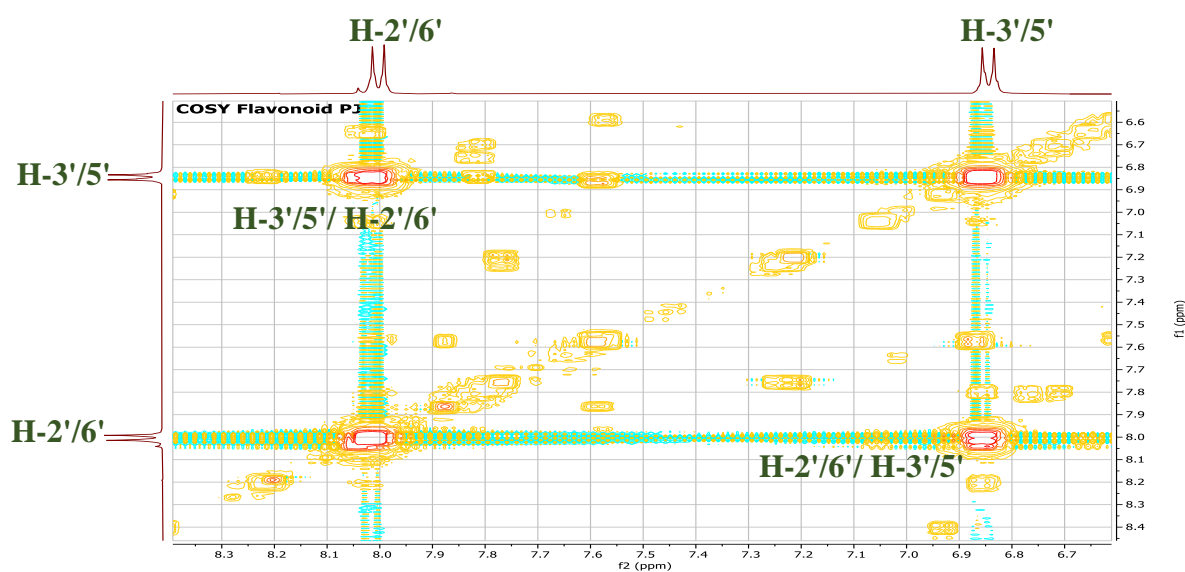


Figure III-B-115-a: COSY spectrum [8.3 – 6.7 ppm] (400 MHz, CD₃OD) of compound PJ

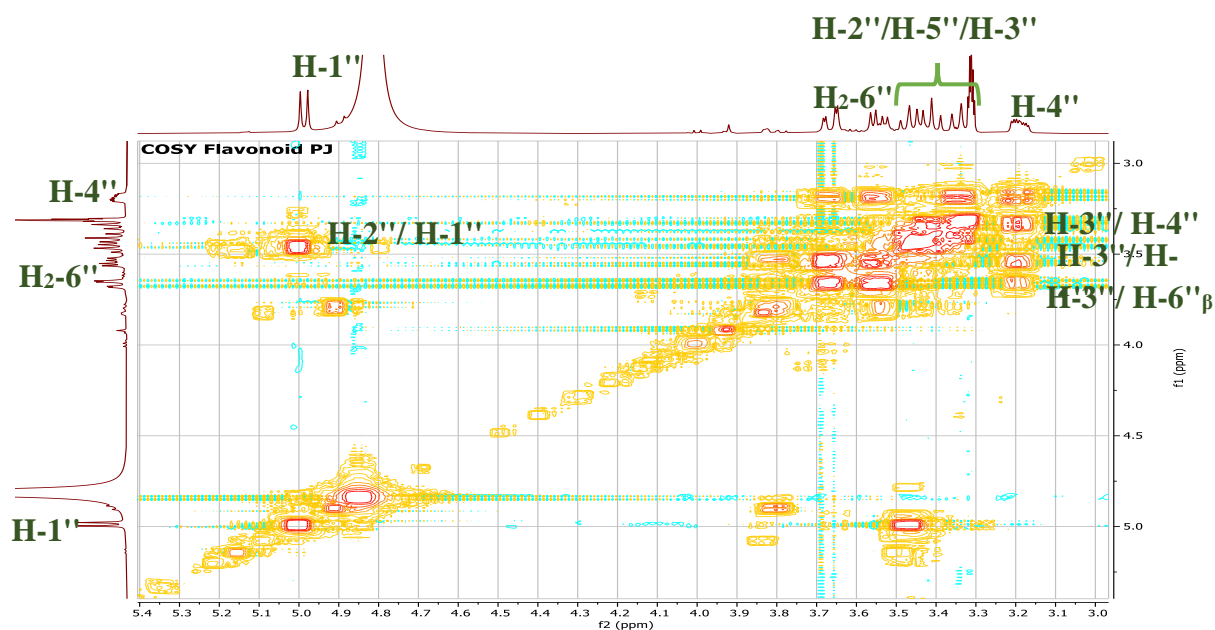


Figure III-B-115-b: COSY spectrum [5.4 – 3.0 ppm] (400 MHz, CD₃OD) of compound PJ

All these spectral data as well as the comparison with the literature [125] allowed us to attribute the structure of **6,8-dihydroxyKaempferol-3-O-β-glucopyranosyl** to compound PJ, which is isolated for the first time as a new compound from *P. tomentosa*. Its chemical structure is illustrated in figure III-B-116:

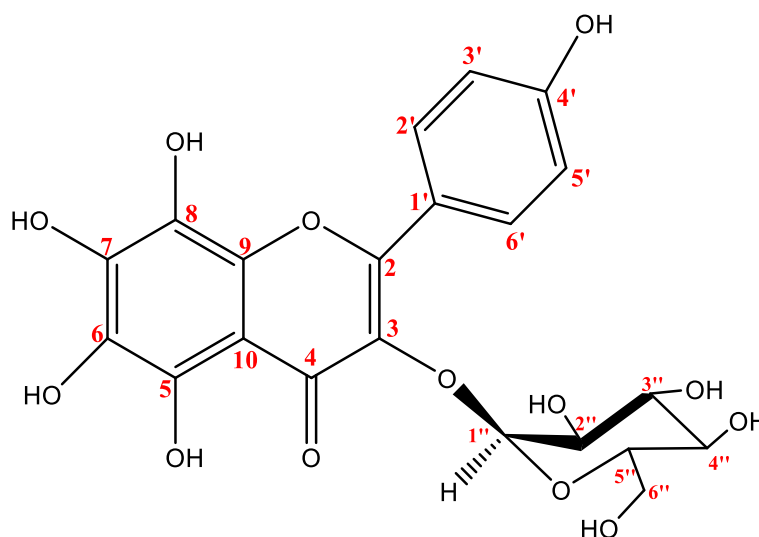


Figure III-B-116: Chemical structure of compound PJ, which is a flavonoid named **6,8-dihydroxyKaempferol-3-O-β-glucopyranosyl**

III-B-3-2-Compound PR

Compound PR was obtained as a colorless amorphous; it takes a red color after revelation with a vanillin sulphuric solution and heating. Its structure was characterized using NMR spectroscopic analysis methods, which are 1D: ^1H NMR and ^{13}C NMR and 2D: HSQC, HSQC-TOCSY, HMBC and COSY. Its spectra recorded in CD_3OD .

- ❖ The ^1H NMR spectrum (Figure III-B-117) of compound PR showed:
 - Two doublet and one doublet of doublet signals with an integration of one proton of each, at δ_{H} 6.66 and δ_{H} 6.61 and δ_{H} 6.50 with a coupling constant $J= 2.65$ Hz, $J= 8.64$ Hz and $J= 8.64; 2.68$ Hz, respectively. These signals are assignable to three characteristic aromatic protons.
 - Two doublet anomeric signals with an integration of one proton at δ_{H} 4.87 and δ_{H} 4.61 with a coupling constant $J= 2.47$ Hz and $J= 7.37$ Hz, respectively. These coupling constants is characteristic of α and β configuration, respectively.
 - The signals corresponding to two no-equivalent protons of CH_2 groups which are:
 - ✓ Two doublet of doublet signals with an integration of one proton of each, at δ_{H} 3.91 and δ_{H} 3.50 with a coupling constant $J= 11.07; 1.61$ Hz and $J= 11.91; 5.28$ Hz, respectively.
 - ✓ Two doublet signals with an integration of one proton of each, at δ_{H} 3.85 and δ_{H} 3.65 with a coupling constant $J= 9.65$ Hz and $J= 9.66$ Hz.
 - Seven multiplet signals with an integration of one proton of each, at δ_{H} 3.55, δ_{H} 3.96, δ_{H} 3.80, δ_{H} 3.25, δ_{H} 3.44, δ_{H} 3.30 and δ_{H} 3.31.
 - One broad singlet signal with an integration of two proton at δ_{H} 3.47.
 - One singlet methoxy signal at δ_{H} 3.74.
 - One doublet methyl signal at: δ_{H} 1.24 with a coupling constant $J= 6.77$.

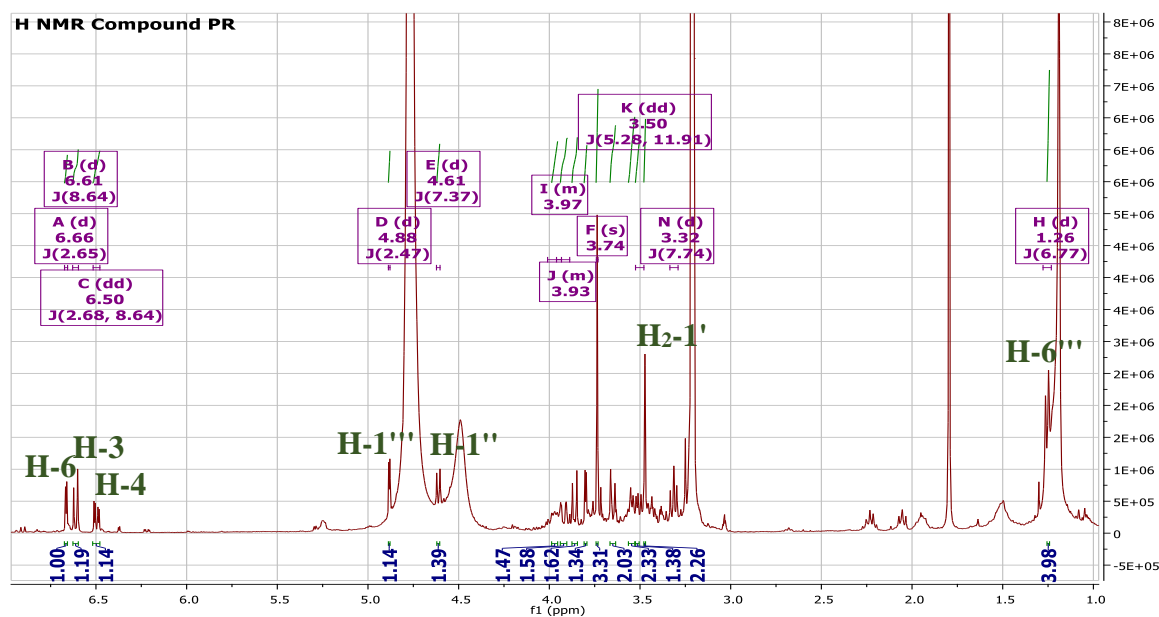


Figure III-B-117: ^1H NMR spectrum (400 MHz, CD_3OD) of compound PR

❖ The ^{13}C NMR spectrum (Figure III-B-118) of compound PR showed the presence of 21 carbon signals, 12 signals of them are typical signals of two sugar units. The type of each carbon was determined according to ^{13}C DEPT (135 and 90) NMR spectra (Figure III-B-119 and III-B-120). These spectra showed:

- Three aromatic carbon signals at δ_{C} 114.70, δ_{C} 108.71 and δ_{C} 102.60.
- Teen methine signals at δ_{C} 109.56, δ_{C} 102.40, δ_{C} 76.62, δ_{C} 76.56, δ_{C} 75.52, δ_{C} 73.56, δ_{C} 70.25, δ_{C} 69.77, δ_{C} 69.77 and δ_{C} 68.34.
- Three methylene signal at δ_{C} 73.56, δ_{C} 67.37 and δ_{C} 64.12.
- One methoxy signal at δ_{C} 55.10.
- One methyl signal at: δ_{C} 19.82.
- Three signals corresponding to quaternary carbons at δ_{C} 168.94, δ_{C} 151.37 and δ_{C} 147.85.

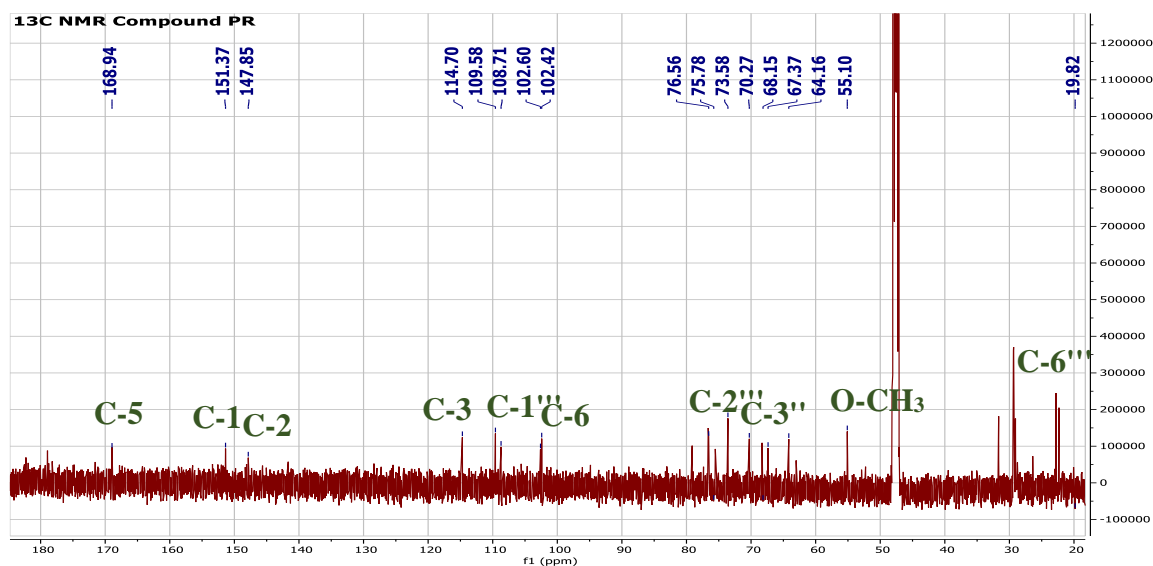


Figure III-B-118: ¹³C NMR spectrum (150 MHz, CD₃OD) of compound PR

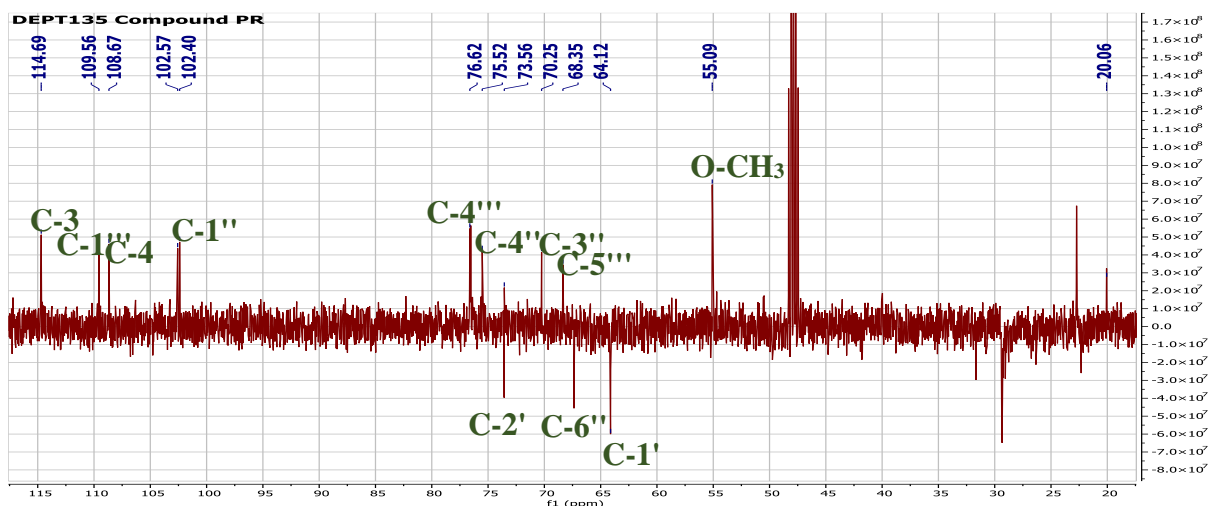


Figure III-B-119: ¹³C NMR DEPT 135 spectrum (100 MHz, CD₃OD) of compound PR

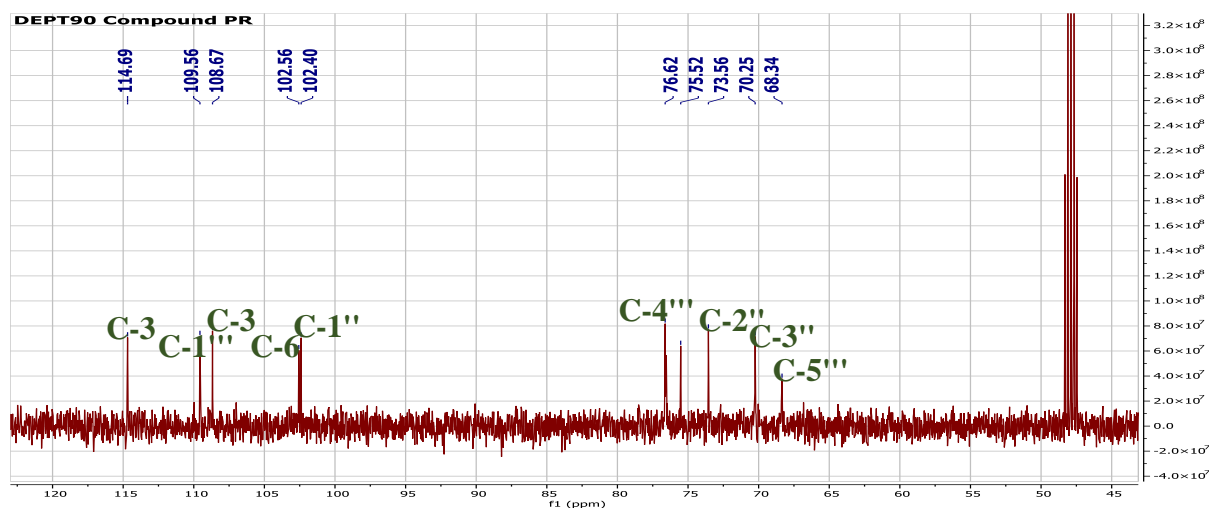


Figure III-B-120: ^{13}C NMR DEPT 90 spectrum (100 MHz, CD_3OD) of compound PR

- Both of ^1H NMR and ^{13}C NMR spectra of this compound confirmed its phenolic nature. They showed characteristic signals of phenol ring which are: two doublet aromatic signals at δ_{C} 6.66 and δ_{C} 6.61 and one doublet of doublet signal at δ_{C} 6.50, as well as, three quaternary aromatic carbon signals at δ_{C} 168.94, δ_{C} 151.37 and δ_{C} 147.85.
 - The presence of two anomeric proton signals at δ_{H} 4.87 and δ_{H} 4.61, in addition of ten carbon signals in the region of sugar carbons in ^{13}C NMR spectrum, indicated the presence of two sugar units linked to phenol ring.
 - The presence of doublet anomeric signal at δ_{H} 4.87 with small coupling constant ($J=2.47$ Hz), in addition of the doublet methyl signal proton at δ_{H} 1.24 with coupling constant $J=6.77$ Hz, confirmed that one of the two sugar units is an α -L-rhamnopyranoside unit.
 - The presence of doublet anomeric signal at δ_{H} 4.61 with coupling constant $J=7.37$ Hz, in addition of the two doublet of doublet signals proton at δ_{H} 3.91 and δ_{H} 3.50, confirmed that the other sugar unit is an β -D-glucopyranoside unit.
- ❖ The assignment of all protons to their corresponding carbons of compound PR was established using HSQC spectrum (Figure III-B-121-a and III-B-121-b) of this compound. Table III-B-12 illustrate the chemical shifts of H and C of compound PR

Table III-B-12: Chemical shifts of ^1H (400 MHz) and ^{13}C (150 MHz) NMR in CD_3OD of compound PR (δ in ppm and J in Hz)

Compound PR		
Position	δ_{H}	δ_{C}
Typical signals of aglycon part		
1	-	151.37
2	-	147.85
3	6.61 (d/J= 8.64 Hz)	114.70
4	6.50 (dd/J= 8.64; 2.68 Hz)	108.71
5	-	168.94
6	6.66 (d/J= 2.65 Hz)	102.60
O-CH₃	3.74	55.10
1'	3.47 (br)	64.12
2'	3.85 (d/J= 9.65 Hz)	73.56
	3.65 (d/J= 9.66 Hz)	
Typical signals of sugar part		
1''	4.61 (d/J= 7.37 Hz)	102.40
2''	3.30 (m)	73.56
3''	3.25 (m)	70.25
4''	3.44 (m)	75.52
5''	3.55 (m)	69.77
6''	3.91 (dd/J= 11.07; 1.61 Hz)	67.37
	3.65 (dd/J= 11.91; 5.28 Hz)	
1'''	4.87 (d/J= 2.47 Hz)	109.56
2'''	3.80 (m)	76.62
3'''	3.55 (m)	69.77

4'''	3.31 (m)	76.56
5'''	3.96 (m)	68.34
6'''	1.24 (d/J= 6.77 Hz)	19.82

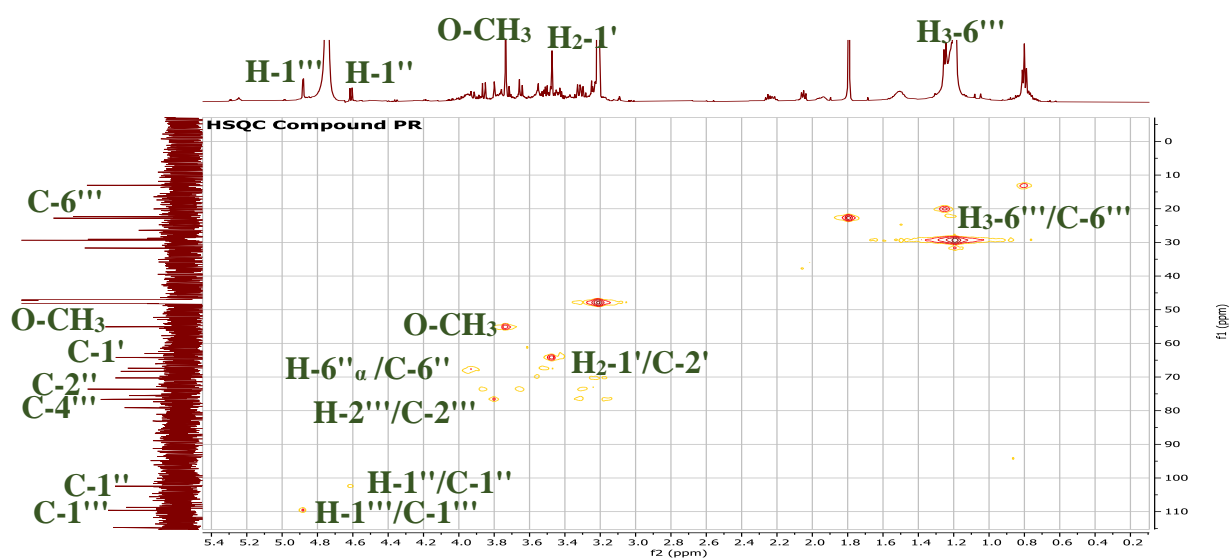


Figure III-B-121-a: HSQC spectrum [5.4 – 0.2 ppm] (600 MHz, CD₃OD) of compound PR

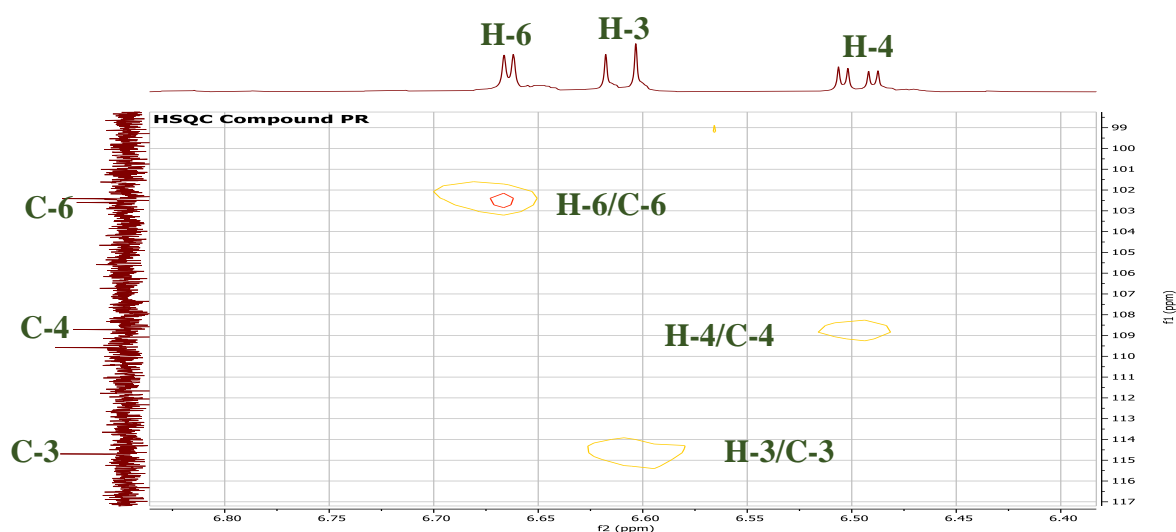


Figure III-B-121-b: HSQC spectrum [6.8 – 6.4 ppm] (600 MHz, CD₃OD) of compound PR

- ❖ In order to confirm the sequence of both phenolic skeleton and the two sugar units, as well as the attachment of the substituents on phenolic ring, HMBC, COSY and HSQC-TOCSY spectra were studied.
- ✓ HSQC-TOCSY experiment is used to identify superimposable osidic protons. From a given osidic carbon, all the protons of the same sugar can be assigned. In the case of this compound, the HSQC-TOCSY spectrum (Figure III-B-124-a and III-B-124-b) also allowed us to determine the attachment of the α -L-rhamnopyranoside unit to the phenolic ring. The correlation between H-3 (δ_H 6.61), C-6 (δ_C 102.60) and H-4'' (δ_H 3.31), indicates that the hydroxyl of the 4'' position is linked to C-1 position of the phenolic ring. HSQC-TOCSY spectrum it also recorded a correlation spots between:
 - H-3 (δ_H 6.61 ppm) has correlated with:
 - C-4 (δ_C 108.71).
 - H-4 (δ_H 6.50) has correlated with:
 - C-3 (δ_C 114.70).

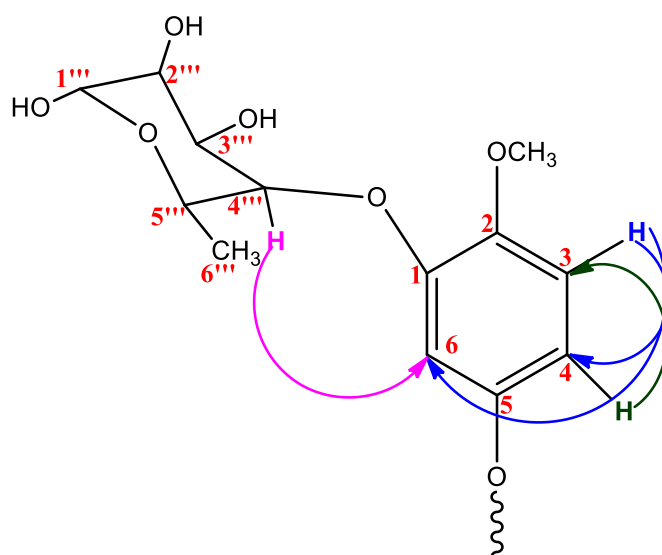


Figure III-B-122: HSQC-TOCSY correlation of H-3, H-4, H-6 and H-4'' of compound PR

- H-2'' (δ_H 3.30) has correlated with:
 - C-4'' (δ_C 75.52).
- H-1''' (δ_H 4.87) has correlated with:
 - C-2''' (δ_C 76.62).
- H₃-6''' (δ_H 1.24) has correlated with:

- C-5''' (δ_c 68.34).

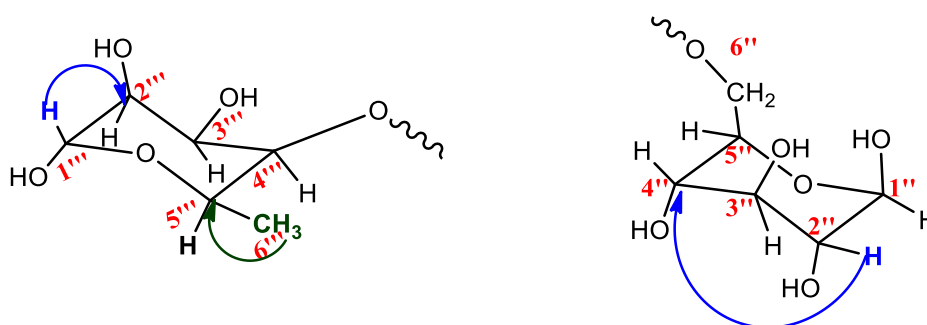


Figure III-B-123: HSQC-TOCSY correlation of the sugar part of compound PR

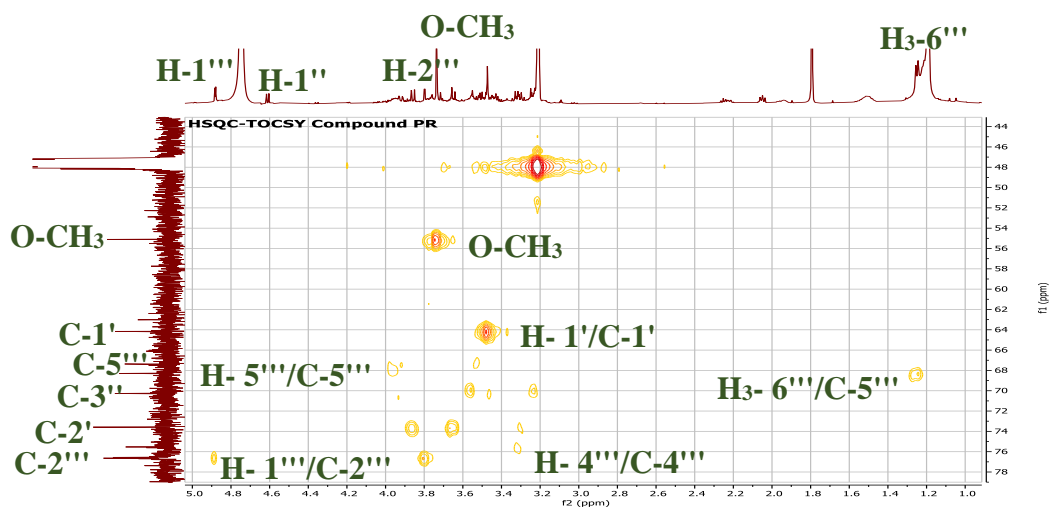


Figure III-B-124-a: HSQC-TOCSY expansion spectrum [5.0 -1.0 ppm] (600 MHz, CD₃OD) of compound PR

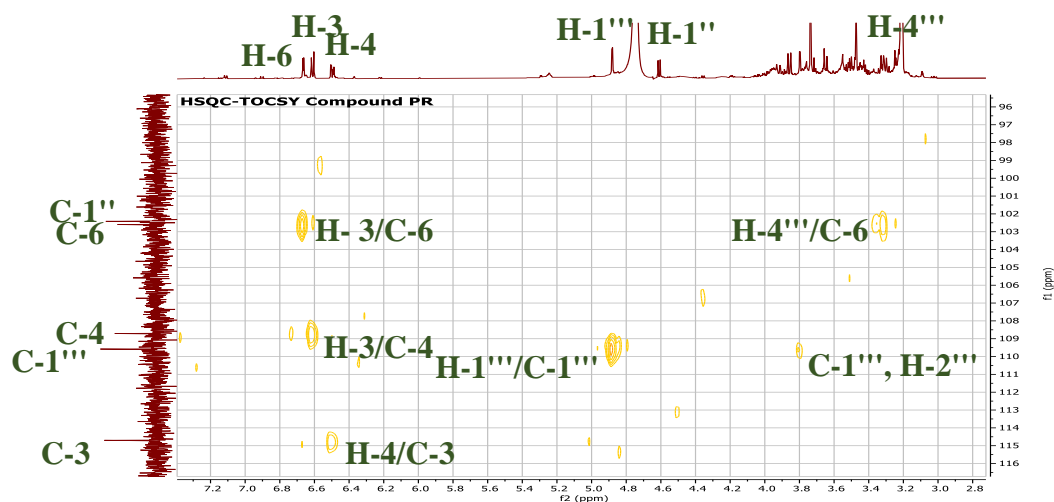


Figure III-B-124-b: HSQC-TOCSY expansion spectrum [7.2 – 2.8 ppm] (600 MHz, CD₃OD) of compound PR

- ✓ The attachment of methoxy group (O-CH₃) at C-2 position of phenolic ring is confirmed using HMBC spectrum (Figure III-B-126), which recorded a correlation spots between C-2 (δ_C 147.85) and both of O-CH₃ (δ_H 3.74) and H-3 (δ_H 6.61).

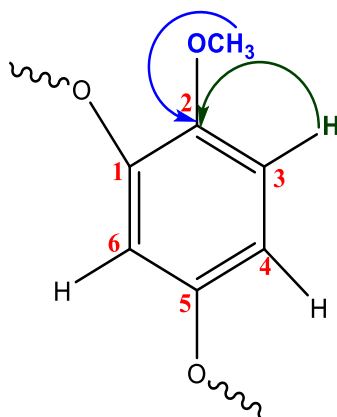


Figure III-B-125: HMBC correlation of H-3 and OCH₃ of compound PR

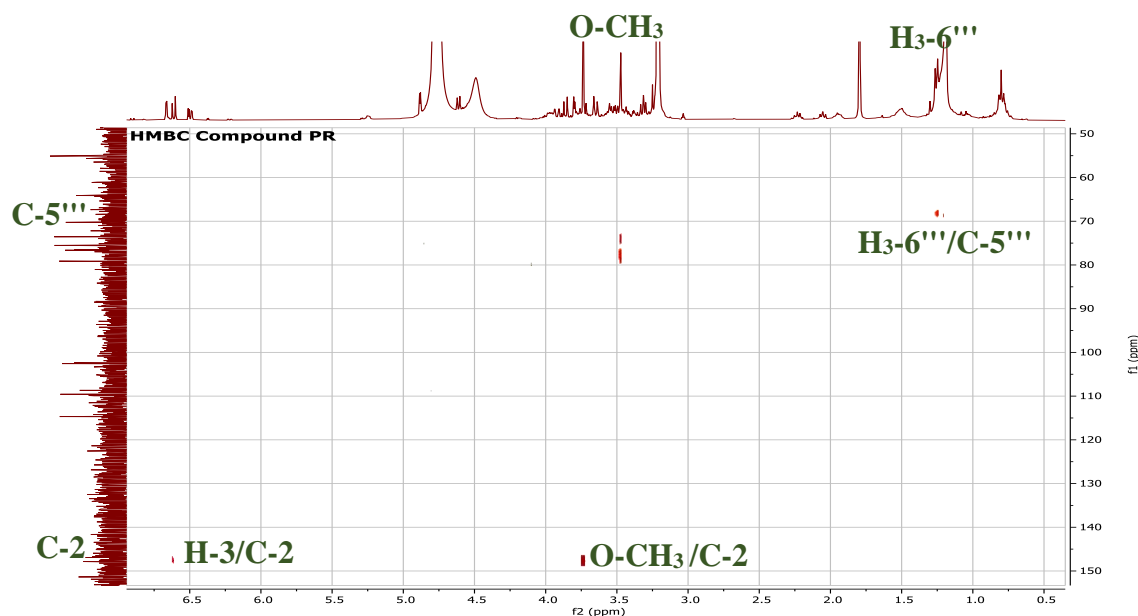


Figure III-B-126: HMBC spectrum (400 MHz, CD₃OD) of compound PR

- ✓ The attachment of C-1' at C-2' is confirmed using COSY spectrum (Figure III-B-129), which recorded correlation spot between H-1' (δ_H 3.47) and H-2' $_{\alpha}$ (δ_H 3.85).
The linkage of β -D-glucopyranoside unit at hydroxyethoxy group (C-1'-C-2'), is confirmed by correlation spot that shown in COSY spectrum between H-6'' $_{\alpha}$ (δ_H 3.91) and H-2' $_{\beta}$ (δ_H 3.65). In the other hand, chemical shift of C-6'' was shifted downfield (δ_C 67.37) which indicate a linked -CH₂OH group of this sugar.
The correlation spot between H-2' $_{\alpha}$ (δ_H 3.85) and H-2' $_{\beta}$ (δ_H 3.65) is also shown in this COSY spectrum.

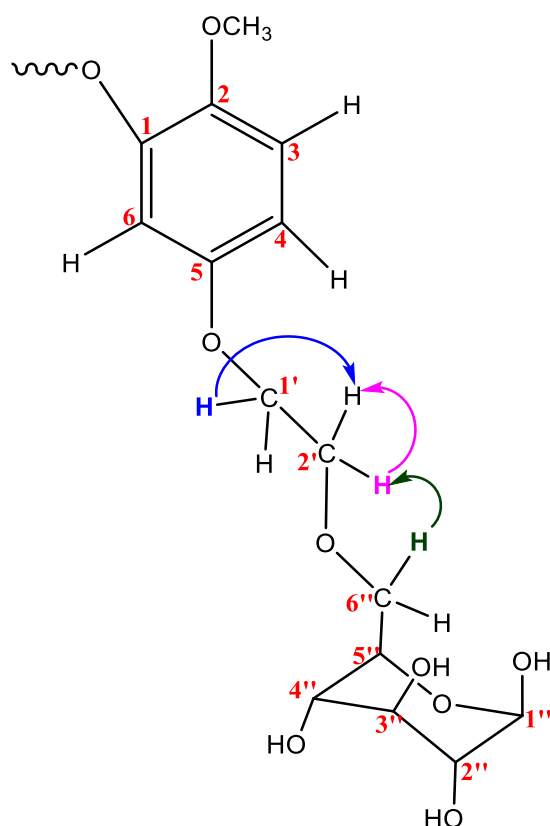


Figure III-B-127: COSY correlation of H-1', H-2' and H-6'' of compound PR

COSY spectrum is also used to confirm the sequence of the two sugar units, it shows the correlation spots between each vicinal protons, which are:

- Correlation spots corresponding to β -D-glucopyranoside unit which are:
 - H-1'' (δ_{H} 4.61) correlated with H-2'' (δ_{H} 3.30).
 - H-2'' (δ_{H} 3.30) correlated with H-3'' (δ_{H} 3.25).
 - H-4'' (δ_{H} 3.44) correlated with H-5'' (δ_{H} 3.55).
 - H-5'' (δ_{H} 3.55) correlated with H-6'' $_{\alpha}$ (δ_{H} 3.91).
 - H-5'' (δ_{H} 3.55) correlated with H-6'' $_{\beta}$ (δ_{H} 3.50).
 - H-6'' $_{\alpha}$ (δ_{H} 3.91) correlated with H-6'' $_{\beta}$ (δ_{H} 3.50).
- Correlation spots corresponding to α -L-rhamnopyranoside unit which are:
 - H-1''' (δ_{H} 4.87) correlated with H-2''' (δ_{H} 3.80).
 - H-2''' (δ_{H} 3.80) correlated with H-3''' (δ_{H} 3.55).
 - H-5''' (δ_{H} 3.96) correlated with H-6''' (δ_{H} 1.24).

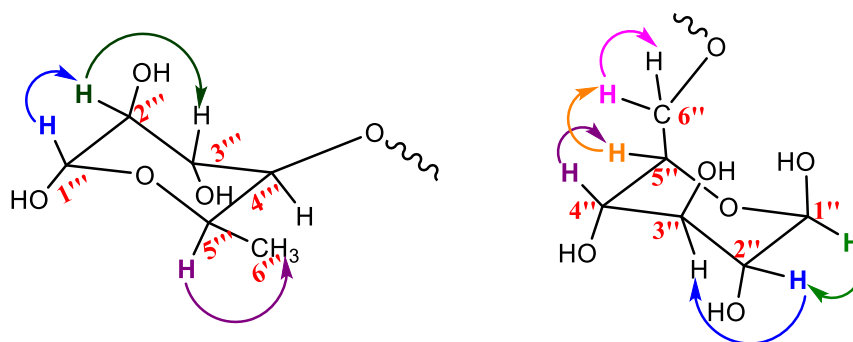


Figure III-B-128: COSY correlation of sugar part of compound PR

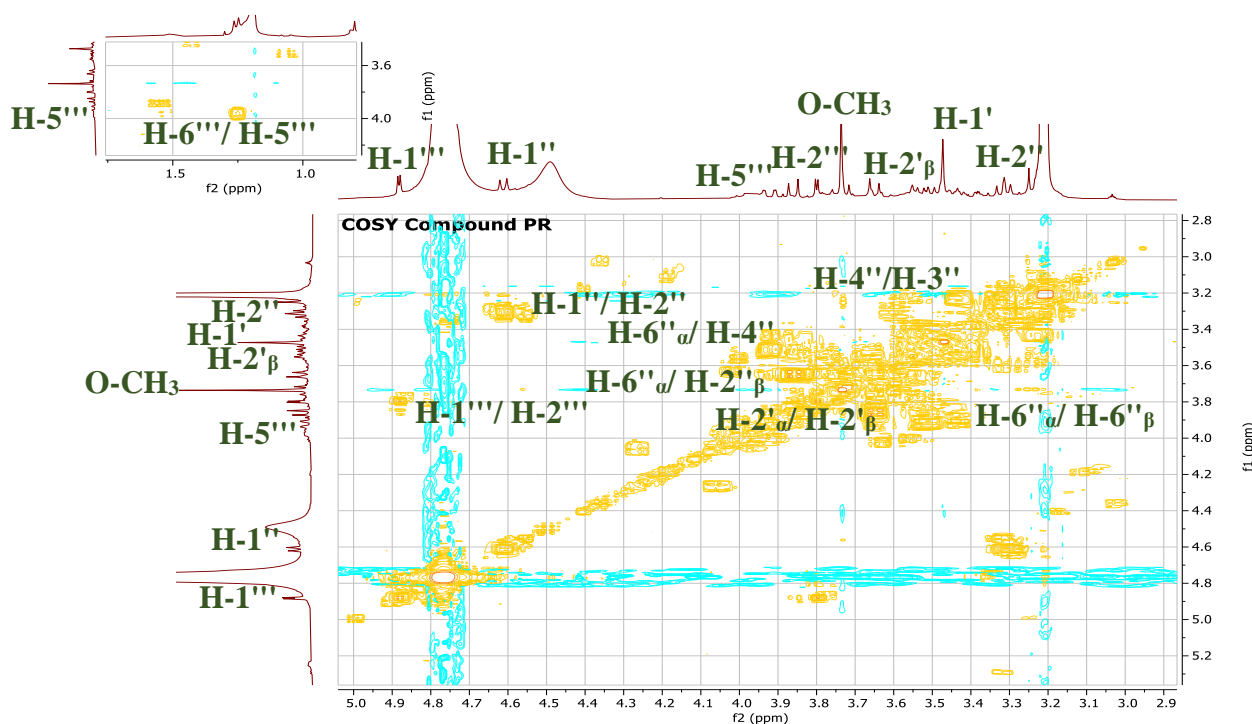


Figure III-B-129: COSY spectrum (400 MHz, CD₃OD) of compound PR

All these spectral data allowed us to attribute the structure of **5-[(2-O-β-glucopyranosyl)ethoxy]-2-methoxy-phenol-O-α-rhamnopyranosyl** to compound PR, which is isolated for the first time as a new compound from *P. tomentosa*. Its chemical structure is illustrated in figure III-B-130:

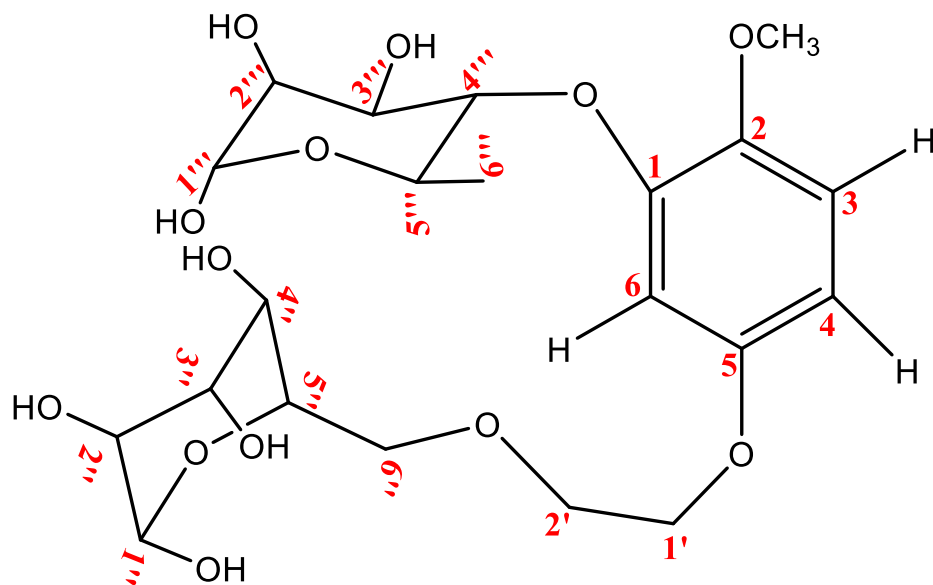


Figure III-B-130: chemical structure of compound PR, which is a phenolic compound named 5-[(2-O- β -glucopyranosyl)ethoxy]-2-methoxy-phenol-O- α -rhamnopyranosyl

General conclusion

General conclusion

Our research is principally devoted to the phytochemical investigation and the biological evaluation of the species found in the Algerian Sahara. In continuation with this context, our work aims to discover and characterize novel compounds of a plant from the Sahara of Algeria named *Pergularia tomentosa*.

The Phytochemical analysis of leaves and stems extracts of *P. tomentosa* showed that this plant contains various secondary metabolites such as cardenolides, alkaloids, flavonoids, saponins, steroids, tannins etc. The quantitative study of the different leaves and stems extracts using colorimetric methods, showed that both leaves and stems extracts contain a significant content of phenolics, flavonoids and tannins. In stems extracts, the highest phenolic content is recorded in chloroform extract (TPC= 0.2246 ± 0.002 mg GAE/g of plant dry weight) and the highest flavonoid and tannin content are recorded in butanol extract (TFC= 0.1249 ± 0.00127 mg QE/g of plant dry weight and TTC= 0.133 ± 0.0211 mg CE/g of plant dry weight). In leaves extracts, the highest phenolic and flavonoid content are recorded in n-butanol extract (TPC= 0.5343 ± 0.045 mg GAE/g of plant dry weight and TFC= 0.1249 ± 0.00127 mg QE/g of plant dry weight) and the highest tannin content is recorded in aqueous extract (TTC= 0.436 ± 0.0046 mg CE/g of plant dry weight). In order to measure *in vitro* antioxidant activity of the different stems and leaves extracts, reducing power assay and DPPH test were employed. According the stems extracts, ethyl acetate extract has the best antiradical activity with $IC_{50} = 0.205 \pm 0.02$ mg/mL. As well as, the best reducing capacity is recorded in the n-butanol extract with $AEAC = 72.48 \pm 8.62$ mM. In the other hand, regarding the leaves extracts, ethyl acetate extract has the best antiradical activity with $IC_{50} = 0.05 \pm 0.02$ mg/mL. Furthermore, the best reducing capacity is recorded in the aqueous extract with $AEAC = 265.85 \pm 8.09$ mM. The *in vitro* investigation of anti-diabetic activity of some leaves and stems extracts, showed that the ethyl acetate stems extract of *P. tomentosa* has strong capacity to inhibit α -amylase enzyme with inhibition percentage estimated 36.44 %.

In order to evaluate some *in vivo* biological activity of *P. tomentosa*, acute toxicity, anti-inflammatory and sedative activities of both the aqueous and crude extracts were performed on male and female albino mice. Oral administration of the both aqueous and crude extracts

General Conclusion

of *P. tomentosa* did not exhibit any symptoms of intoxication in all animals treated with a single dose of 2000 mg/kg. Thus, the LD₅₀ of these extracts was greater than 2000 mg/kg.

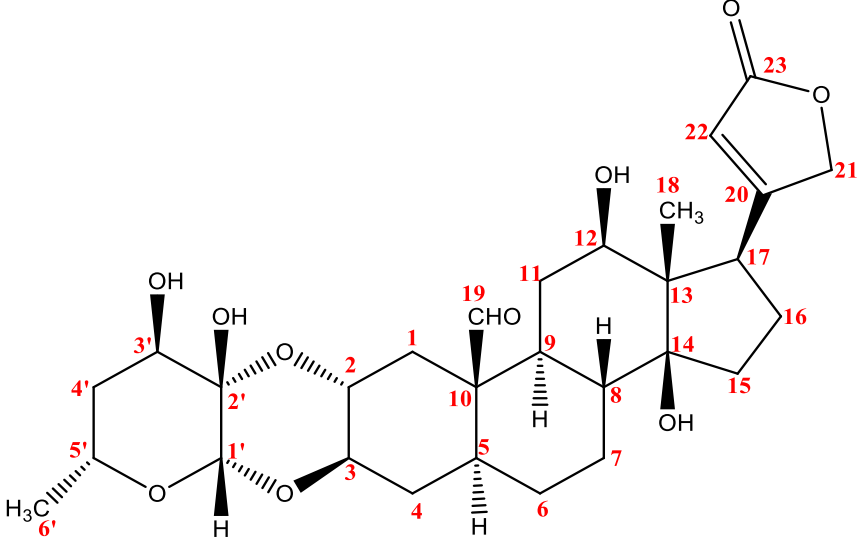
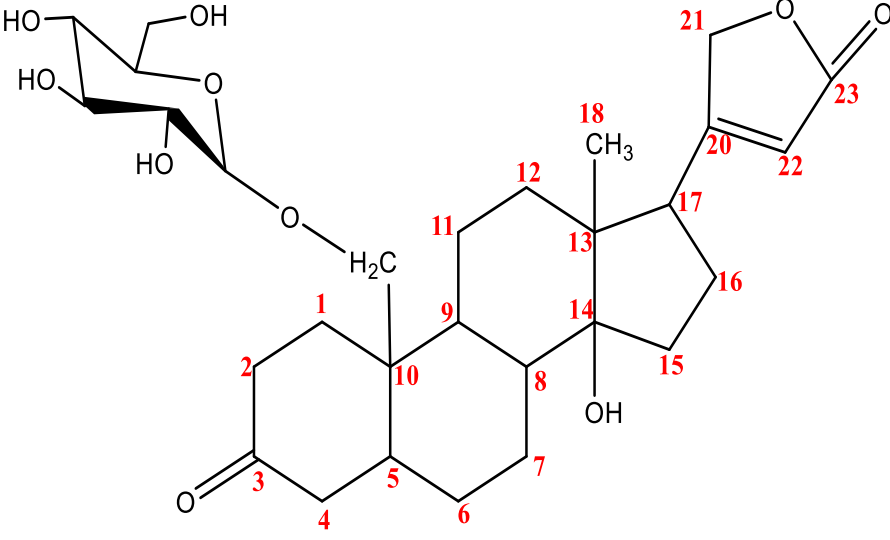
The oral administration of the crude and aqueous extracts at doses of 2000 mg/kg inhibits the development of paw edema. The aqueous extract showed highly significant inhibition of inflammation with a percentage of inhibition very close to that of reference ibuprofen (77.25 % and 83.58 for aqueous and ibuprofen, respectively). While, the crude extract showed lower inhibition than the reference with percentage inhibition 43.00%. As well as the oral administration of these extracts and the reference haloperidol at the same dose, reduced the movement of the animal treated with percentage of reduction of movement of 49.77 %, 60.00 % and 90.77% for aqueous, crude extracts and haloperidol, respectively which indicate that these extracts have good sedative activity.

Our study report for the first time the isolation and purification of alkaloids from *P. tomentosa*. It was performed using different chromatographic methods such as: silica gel column, C18 column, TLC and PTLC. This isolation allows us to obtain twenty-six pure alkaloids, their quantities vary from 1.8 mg to 0.1 mg. Chemical structures of only five alkaloids were determined using nuclear magnetic resonance experiments (¹H, ¹³C, HSQC, HMBC and COSY). Based on these NMR analyses, as well as the comparison with the literature, it turns out that the type of all the isolated alkaloids are macrocyclic diester pyrrolizidine alkaloids. All these compounds are isolated for the first time as new compounds.

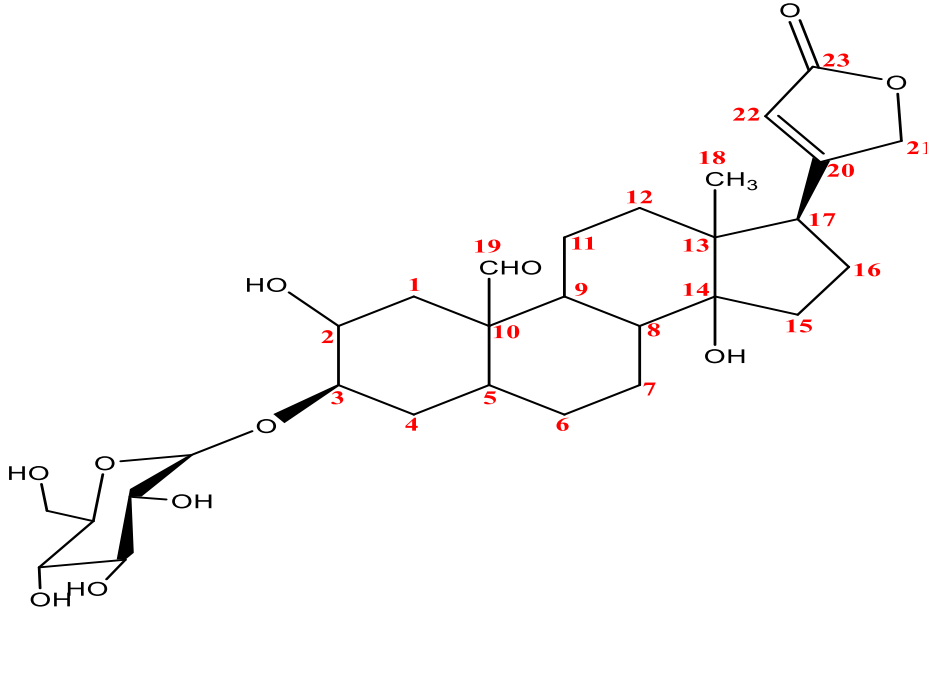
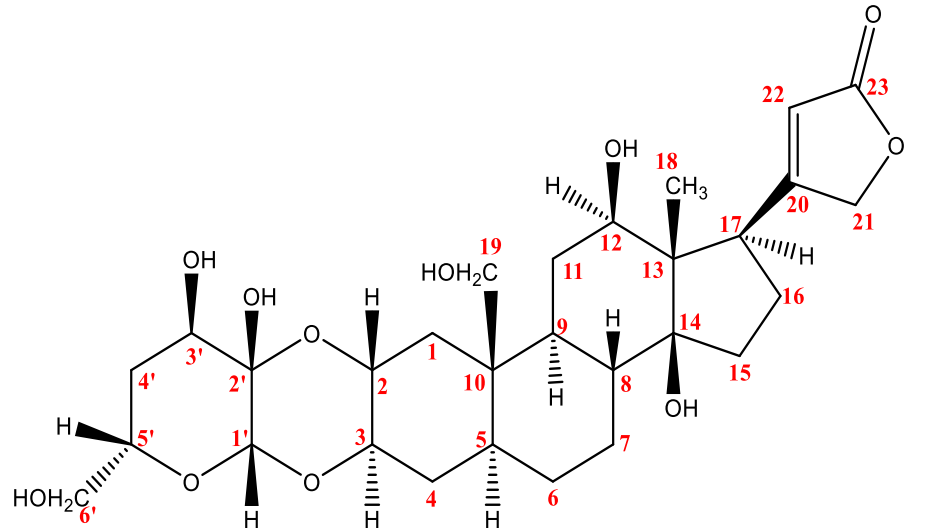
The phytochemical investigation that carried out on the combined butanol and ethyl acetate extracts using different chromatographic methods such as: silica gel column, sephadex LH-20 column, C18 column, TLC and PTLC, lead us to obtain five cardenolide glycosides, two flavonoids and one phenolic compound; their quantities vary from 22.8 mg to 4.3 mg. Six compounds were determined using different NMR spectroscopic analysis methods (¹H, ¹³C, DEPT135, DEPT90, HSQC, TOCSY-HSQC, HMBC and COSY), as well as the comparison with those of literatures. After structural elucidation of these compounds, it turns out that: tow cardenolide glycosides, one flavonoid and one phenolic compounds are new compounds. The two remaining cardenolide glycoside were isolated previously from this plant.

The determination of structures of twenty-one alkaloids, one cardenolide and one flavonoid was impossible due to their small amount which make their NMR spectra unexploitable.

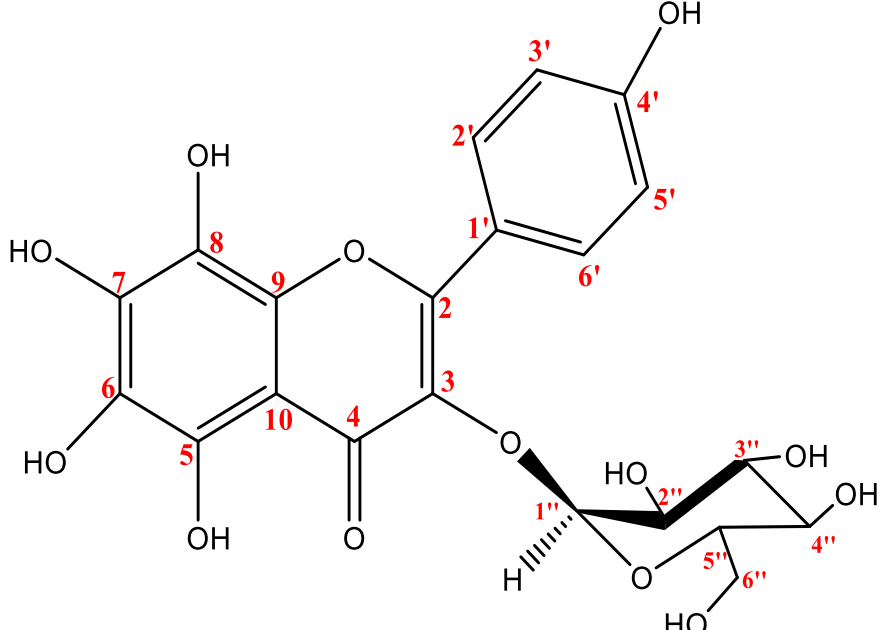
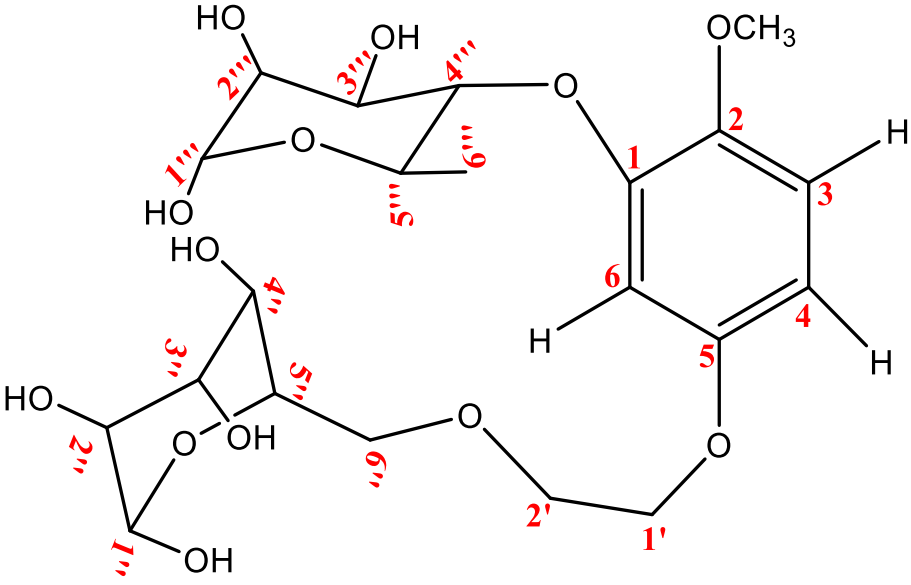
Table III-B-13: Chemical structure of the compounds isolated from *P.tomentosa*

compound	Masse of compound (mg)	Family of compound	Chemical structure	Name of compound	Report
PN	20.4	Cardenolide glycoside		12β-hydroxycalactin	Isolated for second time as a new compound
PM	4.3	Cardenolide glycoside		3-oxo,19-O-β-D-glucopyranosylcoroglaucigenin	Isolated for the first time as a new compound

General Conclusion

<p>PVe</p>	<p>6</p>	<p>Cardenolide glycoside</p>		<p>2-hydroxycorotoxigenin-3-O-glucopyranoside</p>	<p>Isolated for the first time as a new compound</p>
<p>PV</p>	<p>13.1</p>	<p>Cardenolide glycoside</p>		<p>Ghalakinoside</p>	<p>previously isolated from <i>P. tomentosa</i></p>

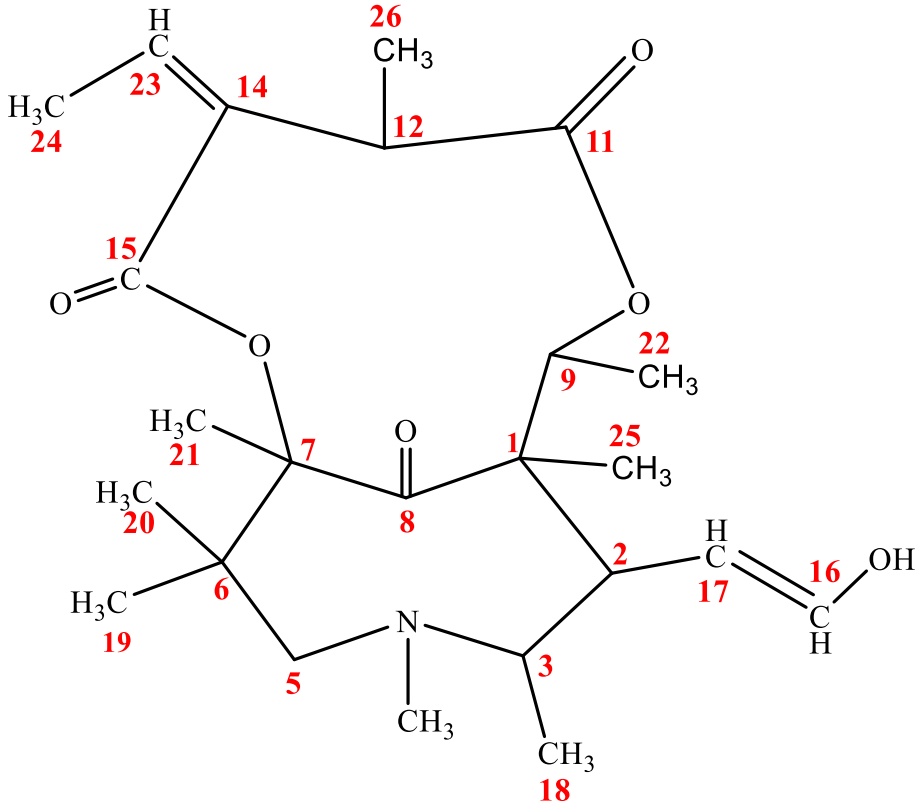
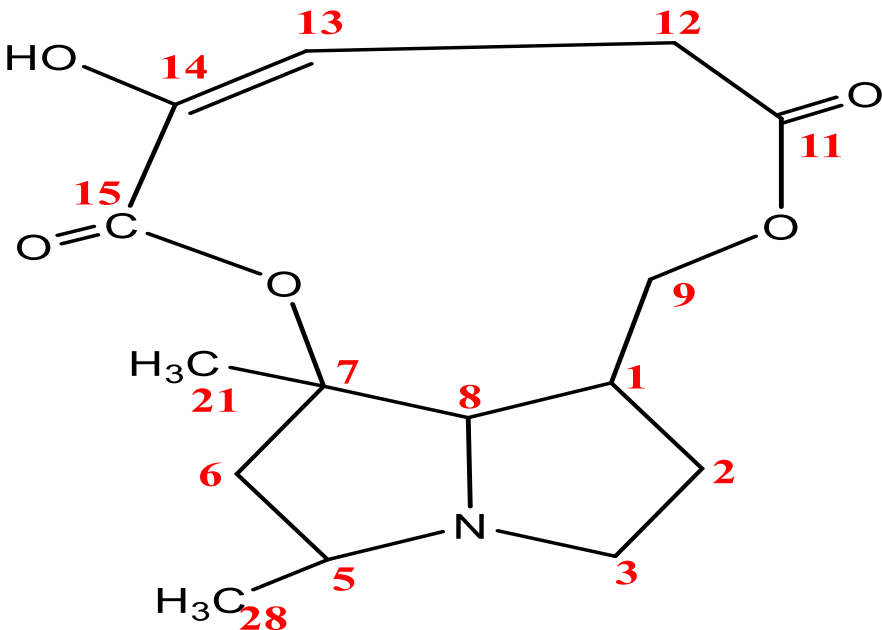
General Conclusion

<p>PJ</p> <p>22.8</p>	<p>Flavonoid</p>		<p>6,8-dihydroxykaempferol-3-O-β-glucopyranosyl</p>	<p>Isolated for the first time as a new compound</p>
<p>PR</p> <p>6</p>	<p>Phenolic compound</p>		<p>5-[(2-O-β-glucopyranosyl)ethoxy]-2-methoxyphenol-O-α-rhamnopyranosyl</p>	<p>Isolated for the first time as a new compound</p>

General Conclusion

P8	0.6	Alkaloid		Tomentonecine A	Isolated for the first time as a new compound
P13	1.7	Alkaloid		Tomentonecine B	Isolated for the first time as a new compound

General Conclusion

P5	0.1	Alkaloid		Tomentonecine C	Isolated for the first time as a new compound
P20	1	Alkaloid		Tomentonecine D	Isolated for the first time as a new compound

General Conclusion

P10	1.2	Alkaloid		Tomentonecine E	Isolated for the first time as a new compound
------------	-----	----------	--	-----------------	-----------------------------------------------

References

References

1. P. Ozenda, *Flore du sahara septentrional et central*. 1958.
2. P. Quézel and S. Santa, *Nouvelle flore de l'algérie et des régions désertiques méridionales*. 1962.
3. A.A. Gohar, M. El-Olemy, E. Abdel-Sattar, M. El-Said, and M. Niwa, *Cardenolides and β -sitosterol glucoside from pergularia tomentosa l*. Natural Product Sciences, 2000. **6**(3): p. 142-146.
4. M. Miladi, K. Abdellaoui, H. Regaieg, G. Omri, F. Acheuk, and H.M. Ben, *Effects of latex from pergularia tomentosa and the aggregation pheromone, phenylacetonitrile, on locusta migratoria larvae*. Tunisian Journal of Plant Protection, 2018. **13**(Special Issue): p. 87-98.
5. E.N. Ads, A.S. Abouzied, and M.K. Alshammari, *Evaluation of cytotoxic effects of methanolic extract of pergularia tomentosa l growing wild in ksa*. Asian Pacific Journal of Cancer Prevention, 2021. **22**(S1): p. 67-72.
6. H.R. El-Seedi, S.A. Khalifa, E.A. Taher, M.A. Farag, A. Saeed, M. Gamal, M.-E.F. Hegazy, D. Youssef, S.G. Musharraf, and M.M. Alajlani, *Cardenolides: Insights from chemical structure and pharmacological utility*. Pharmacological research, 2019. **141**: p. 123-175.
7. B. Sennblad and B. Bremer, *The familial and subfamilial relationships of apocynaceae and asclepiadaceae evaluated with rbcL data*. Plant Systematics and Evolution, 1996. **202**(3): p. 153-175.
8. E. Sundell, *Asclepiadaceae milkweed family*. Journal of the Arizona-Nevada Academy of Science, 1994: p. 169-187.

References

9. I. Yildiz, O. Sen, R. Erenler, I. Demirtas, and L. Behcet, *Bioactivity-guided isolation of flavonoids from cynanchum acutum l. Subsp. Sibiricum (willd.) rech. F. And investigation of their antiproliferative activity*. Natural Product Research, 2017. **31**(22): p. 2629-2633.
10. F. Albers and U. Meve, *Asclepiadaceae*, in *Illustrated handbook of succulent plants: Asclepiadaceae*. 2004, Springer. p. 5-274.
11. K. Swarupandan, J.K. Mangaly, T. Sonny, K. Kishorekumar, and S.C. Basha, *The subfamilial and tribal classification of the family asclepiadaceae*. Botanical Journal of the Linnean Society, 1996. **120**(4): p. 327-369.
12. A.I. Hamed, A. Plaza, M.L. Balestrieri, U.A. Mahalel, I.V. Springuel, W. Oleszek, C. Pizza, and S. Piacente, *Cardenolide glycosides from pergularia tomentosa and their proapoptotic activity in kaposi's sarcoma cells*. Journal of natural products, 2006. **69**(9): p. 1319-1322.
13. S. Piacente, M. Masullo, N. De Nève, J. Dewelle, A. Hamed, R. Kiss, and T. Mijatovic, *Cardenolides from pergularia tomentosa display cytotoxic activity resulting from their potent inhibition of na⁺/k⁺-atpase*. Journal of natural products, 2009. **72**(6): p. 1087-1091.
14. E. Gellert, *The indolizidine alkaloids*. Journal of Natural Products, 1982. **45**(1): p. 50-73.
15. S.S. Subramanian and A. Nair, *Flavonoids of some asclepiadaceous plants*. Phytochemistry, 1968. **7**(9): p. 1703-1704.
16. N. Brown, *The genus pergularia*. Bulletin of Miscellaneous Information (Royal Gardens, Kew), 1907: p. 323-325.
17. D. Goyder, *A revision of the genus pergularia l.(apocynaceae: Asclepiadoideae)*. Kew Bulletin, 2006: p. 245-256.

References

18. S. Liede, *On the position of the genus pergularia (asclepiadaceae)*, in *The biodiversity of african plants*. 1996, Springer. p. 481-488.
19. C. Devaux, *Plantes toxiques ou réputées toxiques pour le bétail en afrique de l'ouest. Note de synthèse n° 4*. 1973.
20. A.M. Hosseini Kahnouj Sh, Azarnivand H, Piacente S, Zare Chahouki Ma, *Pergularia tomentosa, from traditional uses to ecology and phytochemistry*. Journal of Medicinal Plants, 2017. **16**(63): p. 108-118.
21. A. Chehma, *Catalogue des plantes spontanées du sahara septentrional algérien laboratoire de protection des écosystèmes en zone arides et semi arides, univ. Kasdi Merbah, Ouargla*, 2006.
22. A. Kemassi, S. Darem, R. Cherif, Z. Boual, S.E. Sadine, M.S. Aggoune, A. Ould El Hadj-Khelil, and M. Ould El Hadj, *Recherche et identification de quelques plantes médicinales à caractère hypoglycémiant de la pharmacopée traditionnelle des communautés de la vallée du m'zab (sahara septentrional est algérien)*. J Adv Res Sci Technol, 2014. **1**(1): p. 1-5.
23. M. Ould El Hadj, M. Hadj-Mahammed, and H. Zabeirou, *Place of the spontaneous plants samples in the traditional pharmacopoeia of the area of ouargla (septentrional east sahara)*. Courrier du Savoir, 2003. **3**: p. 50-51.
24. N.A. Al-Mekhlafi and A. Masoud, *Phytochemical and pharmacological activities of pergularia tomentosa l.-a review*. Indo American Journal of Pharmaceutical Sciences, 2017. **4**(11): p. 4558-4565.
25. I. Lahmar, H. Belghith, F. Ben Abdallah, and K. Belghith, *Nutritional composition and phytochemical, antioxidative, and antifungal activities of pergularia tomentosa l*. BioMed research international, 2017. **2017**.
26. 2023; Available from: <https://www.gbif.org/species/7877996>.

References

27. M. Hifnawy, M. El-Shanawany, M. Khalifa, A. Youssef, and S. Desoukey, *Cardiotonic activity of pergularia tomentosa different extracts, fractions & isolated compounds*. J Pharm Biol Sci, 2014. **9**: p. 54-60.
28. M. Hosseini, M. Ayyari, A. Meyfour, S. Piacente, A. Cerulli, A. Crawford, and S. Pahlavan, *Cardenolide-rich fraction of pergularia tomentosa as a novel antiangiogenic agent mainly targeting endothelial cell migration*. DARU Journal of Pharmaceutical Sciences, 2020. **28**(2): p. 533-543.
29. W.A. Rayyan, S.A. Alshammari, A.M. Alsammary, M.S. Al-Shammari, N. Seder, and L.F. Abu-Qatouseh, *The phytochemical analysis and antimicrobial activity of pergularia tomentosa in north east kingdom of saudi arabia ksa*. Biomedical and Pharmacology Journal, 2018. **11**(4): p. 1763-1771.
30. F. Acheuk and B. Doumandji-Mitiche, *Insecticidal activity of alkaloids extract of pergularia tomentosa (asclepiadaceae) against fifth instar larvae of locusta migratoria cinerascens (fabricius 1781)(orthoptera: Acrididae)*. International Journal of Science and Advanced Technology, 2013. **3**(6): p. 8-13.
31. F.E. Ghadi, A.R. Ghara, A. Cerulli, and S. Piacente, *Evaluation of the anti-diabetic activity and lc-esi/ltqorbitrap/ms/ms profiling of an aqueous extract of pergularia tomentosa l. Aerial parts*. 2021.
32. R. Yakubu, F. Jibril, A. Lukman, and F. Sheikh, *Trends for antioxidant power of phytochemicals from pergularia tomentosa l. Asclepiadacea) whole plant*. Scholars Academic J Pharm, 2015. **4**(2): p. 74-80.
33. D.A. Ananth, G. Deviram, V. Mahalakshmi, and V.R. Bharathi, *Active status on phytochemistry and pharmacology of pergularia daemia forsk.(trellis-vine): A review*. Clinical Phytoscience, 2021. **7**(1): p. 1-13.

References

34. S.H. Hosseini, M. Masullo, A. Cerulli, S. Martucciello, M. Ayyari, C. Pizza, and S. Piacente, *Antiproliferative cardenolides from the aerial parts of pergularia tomentosa*. Journal of natural products, 2019. **82**(1): p. 74-79.
35. P.W. Green, N.C. Veitch, P.C. Stevenson, and M.S. Simmonds, *Cardenolides from gomphocarpus sinaicus and pergularia tomentosa (apocynaceae: Asclepiadoideae) deter the feeding of spodoptera littoralis*. Arthropod-Plant Interactions, 2011. **5**(3): p. 219-225.
36. Z. Babaamer, M. Abuzarga, N. Al-Abdalla, and L. Sakhri, *Isolation of cardenolide glycosides from pergularia tomentosa. L and their antioxidant activities*. Ann Sci Technol, 2014. **6**: p. 122-128.
37. V. Bhaskar and N. Balakrishnan, *Veliparuthi (pergularia daemia (forsk.) chiov.)-as a phytomedicine: A review*. Int. J. Pharmtech. Res, 2009. **1**: p. 1305-1313.
38. Z.Y. Babaamer, L. Sakhri, H.I. Al-Jaber, M.A. Al-Qudah, and M.H. Abu Zarga, *Two new taraxasterol-type triterpenes from pergularia tomentosa growing wild in algeria*. Journal of Asian natural products research, 2012. **14**(12): p. 1137-1143.
39. H.S. Al Hinai, W.M. Al-Subhi, F.R.S. Al-Rubaiai, S.I. Hassan, N. Sherwani, and M.O. Fatope, *Lupane and ursane-type triterpenoids from pergularia tomentosa*. Chemistry of Natural Compounds, 2018. **54**: p. 790-792.
40. S. Ignacimuthu, M. Pavunraj, V. Duraipandiyan, N. Raja, and C. Muthu, *Antibacterial activity of a novel quinone from the leaves of pergularia daemia (forsk.), a traditional medicinal plant*. Asian Journal of Traditional Medicines, 2009. **4**(1): p. 36-40.
41. J. Bruneton, *Pharmacognosie, phytochimie plantes médicinales*. 5e édition ed. 2015.
42. R. Milcent, *Chimie organique hétérocyclique*, ed. H. Collection. 2003.
43. H. Sayhan, S.G. Beyaz, and A. Çelikleş, *The local anesthetic and pain relief activity of alkaloids*. Intech Open, 2017: p. 57-84.

References

44. T. Aniszewski, *Alkaloid chemistry*. Alkaloids; chemistry, biology, ecology, and applications, 2nd edn. Elsevier BV, Netherlands, 2015: p. 99-193.
45. J. Zhu, M. Wang, W. Wen, and R. Yu, *Biosynthesis and regulation of terpenoid indole alkaloids in catharanthus roseus*. *Pharmacognosy reviews*, 2015. **9**(17): p. 24.
46. E. Lima and J. Medeiros, *Marine organisms as alkaloid biosynthesizers of potential anti-alzheimer agents*. *Marine Drugs*, 2022. **20**(1): p. 75.
47. H.F.L.a.J.F. Jackson, *Modern methods of plant analysis*. Springer-Verlag, 1994.
48. S.B. Malcolm, *Milkweeds, monarch butterflies and the ecological significance of cardenolides*. *Chemoecology*, 1994. **5**(3): p. 101-117.
49. T. Züst, M. Mirzaei, and G. Jander, *Erysimum cheiranthoides, an ecological research system with potential as a genetic and genomic model for studying cardiac glycoside biosynthesis*. *Phytochemistry reviews*, 2018. **17**(6): p. 1239-1251.
50. D. Deepak, S. Srivastava, N. Khare, and A. Khare, *Cardiac glycosides*. *Fortschritte der Chemie organischer Naturstoffe/Progress in the Chemistry of Organic Natural Products*, 1996: p. 71-155.
51. A.F.M. Botelho, F. Pierezan, B. Soto-Blanco, and M.M. Melo, *A review of cardiac glycosides: Structure, toxicokinetics, clinical signs, diagnosis and antineoplastic potential*. *Toxicon*, 2019. **158**: p. 63-68.
52. S. Martucciello, G. Paoletta, A.M. Romanelli, S. Sposito, L. Meola, A. Cerulli, M. Masullo, S. Piacente, and I. Caputo, *Pro-apoptotic and pro-autophagic properties of cardenolides from aerial parts of pergularia tomentosa*. *Molecules*, 2022. **27**(15): p. 4874.
53. J. Cai, B.-D. Zhang, Y.-Q. Li, W.-F. Zhu, T. Akihisa, T. Kikuchi, J. Xu, W.-Y. Liu, F. Feng, and J. Zhang, *Cardiac glycosides from the roots of streblus asper lour*. *With*

References

- activity against epstein-barr virus lytic replication*. Bioorganic Chemistry, 2022. **127**: p. 106004.
54. A.A. Agrawal, G. Petschenka, R.A. Bingham, M.G. Weber, and S. Rasmann, *Toxic cardenolides: Chemical ecology and coevolution of specialized plant–herbivore interactions*. New Phytologist, 2012. **194**(1): p. 28-45.
55. P. Apostolou, M. Toloudi, M. Chatziioannou, E. Ioannou, D.R. Knocke, J. Nester, D. Komiotis, and I. Papatiriou, *Anvirzel™ in combination with cisplatin in breast, colon, lung, prostate, melanoma and pancreatic cancer cell lines*. BMC Pharmacology and Toxicology, 2013. **14**(1): p. 1-6.
56. A.B. Krishna, H.K. Manikyam, V.K. Sharma, and N. Sharma, *Plant cardenolides in therapeutics*. Int J Indigenous Med Plants, 2015. **48**: p. 1871-1896.
57. Z. Rahmani, Eude de la relation structure-activité antioxydante et antihémolyse des érythrocytes humaines par quelques dithiolethiones et composés phénoliques. Thesis, 2015. Université de Ouargla-Kasdi Merbah.
58. C. Tsang, Antioxidant activity, protective effects and absorption of polyphenolic compounds. Thesis, 2004. University of Glasgow.
59. S. Boumerfeg, Antioxidative properties of *tamus communis* l., *carthamus caeruleus* l. And *ajuga iva* l. Extracts. Thesis, 2018.
60. O.-C. Bujor, Extraction, identification and antioxidant activity of the phenolic secondary metabolites isolated from the leaves, stems and fruits of two shrubs of the ericaceae family. Thesis, 2016. Université d'Avignon.
61. N.S. Belinda, Evaluation of antioxidant and anti-inflammatory activities, total phenolic and flavonoid content in selected medicinal plants, non-edible medicinal mushrooms and seaweed. Thesis, 2020. Kenyatta University.

References

62. A.E. Stratariadaki, *Study of phenolic content and antioxidant activity of greek red and white wines by means of classical methods and fir*. 2015.
63. O. Dangles, *Antioxidant activity of plant phenols: Chemical mechanisms and biological significance*. *Current Organic Chemistry*, 2012. **16**(6): p. 692-714.
64. K. Mishra, H. Ojha, and N.K. Chaudhury, *Estimation of antiradical properties of antioxidants using dpph assay: A critical review and results*. *Food chemistry*, 2012. **130**(4): p. 1036-1043.
65. B. G, *Total antioxidant capacity*. *Adv Clin Chem*, 2003. **2423**(03).
66. P. Prieto, M. Pineda, and M. Aguilar, *Spectrophotometric quantitation of antioxidant capacity through the formation of a phosphomolybdenum complex: Specific application to the determination of vitamin e*. *Analytical biochemistry*, 1999. **269**(2): p. 337-341.
67. M. Kebieche and Z. Meraihi, *Activité biochimique des extraits flavonoïdiques de la plante ranunculus repens l*. Thesis, 2009. Constantine: Université Mentouri Constantine.
68. N. Kambouche, B. Merah, A. Derdour, S. Bellahouel, M. Benziane, C. Younos, M. Firkioui, S. Bedouhene, and R. Soulimani, *Étude de l'effet antidiabétique des saponines extraites d'anabasis articulata (forssk) moq, plante utilisée traditionnellement en algérie*. *Phytothérapie*, 2009. **7**(4): p. 197-201.
69. A. Nagappa, P. Thakurdesai, N.V. Rao, and J. Singh, *Antidiabetic activity of terminalia catappa linn fruits*. *Journal of ethnopharmacology*, 2003. **88**(1): p. 45-50.
70. N.M. Hanae, *Étude pharmacologique toxicologique de l'arbutus unedo l. Au maroc*. 2018.
71. W. Sobhi, *Caractérisation de l'huile des graines de nigella sativa et étude de son activité hypoglycémiant et son hépato-toxicité*. Thesis, 2018.

References

72. N. Kebir, Propriétés du lait de chamelle cru sur les profils glucidique et lipidique des rats wistar rendus diabétiques par l'alloxane. Thesis, 2018.
73. A. Guérin-Dubourg, Étude des modifications structurales et fonctionnelles de l'albumine dans le diabète de type 2: Identification de biomarqueurs de glycoxydation et de facteurs de risque de complications vasculaires. Thesis, 2014. Université de la Réunion.
74. T. Nouadri, *L' α -amylase de penicillium camemberti pl21: Production, purification, caractérisation et immobilisation*. Diplôme de Doctorat d'Etat. Biochimie et Biotechnologies. Université Mentouri Constantine. p160, 2011.
75. P. Goetz, *Phytothérapie du diabète*. Phytothérapie, 2007. **5**(4): p. 212-217.
76. M. Merghem, Evaluation of toxicity in mice and rats and antioxydant activities of ruta montana l. Extracts. Thesis, 2018.
77. W. Nouioua, Ecologie, chorologie et phytochimie et activité biologique d'une paeoniaceae endémique algérienne (l.) mill. Thesis, 2017. Université Ferhat Abbas.
78. M.A. Baki, A. Khan, M.a.A. Al-Bari, A. Mosaddik, G. Sadik, and K. Mondal, *Sub-acute toxicological studies of pongamol isolated from pongamia pinnata*. Research Journal of Medicine and Medical Sciences, 2007. **2**(2): p. 53-57.
79. O. Oecd, *Guidelines for testing of chemicals, acute oral toxicity-fixed dose procedure*. Organ. Econ. Coop. Dev, 2001.
80. R. Mebirouk and D. Naimi, Recherche et évaluation des activités biologiques de trois extraits d'helix aspersa (aqueux, hydro alcoolique et organique). Thesis, 2017. Université Frères Mentouri-Constantine 1.
81. A. Bean, Investigating the anti-inflammatory activity of honey. Thesis, 2012. University of Waikato.

References

82. G. Nabil, Contribution à l'étude de l'activité biologique des deux espèces de marrubium vulgare l et marrubium deserti de noé in vitro et in vivo. Thesis, 2018. Univ. Batna 2.
83. M. Chaima, Evaluation des activités biologiques et étude de la composition chimique de la plante scabiosa stellata l. Thesis, 2019. Université de Batna 2.
84. G. Hajjaj, *Screening phytochimique, étude toxicologique et valorisation pharmacologique de matricaria chamomilla l. Et de l'ormenis mixta l.(asteraceae)*. 2017.
85. S. Ferdjoui, Activités biologiques de deux plantes médicinales mentharotundifolia. Et lamium amplexicaulel. Thesis, 2020.
86. A. Bounihi, Criblage phytochimique, étude toxicologique et valorisation pharmacologique de melissa officinalis et de mentha rotundifolia (lamiacées). Thesis, 2016.
87. T. Morita, S. Tsuneto, and Y. Shima, *Definition of sedation for symptom relief: A systematic literature review and a proposal of operational criteria*. Journal of pain and symptom management, 2002. **24**(4): p. 447-453.
88. M. Frasca, E. Treillet, M. Pechard, B. Sardin, and B. Burucoa, *Pratiques médicamenteuses sédatives en situation palliative et de fin de vie. L'essentiel des recommandations has 2020*. Médecine Palliative, 2022. **21**(1): p. 4-10.
89. J. Divya, A. Kumar, and R. Kumar, *Evaluation of diuretic and sedative activity for ethanolic leaves extract of basella alba l. Var rubra*. World Journal of Current Medical and Pharmaceutical Research, 2020: p. 74-84.
90. M.-M. Shi, J.-H. Piao, X.-L. Xu, L. Zhu, L. Yang, F.-L. Lin, J. Chen, and J.-G. Jiang, *Chinese medicines with sedative–hypnotic effects and their active components*. Sleep medicine reviews, 2016. **29**: p. 108-118.

References

91. W.C. Evans, *Trease and evans' pharmacognosy*. 2009: Elsevier Health Sciences.
92. Trease Ge. and E. Wc, *Pharmacognosy*. 11 ed. 1989, London.
93. J. Harborne, *Phytochemical methods chapman and hall*. Ltd. London, 1973. **4**: p. 49-188.
94. R. Yadav and M. Agarwala, *Phytochemical analysis of some medicinal plants*. Journal of phytology, 2011. **3**(12).
95. O. Oloyede, *Chemical profile of unripe pulp of carica papaya*. Pakistan journal of nutrition, 2005. **4**(6): p. 379-381.
96. V.L. Singleton and J.A. Rossi, *Colorimetry of total phenolics with phosphomolybdic-phosphotungstic acid reagents*. American journal of Enology and Viticulture, 1965. **16**(3): p. 144-158.
97. M. Belguidoum, H. Dendougui, Z. Kendour, A. Belfar, C. Bensaci, and M. Hadjadj, *Antioxidant activities, phenolic, flavonoid and tannin contents of endemic zygophyllum cornutum coss. From algerian sahara*. Der Pharma Chemica, 2015. **7**(11): p. 312-317.
98. A. Mansouri, G. Embarek, E. Kokkalou, and P. Kefalas, *Phenolic profile and antioxidant activity of the algerian ripe date palm fruit (phoenix dactylifera)*. Food chemistry, 2005. **89**(3): p. 411-420.
99. C. Boubekri, *Etude de l'activité antioxydante des polyphénols extraits de solanum melongena par des techniques électrochimiques*. Thesis, 2014. Université Mohamed Khider Biskra.
100. A. Fournet and V. Muñoz, *Natural products as trypanocidal, antileishmanial and antimalarial drugs*. Current Topics in medicinal chemistry, 2002. **2**(11): p. 1215-1237.

References

101. Z. Rahmani, A. Douadi, and Z. Rahmani, *In vitro inhibition of α -amylase enzyme, phytochemical study and antioxidant capacity for cupressus sempervirens extracts growing in arid climate*. Asian Journal of Research in Chemistry, 2019. **12**(6): p. 359-365.
102. A.O. Toxicity–Up, *Oecd guideline for testing of chemicals*. 2001.
103. K. Boudjema, N. Nahoui, K. Temmimi, K. Azine, L. Hali, and F. Fazouane, *Screening phytochimique et activités biologiques d'extrait méthanolique obtenu à partir de la plante melissa officinalis l*. Journal of Advanced research in science and technology ISSN: 2352_9989, 2021.
104. Y. Fukushima, T. Ohie, Y. Yonekawa, K. Yonemoto, H. Aizawa, Y. Mori, M. Watanabe, M. Takeuchi, M. Hasegawa, and C. Taguchi, *Coffee and green tea as a large source of antioxidant polyphenols in the japanese population*. Journal of agricultural and food chemistry, 2009. **57**(4): p. 1253-1259.
105. S. Heneidak, R.J. Grayer, G.C. Kite, and M.S. Simmonds, *Flavonoid glycosides from egyptian species of the tribe asclepiadeae (apocynaceae, subfamily asclepiadoideae)*. Biochemical systematics and ecology, 2006. **34**(7): p. 575-584.
106. T. Tanaka, Y. Matsuo, and Y. Saito, *Solubility of tannins and preparation of oil-soluble derivatives*. Journal of Oleo Science, 2018. **67**(10): p. 1179-1187.
107. R.S. Phatak and A.S. Hendre, *Total antioxidant capacity (tac) of fresh leaves of kalanchoe pinnata*. Journal of Pharmacognosy and Phytochemistry, 2014. **2**(5).
108. S.M. Alghanem and Y.A. El-Amier, *Phytochemical and biological evaluation of pergularia tomentosa l.(solanaceae) naturally growing in arid ecosystem*. International Journal of Plant Science and Ecology, 2017. **3**(2): p. 7-15.
109. M. Ali Asgar, *Anti-diabetic potential of phenolic compounds: A review*. International Journal of Food Properties, 2012. **16**(1): p. 91-103.

References

110. P. Jiang, J. Xiong, F. Wang, M.H. Grace, M.A. Lila, and R. Xu, *α -amylase and α -glucosidase inhibitory activities of phenolic extracts from eucalyptus grandis \times e. Urophylla bark*. Journal of Chemistry, 2017.
111. O.A. Oluwagunwa, A.M. Alashi, and R.E. Aluko, *Inhibition of the in vitro activities of α -amylase and pancreatic lipase by aqueous extracts of amaranthus viridis, solanum macrocarpon and telfairia occidentalis leaves*. Frontiers in Nutrition, 2021. **8**.
112. A. Cornish-Bowden, *Cinétique enzymatique*. 2005: EDP sciences.
113. U.N.E.C.F.E. Secretariat, *Globally harmonized system of classification and labelling of chemicals (ghs)*. 2005: Copyright Law of the United St.
114. V.K. Pothagar, M. Elangovan, and R.S. Srinivasan, *Enzymatic and non-enzymatic antioxidant activity of pergularia tomentosa against carbon tetra chloride induced hepatic damage in wistar albino rats*. 2017.
115. V. Kumar and N. Basu, *Anti-inflammatory activity of the latex of calotropis procera*. Journal of Ethnopharmacology, 1994. **44**(2): p. 123-125.
116. G. Lin, P. Rose, K. Chatson, E. Hawes, X. Zhao, and Z. Wang, *Characterization of two structural forms of otonecine-type pyrrolizidine alkaloids from ligularia hodgsonii by nmr spectroscopy*. Journal of natural products, 2000. **63**(6): p. 857-860.
117. R.J. Molyneux, J.N. Roitman, M. Benson, and R.E. Lundin, *^{13}C nmr spectroscopy of pyrrolizidine alkaloids*. Phytochemistry, 1982. **21**(2): p. 439-443.
118. J. Tamariz, E. Burgueño-Tapia, M.A. Vázquez, and F. Delgado, *Pyrrolizidine alkaloids*. The alkaloids: chemistry and biology, 2018. **80**: p. 1-314.
119. C.G. Logie, M.R. Grue, and J.R. Liddell, *Proton nmr spectroscopy of pyrrolizidine alkaloids*. Phytochemistry, 1994. **37**(1): p. 43-109.

References

120. M.S. Al-Said, M.S. Hifnawy, A.T. Mcphail, and D.R. Mcphail, *Ghalakinoside, a cytotoxic cardiac glycoside from pergularia tomentosa*. *Phytochemistry*, 1988. **27**(10): p. 3245-3250.
121. J.-Z. Li, C. Qing, C.-X. Chen, X.-J. Hao, and H.-Y. Liu, *Cytotoxicity of cardenolides and cardenolide glycosides from asclepias curassavica*. *Bioorganic & Medicinal Chemistry Letters*, 2009. **19**(7): p. 1956-1959.
122. L. Rascón-Valenzuela, C. Velázquez, A. Garibay-Escobar, L. Medina-Juárez, W. Vilegas, and R. Robles-Zepeda, *Antiproliferative activity of cardenolide glycosides from asclepias subulata*. *Journal of ethnopharmacology*, 2015. **171**: p. 280-286.
123. A. Harborne, *Phytochemical methods a guide to modern techniques of plant analysis*. 1998: springer science & business media.
124. K.R. Markham, *Techniques of flavonoid identification*. 1982: Academic press.
125. R.M. Facino, M. Carini, L. Franzoi, O. Pirola, and E. Bosisio, *Phytochemical characterization and radical scavenger activity of flavonoids from helichrysum italicum g. Don (compositae)*. *Pharmacological research*, 1990. **22**(6): p. 709-721.